Heterocycles via C–H Functionalization Strategies; Synthesis of Pyrroloindoles and Tanshinone IIA

By

©Simon Nathan Tucker

A thesis submitted to the

School of Graduate Studies

In partial fulfillment of the requirements for the degree of

Master of Science

Department of Chemistry

Memorial University of Newfoundland

July 2022

St. John's, Newfoundland and Labrador

Abstract

This thesis is divided into two projects. Chapter one discusses the development of tandem C–H functionalization and Michael-type annulation using α-diazocarbonyl compounds for the synthesis of fused indole ring systems. Highlights include the use of cheap copper catalysts, high stereoselectivity, and a robust substrate scope showcasing the amenability of the transformation to various indole and diazo substrates. Details of an interesting base-catalyzed olefin isomerization will also be discussed. Chapter two details a newly developed total synthesis of tanshinone IIA, an abietane diterpenoid from the tanshinone family of natural products. This route is highlighted by access to complex coupling partners through multigram scale reactions starting from simple commercially available starting materials. Key transformations include an iridium-catalyzed borylation, a directed metalation/iodination, and a Brook-type rearrangement to furnish a synthetically challenging ortho-quinone ring. Chapter three presents a summary of this thesis work and potential avenues for future research.

Acknowledgements

First, I would like to thank my supervisor Huck, for his constant guidance and encouragement since the day I joined his group in 2018. I would also like to thank my group members, both old and new, for offering their support and suggestions regarding lab troubles.

Thank you to my parents Craig Tucker and Kelly Fewer, and my grandparents who modeled for me the drive and dedication needed to achieve all goals I set my heart on.

Thank you Natalie, for your unrivaled love and support.

Table of Contents

ABSTRACT ..... **II**

ACKNOWLEDGEMENTS ..... **III**

LIST OF TABLES ..... **V**

LIST OF SCHEMES ..... **VI**

LIST OF FIGURES ..... **VIII**

LIST OF ABBREVIATIONS AND SYMBOLS ..... **IX**

CHAPTER 1: SYNTHESIS OF FUSED INDOLE FRAMEWORKS VIA TANDEM C-H INSERTION/MICHAEL-TYPE ANNULATION **1**

STATEMENT OF CO-AUTHORSHIP 1
1.1: INTRODUCTION 2
1.1.1: α-Diazocarbonyl Compounds and Metal Carbenoids *2*
1.1.2: Heteroatom–Hydrogen Insertion *5*
1.1.3: Heteroatom–Hydrogen Insertion and Tandem Electrophile Trapping *7*
1.1.4: Formal Carbon-Hydrogen Insertion with α-Diazocarbonyl Compounds *10*
1.1.5: Formal Carbon-Hydrogen Insertion/Annulation Reactions *12*
1.1.6: Thesis Project Objectives *14*
1.2: RESULTS AND DISCUSSION 15
1.3 EXPERIMENTAL 28
1.3.1: General procedures *28*
1.3.2: Synthetic procedures *29*

REFERENCES **45**

APPENDIX **49**

CHAPTER 2: TOTAL SYNTHESIS OF TANSHINONE IIA **90**

2.1 TANSHINONE NATURAL PRODUCTS 90
2.1.1 Isolation and Applications *90*
2.1.2 Previous Synthetic Efforts *92*
2.1.2 Project Objectives and Initial Retrosynthetic Analysis en Route to Tanshinone IIA *97*
2.2 RESULTS AND DISCUSSION 98
2.2.1 Synthesis of Starting Materials *98*
2.2.2 Initial Coupling Attempts *101*
2.3 EXPERIMENTAL 118
2.3.1: General procedures *118*
2.3.2: Synthetic procedures *119*

REFERENCES **128**

APPENDIX **130**

CHAPTER 3: SUMMARY AND FUTURE WORK **154**

3.1: CHAPTER 1 SUMMARY 154
3.2: CHAPTER 2 SUMMARY 156
3.2.1: Potential Future Work *157*

REFERENCES **160**

List of Tables

Table 1: Optimization of the Diels-Alder reaction..... 101

List of Schemes

Scheme 1.1: Formation of metal carbenoids and common reactions using α-diazocarbonyl compounds. 3
Scheme 1.2: Main factors that control reactivity of metal carbenoids. 4
Scheme 1.3: General reaction profile of an X–H insertion reaction of α-diazocarbonyl compounds. 5
Scheme 1.4: Preliminary research on α-diazocarbonyl compounds by Yates. 6
Scheme 1.5: Efficient rhodium catalyzed O–H insertion reactions by Teyssié. 7
Scheme 1.6: General reaction process of tandem insertion/electrophilic trapping. 8
Scheme 1.7: Aldol-type trapping of diazo O–H insertion intermediates by Hu. 9
Scheme 1.8: Tandem O–H insertion/Michael addition by Xu. 9
Scheme 1.9 A: Formal C–H insertion via metal catalyzed C–H activation. B: Formal C–H insertion via electrophilic addition of a metal carbene. 11
Scheme 1.10: Metal carbene insertion into indole by Kerr 11
Scheme 1.11: Gold-catalyzed insertion/annulation by Zhang. 12
Scheme 1.12: Copper-catalyzed insertion/annulation by Xu. 13
Scheme 1.13: Tandem C–H insertion/Conia-ene cyclization by Grover. 14
Scheme 1.14: Copper-catalyzed C-H insertion/Michael-type cyclization. 15
Scheme 1.15: Proposed mechanism of the insertion/annulation process. 16
Scheme 1.16: Effects of ester group on the yield of the insertion/annulation process. 17
Scheme 1.17: Effect of alkyne substitution on the insertion/annulation process. 18
Scheme 1.18: A: Varying the length of the tethered electrophile. B: Varying the location of the tethered electrophile. 20
Scheme 1.19: Effect of different acceptor/acceptor diazo groups. 21
Scheme 1.20: Effect of different donor/acceptor diazo groups. 22
Scheme 1.21: Mono-activation pathway leading to E-isomer. 23
Scheme 1.22: Base-mediated conversion of crude reaction mixtures to olefin isomerized product. ..... **Error! Bookmark not defined.**
Scheme 1.23: Base-promoted cyclization/olefin isomerization process. 25
Scheme 1.24: Base-promoted cyclization on substrates that did not undergo olefin isomerization. 26
Scheme 1.25: Base-promoted annulation using traditional Michael acceptors. 27
Scheme 2.1: Select examples of tanshinones. 91
Scheme 2.2: Key ring forming steps in Kakisawa's synthesis of tanshinone IIA. 93
Scheme 2.3: Diels-Alder strategy for synthesis of tanshinone IIA by Kakisawa and Inouye. 94
Scheme 2.4: Photochemical annulation strategy for the synthesis of tanshinone IIA by Danheiser. 95
Scheme 2.5: Remote functionalization strategy in the synthesis of tanshinone IIA by Jiang. 96
Scheme 2.6: Total synthesis of tanshinone IIA by Huang. 97
Scheme 2.7: Retrosynthetic analysis of the proposed route to tashninone IIA. 98
Scheme 2.8: Two-step synthesis of key carboxylic acid **28**. 99
Scheme 2.9: Synthesis of oxazole **34.** 100

Scheme 2.10: A: Rh(III) catalyzed coupling between benzoic acids and furans.[30] B: Rh(III) catalyzed coupling attempts between **28** and **29.** 102
Scheme 2.11: Palladium-catalyzed biaryl coupling attempt..... 104
Scheme 2.12: Rh(III)-catalyzed dimerization of benzoic acids by Li..... 105
Scheme 2.13: Rhodium-catalyzed cross-coupling attempt using carboxylic acids. 105
Scheme 2.14: Further attempts at carboxylic acid cross-coupling..... 106
Scheme 2.15: A: Literature reported coupling of aryl bromides with furan esters. B: Iodination and subsequent coupling attempt with furoate **29.** 107
Scheme 2.16: Further attempts at directed couplings using aryl iodides. 108
Scheme 2.17: Synthesis and coupling attempt of iodofuran **50** with aryl carboxylic acid 109
Scheme 2.18: Esterification of aryl iodo-carboxylic acid **48.**..... 110
Scheme 2.19: Synthesis attempts of alternate coupling partners. 110
Scheme 2.20: Synthesis of biaryl coupling product **54** via Stille coupling. 111
Scheme 2.21: Synthesis of boronic ester **55** via Miyaura borylation. 113
Scheme 2.22: Two-step synthesis of boronic ester **54** using iridium catalysis..... 113
Scheme 2.23: Strategies for synthesis of iodo-furan coupling partners. 114
Scheme 2.24: Attempts at forming diester **59** using Suzuki reaction. 115
Scheme 2.25: Failed acyloin condensation of diester **59.**..... 115
Scheme 2.26: Mechanism of Stanna-Brook rearrangement by Sardina. 116
Scheme 2.27: Stanna-Brook rearrangement allows the synthesis of tanshinone IIA..... 117
Scheme 3.1: Representative example of pyrroloindole synthesis. 154
Scheme 3.2: A: Interesting result from attempted insertion/annulation. B: Initial attempts at the synthesis of indolizines via tandem insertion/annulation..... 156
Scheme 3.3: Total synthesis of tanshinone IIA..... 157
Scheme 3.4: One-pot Negishi coupling attempt. 158
Scheme 3.5: Progress towards the synthesis of normiltirone and miltirone. 159

List of Figures

Figure 1.1: Classes of diazo reagents. 3
Figure 2.1: ^{1}H NMR spectrum of undesired coupled product **38.** 103
Figure 2.2: ^{1}H NMR spectrum of desired coupled product **54.** 112

List of Abbreviations and Symbols

Å: Ångstroms

Ac: acetyl

acac: Acetylacetonate

APPI: Atmospheric pressure photo-ionization

Bn: Benzyl

BPin: Pinacolatoborane

COD: 1,5-Cyclooctadiene

Cp*: Cyclopentadiene

dba: Dibenzylideneacetone

DCE: 1,2-Dicholoroethane

DCM: Dichloromethane

DDQ: 2,3-Dicholoro-5,6-dicyano-1,4-benzoquinone

DME: Dimethoxyethane

DMF: Dimethylformamide

dppf: 1,1'-Bis(diphenylphosphino)ferrocene

EDG: Electron donating group

EI: Electrospray-ionization

Et: Ethyl

EWG: Electron withdrawing group

g: Gram

h: Hour

HRMS: High resolution mass spectrometry

hv: Light

Hz: Hertz

^{i}Bu : Isobutyl

^{i}Pr : Isopropyl

IR: Infrared

J: Coupling constant (Hz)

L: Litre

LDA: lithium diisopropylamide

Me: Methyl

mg: Milligram

min: Minute

mL: Millilitre

mmol: Millimole

MS: Mass spectrometry

n-Bu: Butyl

NMR: Nuclear magnetic resonance

Ph: Phenyl

PIDA: Phenyliodine(III)diacetate

R_f: Retention factor

rt: Room Temperature

TBS: *tert*-Butyldimethylsilyl

t-Bu: *tert*-Butyl

Tf: Triflyl

tfacac: Trifluoroacetylacetonate

TFP: Tri-2-furylphosphine

THF: Tetrahydrofuran

TIPS: Triisopropylsilyl

TLC: Thin-layer chromatography

TMP: 2,2,6,6-Tetremethylpiperidine

TOF: Time of flight

UV: Ultraviolet

XPhos: 2-Dicyclohexylphosphino-2',4',6'-triisopropylbiphenyl

δ: Chemical shift (ppm)

ν: wavenumber (cm^{-1})

Chapter 1: Synthesis of Fused Indole Frameworks via Tandem C-H Insertion/Michael-type Annulation

Statement of Co-Authorship

This chapter has been published under the title "Stereoselective Copper-Catalyzed Heteroarene C–H Functionalization/Michael-Type Annulation Cascade With α-Diazocarbonyls" in *Chem. Commun.,* **2021**, *57*, 10556-10559.

Authors: Aabid Bhat, Nathan Tucker, Dr. Jian-Bin Lin, Dr. Huck Grover

This article was a combined effort on the parts of graduate students Aabid Bhat and Nathan Tucker, under the supervision of Dr. Huck Grover.

Nathan Tucker (listed in this article as the 2nd author): contributed significantly to the synthetic work, physical data collection, and preparation of the manuscript and supporting information.

Aabid Bhat (listed in this article as the 1st author): contributed significantly to the synthetic work, physical data collection, and preparation of the manuscript and supporting information.

Dr. Jian-Bin Lin: Performed crystallographic structure determination to elucidate stereochemistry of several compound.

Dr. Huck Grover: Is the principal investigator of this work, who led the project and contributed to the interpretation/analysis of data and the writing of the manuscript.

The article has been reproduced in this Chapter in a modified form that includes the contributions of all the co-authors for the purpose of a complete discussion.

1.1: Introduction

1.1.1: *α*-Diazocarbonyl Compounds and Metal Carbenoids

The development of specialized reagents aimed at increasing the efficiency of bond forming reactions is of great importance to organic chemists.[1] Molecules that are easy to synthesize, straightforward to use, and demonstrate controlled reactivity are ideal for synthesis. One such class of reagents are *α*-diazocarbonyl compounds (**1**) . These reagents consist of a carbonyl group that is substituted at the *α*-carbon with a dinitrogen (diazo) moiety. Since the first reported synthesis of an *α*-diazocarbonyl by Curtius in 1883,[2] many different types of *α*-diazocarbonyl compounds have been developed.

These *α*-diazocarbonyl compounds (**1**) can be decomposed by reaction with a suitable transition metal to lose a molecule of N_2 and form a metal carbenoid as the reactive intermediate (**2**).[3] These metal carbenoids can undergo a myriad of synthetic transformations. Some of the most common include ylide formation,[4] cyclopropanation,[5] and bond insertion reactions,[6] among other reactions (Scheme 1.1).[7]

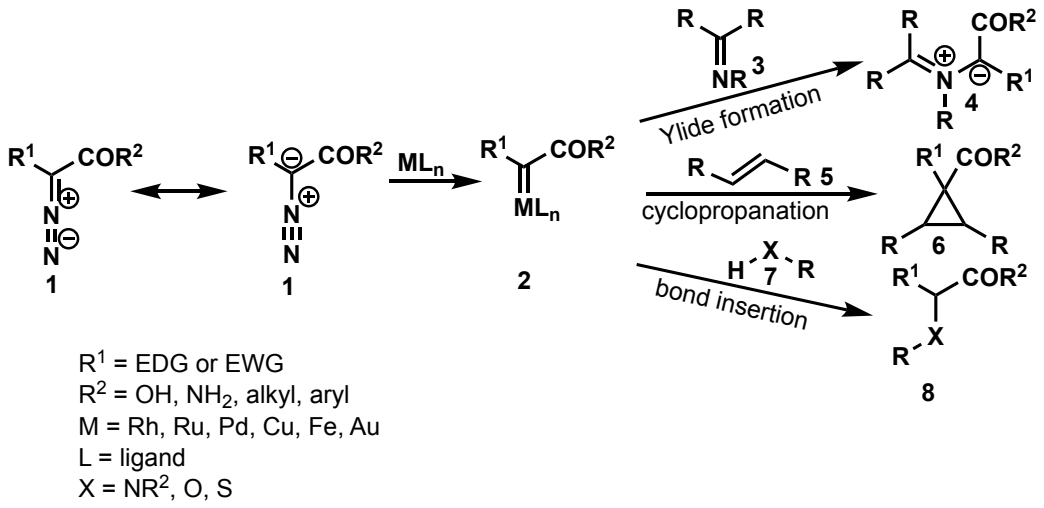

Scheme 1.1: Formation of metal carbenoids and common reactions using α-diazocarbonyl compounds.

In general, diazo reagents can be classified based on the number and type of substituents connected to the carbon containing the diazo moiety. For example, a diazo reagent that is substituted with one electron withdrawing group (EWG) is classified as an acceptor diazo reagent (**9**), whereas a diazo reagent containing an electron donating group (EDG) is classified as a donor diazo reagent (**13** Figure 1.1). Among these various classes of diazo reagents, **9**, **10**, and **11**, where the EWG is a carbonyl moiety, commonly referred to as *α*-diazocarbonyls, are the most common/explored classes of diazo reagents.

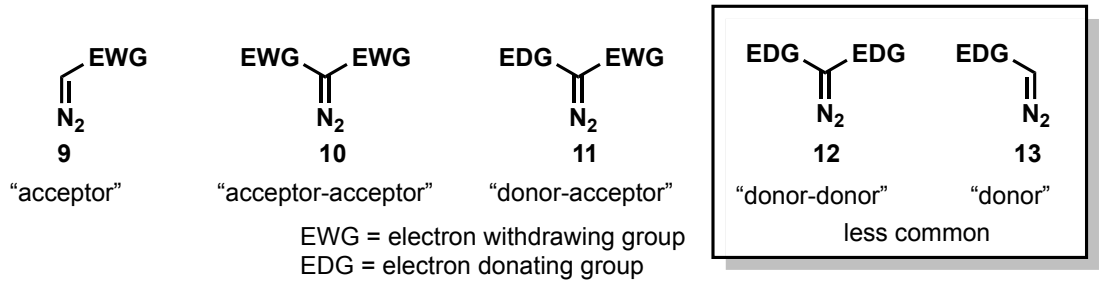

Figure 1.1: Classes of diazo reagents.

In addition to providing an easy method of classifying diazo reagents, the variation of functional groups appended to the diazo carbon are also known to have a marked influence on the reactivity and stability of carbene or carbenoid generated upon loss of dinitrogen.[8] For instance, several different types of reactions (e.g. intramolecular insertions) involving acceptor/acceptor diazo reagents have displayed faster reaction rates and improved yields when compared to the donor/acceptor or acceptor classes of diazo reagents.[9] Alternatively, in other types of transformations (e.g. intermolecular insertions) the donor/acceptor reagents have provided higher levels of chemoselectivity and yields.[10] In essence, the stability and reactivity of the carbene/carbenoid, generated from the diazo reagent, can be tuned for a specific transformation by varying the substituents at the diazo carbon (Scheme 1.2). However, this is not the only factor that influences the reactivity of the carbene. Another key factor that must be taken into account is the catalyst used to activate the diazo compound.[8] Different transition metals, as well as the ligands that make up said transition metal complexes, can have a nuanced effect on the reactivity of the resulting carbene. Further discussion on catalyst control will be reported in the next sections.

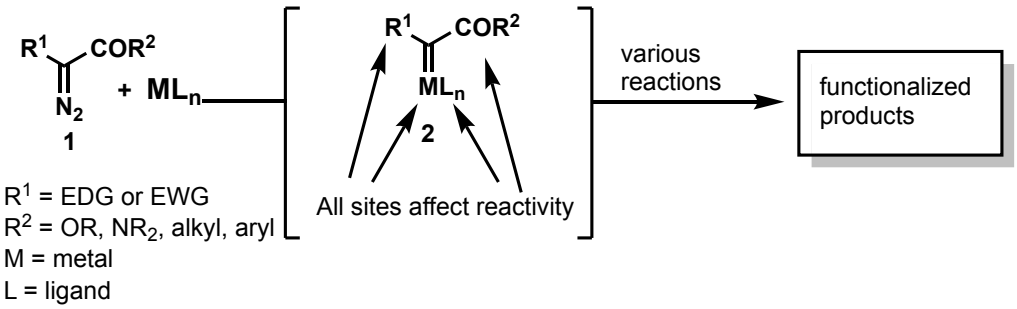

Scheme 1.2: Main factors that control reactivity of metal carbenoids.

1.1.2: Heteroatom–Hydrogen Insertion

Heteroatom–carbon bonds are one of the most prevalent types of chemical bonds, present in a wide array of organic molecules, including natural products,[11] drug molecules,[12] and polymers.[13] Thus, chemists are devoted to developing methods that construct these bonds, not only in the most efficient way possible, but using strategies that incorporate diverse functionality in the obtained products. To this end, *α*-diazocarbonyl compounds have emerged as a powerful reagents as a means to form desirable heteroatom–carbon bonds. With the aid of an appropriate catalyst, *α*-diazocarbonyl compounds can generate a reactive metal-carbenoid intermediate which can undergo formal heteroatom–H insertion; (termed X–H insertion where X is a heteroatom), by route of a protic onium ylide intermediate (Scheme 1.3).[14]

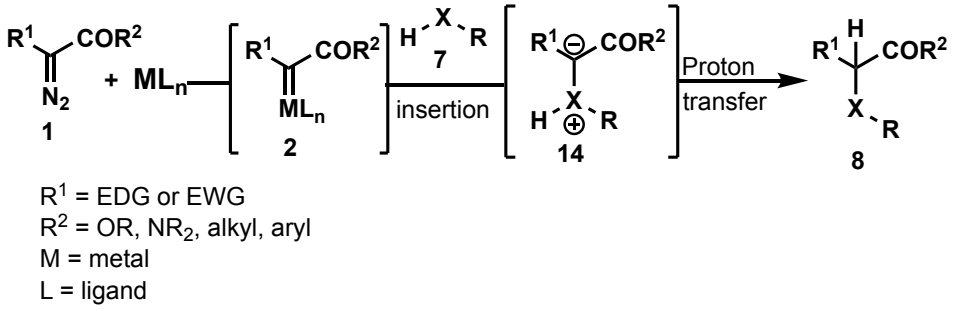

Scheme 1.3: General reaction profile of an X–H insertion reaction of α-diazocarbonyl compounds.

One of the first reported X–H bond insertion reactions of an *α*-diazocarbonyl compound was reported by Yates in 1952.[15] He demonstrated that when l-diazo-2-nonadecanone (**15**) was decomposed under the presence of copper in ethanol, the product that formed was not the expected ester ethyl nonadecanoate (**17**), but the keto-ether 1-ethoxy-2-nonadecanone (**16**) (Scheme 1.4). Yates was further able to demonstrate the

utility of diazo compound **15** by subjecting it to reaction with amines and thiols under the copper conditions to generate the corresponding keto-amines and thioethers respectively. This pioneering work by Yates sparked a large increase in research in the area of diazo compounds and their reactivity.

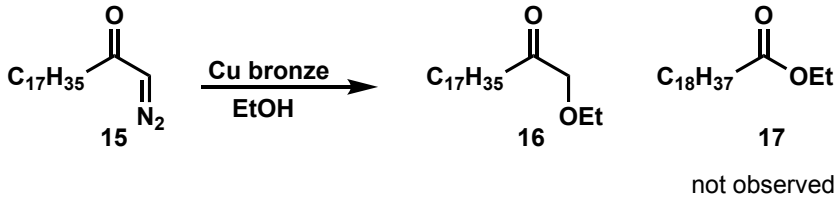

Scheme 1.4: Preliminary research on α-diazocarbonyl compounds by Yates.

Over the last few decades, the amount of reported heteroatom–hydrogen bond insertion reactions with *α*-diazocarbonyl compounds increased dramatically. The efforts in this area have provided a greater understanding behind the mechanism of these transformations, as well as the development of new catalysts that can promote these transformations. Noyori and Nozaki[16] were the first to propose that the reactive species is a metal carbenoid which enhances the reactivity and stability of the carbene generated from the decomposition of the diazo functional group. Since this proposal by Noyori and Nozaki it has been shown that the generation of the reactive metal carbenoid species is not limited to copper catalysts, but can be produced by many transition metal catalysts.[17] Among the metals that are known to decompose diazo compounds, rhodium was one of the first catalysts to be reported. Rhodium was first demonstrated by Teyssié to decompose ethyl diazoacetate (**18**)[18] to generate a rhodium carbenoid, which efficiently underwent insertion into O–H bonds of various alcohols in excellent overall yields (Scheme 1.5). Teyssié also reported the success of these reaction conditions to insert into N–H and S–H bonds.[19]

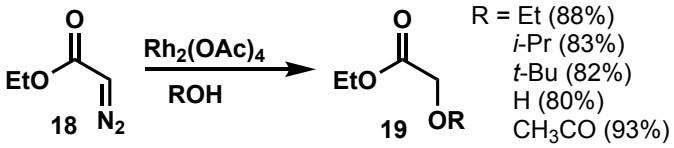

Scheme 1.5: Efficient rhodium catalyzed O–H insertion reactions by Teyssié.

Sparked by this initial report by Teyssié, many researchers chose to focus on rhodium for use in diazo insertion chemistry. Several reports emerged of not only rhodium catalyzed insertion of α-diazocarbonyls into O–H bonds[20,21] but also N–H bonds.[22,23] This cemented rhodium as the catalyst of choice for almost all types of diazo insertion reactions for many years. However, yield is not the only factor that one must take into account when conducting a transformation of this type. Stereoselectivity is of the utmost importance in many synthetic transformations, and diazo insertion reactions are no exception. Much work on diazo insertion chemistry over the last few decades has been focused on the development of alternate or improved catalysis, with a focus on stereoselective transformations and applications of this bond-forming strategy in total synthesis.[24–33]

1.1.3: Heteroatom–Hydrogen Insertion and Tandem Electrophile Trapping

Generating complex functionality in one step is very synthetically useful for any chemist. One way to achieve complex functionality is made available through exploiting the dual reactivity of α-diazocarbonyl compounds. For example, if the proton transfer from the ylide (**3**) that is generated from the nucleophilic addition of a heteroatom to a metal carbenoid is delayed, the ylide could be intercepted by an electrophile (Scheme 1.6). Following a final proton transfer, **21** would be produced, in a net process in which two new

sigma bonds, to non-hydrogen atoms, are formed to the diazo carbon in a single step in a tandem bond-forming fashion.

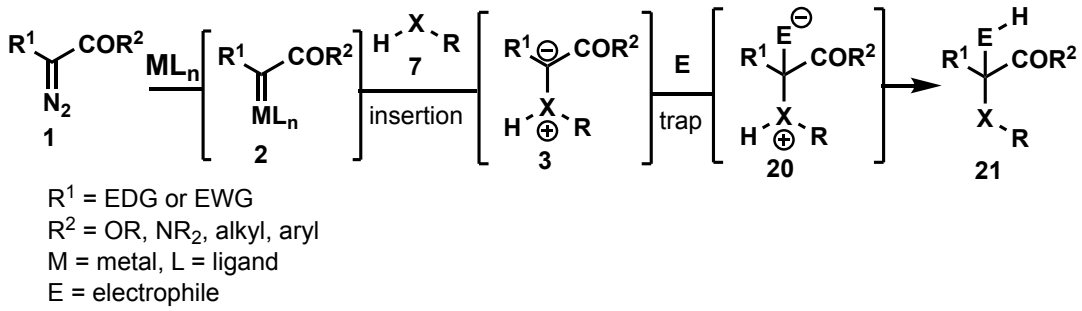

Scheme 1.6: General reaction process of tandem insertion/electrophilic trapping.

The nucleophilic attack of an enolate/enol to an electrophilic carbonyl is one of the most common bond-forming reactions in organic chemistry, encompassing common examples including the aldol and Claisen reactions. As such, one of the most explored electrophilic species that has been used in these tandem couplings are carbonyls. Leveraging the electrophilicity of the carbonyl functional group to be attacked by a nucleophilic enolate generated by a carbene insertion can give way to some interesting and complex products. For example, Hu and colleagues published a tandem three component coupling between donor/acceptor diazo **22**, benzyl alcohol **23**, and *p*–nitro benzaldehyde **24** under rhodium catalysis (Scheme 1.7). Mechanistically, this reaction is proposed to proceed via an O–H insertion into the alcohol **23**, which forms a protic oxonium ylide that can undergo nucleophilic attack on aldehyde **24** (Scheme 1.7).[34] This is a wonderful example of a tandem diazo reaction which forms two chiral centers in one pot, while providing a product with multiple functional groups available for further reactions.

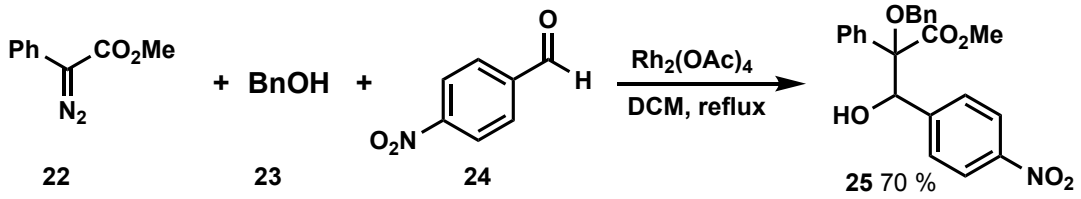

Scheme 1.7: Aldol-type trapping of diazo O–H insertion intermediates by Hu.

Over the last several decades, there has been much advancement in multicomponent reactions via trapping of protic onium ylides, generated from diazo reagents, with electrophiles.[35] Researchers in this area have successfully explored various heteroatom nucleophiles (S, O, N), electrophiles (e.g. imines, ketones, alkynes, Michael-acceptors),[36–39] and catalyst systems for both racemic and asymmetric transformations. Of these classes of electrophiles, pi systems such as alkynes and *α,β*-unsaturated carbonyls have seen the most use.[40–49] Their synthetic utility is highlighted in this example by Xu. Here the *α*-diazocarbonyl **22** does an O–H insertion into the alcohol **26**, which has a tethered *α,β*-unsaturated ketone that is susceptible to nucleophilic attack via a Michael addition, resulting in the formation of benzopyran **27** (Scheme 1.8).[40]

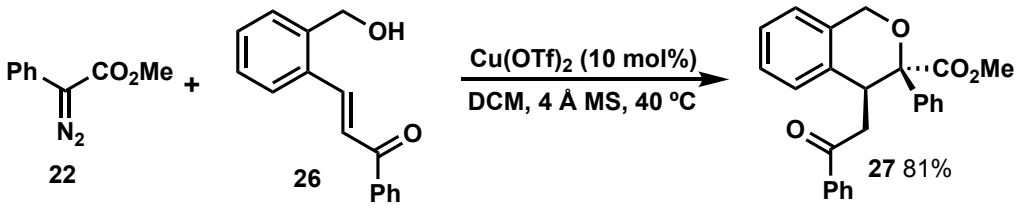

Scheme 1.8: Tandem O–H insertion/Michael addition by Xu.

While this tandem insertion/trapping strategy is well studied when the insertion step occurs on a heteroatom, the same cannot be said for C–H insertion reactions. Applying

these types of transformations to C–H insertions has seen less use, due to the challenges associated with C–H insertion reactions. Overcoming this challenge and invoking these types of transformations via C–H insertion is a rapidly developing field.

1.1.4: Formal Carbon–Hydrogen Insertion with *α*-Diazocarbonyl Compounds

While the direct insertion of diazo compounds into C–H bonds is well known, it suffers from a lack of selectivity in the insertion process when compared to X–H insertion reactions.[50–52] Over the past 70 years, there have been several established strategies developed to overcome selectivity issues associated with C–H insertion chemistry.[8] One strategy relies on metal catalyzed C–H activation, where the metal itself activates the C–H bond in question to generate organometallic intermediate **29**, which can then react with a diazo compound to generate a metal carbene (**30**), which finally undergoes a migratory insertion to give a formal C–H insertion product **31** after protonation (Scheme 1.9 A). Another method that is relevant to the research described in the following section of this thesis is the electrophilic addition to a metal carbene with a nucleophilic double bond (most commonly an arene) to give a zwitterionic intermediate **33** (Scheme 1.9 B). In a similar process to X–H insertion reactions, this intermediate can then undergo a proton transfer to reinstall the double bond and deliver the formal insertion product **31**.

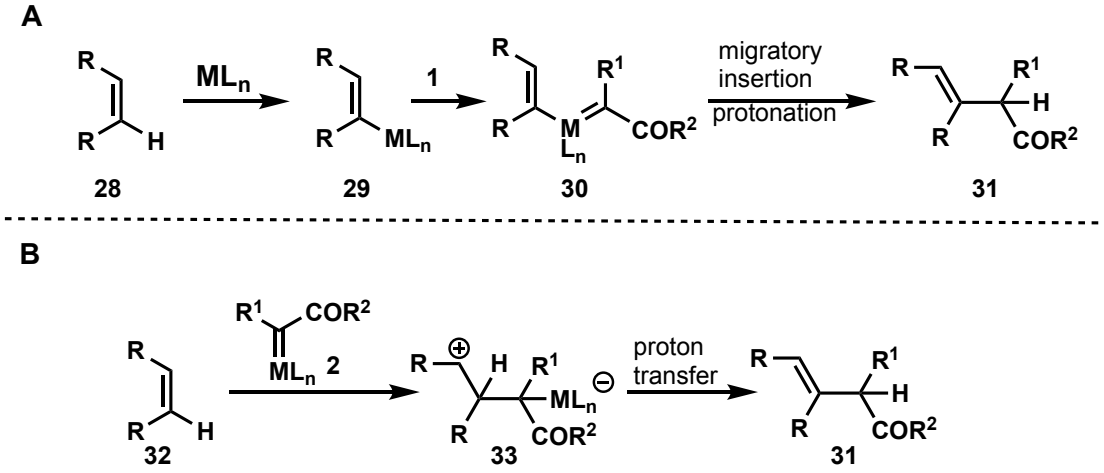

Scheme 1.9 A: Formal C–H insertion via metal catalyzed C–H activation. B: Formal C–H insertion via electrophilic addition of a metal carbene.

Among the myriad of nucleophilic arene coupling partners that have been shown to be compatible with diazo regents in this type of formal C–H insertion method, none are more important to this thesis work than the example illustrated by Kerr and coworkers in 2010. In this example by Kerr, skatole **35** acts as a suitable nucleophile to react with a copper carbenoid derived from α-diazocarbonyl **34** to give insertion product **36** (Scheme 1.10).[53] Of notable importance in this work is the site selectivity of the formal C–H insertion, occurring exclusively at the C2 position of the indole ring and the use of a cheap copper catalyst to generate the reactive carbene intermediate.

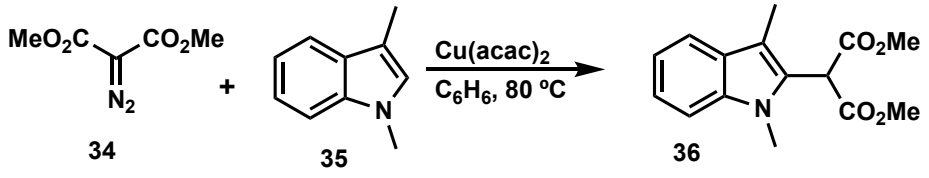

Scheme 1.10: Metal carbene insertion into indole by Kerr.

Although the work by Kerr is certainly not the first example of this type of formal C–H insertion reaction, it does highlight the simplicity and selectivity that can be achieved by using diazo compounds to generate new C–C bonds. Over the last two decades, there have been significant advancements in this area of C–H insertion reactions, including catalyst development, enantioselective transformations, as well as studies on a wide array of coupling partners.[54–58] Due to the robust nature of this reaction, it has also been attracting attention for use in insertion/annulation chemistry.

1.1.5: Formal Carbon–Hydrogen Insertion/Annulation Reactions

The challenge associated with utilizing C–H insertion chemistry in combination with annulation strategies has been the lack of selectivity in the insertion step. However, with the development of selective C–H insertion strategies similar to the previous example by Kerr, many chemists are starting to develop this tandem bond forming approach for the synthesis of carbocyclic rings. One of the pioneering examples of this transformation was reported by Zhang and coworkers. They subjected α-diazocarbonyl **37**, which contains an electrophilic alkyne, to insertion with anisole **38** followed by subsequent annulation with the tethered alkyne to form indene **39** (Scheme 1.11).[59]

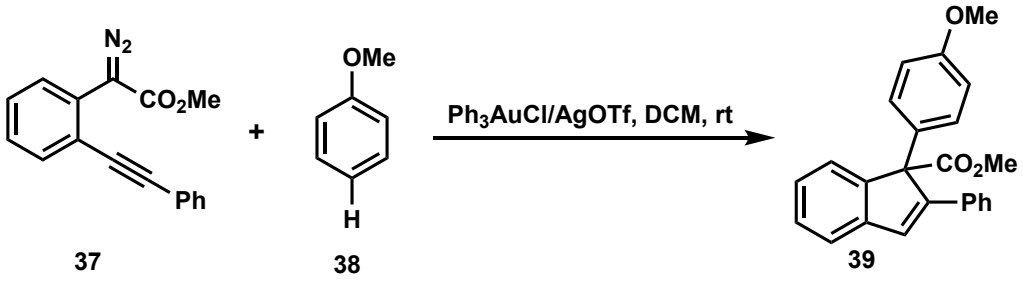

Scheme 1.11: Gold-catalyzed insertion/annulation by Zhang.

The scope of electrophiles in this tandem bond forming sequence is not limited to alkynes. Just like the tandem X–H insertion/annulation strategies, many different types of electrophiles can be used.[60–63] For example, in the report from Xu et al., donor acceptor diazo **22** does a formal C–H insertion into indole **40**, and then undergoes a concerted annulation with the *α,β*-unsaturated ester moiety to give a highly functionalized fused indole **41** (Scheme 1.12).[61]

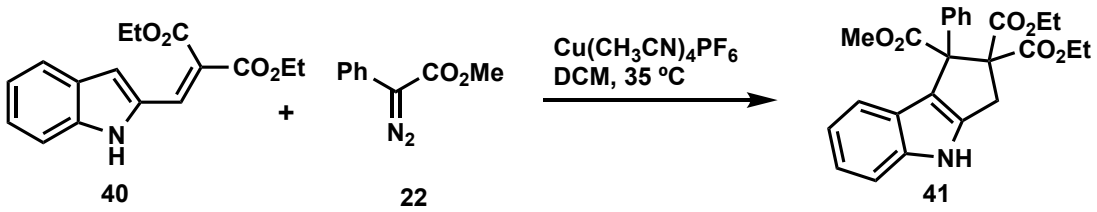

Scheme 1.12: Copper-catalyzed insertion/annulation by Xu.

Inspired by literature precedent, our group has previously reported a tandem insertion/cyclization process to furnish pyrroloindoles. (Scheme 1.13).[64] In this work, **42** is reacted with *N*–propargylskatole **43** under rhodium catalysis to promote a C–H insertion event. Following insertion, a zinc enolate forms, which can be trapped by a terminal alkyne via a Conia-ene type cyclization to yield ring systems with an *exo*–methylene group. Given that this transformation is very synthetically useful for accessing pyrroloindole systems, further development was undertaken to improve upon it.

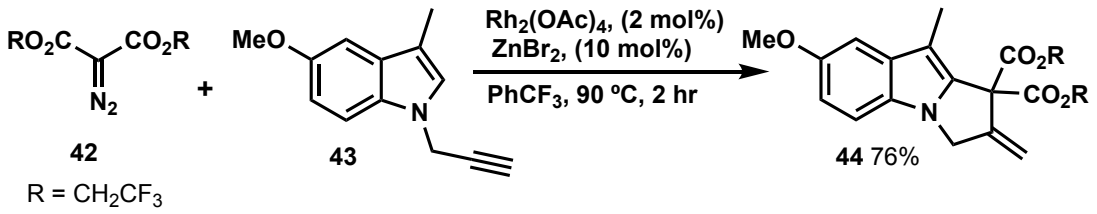

Scheme 1.13: Tandem C–H insertion/Conia-ene cyclization by Grover.

1.1.6: Thesis Project Objectives

While the tandem C–H insertion/Conia-ene transformation described in Scheme 1.13 is indeed useful and can lead to some highly functionalized ring systems, there are some drawbacks that need to be addressed. First, this reaction, like many others, requires a dual catalyst system; one to generate the metal carbenoid and promote the C–H insertion and the other to promote the annulation. It was envisioned that efficiency of this transformation could be improved if a single catalyst could be identified to promote both steps of the tandem reaction. A second issue was that the electrophile in the preliminary project was limited to terminal alkynes. Subjecting internal alkynes to the dual catalyst reaction conditions led to products that had only undergone the C–H insertion step and not the Conia-ene cyclization. Finally, the only classes of α-diazocarbonyls that were successful in this transformation were acceptor/acceptor, with the more electron withdrawing trifluoroethyl esters being the best yielding. Attempts at using donor/acceptor diazo reagents were unsuccessful.

To address these issues, the focus of my honors project (September 2019-May 2020) was twofold. The first objective was to develop a single catalyst system that could accomplish both insertion and cyclization by exploring a different type of electrophile. The

second objective was to prepare a library of indole substrates containing the new electrophile to explore the scope and limitations of the new single catalyst system. After much work, objective one was realized by changing the electrophile from a terminal alkyne to a Michael-type acceptor (**45** Scheme 1.14). Throughout the duration of my honors the reaction between **45** and **46** was optimized and the ideal reaction conditions for this transformation were found to be copper trifluoroacetylacetonate in benzene at 80 ºC (Scheme 1.14). In addition, a number of differently substituted α-diazocarbonyls and tethered indole alkynes were synthesized. Thus, the primary objective of this chapter of my thesis was to explore the compatibility of the optimized reaction conditions with various starting materials. The results of the substrate scope are described in the next section.

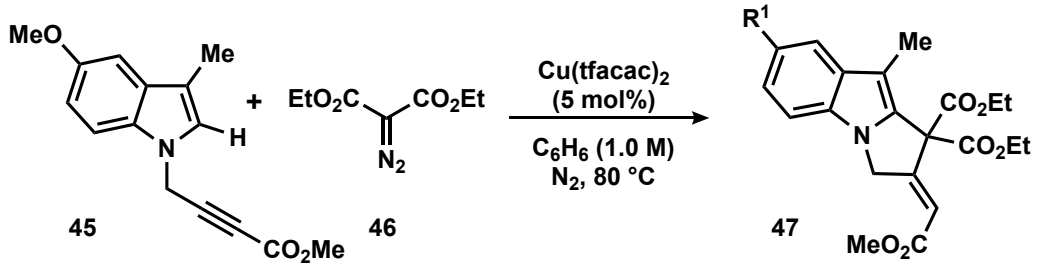

Scheme 1.14: Copper-catalyzed C-H insertion/Michael-type cyclization.

1.2: Results and Discussion

It is believed that the copper serves two purposes in the mechanism of this reaction (Scheme 1.15). First, copper can activate the α-diazocarbonyl **46** to form a copper carbenoid reactive intermediate **A**, which can undergo a formal C–H insertion with skatole **45** to form copper complex **B**. The copper-bound enolate can then activate the alkyne electrophile (**C**), to invoke a *5-exo-dig* cyclization in a *syn*-addition fashion to give cyclized

intermediate **D**. It is hypothesized that this dual activation set by the catalyst where the copper activates both the nucleophile and the electrophile (enolate and Michael acceptor) is the root of the observed stereoselectivity.[65] Finally, protodemetalation of **D** generates the *Z*-alkene isomer **47** and regenerates the active catalytic species. After establishing optimal conditions and a reasonable mechanism, it was then decided to see what variations on the starting material structure could affect the yield and selectivity of this transformation.

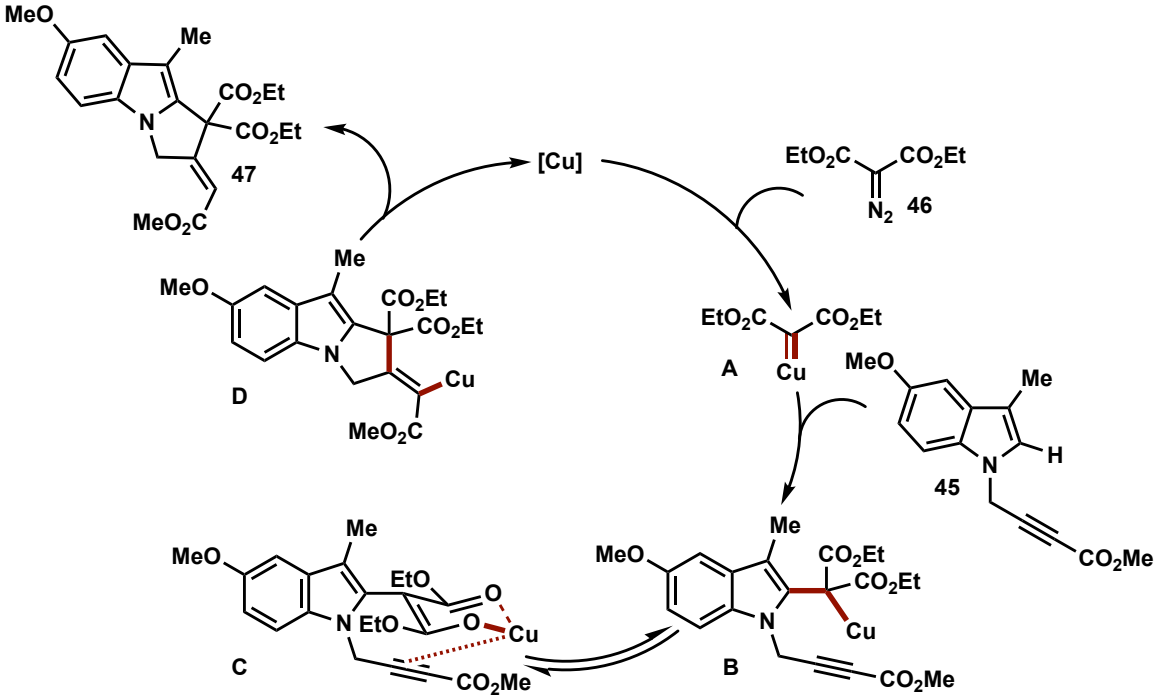

Scheme 1.15: Proposed mechanism of the insertion/annulation process.

The first variation in starting material structure that was explored was substitution on the benzenoid ring of the indole (**45** vs **48**, Scheme 1.16). As was expected based on our previous report,[64] when there is no substitution on the benzenoid ring of the indole substrate, **53** (R1 = H), a slight decrease in yield in comparison to the optimized substrate, **47** (R1 = OMe) is observed. Presumably, this decrease in yield is due to lack of regioselectivity during the C–H insertion event leading to undesired benzenoid

functionalized products. To this end, the project was continued with indole starting materials containing a C5-OMe group to help maximize the selectivity of the desired tandem reaction. This material was chosen because it is cheap, commercially available and in previous works was determined to be a high yielding substrate when compared to other C5 and C6 substituted skatoles.

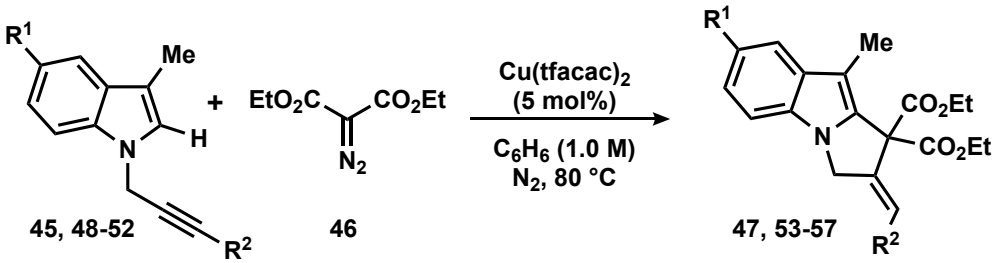

47: R^1 = OMe R^2 = CO_2Me, 78%

53: R^1 = H R^2 = CO_2Me, 69%

54: R^1 = OMe R^2 = CO_2Et, 78%

55: R^1 = OMe R^2 = CO_2Ph, 78%

56: R^1 = OMe R^2 = CO_2Bn, 73%

57: R^1 = OMe R^2 = $CO_2{}^i$Bu, 81%

Scheme 1.16: Effects of ester group on the yield of the insertion/annulation process.

Next, we evaluated the efficiency of the reaction conditions when the substituent attached to the alkyne (R^2, Scheme 1.16) were varied. Substrates containing a number of different ester groups **49-52** were subjected to the optimized reaction conditions. Notably varying the ester group with different alky and aryl groups **54-57** had no significant effect on the yield (yields 73-81%), and in all cases the *Z*-stereoisomer was formed with complete selectivity.

Although all ester substituents performed well under the current reaction conditions, to date, it appears that the carbonyl substitution at this position (R^2) is limited

to esters. As noted in previous work (Honours thesis), the use of ketones at this position instead of esters led to complex intractable mixtures of products. As further proof of the importance of the electron withdrawing ester group in the current transformation, indole **58**, containing a methyl substituent on the alkyne, was subjected to the optimized reaction conditions (Scheme 1.17). As expected only the insertion product **59** was obtained from this reaction, and no cyclization was observed, even with prolonged heating. This result indicates the importance of the electronic nature of the electrophile in this transformation.

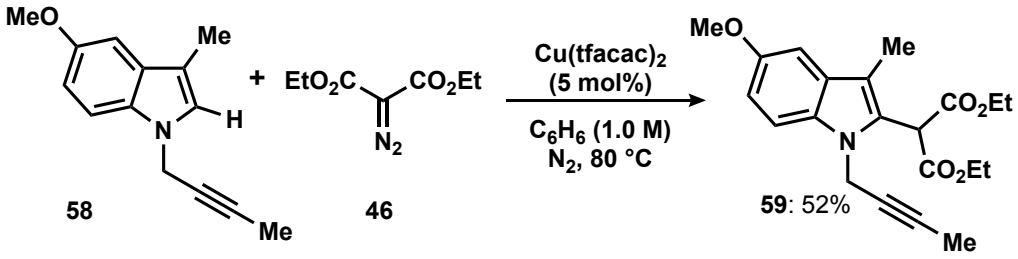

Scheme 1.17: Effect of alkyne substitution on the insertion/annulation process.

It was also found that the length and position of the tethered alkyne could be varied to provide several other unique tricyclic indole-fused structures (Scheme 1.18). When the carbon chain length between the indole nitrogen and the alkyne of the starting material was extended by one carbon, pyridoindole **61** could be obtained in 68% yield (Scheme 1.18A). However, attempts to generate larger ring systems by further extending any chain length between the indole nitrogen and the alkyne resulted solely in the formation of the insertion product. This is presumably due to the increased distance between the nucleophile (enolate from C–H insertion) and the electrophile (Michael acceptor), which may prevent copper from properly coordinating both moieties to promote the annulation.

Further experiments exploring the compatibility of our reaction conditions with varying locations of the electrophilic alkyne unit also proved effective. When the alkyne was tethered from the C2 or C3 position of the indole, tetrahydrocarbazole products **63** and **65** were obtained in good overall yields (Scheme 1.18 B). Tetrahydrocarbazoles are a common tricyclic motif that is present in a number of different natural products,[67] meaning a new synthetic method to easily access them is an important development. The slightly increased yield of **63** is due to the fact that indole is more nucleophilic through the C3 position.[68] It is worth noting that in all the aforementioned reactions, the products are obtained solely as the single alkene isomer. These results stand to illustrate the high level of stereocontrol associated with this transformation.

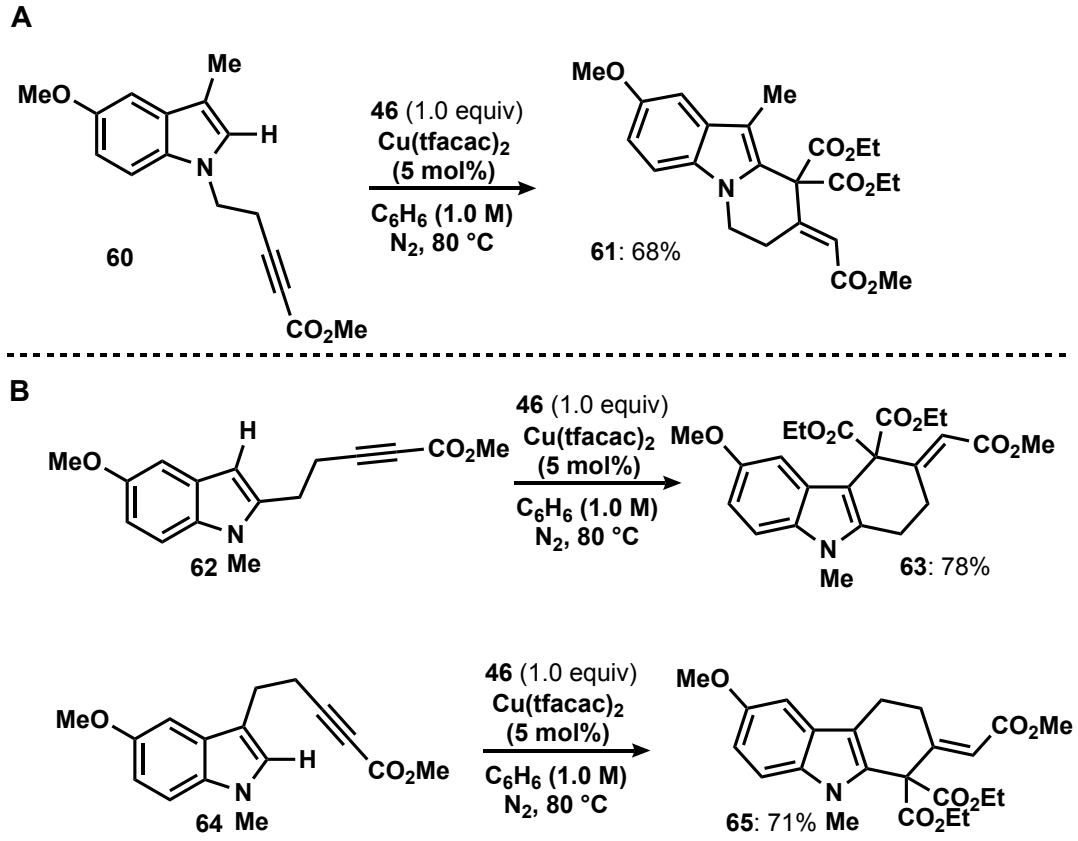

Scheme 1.18: A: Varying the length of the tethered electrophile. B: Varying the location of the tethered electrophile.

Having established the validity of the copper catalyzed reaction conditions with diazo-diester **46** and various indole substrates, the compatibility of our reaction conditions with other α-diazocarbonyl compounds was explored. It was found that these reaction conditions were applicable with a number of differently substituted α-diazocarbonyls, both of the acceptor/acceptor and donor/acceptor classes. When subjected to the reaction conditions with indole **45**, acceptor/acceptor diazo compounds **66** and **67** undergo the desired transformation with the same stereoselectivity as previous examples (Scheme 1.19). However, there is a significant decrease in yield when diazo **67**, derived from methyl

acetoacetate is utilized. This is theorized to be a result of the thermal instability of **67**, due to the fact that pyrroloindole **69** is isolated along with a complex mixture of compounds that seemingly incorporated the diazo component but not the indole component.

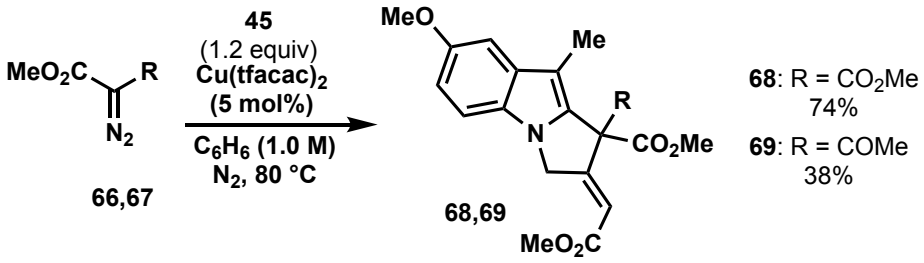

Scheme 1.19: Effect of different acceptor/acceptor diazo groups.

Moving to the donor/acceptor diazo compounds, delightfully, this class of reagent did undergo the desired tandem transformation under the copper catalyzed conditions (Scheme 1.20). However, in contrast to the acceptor/acceptor diazo reagents a sharp decrease in the selectivity of the annulation step was observed. In fact, all pyrroloindole products **74-77** obtained from these experiments were isolated as separable mixtures of olefin isomers. The isomers were assigned by the differences in chemical shift between H_a and H_b (Scheme 1.20). In the *E*-isomers, the chemical shift of proton H_a is found approximately 0.3 ppm downfield compared to the *Z*-isomer, and the chemical shift of H_b (observed as a multiplet for 2 protons) is found approximately 0.4 ppm upfield compared to the *Z*-isomer (see Appendix for further details).

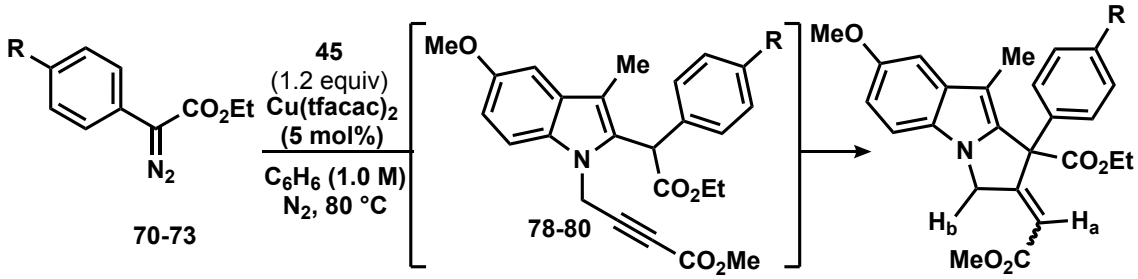

74: R = H, 24%, 5:1 (*Z*:*E*)
(+ **78**: 32%)

75: R = OMe, 34%, 3.3:1.0 (*Z*:*E*)
(+ **79**: 32%)

76: R = Br, 45%, 2.5:1.0 (*Z*:*E*)
(+ **80**: 18%)

77: R = NO_2, 65%, 1.5:1.0 (*Z*:*E*)

Scheme 1.20: Effect of different donor/acceptor diazo groups.

In each of the above reactions with donor/acceptor diazo reagents, the *Z*-isomer was isolated as the major product, however, the reason for the decrease in selectivity is still unclear. It is postulated that the *E*-isomer can arise from a mono-activation pathway in the annulation step, where the role of the copper catalyst in this step is only to activate the alkyne electrophile leading to a *5-exo-dig* cyclization in an *anti*-addition fashion (Scheme 1.21).[66] Alternatively, the *Z*-isomer could come from the double activation pathway described previously for the acceptor/acceptor diazo reagents. The variation in activation pathways is presumably due to the fact that there are no longer two carbonyl groups on the diazo reagent, and thus there is less catalyst coordination for the donor/acceptor diazo compounds.

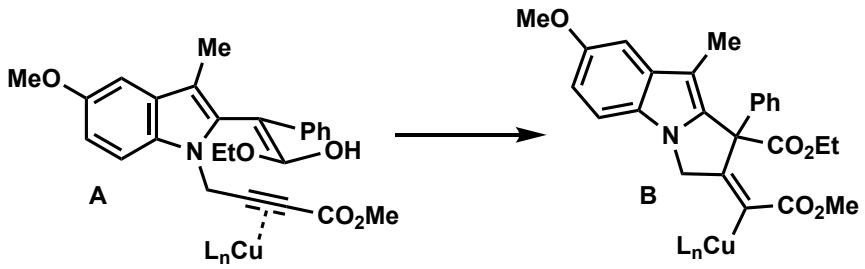

Scheme 1.21: Mono-activation pathway leading to E-isomer.

In addition to the isolation of a mixtures of stereoisomers in the experiments conducted with donor/acceptor diazo reagents, there was also a significant amount of non-cyclized materials (insertion products **78**, **79**, and **80**) isolated as well. In contrast, the insertion product was never observed when acceptor/acceptor reagents were utilized, a difference that could potentially indicate the importance of enolization in the annulation step. In fact, the only donor/acceptor diazo reagent that underwent insertion and complete cyclization to the pyrroloindole isomer products (**77**), was diazo **73** (Scheme 1.20). This is presumably due to the electron withdrawing nature of the aryl-NO_2 group, providing stability to the enolate which is essential to promote the annulation. Overall, the combined yields of the insertion and annulation products were still moderate, however the incomplete conversion exhibited by the donor/acceptor diazo reagents was an undesirable result that needed to be amended.

To tackle this issue, it was envisioned that a base could be added into the reaction after the C–H insertion step was complete to hopefully increase enolization and ensure complete conversion to the pyrroloindole framework. To test this hypothesis, the crude reaction mixture consisting of insertion product **78** and annulation products **74** was

subjected to Cs_2CO_3, due to its compatible solubility in the reaction solvent. Fortunately, the basic conditions funneled all three products from the crude reaction mixture to a single product **81**, which intriguingly had undergone a double bond isomerization (Scheme 1.22). The structure was confirmed by X-ray crystallography (see Appendix for details). In a related experiment, pyrroloindole **47** was subjected to reaction with Cs_2CO_3 and converted to product **82** quantitatively. While this does not rule out the initial formation of an allene followed by cyclization, this result indicates isomerization occurs after the annulation.

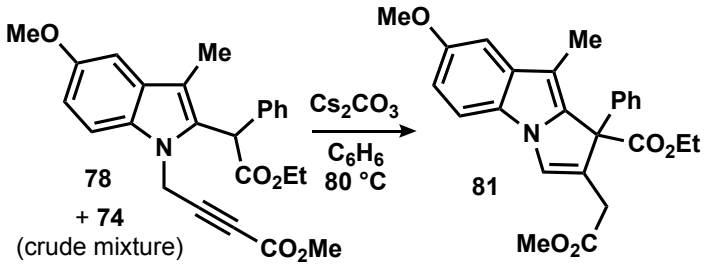

Scheme 1.22: Base-mediated conversion of crude reaction mixtures to olefin isomerized product.

Encouraged by this positive result, it was then theorized that a base could simply be added to the reaction and convert the mixture of products to this single olefin isomerized product in one-pot. Pleasingly, this transformation was able to be accomplished with several different starting materials. For example, when diazo reagents **70** and **46** were subjected to the standard copper catalyzed reaction conditions with indole **45**, followed by addition of Cs_2CO_3, the olefin isomerized products **81** and **82** were obtained in 63% and 57% yields respectively (Scheme 1.23).

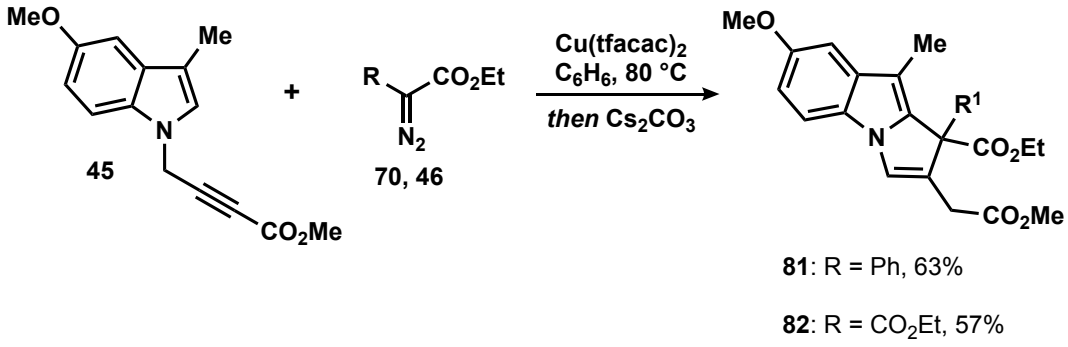

Scheme 1.23: Base-promoted cyclization/olefin isomerization process.

Utilizing these one-pot telescoped reaction conditions also proved successful on substrates that had previously been challenging to convert under copper catalyzed conditions alone. When indoles **83** and **84**, which contain aromatic substituted alkynes, were subjected to these reaction conditions with diazo **46**, pyrroloindole products **85** and **86**, which have notably not undergone an olefin isomerization, were isolated in modest overall yields (Scheme 1.24). It is important to note that previously, without addition of Cs_2CO_3, these two substrates **83** and **84** only yielded primarily insertion products, with only trace amounts of annulation products **85** and **86**. This is presumably due to the weakly electron withdrawing nature of the substituted benzene ring, which results in the alkyne being a weaker electrophile than when substituted with an ester, hence explaining why the base was needed to overcome the challenge of annulation.

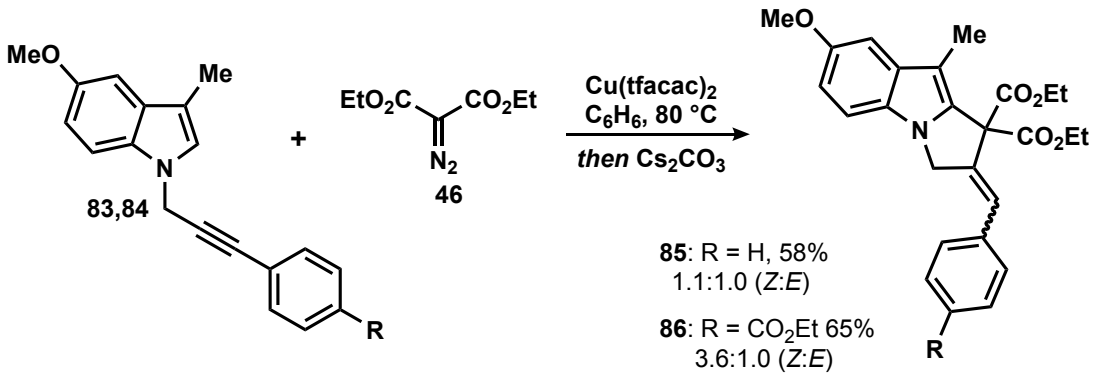

Scheme 1.24: Base-promoted cyclization on substrates that did not undergo olefin isomerization.

Finally, it was proposed that if substituted alkynes are able to act as electrophiles for this reaction, then so should alternate forms of *α,β*-unsaturated carbonyls. Initial attempts to subject indole **87** to the optimized reaction conditions without the addition of base ($Cu(tfacac)_2$, benzene, 80 °C) resulted in only isolation of the insertion product. However, when the same substrate was treated with the new combined copper/cesium conditions, pyrroloindole **88** was isolated in moderate yield (Scheme 1.25A). Gratifyingly, these copper/cesium conditions were also amendable to the synthesis of tetrahydrocarbazoles **91** and **92** from substituted indoles **89** and **90** (Scheme 1.25B).

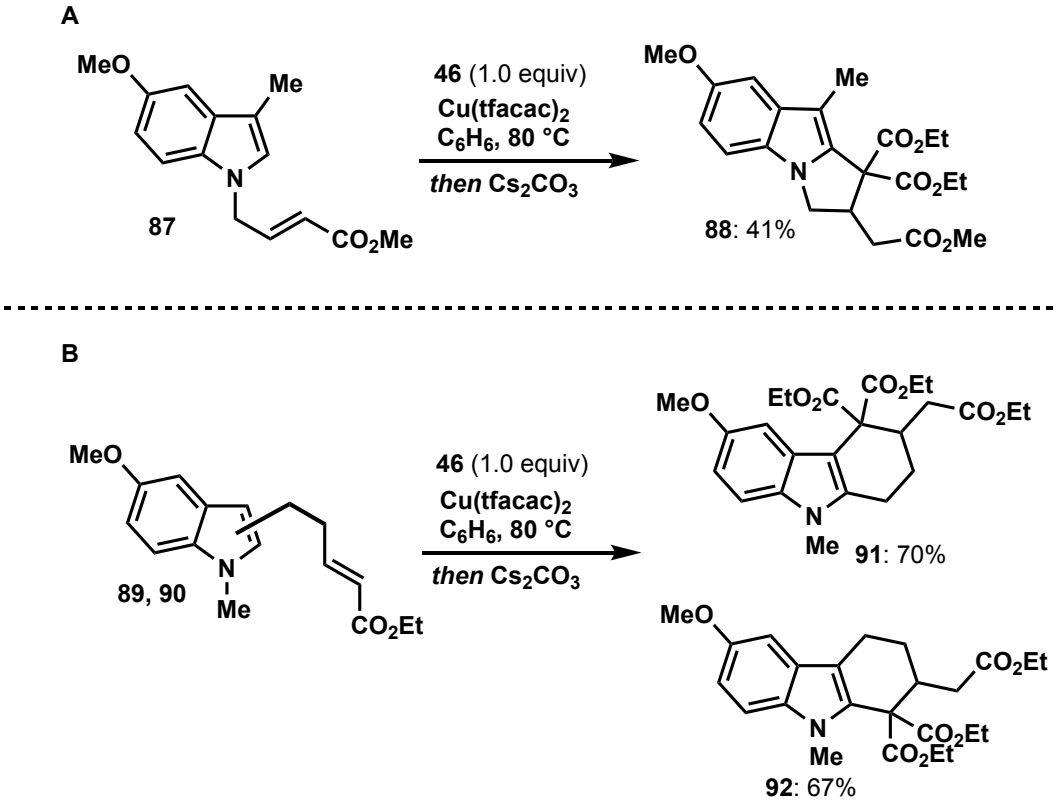

Scheme 1.25: Base-promoted annulation using traditional Michael acceptors.

In conclusion, a number of different pyrroloindole, pyridoindole, and tetrahydrocarbazole substrates have been synthesized through a tandem C–H functionalization/Michael-type annulation. Highlights of this methodology include a single inexpensive catalyst system, moderate to high yields, and satisfactory stereoselectivity. Further synthetic value was accomplished using a one-pot insertion/base-promoted annulation sequence to enable the use of less conventional electrophiles.

1.3 Experimental

1.3.1: General procedures

Unless otherwise stated, all reactions were performed in flame-dried glassware under a nitrogen atmosphere. Dry solvents were obtained from Sigma Aldrich SureSeal™ bottles or by passing these solvents through activated alumina columns. Unless stated elsewhere, chemicals were purchased from commercial suppliers and used directly as received. Reactions were monitored by thin layer chromatography (TLC) on Silicycle Siliaplate™ glass backed TLC plates (250 μm thickness, 60 Å porosity, F-254 indicator) and visualized by UV irradiation or development with anisaldehyde stain. Volatile solvents were removed under reduced pressure using a rotary evaporator. All column chromatography was performed using Silicycle SiliaFlash® F60, 230-400 mesh silica gel (40-63 μm). ^{1}H and ^{13}C NMR spectra were measured on a Bruker Avance III 300 MHz multinuclear spectrometer or a Bruker AVANCE 500 MHz spectrometer, using $CDCl_3$ as solvent. Except when noted otherwise, chemical shifts are reported relative to the residual solvent signal (^{1}H NMR = 7.26 ($CHCl_3$); ^{13}C NMR = 77.16 ($CDCl_3$)). Coupling constants (*J*) are given in Hz. NMR data is reported as follows: chemical shift (multiplicity, coupling constant, number of hydrogens). Splitting is reported with the following symbols: s = singlet, bs = broad singlet, d = doublet, t = triplet, dd = doublet of doublets, q = quartet, m = multiplet. Infrared (IR) spectra were recorded using neat samples on a Bruker Alpha spectrometer. High resolution mass spectrometry (HRMS) data were obtained using an Agilent 6200 series instrument, employing a TOF mass analyzer. Melting points (**MP**)

were obtained on an OptiMelt instrument (a digital apparatus) produced by Stanford Research Systems by scanning temperature ranges from 40 - 150 °C at a rate of 3 °C/min.

1.3.2: Synthetic procedures

General Synthetic Procedure A:

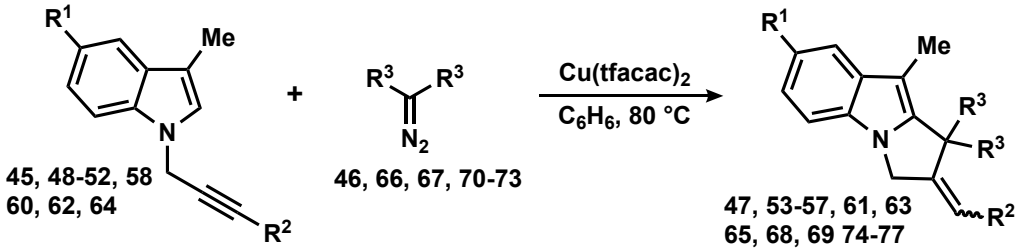

The indole starting material (**45**, **48-52**, **58**, **60**, **62**, **64** 1.2 equiv) was added to a reaction vessel equipped with a stir bar, and the vessel was then evacuated and backfilled with N_2. This cycle was repeated two times, followed by the addition of benzene (5 mL/mmol of indole) under an N_2 atmosphere. $Cu(tfacac)_2$ (5 mol %) was then added to the reaction vessel, and again the vessel was evacuated (quickly) and backfilled with N_2. Diazo reagent (**46**, **66**, **67**, **70-73** 1.0 equiv) was added to a separate reaction vessel, and the vessel was then evacuated and backfilled with N_2. This cycle was repeated two times. The diazo reagent was then dissolved in benzene (3 mL/mmol of diazo) under an N_2 atmosphere and transferred dropwise by syringe to the solution of indole starting material. Two sequential rinses and transfers using small quantities of benzene were then conducted to ensure complete transfer of the diazo reagent. The reaction mixture was then heated to 80 °C and stirred at this temperature for 12 h. The reaction progress was monitored by TLC analysis and considered complete upon consumption of diazo reagent. Upon completion, the reaction mixture was concentrated *in vacuo* and purified by silica gel flash column

chromatography (hexanes/EtOAc gradient) to yield annulation products **47, 53-57, 61, 63, 65, 68, 69 74-77,** and insertion products **59, 78-80.**

General Synthetic Procedure B:

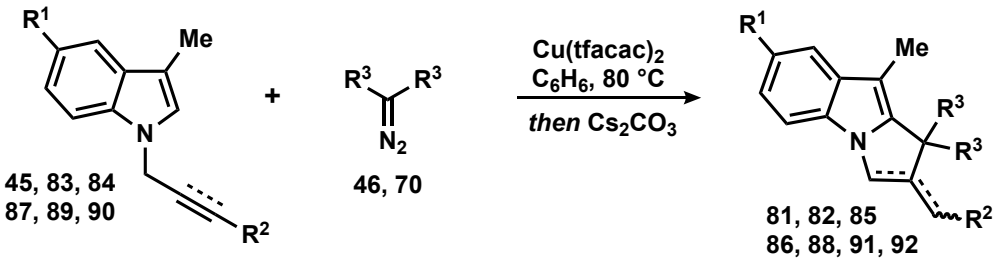

Indole starting material (**45 83, 84, 87, 89, 90**, 1.2 equiv) was added to a reaction vessel equipped with a stir bar, and the vessel was then evacuated and backfilled with N_2. This cycle was repeated two times, followed by the addition of benzene (5 mL/mmol of indole) under an N_2 atmosphere. $Cu(tfacac)_2$ (5 mol %) was then added to the reaction vessel, and again, the vessel was evacuated (quickly) and backfilled with N_2. Diazo reagent (**46, 70**, 1.0 equiv) was added to a separate reaction vessel, and the vessel was then evacuated and backfilled with N_2. This cycle was repeated two times. The diazo reagent was then dissolved in benzene (3 mL/mmol of diazo) under an N_2 atmosphere and transferred dropwise by syringe to the solution of indole starting material. Two sequential rinses and transfers using small quantities of benzene were then conducted to ensure complete transfer of the diazo reagent. The reaction mixture was then heated to 80 °C and stirred at this temperature for 12 h. The reaction progress was monitored by TLC analysis and considered complete upon consumption of diazo reagent. Upon completion, Cs_2CO_3 (1.2 equiv) was added and allowed to stir for an additional 12 h. After 12 h had elapsed, the reaction mixture was filtered through Celite, concentrated *in vacuo*, and purified by silica gel flash column

chromatography (hexanes/EtOAc gradient) to yield annulation products **81, 82, 85, 86, 88, 91, 92**.

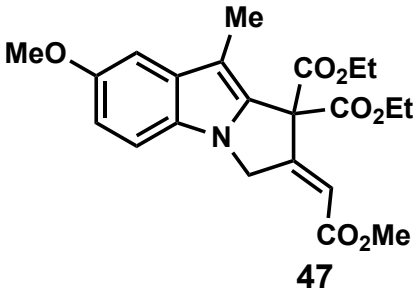

47

47 was prepared using General Experimental Procedure A. Reagents employed: substituted *N*-propargyindole **45** (309 mg, 1.20 mmol), diethyl diazomalonate **46** (187 mg, 1.00 mmol), $Cu(tfacac)_2$ (18.5 mg, 0.0500 mmol). **47** (322 mg, 0.775 mmol, 78%) was obtained as a brown oil:
R_f = 0.47, 25% EtOAc in hexanes;
^{1}H NMR (300 MHz, $CDCl_3$) δ = 7.19 (d, *J* = 8.8 Hz, 1H), 7.02 (d, *J* = 2.2 Hz, 1H), 6.88 (dd, *J* = 8.8, 2.4 Hz, 1H), 6.49 (t, *J* = 2.6 Hz, 1H), 5.22 (d, *J* = 2.6 Hz, 2H), 4.32 – 4.19 (m, 4H), 3.87 (s, 3H), 3.81 (s, 3H), 2.30 (s, 3H), 1.28 (t, *J* = 7.1 Hz, 6H) ppm;
^{13}C NMR (75 MHz, $CDCl_3$) δ = 166.9, 166.0, 156.3, 154.1, 133.6, 133.0, 127.6, 119.1, 112.3, 110.6, 105.6, 101.3, 64.3, 62.8, 56.0, 51.8, 48.9, 14.0, 9.1 ppm;
IR (neat): ν_{max} = 2981, 2361, 1722, 1484, 1351, 1213, 1043, 795 cm^{-1};
HRMS (APPI+): calc'd for $C_{22}H_{25}NO_7$ $[M]^+$ 415.1631, found 415.1631.

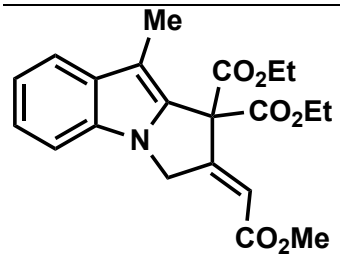

53

53 was prepared using General Experimental Procedure A. Reagents employed: indole **48** (146 mg, 0.644 mmol), diethyl diazomalonate **46** (0.100 g, 0.537 mmol), $Cu(tfacac)_2$ (0.010 g, 0.027 mmol). **53** (143 mg, 0.371 mmol, 69%) was obtained as a dark yellow oil:
R_f = 0.50, 60% CH_2Cl_2 in hexanes;
^{1}H NMR (300 MHz, $CDCl_3$) δ = 7.60 (d, *J* = 7.9 Hz, 1H), 7.30 (d, *J* = 8.2 Hz, 1H), 7.25 – 7.19 (m, 1H), 7.16 – 7.11 (m, 1H), 6.51 (t, *J* = 2.6 Hz, 1H), 5.26 (d, *J* = 2.7 Hz, 2H), 4.35 – 4.18 (m, 4H), 3.82 (s, 3H), 2.34 (s, 3H), 1.28 (t, *J* = 7.1 Hz, 6H) ppm;
^{13}C NMR (75 MHz, $CDCl_3$) δ = 167.0, 166.1, 156.4, 133.0, 132.8, 132.3, 122.1, 119.6, 119.4, 119.3, 109.9, 106.2, 64.2, 63.0, 52.0, 48.8, 14.1, 9.1 ppm;
IR (neat): ν_{max} = 2979, 2360, 1732, 1454, 1365, 1215, 743 cm^{-1};
HRMS (APPI+): calc'd for $C_{21}H_{24}NO_6$ $[M+H]^+$ 386.1595, found 386.1621.

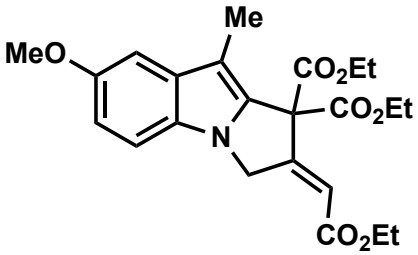

54

54 was prepared using General Experimental Procedure A. Reagents employed: substituted *N*-propargyindole **49** (175 mg, 0.644 mmol), diethyl diazomalonate **46** (0.100 g, 0.537 mmol), $Cu(tfacac)_2$ (0.010 g, 0.027 mmol). **54** (179 mg, 0.417 mmol, 78%) was obtained as a dark brown oil:

R_f = 0.60, 50% CH_2Cl_2 in hexanes;

^{1}H NMR (300 MHz, $CDCl_3$) δ = 7.19 (d, *J* = 8.8 Hz, 1H), 7.02 (d, *J* = 2.3 Hz, 1H), 6.88 (dd, *J* = 8.8, 2.4 Hz, 1H), 6.48 (t, *J* = 2.6 Hz, 1H), 5.23 (d, *J* = 2.6 Hz, 2H), 4.36 – 4.18 (m, 6H), 3.87 (s, 3H), 2.31 (s, 3H), 1.34 (t, *J* = 7.1 Hz, 3H), 1.28 (t, *J* = 7.1 Hz, 6H) ppm;

^{13}C NMR (75 MHz, $CDCl_3$) δ = 167.0, 165.7, 156.1, 154.2, 133.7, 133.1, 127.7, 119.6, 112.4, 110.6, 105.6, 101.4, 64.4, 62.9, 60.9, 56.1, 49.0, 14.3, 14.1, 9.2 ppm;

IR (neat): ν_{max} = 2978, 1731, 1473,1443, 1261, 1253, 1216, 1024, 855, 808 cm^{-1};

HRMS (APPI+): calc'd for $C_{23}H_{28}NO_7$ $[M+H]^+$ 430.1858, found 430.1872.

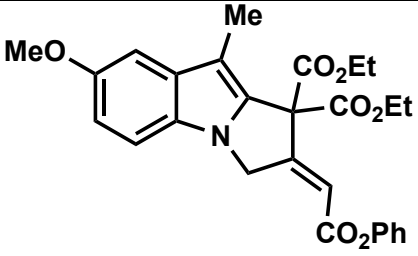

55

55 was prepared using General Experimental Procedure A. Reagents employed: substituted *N*-propargyindole **50** (206 mg, 0.644 mmol), diethyl diazomalonate **46** (0.100 g, 0.537 mmol), $Cu(tfacac)_2$ (0.010 g, 0.027 mmol). **55** (201 mg, 0.421 mmol, 78%) was obtained as a dark brown oil:

R_f = 0.60, 40% CH_2Cl_2 in hexanes;

^{1}H NMR (300 MHz, $CDCl_3$) δ = 7.45 – 7.39 (m, 2H), 7.30 – 7.24 (m, 1H), 7.19 – 7.14 (m, 3H), 7.03 (d, *J* = 2.1 Hz, 1H), 6.88 (dd, *J* = 8.7, 2.2 Hz, 1H), 6.73 (t, *J* = 2.6 Hz, 1H), 5.27 (d, *J* = 2.6 Hz, 2H), 4.40 – 4.22 (m, 4H), 3.87 (s, 3H), 2.33 (s, 3H), 1.31 (t, *J* = 7.1 Hz, 6H) ppm;

^{13}C NMR (75 MHz, $CDCl_3$) δ = 166.9, 164.1, 158.7, 154.3, 150.5, 133.5, 133.1, 129.6, 127.7, 126.2, 121.6, 118.8, 112.5, 110.6, 105.8, 101.5, 64.6, 63.1, 56.1, 49.2, 14.2, 9.2 ppm;

IR (neat): ν_{max} = 2972, 2928, 1732, 1484, 1185, 1161, 1041, 688 cm^{-1};

HRMS (APPI+): calc'd for $C_{27}H_{28}NO_7$ $[M+H]^+$ 478.1858, found 478.1878.

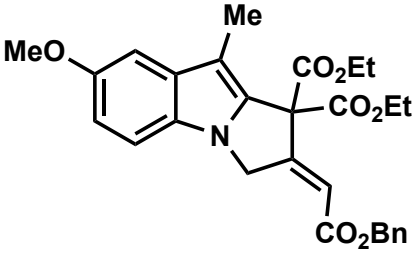

56

56 was prepared using General Experimental Procedure A. Reagents employed: substituted *N*-propargyindole **51** (215 mg, 0.644 mmol), diethyl diazomalonate **46** (0.100 g, 0.537 mmol), $Cu(tfacac)_2$ (0.010 g, 0.027 mmol). **56** (192 mg, 0.391 mmol, 73%) was obtained as a pale-yellow solid:

R_f = 0.50, 60% CH_2Cl_2 in hexanes;

M.P. = 107-109 °C

^{1}H NMR (300 MHz, $CDCl_3$) δ = 7.43 – 7.33 (m, 5H), 7.17 (d, *J* = 8.8 Hz, 1H), 7.02 (d, *J* = 2.3 Hz, 1H), 6.88 (dd, *J* = 8.8, 2.4 Hz, 1H), 6.53 (t, *J* = 2.6 Hz, 1H), 5.23 (bs, 4H), 4.34 – 4.17 (m, 4H), 3.87 (s, 3H), 2.30 (s, 3H), 1.27 (t, *J* = 7.1 Hz, 6H) ppm;
^{13}C NMR (75 MHz, $CDCl_3$) δ = 166.9, 165.5, 156.8, 154.1, 135.7, 133.7, 133.1, 128.8, 128.6, 128.6, 127.8, 119.3, 112.5, 110.6, 105.7, 101.4, 66.8, 64.4, 63.0, 56.1, 49.1, 14.1, 9.2 ppm;
IR (neat): ν_{max} = 2969, 2360, 1736, 1238, 1191, 1162, 1028, 846, 748 cm^{-1};
HRMS (APPI+): calc'd for $C_{28}H_{30}NO_7$ $[M+H]^+$ 492.2014, found 492.2011.

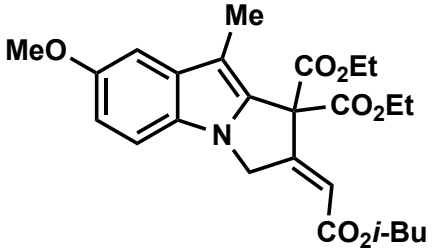

57

57 was prepared using General Experimental Procedure A. Reagents employed: substituted *N*-propargylindole **52** (193 mg, 0.644 mmol), diethyl diazomalonate **46** (0.100 g, 0.537 mmol), $Cu(tfacac)_2$ (0.010 mg, 0.027 mmol). **57** (198 mg, 0.433 mmol, 81%) was obtained as a yellow oil:

R_f = 0.60, 40% CH_2Cl_2 in hexanes;
^{1}H NMR (300 MHz, $CDCl_3$) δ = 7.19 (d, *J* = 8.2 Hz, 1H), 7.02 (d, *J* = 2.4 Hz, 1H), 6.88 (dd, *J* = 8.8, 2.4 Hz, 1H), 6.50 (t, *J* = 2.6 Hz, 1H), 5.23 (d, *J* = 2.7 Hz, 2H), 4.37 – 4.16 (m, 4H), 3.98 (d, *J* = 6.6 Hz, 2H), 3.87 (s, 3H), 2.31 (s, 3H), 2.09 – 1.94 (m, 1H), 1.28 (t, *J* = 7.1 Hz, 6H), 0.99 (d, *J* = 6.7 Hz, 6H) ppm;
^{13}C NMR (75 MHz, $CDCl_3$) δ = 167.1, 165.8, 156.1, 154.2, 133.7, 133.1, 127.7, 119.6, 112.4, 110.6, 105.6, 101.4, 71.1, 64.4, 62.9, 56.1, 49.0, 27.9, 19.3, 14.1, 9.2 ppm;
IR (neat): ν_{max} = 2964, 1726, 1477, 1214, 1040, 795 cm^{-1};
HRMS (APPI+): calc'd for $C_{25}H_{32}NO_7$ $[M+H]^+$ 458.2171, found 458.2195.

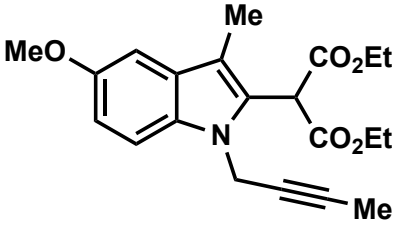

59

59 was prepared using General Experimental Procedure A. Reagents employed: substituted *N*-propargylindole **58** (137 mg, 0.644 mmol), diethyl diazomalonate **46** (0.100 g, 0.537 mmol), $Cu(tfacac)_2$ (0.010 g, 0.027 mmol). **59** (104 mg, 0.280 mmol, 52%) was obtained as a yellow solid:

R_f = 0.50, 20% acetone in hexanes;
^{1}H NMR (300 MHz, $CDCl_3$) δ = 7.32 (d, *J* = 8.8 Hz, 1H), 6.99 (d, *J* = 2.4 Hz, 1H), 6.91 (dd, *J* = 8.8, 2.5 Hz, 1H), 5.07 (s, 1H), 4.86 (q, *J* = 2.4 Hz, 2H), 4.36 – 4.16 (m, 4H), 3.87 (s, 3H), 2.28 (s, 3H), 1.73 (t, *J* = 2.4 Hz, 3H), 1.28 (t, *J* = 7.1 Hz, 6H) ppm;
^{13}C NMR (75 MHz, $CDCl_3$) δ = 167.4, 154.2, 131.9, 128.6, 126.9, 112.7, 111.3, 110.8, 101.1, 80.1, 74.1, 62.3, 56.1, 49.7, 34.5, 14.2, 9.3, 3.7 ppm;
IR (neat): ν_{max} = 2933, 1729, 1306, 1207, 1163, 1030, 831 cm^{-1};
HRMS (APPI+): calc'd for $C_{21}H_{26}NO_5$ $[M+H]^+$ 372.1803, found 372.1786.

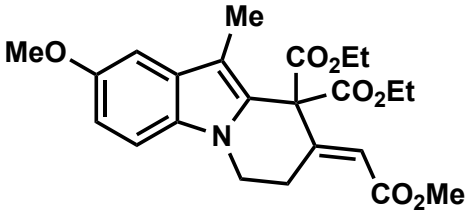

61

61 was prepared using General Experimental Procedure A. Reagents employed: substituted indole **60** (175 mg, 0.644 mmol), diethyl diazomalonate **46** (0.100 g, 0.537 mmol), $Cu(tfacac)_2$ (0.010 g, 0.027 mmol). **61** (158 mg, 0.368 mmol, 68%) was obtained as a pale-yellow crystal:

R_f = 0.45, 30% EtOAc in hexanes;

M.P. = 115-118 °C

^{1}H NMR (300 MHz, $CDCl_3$) δ = 7.17 (d, *J* = 8.8 Hz, 1H), 7.00 (d, *J* = 2.3 Hz, 1H), 6.89 (dd, *J* = 8.8, 2.4 Hz, 1H), 5.97 (s, 1H), 4.30 – 4.20 (m, 4H), 4.13 (t, *J* = 6.2 Hz, 2H), 3.87 (s, 3H), 3.76 (s, 3H), 3.54 (t, *J* = 6.1 Hz, 2H), 2.21 (s, 3H), 1.25 (t, *J* = 7.1 Hz, 6H) ppm;

^{13}C NMR (75 MHz, $CDCl_3$) δ = 168.0, 166.2, 154.2, 151.7, 130.5, 129.0, 127.4, 119.5, 112.2, 109.7, 109.6, 100.6, 63.7, 62.7, 56.0, 51.6, 41.6, 26.1, 14.0, 9.6 ppm;

IR (neat): ν_{max} = 2926, 1728, 1255, 1162, 1068, 1023, 743 cm^{-1};

HRMS (APPI+): calc'd for $C_{23}H_{28}NO_7$ $[M+H]^+$ 430.1858, found 430.1875.

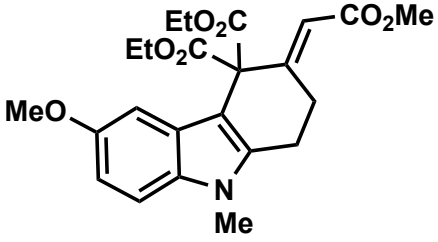

63

63 was prepared using General Experimental Procedure A. Reagents employed: substituted indole **62** (175 mg, 0.644 mmol), diethyl diazomalonate **46** (0.100 g, 0.537 mmol), $Cu(tfacac)_2$ (0.010 g, 0.027 mmol). **63** (180 mg, 0.42 mmol, 78%) was obtained as yellow crystals:

R_f = 0.50, 40% acetone in hexanes;

M.P. = 161-163 °C

^{1}H NMR (300 MHz, $CDCl_3$) δ = 7.13 (d, *J* = 8.8 Hz, 1H), 6.96 (d, *J* = 2.4 Hz, 1H), 6.82 (dd, *J* = 8.8, 2.5 Hz, 1H), 5.87 (s, 1H), 4.34 – 4.15 (m, 4H), 3.81 (s, 3H), 3.73 (s, 3H), 3.57 (s, 3H), 3.44 (t, *J* = 6.4 Hz, 2H), 2.91 (t, *J* = 6.4 Hz, 2H), 1.25 (t, *J* = 7.1 Hz, 6H) ppm;

^{13}C NMR (75 MHz, $CDCl_3$) δ = 169.9, 166.6, 155.0, 154.0, 137.5, 132.9, 126.2, 118.1, 111.2, 109.6, 105.4, 102.7, 63.8, 62.1, 55.9, 51.4, 29.4, 24.9, 23.2, 14.2 ppm;

IR (neat): ν_{max} = 2926, 1728, 1649, 1487, 1255, 1162, 1068, 802 cm^{-1};

HRMS (APPI+): calc'd for $C_{23}H_{28}NO_7$ $[M+H]^+$ 430.1858, found 430.1875.

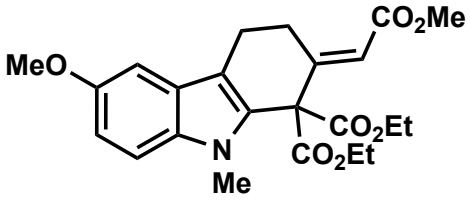

65

65 was prepared using General Experimental Procedure A. Reagents employed: substituted indole **64** (175 mg, 0.644 mmol), diethyl diazomalonate **46** (0.100 g, 0.537 mmol), $Cu(tfacac)_2$ (0.010 g, 0.027 mmol). **65** (164 mg, 0.382 mmol, 71%) was obtained as a light green oil:

R_f = 0.40, 20% EtOAc in hexanes;
^{1}H NMR (300 MHz, $CDCl_3$) δ = 7.20 (d, *J* = 8.8 Hz, 1H), 6.96 (d, *J* = 2.3 Hz, 1H), 6.91 (dd, *J* = 8.8, 2.5 Hz, 1H), 5.78 (s, 1H), 4.28 (q, *J* = 7.1 Hz, 4H), 3.86 (s, 3H), 3.75 (s, 3H), 3.64 (s, 3H), 3.30 (t, *J* = 6.3 Hz, 2H), 2.91 (t, *J* = 6.3 Hz, 2H), 1.27 (t, *J* = 7.1 Hz, 6H) ppm;
^{13}C NMR (75 MHz, $CDCl_3$) δ = 168.6, 166.3, 155.5, 154.0, 133.7, 129.8, 125.6, 118.0, 112.7, 112.5, 110.1, 100.6, 64.6, 62.7, 56.0, 51.4, 31.3, 25.9, 21.7, 13.9 ppm;
IR (neat): ν_{max} = 2932, 1728, 1663, 1487, 1250, 1162, 1068, 779 cm^{-1};
HRMS (APPI+): calc'd for $C_{23}H_{28}NO_7$ $[M+H]^+$ 430.1858, found 430.1875.

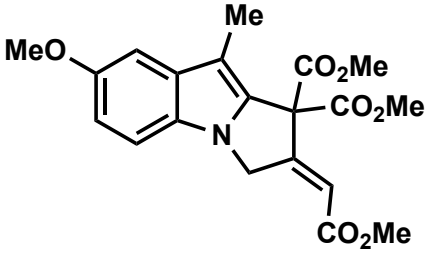

68

68 was prepared using General Experimental Procedure A. Reagents employed: substituted *N*-propargylindole **45** (154 mg, 0.600 mmol), dimethyl diazomalonate **66** (79 mg, 0.50 mmol), $Cu(tfacac)_2$ (9.2 mg, 0.025 mmol). **68** (144 mg, 0.372 mmol, 74%) was obtained as a dark brown oil:

R_f = 0.47, 25% EtOAc in hexanes;
^{1}H NMR (300 MHz, $CDCl_3$) δ = 7.19 (d, *J* = 8.7 Hz, 1H), 7.02 (d, *J* = 2.2 Hz, 1H), 6.88 (dd, *J* = 8.7, 2.3 Hz, 1H), 6.48 (t, 2.3 Hz, 1H), 5.23 (d, *J* = 2.5 Hz, 2H), 3.86 (s, 3H), 3.80 (s, 3H), 3.79 (s, 6H), 2.28 (s, 3H) ppm;
^{13}C NMR (75 MHz, $CDCl_3$) δ = 167.4, 165.9, 156.2, 154.3, 133.4, 132.9, 127.7, 119.3, 112.6, 110.7, 105.7, 101.4, 63.9, 56.1, 53.7, 51.9, 48.9, 8.8 ppm;
IR (neat): ν_{max} = 2951, 2361, 1716, 1435, 1231, 1211, 1046, 904, 785 cm^{-1};
HRMS (APPI+): calc'd for $C_{20}H_{22}NO_7$ $[M+H]^+$ 388.1391, found 388.1406.

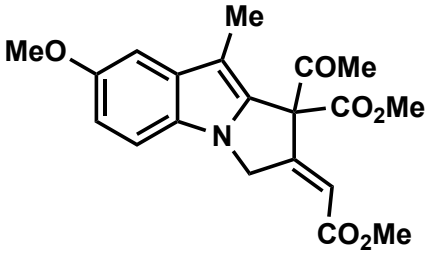

69

69 was prepared using General Experimental Procedure A. Reagents employed: substituted *N*-propargylindole **45 (**154 mg, 0.600 mmol), Methyl 2-diazoacetoacetate **67** (71 mg, 0.50 mmol), $Cu(tfacac)_2$ (9.2 mg, 0.025 mmol). **69** (70 mg, 0.19 mmol, 38%) was obtained as a brown oil:

R_f = 0.47, 25% EtOAc in hexanes;

^{1}H NMR (300 MHz, $CDCl_3$) δ = 7.23 (d, *J* = 8.8 Hz, 1H), 7.03 (d, *J* = 2.4 Hz, 1H), 6.92 (dd, *J* = 8.8, 2.4 Hz, 1H), 6.34 (t, *J* = 2.6 Hz, 1H), 5.35 – 5.19 (m, 2H), 3.88 (s, 3H), 3.82 (s, 3H), 3.81 (s, 3H), 2.28 (s, 3H), 2.05 (s, 3H) ppm;
^{13}C NMR (75 MHz, $CDCl_3$) δ = 199.1, 167.6, 165.9, 155.8, 154.4, 134.0, 133.1, 128.0, 120.1, 112.9, 110.8, 105.9, 101.4, 70.9, 56.1, 53.5, 52.0, 49.1, 26.7, 9.1 ppm;
IR (neat): ν_{max} = 2952, 2360, 2191, 1715, 1485, 1349, 1218, 1162, 1041, 792 cm^{-1};
HRMS (APPI+): calc'd for $C_{20}H_{21}NO_6$ $[M]^+$ 371.1369, found 371.1373.

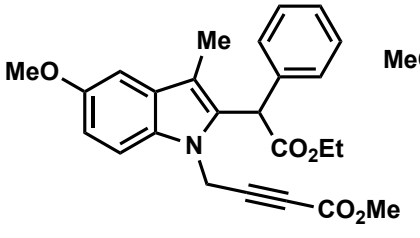

78

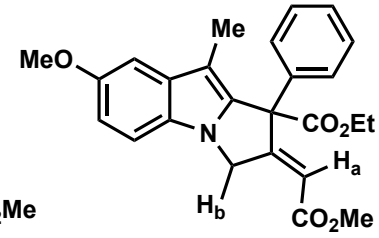

74-*Z*

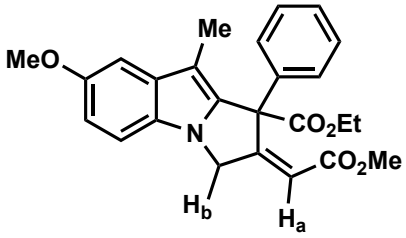

74-*E*

Product **78**, **74-*(Z)***, and **74-*(E)*** were prepared following General Experimental Procedure A. Reagents employed: substituted *N*-propargylindole **45** (154 mg, 0.600 mmol), ethyl 2-phenyldiazoacetate **70** (95 mg, 0.50 mmol), $Cu(tfacac)_2$ (9.2 mg, 0.025 mmol). **78** (65 mg, 0.16 mmol, 32%) was obtained as a brown oil, **74-*(Z)*** (43 mg, 0.10 mmol, 20%) was obtained as a brown oil, and **74-*(E)*** (9 mg, 0.02 mmol, 4%) was obtained as a brown oil:

NOTE: Diagnostic ^{1}H NMR signals between *Z* and *E* isomers; **74-*(Z)*** H_a δ = 5.92 (t, *J* = 2.5 Hz, 1H), H_b δ = 5.45 – 5.12 (m, 2H). **74-*(E)*** H_a δ = 6.11 (t, *J* = 1.9 Hz, 1H), H_b δ = 4.97 (d, *J* = 1.5 Hz, 2H)

Compound **78**:
R_f = 0.50, 25% EtOAc in hexanes;
^{1}H NMR (300 MHz, $CDCl_3$) δ = 7.35 – 7.14 (m, 6H), 7.03 (d, *J* = 2.4 Hz, 1H), 6.92 (dd, *J* = 8.8, 2.5 Hz, 1H), 5.50 (s, 1H), 4.97 – 4.76 (m, 2H), 4.37 – 4.20 (m, 2H), 3.89 (s, 3H), 3.68 (s, 3H), 2.30 (s, 3H), 1.30 (t, *J* = 7.1 Hz, 3H) ppm;
^{13}C NMR (75 MHz, $CDCl_3$) δ = 171.3, 154.6, 153.5, 136.3, 131.9, 131.4, 129.0, 128.9, 127.9, 127.5, 112.6, 111.5, 110.2, 101.3, 82.4, 75.3, 61.9, 56.2, 52.7, 48.0, 34.5, 14.3, 9.2 ppm;
IR (neat): ν_{max} = 2945, 2327, 2240, 1716, 1483, 1253, 1158, 1034, 734 cm^{-1};
HRMS (APPI+): calc'd for $C_{25}H_{26}NO_5$ $[M+H]^+$ 420.1803, found 420.1825.

Compound **74-*(Z)***:
R_f = 0.59, 25% EtOAc in hexanes;
^{1}H NMR (300 MHz, $CDCl_3$) δ = 7.37 – 7.30 (m, 3H), 7.27 – 7.18 (m, 3H), 7.03 (d, *J* = 2.4 Hz, 1H), 6.90 (dd, *J* = 8.8, 2.4 Hz, 1H), 5.93 (t, *J* = 2.5 Hz, 1H), 5.40 – 5.19 (m, 2H), 4.33 – 4.12 (m, 2H), 3.88 (s, 3H), 3.73 (s, 3H), 2.06 (s, 3H), 1.22 (t, *J* = 7.1 Hz, 3H) ppm;

^{13}C NMR (75 MHz, $CDCl_3$) δ = 170.3, 166.4, 163.2, 154.2, 139.5, 138.0, 133.2, 128.8, 127.9, 127.7, 127.5, 119.0, 112.0, 110.6, 104.8, 101.3, 63.5, 62.5, 56.1, 51.7, 49.1, 14.1, 9.0 ppm;
IR (neat): ν_{max} = 2922, 1730, 1438, 1305, 1212, 1024, 806, 703 cm^{-1};
HRMS (APPI+): calc'd for $C_{25}H_{26}NO_5$ $[M+H]^+$ 420.1803, found 420.1829.

Compound **74-*(E)***:
R_f = 0.50, 25% EtOAc in hexanes;
^{1}H NMR (300 MHz, $CDCl_3$) δ = 7.45 – 7.42 (m, 2H), 7.23 – 7.16 (m, 4H), 6.99 (d, *J* = 2.5 Hz, 1H), 6.88 (dd, *J* = 8.7, 2.4 Hz, 1H), 6.11 (t, *J* = 1.9 Hz, 1H), 4.97 (d, *J* = 1.5 Hz, 2H), 4.35 – 4.11 (m, 2H), 3.87 (s, 3H), 3.64 (s, 3H), 2.04 (s, 3H), 1.19 (t, *J* = 7.1 Hz, 3H) ppm;
^{13}C NMR (75 MHz, $CDCl_3$) δ = 168.8, 164.9, 161.1, 154.3, 139.5, 133.5, 128.5, 127.9, 127.3, 127.1, 116.1, 111.9, 110.4, 103.8, 101.5, 61.7, 56.1, 51.6, 50.3, 14.2, 8.0 (Note: two carbon signals are missing presumably due to overlap with the signals at 139.5 and 61.7 ppm)
IR (neat): ν_{max} = 2941, 1730, 1582, 1480, 1350, 1216, 1116, 1033, 855 cm^{-1};
HRMS (APPI+): calc'd for $C_{25}H_{26}NO_5$ $[M+H]^+$ 420.1803, found 420.1832.

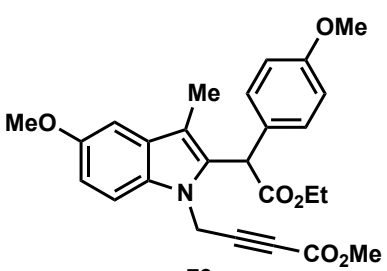

79

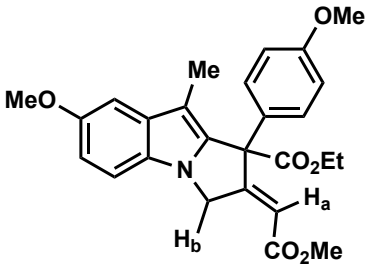

75-*Z*

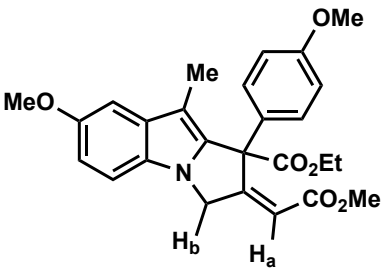

75-*E*

Product **79**, **75-*(Z)***, and **75-*(E)*** were prepared following General Experimental Procedure A. Reagents employed: substituted *N*-propargylindole **45** (154 mg, 0.600 mmol), ethyl 2-(4-methoxyphenyl) diazoacetate **71** (110 mg, 0.50 mmol), $Cu(tfacac)_2$ (9.2 mg, 0.025 mmol). **79** (72 mg, 0.16 mmol, 32%) was obtained as a brown oil, **75-*(Z)*** (58 mg, 0.13 mmol, 26%) was obtained as a brown oil, and **75-*(E)*** (17 mg, 0.038 mmol, 8%) was obtained as a brown oil:

NOTE: Diagnostic ^{1}H NMR signals between *Z* and *E* isomers; **75-*(Z)*** H_a δ = 5.91 (t, *J* = 2.5 Hz, 1H), H_b δ = 5.39 – 5.17 (m, 2H). **75-*(E)*** H_a δ = 6.07 (t, *J* = 1.9 Hz, 1H), H_b δ = 4.94 (d, *J* = 1.5 Hz, 2H)

Compound **79**:
R_f = 0.49, 25% EtOAc in hexanes;
^{1}H NMR (300 MHz, $CDCl_3$) δ = 7.21 (d, *J* = 8.8 Hz, 1H), 7.07 (d, *J* = 8.1 Hz, 2H), 7.03 (d, *J* = 2.5 Hz, 1H), 6.92 (dd, *J* = 8.8, 2.4 Hz, 1H), 6.84 (d, *J* = 8.8 Hz, 2H), 5.43 (s, 1H), 5.01 – 4.76 (m, 2H), 4.34 – 4.21 (m, 2H), 3.88 (s, 3H), 3.78 (s, 3H), 3.68 (s, 3H), 2.30 (s, 3H), 1.30 (t, *J* = 7.1 Hz, 3H) ppm;

^{13}C NMR (75 MHz, $CDCl_3$) δ = 171.6, 159.0, 154.6, 153.5, 131.9, 131.8, 129.1, 128.2, 114.3, 113.8, 112.6, 111.2, 110.2, 101.4, 82.5, 75.2, 61.9, 56.2, 55.4, 52.7, 47.3, 34.4, 14.3, 9.2 ppm;
IR (neat): ν_{max} = 2928, 2247, 1715, 1444, 1260, 1169 1026, 810 cm^{-1};
HRMS (APPI+): calc'd for $C_{26}H_{28}NO_6$ $[M+H]^+$ 450.1917, found 450.1955.

Compound **75-*(Z)***:
R_f = 0.49, 25% EtOAc in hexanes;
^{1}H NMR (300 MHz, $CDCl_3$) δ = 7.24 (d, *J* = 8.8 Hz, 1H), 7.14 (d, *J* = 8.8 Hz, 2H), 7.03 (d, *J* = 2.4 Hz, 1H), 6.90 (dd, *J* = 8.8, 2.4 Hz, 1H), 6.86 (d, *J* = 8.9 Hz, 2H), 5.91 (t, *J* = 2.5 Hz, 1H), 5.39 – 5.17 (m, 2H), 4.29 – 4.12 (m, 2H), 3.88 (s, 3H), 3.80 (s, 3H), 3.73 (s, 3H), 2.07 (s, 3H), 1.22 (t, *J* = 7.1 Hz, 3H) ppm;
^{13}C NMR (75 MHz, $CDCl_3$) δ = 170.5, 166.5, 163.7, 159.2, 154.2, 138.2, 133.2, 131.5, 128.7, 127.8, 118.7, 114.2, 112.0, 110.6, 104.7, 101.3, 62.9, 62.5, 56.2, 55.4, 51.7, 49.1, 14.2, 9.0 ppm;
IR (neat): ν_{max} = 2923, 2855, 2242 1721, 1453, 1249, 1175, 1026, 803 cm^{-1};
HRMS (APPI+): calc'd for $C_{26}H_{28}NO_6$ $[M+H]^+$ 450.1917, found 450.1964.

Compound **75-*(E)***:
R_f = 0.41, 25% EtOAc in hexanes;
^{1}H NMR (300 MHz, $CDCl_3$) δ = 7.34 (d, *J*= 8.9 Hz, 2H), 7.17 (d, *J* = 8.8 Hz, 1H), 6.99 (d, *J* = 2.4 Hz, 1H), 6.87 (dd, *J* = 8.7, 2.4 Hz, 1H), 6.75 (d, *J* = 9.0 Hz, 2H), 6.07 (t, *J* = 1.9 Hz, 1H), 4.94 (d, *J* = 1.9 Hz, 2H), 4.28 – 4.12 (m, 2H), 3.87 (s, 3H), 3.75 (s, 3H), 3.66 (s, 3H), 2.05 (s, 3H), 1.18 (t, *J* = 7.1 Hz, 3H) ppm;
^{13}C NMR (75 MHz, $CDCl_3$) δ = 169.0, 165.0, 161.4, 158.7, 154.3, 142.5, 133.5, 131.6, 129.8, 127.2, 115.6, 113.2, 111.9, 110.4, 103.6, 101.5, 61.7, 60.0, 56.1, 55.3, 51.6, 50.3, 14.2, 8.0. ppm;
IR (neat): ν_{max} = 2943, 1730, 1607, 1447, 1349, 1215, 1178, 1033, 730 cm^{-1};
HRMS (APPI+): calc'd for $C_{26}H_{28}NO_6$ $[M+H]^+$ 450.1917, found 450.1941.

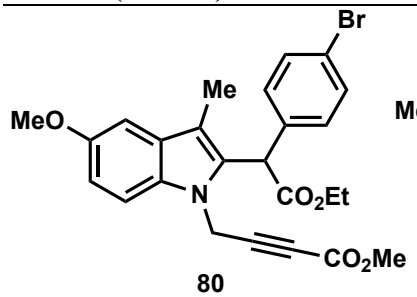

80

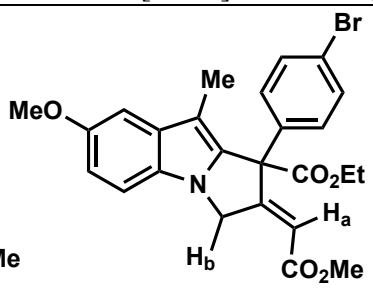

76-*Z*

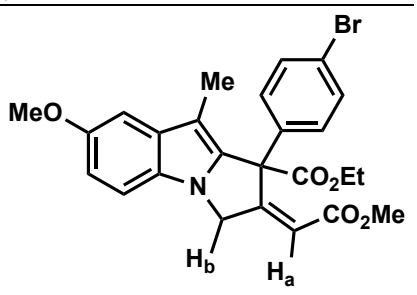

76-*E*

Product **80**, **76-*(Z)***, and **76-*(E)*** were prepared following General Experimental Procedure A. Reagents employed: substituted N-propargylindole **45** (155 mg, 0.602 mmol), ethyl 2-(4-bromophenyl)diazoacetate **72** (135 mg, 0.502 mmol), $Cu(tfacac)_2$ (9.2 mg, 0.025 mmol). **80** (46 mg, 0.092 mmol, 18%) was obtained as a brown oil, **76-*(Z)*** (79 mg, 0.16 mmol, 32%) was obtained as a brown oil, and **76-*(E)*** (33 mg, 0.066 mmol, 13%) was obtained as a brown oil:

NOTE: Diagnostic ^{1}H NMR signals between *Z* and *E* isomers; **76-*(Z)*** H_a δ = 5.88 (t, *J* = 2.5 Hz, 1H), H_b δ = 5.40 – 5.18 (m, 2H). **76-*(E)*** H_a δ = 6.10 (t, *J* = 1.9 Hz, 1H), H_b δ = 4.97 (d, *J* = 2.1 Hz, 2H)

Compound **80**:
R_f = 0.54, 25% EtOAc in hexanes;
^{1}H NMR (300 MHz, $CDCl_3$) δ = 7.44 (d, *J* = 8.5 Hz, 2H), 7.20 (d, *J* = 8.8 Hz, 1H), 7.07 – 6.91 (m, 3H), 6.93 (dd, *J* = 8.8, 2.4 Hz, 1H), 5.40 (s, 1H), 5.02 – 4.74 (m, 2H), 4.37-4.19 (m, 2H), 3.89 (s, 3H), 3.70 (s, 3H), 2.29 (s, 3H), 1.29 (t, *J* = 7.1 Hz, 3H) ppm;
^{13}C NMR (75 MHz, $CDCl_3$) δ = 170.9, 154.7, 153.4, 135.3, 132.0, 131.9, 130.9, 129.8, 129.0, 121.7, 112.9, 111.7, 110.2, 101.4, 82.0, 75.4, 62.1, 56.2, 52.9, 47.4, 34.3, 14.3, 9.3, ppm;
IR (neat): ν_{max} = 2971, 2925, 2361, 1716, 1484, 1436, 1300, 1158, 1035, 798 cm^{-1};
HRMS (APPI+): calc'd for $C_{25}H_{25}{}^{79}BrNO_5$ $[M+H]^+$ 498.0908, found 498.0929.

Compound **76-*(Z)***:
R_f = 0.66, 25% EtOAc in hexanes;
^{1}H NMR (300 MHz, $CDCl_3$) δ = 7.47 (d, *J* = 8.6 Hz, 2H), 7.25 (d, *J* = 8.8 Hz, 1H), 7.11 (d, *J* = 8.6 Hz, 2H), 7.03 (d, *J* = 2.4 Hz, 1H), 6.91 (dd, *J* = 8.8, 2.4 Hz, 1H), 5.88 (t, *J* = 2.5 Hz, 1H), 5.40 – 5.18 (m, 2H), 4.29 – 4.11 (m, 2H), 3.88 (s, 3H), 3.74 (s, 3H), 2.05 (s, 3H), 1.21 (t, *J* = 7.1 Hz, 3H) ppm;
^{13}C NMR (75 MHz, $CDCl_3$) δ = 169.9, 166.2, 162.8, 154.3, 138.6, 137.5, 133.1, 132.0, 129.3, 127.8, 122.1, 119.0, 112.3, 110.7, 104.8, 101.3, 62.9, 62.7, 56.1, 51.8, 49.1, 14.1, 9.0 ppm;
IR (neat): ν_{max} = 2923, 1718, 1482, 1298, 1204, 1014, 798 cm^{-1};
HRMS (APPI+): calc'd for $C_{25}H_{25}{}^{79}BrNO_5$ $[M+H]^+$ 498.0908, found 498.0932.

Compound **76-*(E)***:
R_f = 0.51, 25% EtOAc in hexanes;
^{1}H NMR (300 MHz, $CDCl_3$) δ = 7.33 (apt s, (AA` BB`) 4H), 7.18 (d, *J* = 8.7 Hz, 1H), 6.98 (d, *J* = 2.4 Hz, 1H), 6.89 (dd, *J* = 8.7, 2.4 Hz, 1H), 6.10 (t, *J* = 1.9 Hz, 1H), 4.97 (t, *J* = 2.1 Hz, 2H), 4.31 – 4.09 (m, 2H), 3.87 (s, 3H), 3.65 (s, 3H), 2.02 (s, 3H), 1.18 (t, *J* = 7.1 Hz, 3H) ppm;
^{13}C NMR (75 MHz, $CDCl_3$) δ = 168.4, 164.8, 161.0, 154.4, 141.8, 138.7, 133.4, 130.9, 130.4, 127.2, 121.5, 116.2, 112.2, 110.5, 103.9, 101.5, 61.9, 59.9, 56.1, 51.8, 50.2, 14.1, 8.0 ppm;
IR (neat): ν_{max} = 2923, 2854, 2361, 1735, 1483, 1349, 1213, 1076, 797 cm^{-1};
HRMS (APPI+): calc'd for $C_{25}H_{25}{}^{79}BrNO_5$ $[M+H]^+$ 498.0908, found 498.0937.

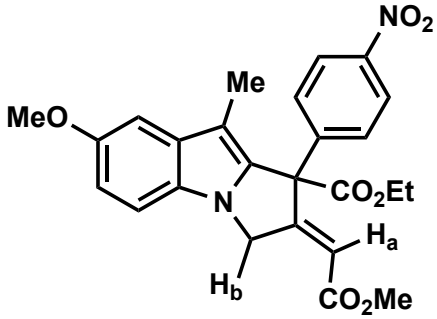

77-*Z*

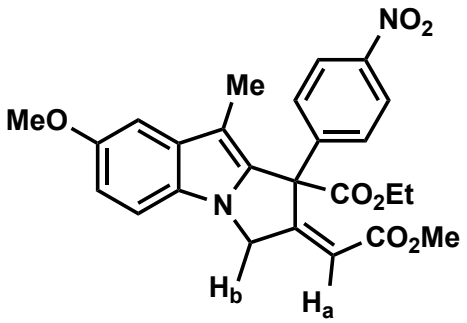

77-*E*

Product **77-*(Z)*** and **77-*(E)*** were prepared following General Experimental Procedure A. Reagents employed: substituted *N*-propargylindole **45** (155 mg, 0.602 mmol), ethyl 2-(4-nitrophenyl)diazoacetate **73** (118 mg, 0.502 mmol), $Cu(tfacac)_2$ (9.2 mg, 0.025 mmol). **77-*(Z)*** (90.0 mg, 0.194 mmol, 39%) was obtained as a brown oil and **77-*(E)*** **(**60.0 mg, 0.129 mmol, 26%) was obtained as a brown oil:

NOTE: Diagnostic ^{1}H NMR signals between *Z* and *E* isomers; **77-*(Z)*** H_a δ = 5.87 (t, *J* = 2.5 Hz, 1H), H_b δ = 5.42 – 5.22 (m, 2H). **77-*(E)*** H_a δ = 6.17 (t, *J* = 2.0 Hz, 1H), H_b δ = 5.04 (d, *J* = 1.9 Hz, 2H)

Compound **77-*(Z)***:
R_f = 0.51, 25% EtOAc in hexanes;
^{1}H NMR (300 MHz, $CDCl_3$) δ = 8.21 (d, *J* = 8.8 Hz, 2H), 7.44 (d, *J* = 8.8 Hz, 2H), 7.26 (d, *J* = 2.4 Hz, 1H), 7.03 (d, *J* = 2.3 Hz, 1H), 6.94 (dd, *J* = 8.8, 2.4 Hz, 1H), 5.87 (t, *J* = 2.5 Hz, 1H), 5.42 – 5.22 (m, 2H), 4.30 – 4.19 (m, 2H), 3.89 (s, 3H), 3.75 (s, 3H), 2.03 (s, 3H), 1.23 (t, *J* = 7.2 Hz, 3H) ppm;
^{13}C NMR (75 MHz, $CDCl_3$) δ = 169.4, 165.9, 162.1, 154.4, 147.5, 146.6, 136.9, 133.1, 128.8, 127.8, 124.1, 119.5, 112.7, 110.8, 105.0, 101.4, 62.99, 62.96, 56.1, 51.9, 49.2, 14.1, 9.0 ppm;
IR (neat): ν_{max} = 2936, 1726, 1606, 1521, 1445, 1349, 1219, 1028, 733 cm^{-1};
HRMS (APPI+): calc'd for $C_{25}H_{25}N_2O_7$ $[M+H]^+$ 465.1656, found 465.1666.

Compound **77-*(E)***:
R_f = 0.38, 25% EtOAc in hexanes;
^{1}H NMR (300 MHz, $CDCl_3$) δ = 8.07 (d, *J* = 9.0 Hz, 2H), 7.69 (d, *J* = 9.0 Hz, 2H), 7.20 (d, *J* = 8.7 Hz, 1H), 6.98 (d, *J* = 2.3 Hz, 1H), 6.91 (dd, *J* = 8.8, 2.4 Hz, 1H), 6.17 (t, *J* = 2.0 Hz, 1H), 5.04 (t, *J* = 1.9 Hz, 2H), 4.34 – 4.10 (m, 2H), 3.86 (s, 3H), 3.64 (s, 3H), 2.00 (s, 3H), 1.19 (t, *J* = 7.1 Hz, 3H) ppm;
^{13}C NMR (75 MHz, $CDCl_3$) δ = 167.8, 164.7, 160.8, 154.5, 146.9, 146.8, 141.2, 133.5, 129.7, 127.3, 122.8, 116.8, 112.6, 110.6, 104.3, 101.5, 62.1, 59.9, 56.1, 51.9, 50.3, 14.1, 7.9 ppm;
IR (neat): ν_{max} = 2958, 1729, 1519, 1445, 1346, 1218, 1111, 1031, 802, 731 cm^{-1};
HRMS (APPI+): calc'd for $C_{25}H_{25}N_2O_7$ $[M]^+$ 464.1584, found 464.1615.

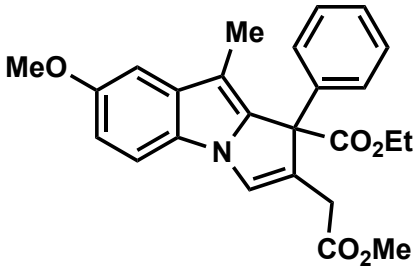

81

81 was prepared using General Experimental Procedure B. Reagents employed: substituted *N*-propargylindole **45** (50.0 mg, 0.194 mmol), ethyl 2-phenyldiazoacetate **70** (31 mg, 0.16 mmol), $Cu(tfacac)_2$ (4.0 mg, 0.0097 mmol), Cs_2CO_3 (63 mg, 0.19 mmol). **81** (43 mg, 0.10 mmol, 63%) was obtained as a brown oil:
X-ray quality crystal prepared by vapor diffusion in ether with pentane.
R_f = 0.44, 25% EtOAc in hexanes;
^{1}H NMR (300 MHz, $CDCl_3$) δ = 7.31 – 7.26 (m, 5H), 7.13 – 7.00 (m, 2H), 7.00 (d, *J* = 2.4 Hz, 1H), 6.89 (dd, *J* = 8.7, 2.4 Hz, 1H), 4.26 (q, *J* = 7.1 Hz, 2H), 3.87 (s, 3H), 3.58 (s, 3H), 3.50 – 3.12 (m, 2H), 2.14 (s, 3H), 1.27 (t, *J* = 7.1 Hz, 3H) ppm;
^{13}C NMR (75 MHz, $CDCl_3$) δ = 171.5, 170.6, 154.1, 140.0, 137.2, 132.7, 128.8, 127.8, 127.1, 125.6, 124.4, 123.0, 112.2, 110.2, 109.4, 101.8, 64.2, 62.1, 56.1, 52.0, 31.9, 14.3, 9.2 ppm;
IR (neat): ν_{max} = 2948, 2361, 1727, 1483, 1446, 1365, 1231, 1043, 796 cm^{-1};
HRMS (APPI+): calc'd for $C_{25}H_{26}NO_5$ $[M+H]^+$ 420.1806, found 420.1838.

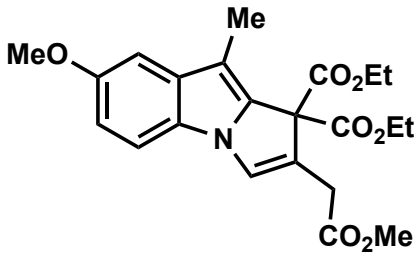

82

82 was prepared using General Experimental Procedure B. Reagents employed: substituted *N*-propargylindole **45** (154 mg, 0.600 mmol), diethyl diazomalonate **46** (93 mg, 0.50 mmol), $Cu(tfacac)_2$ (9.0 mg, 0.025 mmol), Cs_2CO_3 (195 mg, 0.600 mmol). **82** (118 mg, 0.284 mmol, 57%) was obtained as a brown oil:

R_f = 0.32, 25% EtOAc in hexanes;
^{1}H NMR (300 MHz, $CDCl_3$) δ = 7.31 (t, *J* = 1.4 Hz, 1H), 7.22 (d, *J* = 8.8 Hz, 1H), 7.00 (d, *J* = 2.4 Hz, 1H), 6.87 (dd, *J* = 8.8, 2.5 Hz, 1H), 4.24 (q, *J* = 7.1 Hz, 4H), 3.86 (s, 3H), 3.72 (s, 3H), 3.56 (d, *J* = 1.4 Hz, 2H), 2.36 (s, 3H), 1.28 (t, *J* = 7.1 Hz, 6H) ppm;
^{13}C NMR (75 MHz, $CDCl_3$) δ = 171.6, 166.9, 154.2, 134.6, 132.8, 127.5, 125.7, 117.0, 112.7, 110.8, 110.2, 102.0, 65.1, 62.5, 56.1, 52.2, 32.0, 14.2, 9.2 ppm;
IR (neat): ν_{max} = 2983, 1732, 1484, 1447, 1366, 1234, 1157, 1044, 799 cm^{-1};
HRMS (APPI+): calc'd for $C_{22}H_{26}NO_7$ $[M+H]^+$ 416.1704, found 416.1738.

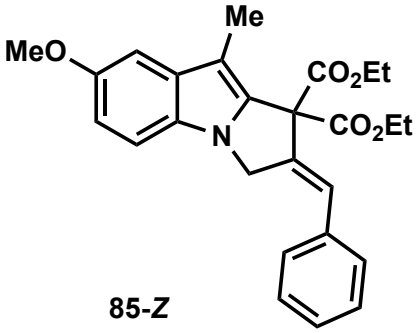

85-*Z*

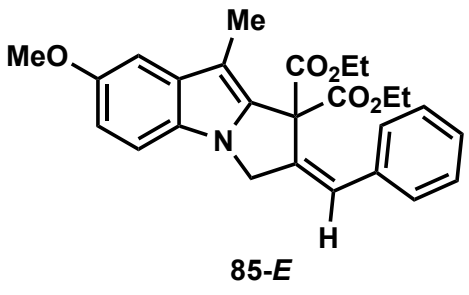

85-*E*

Product **85-*(Z)*** and **85-*(E)*** were prepared following General Experimental Procedure B. Reagents employed: substituted *N*-propargylindole **83** (154 mg, 0.600 mmol), diethyl diazomalonate **46** (93 mg, 0.50 mmol), $Cu(tfacac)_2$ (9.2 mg, 0.025 mmol), Cs_2CO_3 (195 mg, 0.600 mmol). **85-*(Z)*** (67 mg, 0.15 mmol, 30%) was obtained as a brown oil and **85-*(E)*** (62 mg, 0.14 mmol, 28%) was obtained as a brown oil:

Compound **85-*(Z)***:
R_f = 0.63, 25% EtOAc in hexanes;
^{1}H NMR (300 MHz, $CDCl_3$) δ = 7.47 – 7.30 (m, 5H), 7.19 (d, *J* = 8.8 Hz, 1H), 7.04 (d, *J* = 2.6 Hz, 2H), 6.87 (dd, *J* = 8.8, 2.4 Hz, 1H), 5.03 (d, *J* = 2.5 Hz, 2H), 4.37 – 4.20 (m, 4H), 3.88 (s, 3H), 2.32 (s, 3H), 1.29 (t, *J* = 7.1 Hz, 6H) ppm;
^{13}C NMR (75 MHz, $CDCl_3$) δ = 168.2, 154.1, 137.1, 136.1, 135.1, 133.1, 129.1, 128.8, 128.1, 127.9, 112.1, 110.5, 105.3, 101.5, 64.2, 62.5, 56.1, 47.7, 14.2, 9.2 ppm;
(Note: one carbon signal is missing presumably due to overlap with the signal at 128.8 ppm)
IR (neat): ν_{max} = 2927, 2361, 1730, 1485, 1388, 1241, 1161, 1035, 767 cm^{-1};
HRMS (APPI+): calc'd for $C_{26}H_{28}NO_5$ $[M+H]^+$ 434.1962, found 434.1981.

Compound **85-*(E)***:
R_f = 0.63, 25% EtOAc in hexanes;
^{1}H NMR (300 MHz, $CDCl_3$) δ = 7.42 – 7.24 (m, 5H), 7.16 (d, *J* = 8.8 Hz, 1H), 6.99 (d, *J* = 2.4 Hz, 1H), 6.94 (bs, 1H), 6.86 (dd, *J* = 8.8, 2.4 Hz, 1H), 4.89 (d, *J* = 1.9 Hz, 2H), 4.00 – 3.85 (m, 4H), 3.87 (s, 3H), 2.21 (s, 3H), 1.07 (t, *J* = 7.1 Hz, 6H) ppm;
^{13}C NMR (75 MHz, $CDCl_3$) δ = 167.6, 154.0, 137.9, 137.7, 135.0, 132.6, 129.0, 128.9, 128.1, 128.0, 127.5, 112.0, 110.5, 104.5, 101.4, 62.5, 62.3, 56.1, 50.7, 13.9, 8.6 ppm;
IR (neat): ν_{max} = 2961, 2924, 2361, 1730, 1482, 1368, 1231, 1161, 1043, 759 cm^{-1};
HRMS (APPI+): calc'd for $C_{26}H_{28}NO_5$ $[M+H]^+$ 434.1962, found 434.1993.

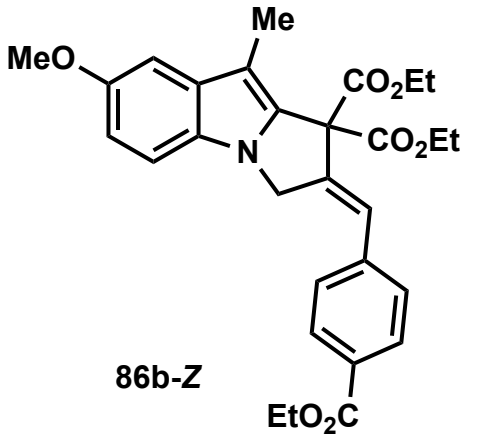

86b-*Z*

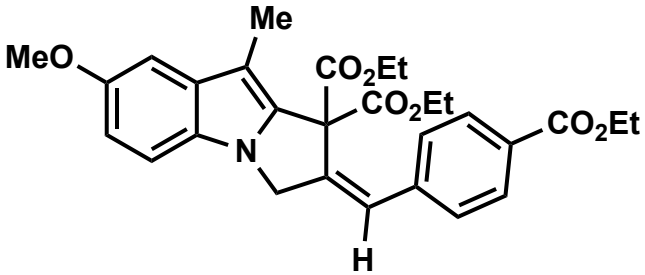

86b-*E*

Product **86-*(Z)*** and **86-*(E)*** were prepared following General Experimental Procedure B. Reagents employed: substituted *N*-propargylindole **84** (154 mg, 0.600 mmol), diethyl diazomalonate **46** (93.1 mg, 0.500 mmol), $Cu(tfacac)_2$ (9.25 mg, 0.0500 mmol), Cs_2CO_3

(195 mg, 0.600 mmol). **86-*(Z)*** (129 mg, 0.255 mmol, 51%) was obtained as a brown oil and **86-*(E)*** (35 mg, 0.069 mmol, 14%) was obtained as a brown oil:

Compound **86-*(Z)***:
R_f = 0.47, 25% EtOAc in hexanes;
^{1}H NMR (300 MHz, $CDCl_3$) δ = 8.11 (d, *J* = 8.4 Hz, 2H), 7.43 (d, *J* = 8.4 Hz, 2H), 7.18 (d, *J* = 8.8 Hz, 1H), 7.08 (t, *J* = 2.6 Hz, 1H), 7.04 (d, *J* = 2.4 Hz, 1H), 6.87 (dd, *J* = 8.8, 2.4 Hz, 1H), 5.04 (d, *J* = 2.5 Hz, 2H), 4.40 (q, *J* = 7.2 Hz, 2H), 4.38 – 4.20 (m, 4H), 3.88 (s, 3H), 2.33 (s, 3H), 1.42 (t, *J* = 7.1 Hz, 3H), 1.30 (t, *J* = 7.1 Hz, 6H). ppm;
^{13}C NMR (75 MHz, $CDCl_3$) δ = 168.0, 166.3, 154.2, 140.3, 139.5, 134.7, 133.1, 130.0, 129.8, 128.7, 128.4, 127.8, 112.2, 110.5, 105.5, 101.5, 64.3, 62.6, 61.3, 56.1, 47.7, 14.5, 14.2, 9.2 ppm;
IR (neat): ν_{max} = 2984, 2853, 2361, 1716, 1607, 1485, 1366, 1241, 1101, 1026, 764 cm^{-1};
HRMS (APPI+): calc'd for $C_{29}H_{32}NO_7$ $[M+H]^+$ 506.2175, found 506.2178.

Compound **86-*(E)***:
R_f = 0.47, 25% EtOAc in hexanes;
^{1}H NMR (300 MHz, $CDCl_3$) δ = 8.01 (d, *J* = 8.4 Hz, 2H), 7.48 (d, *J* = 8.3 Hz, 2H), 7.16 (d, *J* = 8.7 Hz, 1H), 7.00 (d, *J* = 2.4 Hz, 1H), 6.95 (t, *J* = 2.0 Hz, 1H), 6.87 (dd, *J* = 8.7, 2.4 Hz, 1H), 4.91 (d, *J* = 1.9 Hz, 2H), 4.38 (q, *J* = 7.2 Hz, 2H), 3.87 (s, 3H), 4.03 – 3.85 (m, 4H), 2.21 (s, 3H), 1.40 (t, *J* = 7.2 Hz, 3H), 1.09 (s, 6H). ppm;
^{13}C NMR (75 MHz, $CDCl_3$) δ = 167.4, 166.5, 154.1, 139.6, 139.5, 137.5, 132.7, 129.8, 129.4, 128.9, 128.2, 127.5, 112.2, 110.5, 104.7, 101.4, 62.7, 62.4, 61.2, 56.1, 50.7, 14.5, 13.9, 8.6 ppm;
IR (neat): ν_{max} = 2981, 2928, 2361, 1718, 1608, 1483, 1390, 1274, 1228, 1045, 768 cm^{-1};
HRMS (APPI+): calc'd for $C_{29}H_{32}NO_7$ $[M+H]^+$ 506.2175, found 506.2204.

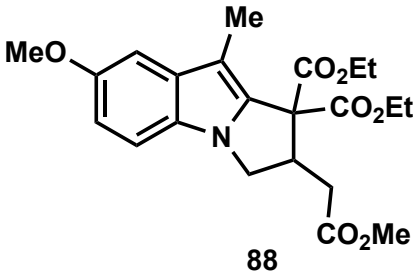

88

88 was prepared using General Experimental Procedure B. Reagents employed: indole **87** (84 mg, 0.32 mmol), diethyl diazomalonate **46** (0.050 mg, 0.27 mmol), $Cu(tfacac)_2$ (5.0 mg, 0.014 mmol) and Cs_2CO_3 (9.0 mg, 0.027 mmol). **88** (45 mg, 0.11 mmol, 41%) was obtained as a brown oil:
(Note: 10 mol% of Cs_2CO_3 was used)

R_f = 0.50, 20% EtOAc in hexanes;
^{1}H NMR (300 MHz, $CDCl_3$) δ = 7.11 (d, *J* = 8.8 Hz, 1H), 7.00 (d, *J* = 2.4 Hz, 1H), 6.84 (dd, *J* = 8.8, 2.4 Hz, 1H), 4.49 – 4.42 (m, 1H), 4.36 – 4.13 (m, 4H), 3.89 – 3.80 (m, 5H), 3.73 (s, 3H), 2.93 – 2.74 (m, 2H), 2.30 (s, 3H), 1.31 (t, *J* = 7.1 Hz, 3H), 1.26 (t, *J* = 7.1 Hz, 3H) ppm;
^{13}C NMR (75 MHz, $CDCl_3$) δ = 172.5, 168.5, 167.8, 154.0, 135.0, 133.1, 128.2, 112.2, 110.5, 105.9, 101.4, 62.3, 62.1, 56.1, 52.1, 48.2, 45.9, 34.2, 14.24, 14.17, 9.3 ppm; (Note: one carbon signal is missing presumably due to overlap with the signal at 62.09)
IR (neat): ν_{max} = 2933, 2361, 1732, 1444, 1370, 1256, 1160, 1038, 795 cm^{-1};

HRMS (APPI+): calc'd for $C_{22}H_{28}NO_7$ $[M+H]^+$ 418.1858, found 418.1873.

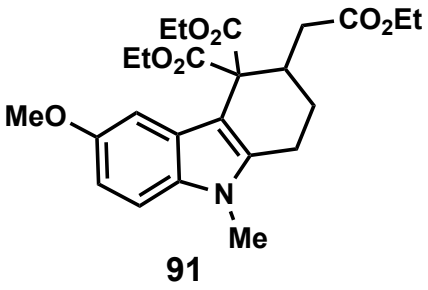

91

91 was prepared using General Experimental Procedure B. Reagents employed: indole **89** (92 mg, 0.32 mmol), diethyl diazomalonate **46** (0.050 g, 0.27 mmol), $Cu(tfacac)_2$ (5.0 mg, 0.014 mmol) and Cs_2CO_3 (9.0 mg, 0.027 mmol). **91** (86 mg, 0.19 mmol, 70%) was obtained as yellow crystals:
(Note: 10 mol% of Cs_2CO_3 was used)

MP: 161-163 °C
R_f = 0.40, 25% acetone in hexanes;
^{1}H NMR (300 MHz, $CDCl_3$) δ = 7.14 (d, *J* = 8.8 Hz, 1H), 7.00 (d, *J* = 2.5 Hz, 1H), 6.82 (dd, *J* = 8.8, 2.5 Hz, 1H), 4.29 – 4.09 (m, 6H), 3.82 (s, 3H), 3.59 (s, 3H), 3.08 – 2.93 (m, 1H), 2.76 (t, *J* = 6.5 Hz, 2H), 2.69 – 2.52 (m, 2H), 2.30 – 2.08 (m, 2H), 1.30 – 1.22 (m, 9H) ppm;
^{13}C NMR (75 MHz, $CDCl_3$) δ = 172.9, 171.2, 170.1, 153.7, 137.5, 132.6, 126.7, 110.8, 109.3, 105.1, 103.7, 61.6, 61.3, 60.5, 58.1, 55.9, 37.0, 35.3, 29.3, 24.6, 20.3, 14.34, 14.28, 14.25 ppm;
IR (neat): ν_{max} = 2981, 1726, 1621, 1486, 1371, 1251, 1188, 1071, 798 cm^{-1};
HRMS (APPI+): calc'd for $C_{24}H_{32}NO_7$ $[M+H]^+$ 445.2178, found 446.2207.

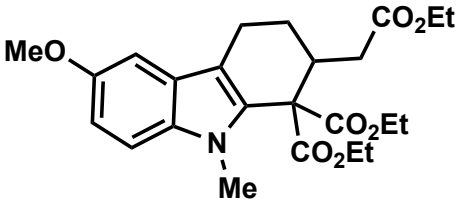

92

92 was prepared using General Experimental Procedure B. Reagents employed: indole **90** (92 mg, 0.32 mmol), **46** diethyl diazomalonate (0.050 g, 0.27 mmol), $Cu(tfacac)_2$ (5.0 mg, 0.014 mmol) and Cs_2CO_3 (9.0 mg, 0.027 mmol). **92** (82 mg, 0.18 mmol, 67%) was obtained as light green oil:
(Note: 10 mol% of Cs_2CO_3 was used)

R_f = 0.40, 20% Acetone in hexanes;
^{1}H NMR (300 MHz, $CDCl_3$) δ = 7.19 (d, *J* = 8.8 Hz, 1H), 6.95 (d, *J* = 2.4 Hz, 1H), 6.91 (dd, *J* = 8.8, 2.5 Hz, 1H), 4.28 – 4.10 (m, 6H), 3.86 (s, 3H), 3.63 (s, 3H), 3.20 – 3.12 (m, 1H), 2.80 (t, *J* = 6.4 Hz, 2H), 2.73 – 2.57 (m, 2H), 2.11 – 1.96 (m, 2H), 1.29 – 1.23 (m, 9H) ppm;
^{13}C NMR (75 MHz, $CDCl_3$) δ = 172.9, 170.2, 169.1, 154.0, 133.5, 130.6, 126.0, 112.6, 111.5, 110.1, 100.6, 62.3, 62.1, 60.6, 59.2, 56.2, 38.9, 35.6, 31.8, 25.8, 19.4, 14.4, 14.12, 14.08 ppm;
IR (neat): ν_{max} = 2975, 2935, 2360, 1738, 1489, 1273, 1162, 1035, 798 cm^{-1};
HRMS (APPI+): calc'd for $C_{24}H_{32}NO_7$ $[M+H]^+$ 445.2178 found 446.219

References

(1) Sheldon, R. A. *Pure Appl. Chem.* **2000**, *72*, 1233–1246.

(2) Curtius, T. *Ber. Dtsch. Chem. Ges.* **1883**, *16*, 2230–2231.

(3) Gessner, V. H. *Chem. Commun.* **2016**, *52*, 12011–12023.

(4) Padwa, A. *Helv. Chim. Acta.* **2005**, *88*, 1357–1374.

(5) Lindsay, V. N. G.; Nicolas, C.; Charette, A. B. *J. Am. Chem. Soc.* **2011**, *133*, 8972–8981.

(6) Bergstrom, B. D.; Nickerson, L. A.; Shaw, J. T.; Souza, L. W. *Angew. Chem. Int. Ed.* **2021**, *60*, 6864–6878.

(7) Ye, T.; McKervey, M. A. *Chem. Rev.* **1994**, *94*, 1091–1160.

(8) Davies, H. M. L.; Beckwith, R. E. J. *Chem. Rev.* **2003**, *103*, 2861–2903.

(9) Takahashi, T.; Tsutsui, H.; Tamura, M.; Kitagaki, S.; Nakajima, M.; Hashimoto, S. *Chem. Commun.* **2001**, 1604–1605.

(10) Davies, H. M. L.; Ren, P.; Jin, Q. *Org. Lett.* **2001**, *3*, 3587–3590.

(11) Flynn, K. M.; Myeong, I. S.; Pinto, T.; Movassaghi, M. *J. Am. Chem. Soc.* **2022**, *144*, 9126–9131.

(12) Campos, K. R.; Coleman, P. J.; Alvarez, J. C.; Dreher, S. D.; Garbaccio, R. M.; Terrett, N. K.; Tillyer, R. D.; Truppo, M. D.; Parmee, E. R. *Science.* **2019**, *363,* 1-8.

(13) Wang, K.; Qi, D.; Li, Y.; Wang, T.; Liu, H.; Jiang, J. *Coord. Chem. Rev.* **2019**, *378*, 188–206.

(14) Zhang, D.; Hu, W. *Chem. Rec.* **2017**, *17*, 739–753.

(15) Yates, P. *J. Am. Chem. Soc.* **1952**, *74*, 5376–5381.

(16) Nozaki, H.; Takaya, H.; Moriuti, S.; Noyori, R. *Tetrahedron* **1968**, *24*, 3655–3669.

(17) Fructos, M. R.; Belderrain, T. R.; De Frémont, P.; Scott, N. M.; Nolan, S. P.; Díaz-Requejo, M. M.; Pérez, P. J. *Angew. Chem. Int. Ed.* **2005**, *44*, 5284–5288.

(18) Paulissen, R.; Reimlinger, H.; Hayez, E.; Hubert, A. J.; Teyssié, P. *Tetrahedron Lett.* **1973**, *24*, 2233–2236.

(19) Paulissen, R.; Hayez, E.; Hubert, A. J.; Teyssie, P. *Tetrahedron Lett.* **1974**, *15*, 607–608.

(20) Cox, G. G.; Miller, D. J.; Moody, C. J.; Sie, E. R. H. B.; Kulagowski, J. J. *Tetrahedron* **1994**, *50*, 3195–3212.

(21) Nelson, T. D.; Song, Z. J.; Thompson, A. S.; Zhao, M.; Demarco, A.; Reamer, R. A.; Huntington, M. F.; Grabowski, E. J. J.; Reider, P. J. *Tetrahedron Lett.* **2000**, *41*, 1877–1881.

(22) Bertelsen, S.; Nielsen, M.; Bachmann, S.; Jørgensen, K. A. *Synthesis.* **2005**, 2234–2238.

(23) Ferris, L.; Haigh, D.; Moody, C. J. *J. Chem. Soc. - Perkin Trans. 1* **1996**, 2885–2888.

(24) Nicoud, J.; Kagan, H. B. *Tetrahedron Lett.* **1971**, 2065–2068.

(25) Morilla, M. E.; Díaz-Requejo, M. M.; Belderrain, T. R.; Nicasio, M. C.; Trofimenko, S.; Pérez, P. J. *Chem. Commun.* **2002**, *38*, 2998–2999.

(26) Bachmann, S.; Fielenbach, D.; Jørgensen, K. A. *Org. Biomol. Chem.* **2004**, *2*, 3044–3049.

(27) Maier, T. C.; Fu, G. C. *J. Am. Chem. Soc.* **2006**, *128*, 4594–4595.

(28) Zhang, X.; Ma, M.; Wang, J. *Arkivoc* **2003**, *2*, 84–91.

(29) Hyde, S.; Veliks, J.; Liégault, B.; Grassi, D.; Taillefer, M.; Gouverneur, V. *Angew. Chem. Int. Ed.* **2016**, *55*, 3785–3789.

(30) Zhang, Y. Z.; Zhu, S. F.; Wang, L. X.; Zhou, Q. L. *Angew. Chem. Int. Ed.* **2008**, *47*, 8496–8498.

(31) García, C. F.; McKervey, M. A.; Ye, T. *Chem. Commun.* **1996**, 1465–1466.

(32) Buck, R. T.; Doyle, M. P.; Drysdale, M. J.; Ferris, L.; Forbes, D. C.; Haigh, D.; Moody, C. J.; Pearson, N. D.; Zhou, Q. L. *Tetrahedron Lett.* **1996**, *37*, 7631–7634.

(33) Davies, H. M. L.; Hansen, T.; Rutberg, J.; Bruzinski, P. *Tetrahedron Lett.* **1997**, *38*, 1741–1744.

(34) Lu, C. D.; Liu, H.; Chen, Z. Y.; Hu, W. H.; Mi, A. Q. *Org. Lett.* **2005**, *7*, 83–86.

(35) Guo, X.; Hu, W. *Acc. Chem. Res.* **2013**, *46*, 2427–2440.

(36) Jiang, J.; Xu, H. D.; Xi, J. B.; Ren, B. Y.; Lv, F. P.; Guo, X.; Jiang, L. Q.; Zhang, Z. Y.; Hu, W. H. *J. Am. Chem. Soc.* **2011**, *133*, 8428–8431.

(37) Xiao, G.; Chen, T.; Ma, C.; Xing, D.; Hu, W. *Org. Lett.* **2018**, *20*, 4531–4535.

(38) Ma, B.; Wu, Z.; Huang, B.; Liu, L.; Zhang, J. *Chem. Commun.* **2016**, *52*, 9351–9354.

(39) Jing, C.; Xing, D.; Hu, W. *Chem. Commun.* **2014**, *50*, 951–953.

(40) Alavala, G. K. R.; Sajjad, F.; Shi, T.; Kang, Z.; Ma, M.; Xing, D.; Hu, W. *Chem. Commun.* **2018**, *54*, 12650–12653.

(41) Liu, K.; Zhu, C.; Min, J.; Peng, S.; Xu, G.; Sun, J. *Angew. Chem. Int. Ed.* **2015**, *54*, 12962–12967.

(42) Medvedev, J. J.; Meleshina, M. V.; Panikorovskii, T. L.; Schneider, C.; Nikolaev, V. A. *Org. Biomol. Chem.* **2015**, *13*, 9107–9117.

(43) Medvedev, J. J.; Galkina, O. S.; Klinkova, A. A.; Giera, D. S.; Hennig, L.; Schneider, C.; Nikolaev, V. A. *Org. Biomol. Chem.* **2015**, *13*, 2640–2651.

(44) Xu, X.; Han, X.; Yang, L.; Hu, W. *Eur. J. Chem.* **2009**, *15*, 12604–12607.

(45) Jing, C.; Xing, D.; Qian, Y.; Shi, T.; Zhao, Y.; Hu, W. *Angew. Chem. Int. Ed.* **2013**, *52*, 9289–9292.

(46) Hunter, A. C.; Schlitzer, S. C.; Stevens, J. C.; Almutwalli, B.; Sharma, I. *J. Org. Chem.* **2018**, *83*, 2744–2752.

(47) Hunter, A.; Chinthapally, K.; Bain, A. I.; Stevens, J. C.; Sharma, I. *Adv. Synth. Catal.* **2014**, *361,* 2951-2958.

(48) Hunter, A. C.; Schlitzer, S. C.; Sharma, I. *Chem. Eur. J.* **2016**, *22*, 16062–16065.

(49) Urabe, F.; Miyamoto, S.; Takahashi, K.; Ishihara, J.; Hatakeyama, S. *Org. Lett.* **2014**, *16*, 1004–1007.

(50) Meerwein, H.; Rathjen, H.; Werner, H. *Ber. Dtsch. Chem. Ges.* **1942**, *75*, 1610–1622.

(51) Demonceau, A.; Noels, A. F.; Hubert, A. J.; Teyssié, P. *Bull. Soc. Chim. Belg*. **1984**, *93,* 945–948.

(52) Demonceau, A.; Noels, A. F.; Hubert, A. J.; Teyssié, P. *J. Chem. Soc. Chem. Commun.* **1981**, *14*, 688–689.

(53) Johansen, M. B.; Kerr, M. A. *Org. Lett.* **2010**, *12*, 4956–4959.

(54) Vorobyeva, D. V.; Osipov, S. N. *Synthesis.* **2018**, *50*, 227–240.

(55) Ciszewski, L. W.; Durka, J.; Gryko, D. *Org. Lett.* **2019**, *21*, 7028–7032.

(56) Gao, X.; Wu, B.; Yan, Z.; Zhou, Y. G. *Org. Biomol. Chem.* **2016**, *14*, 8237–8240.

(57) Gao, X.; Wu, B.; Huang, W. X.; Chen, M. W.; Zhou, Y. G. *Angew. Chem. Int. Ed.*

2015, *54*, 11956–11960.

(58) Lv, H.; Xu, W. L.; Lin, K.; Shi, J.; Yi, W. *Eur. J. Org. Chem.* **2016**, *34*, 5637–5641.

(59) Ma, B.; Wu, Z.; Huang, B.; Liu, L.; Zhang, J. *Chem. Commun.* **2016**, *52*, 9351–9354.

(60) Jia, S.; Lei, Y.; Song, L.; Krishna Reddy, A. G.; Xing, D.; Hu, W. *Adv. Synth. Catal.* **2017**, *359*, 58–63.

(61) Dong, K.; Pei, C.; Zeng, Q.; Qiu, L.; Hu, W.; Qian, Y.; Xu, X. *Chem. Commun.* **2019**, *55*, 6393–6396.

(62) Song, L.; Ni, D.; Jia, S.; Pi, R.; Dong, S.; Yang, F.; Tang, J.; Liu, S. *Org. Lett.* **2020**, *22*, 1846–1851.

(63) Li, Y.; Tang, Z.; Zhang, J.; Liu, L. *Chem. Commun.* **2020**, *56*, 8202–8205.

(64) Bhat, A.; Alavi, S.; Grover, H. *Org. Lett.* **2020**, *22*, 224–229.

(65) Hack, D.; Blümel, M.; Chauhan, P.; Philipps, A. R.; Enders, D. *Chem. Soc. Rev.* **2015**, *44*, 6059–6093.

(66) Bhat, A.; Tucker, N.; Lin, J.-B.; Grover, H. *Chem. Commun.* **2021**, *57*, 10556–10559

(67) Chaudhari, T. Y.; Tandon, V. *Org. Biomol. Chem.* **2021**, *19*, 1926–1939.

(68) Mohammadi Ziarani, G.; Moradi, R.; Ahmadi, T.; Lashgari, N. *RSC Adv.* **2018**, *8*, 12069–12103.

Appendix

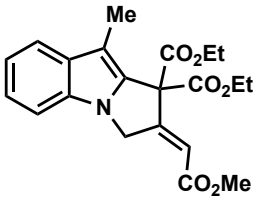
Me
CO2Et
CO2Et
N
CO2Me

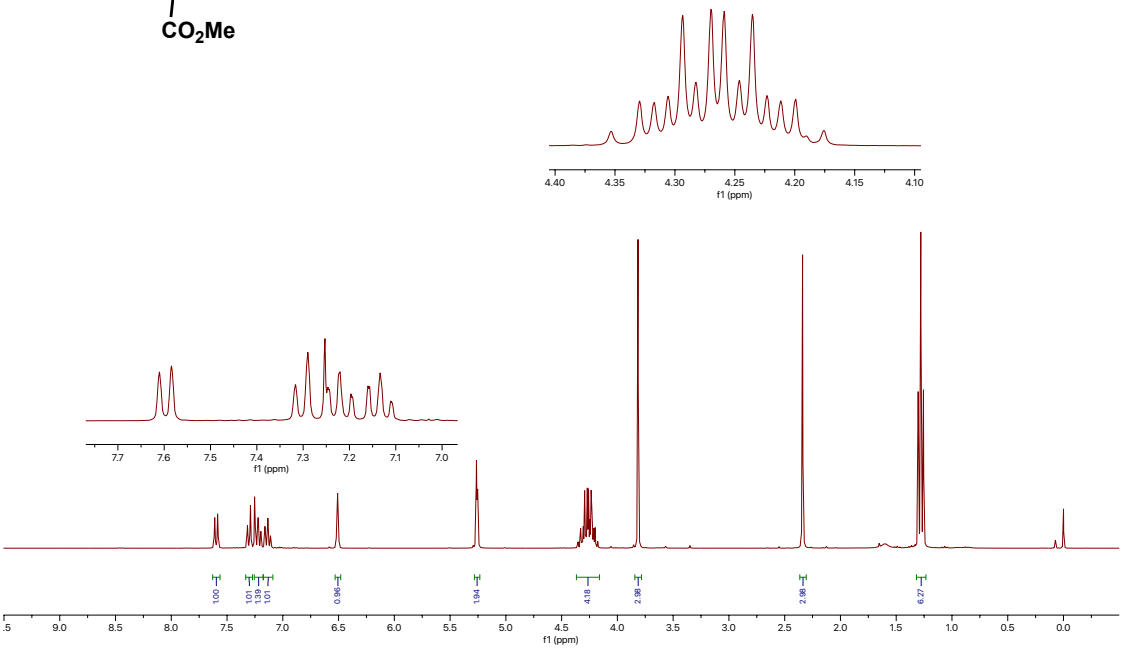
f1 (ppm)

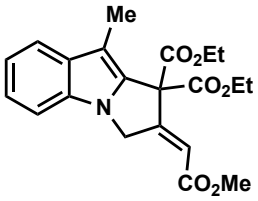
Me
CO2Et
CO2Et
N
CO2Me

f1 (ppm)

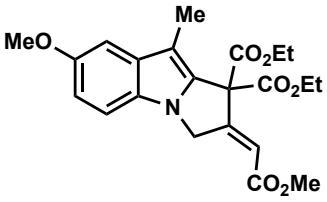
Me
MeO
CO2Et
CO2Et
N
CO2Me

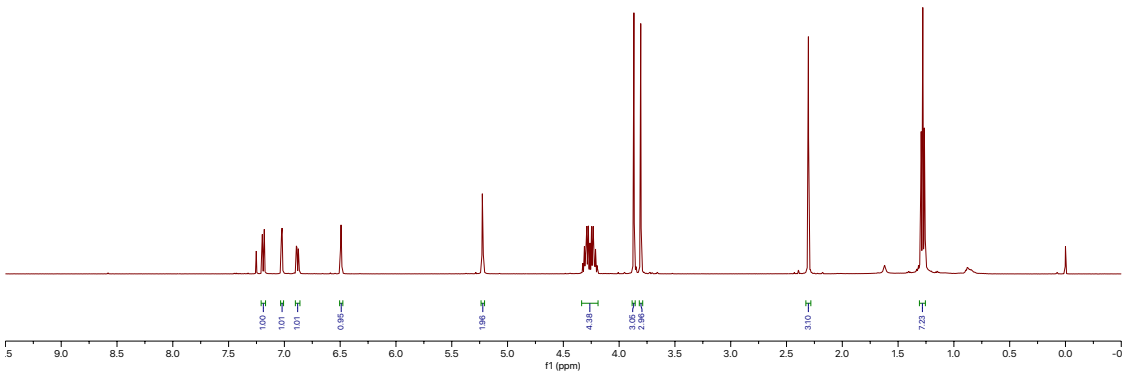
1.00
1.01
1.01
0.95
1.96
4.38
3.05
2.96
3.10
7.23
f1 (ppm)


166.90
166.05
156.38
154.16
133.63
133.02
127.69
119.14
112.39
110.60
105.60
101.35
64.32
62.89
56.03
51.87
48.96
14.07
9.10

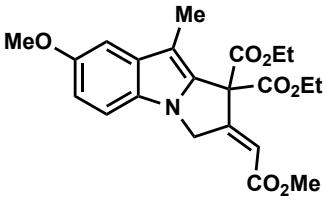
Me
MeO
CO2Et
CO2Et
N
CO2Me

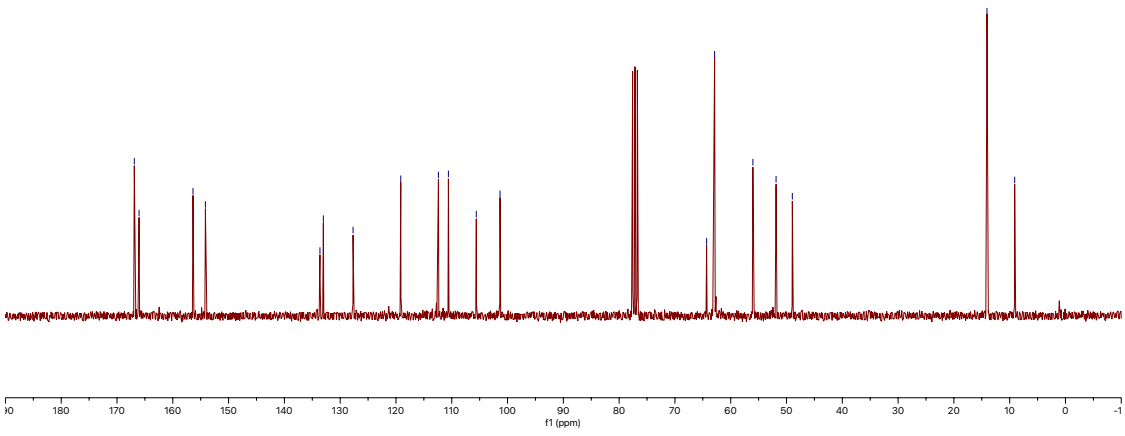
f1 (ppm)

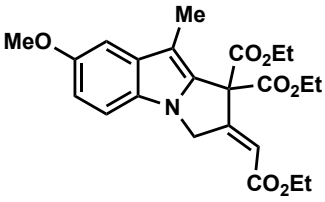
Me
MeO
CO2Et
CO2Et
N
CO2Et

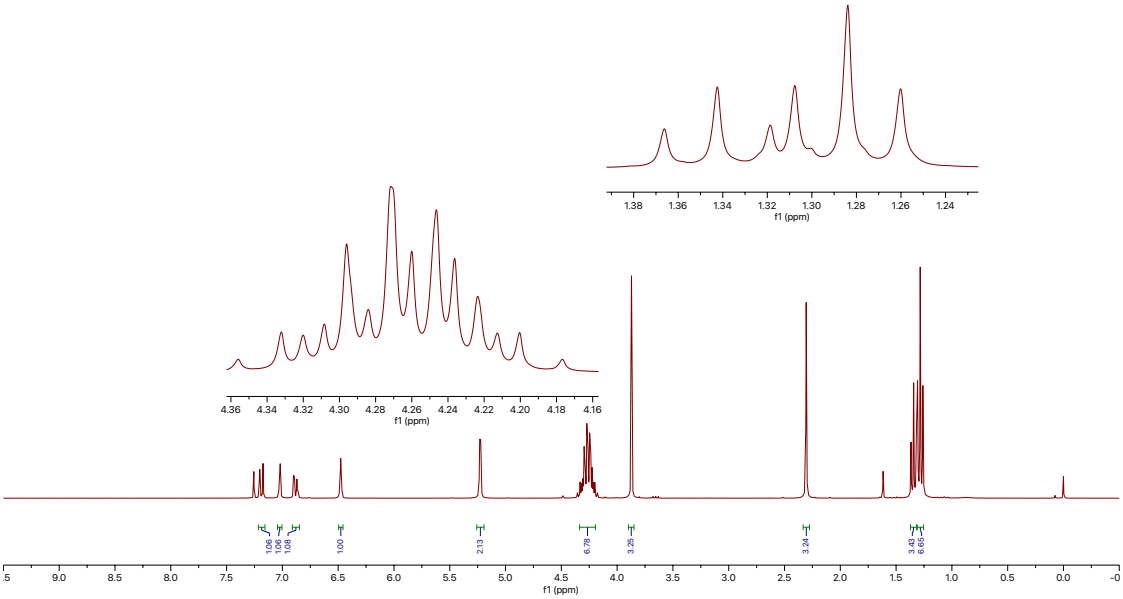
1.38 1.36 1.34 1.32 1.30 1.28 1.26 1.24
f1 (ppm)
4.36 4.34 4.32 4.30 4.28 4.26 4.24 4.22 4.20 4.18 4.16
f1 (ppm)
1.06 1.06 1.08 1.00 2.13 6.78 3.25 3.24 3.42 6.65
f1 (ppm)

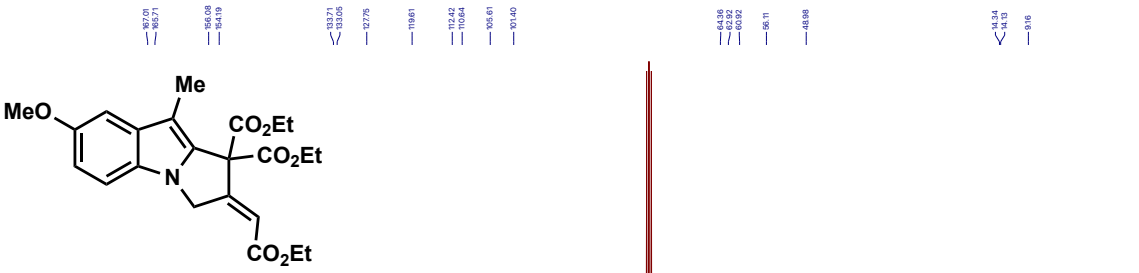
167.01
165.71
156.08
154.19
133.71
133.05
127.75
119.61
112.42
110.64
105.61
101.40
64.36
62.92
60.92
56.11
48.88
14.34
14.13
9.16

Me
MeO
CO2Et
CO2Et
N
CO2Et

180 170 160 150 140 130 120 110 100 90 80 70 60 50 40 30 20 10 0
f1 (ppm)

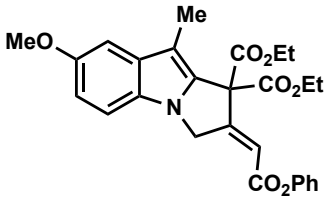
Me
MeO
CO2Et
CO2Et
N
CO2Ph

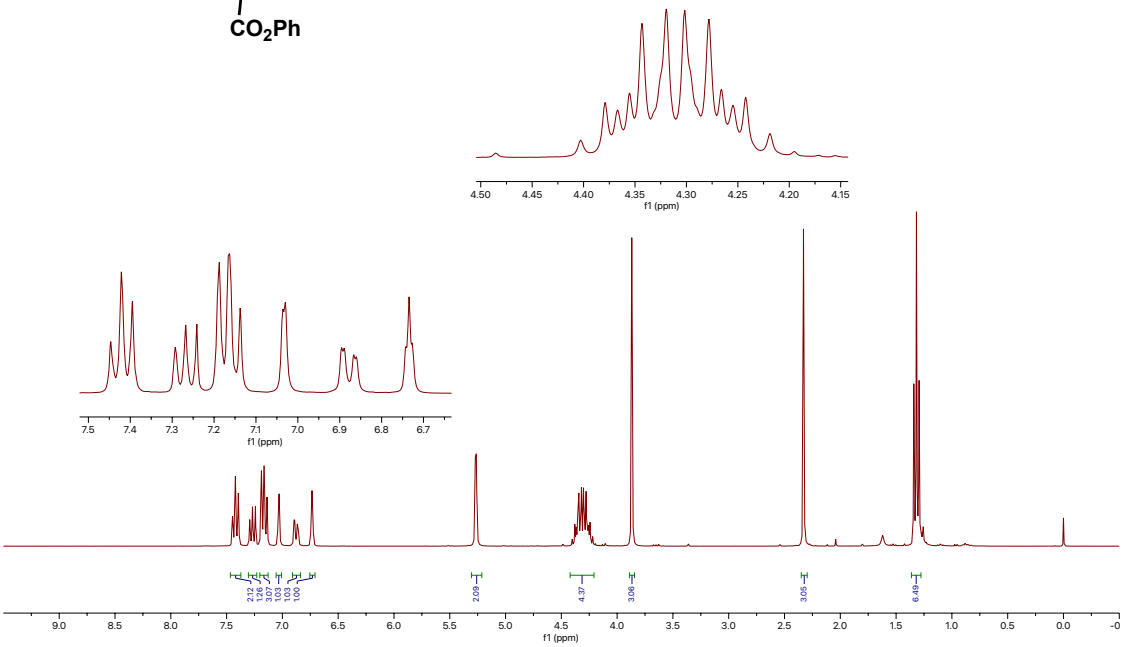
f1 (ppm)

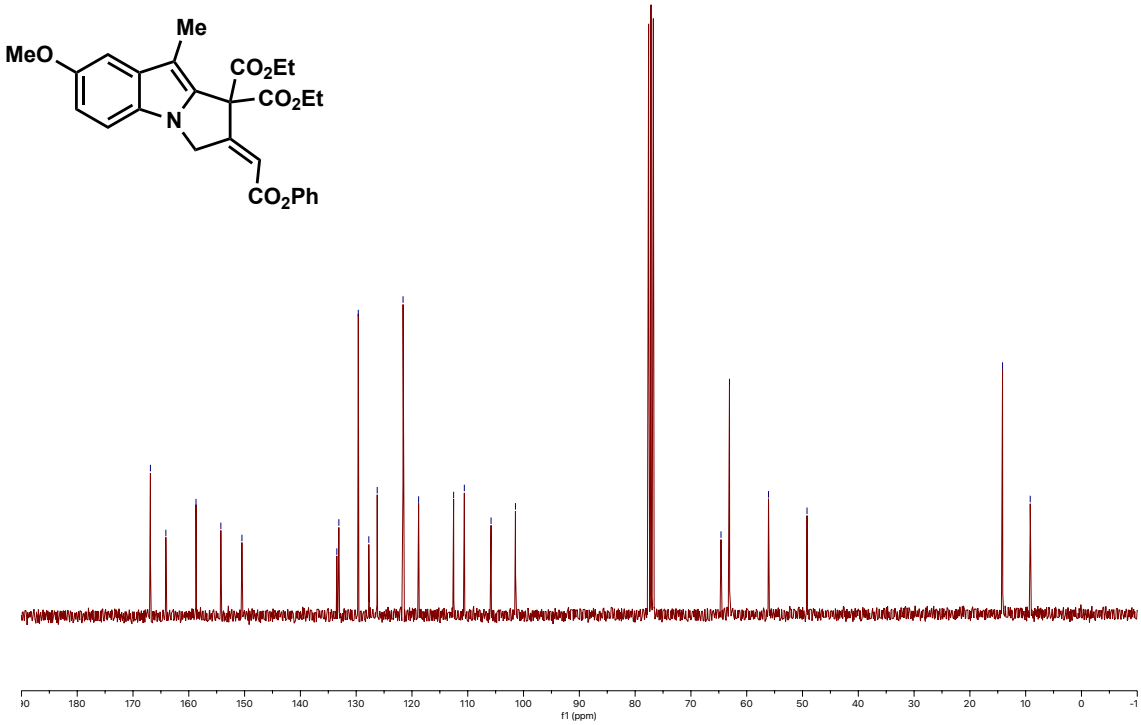
Me
MeO
CO2Et
CO2Et
N
CO2Ph
f1 (ppm)

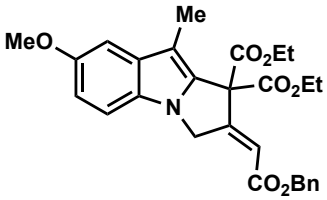
Me
MeO
CO2Et
CO2Et
N
CO2Bn

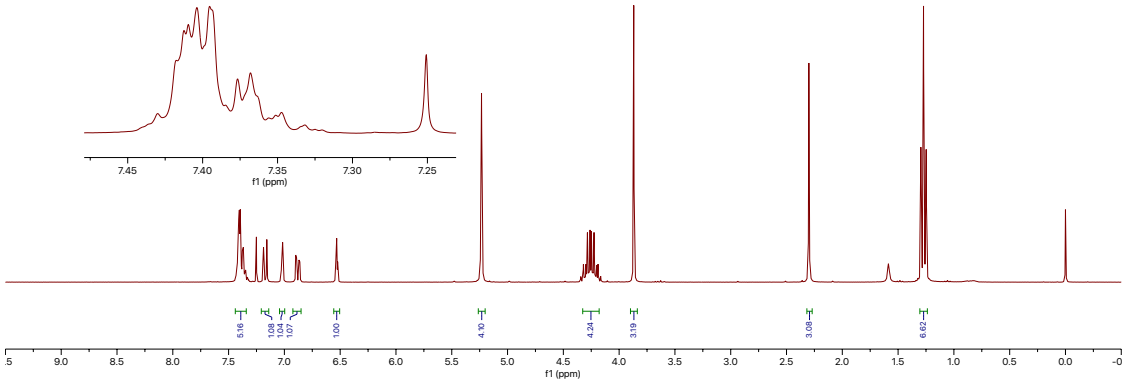
7.45
7.40
7.35
7.30
7.25
f1 (ppm)
5.16
1.08
1.04
1.07
1.00
4.30
4.24
3.19
3.08
6.62
f1 (ppm)

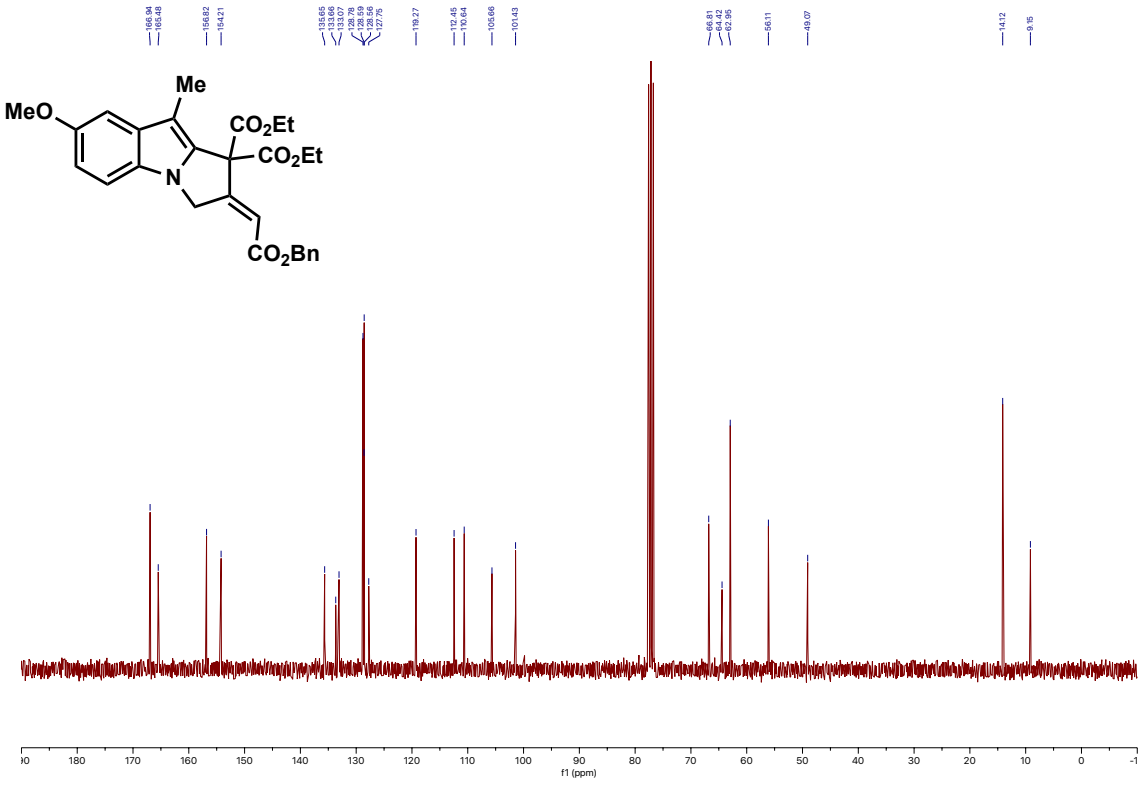
166.94
165.48
156.82
154.21
135.65
133.66
133.07
128.78
128.59
128.58
127.75
119.27
112.45
110.64
105.66
101.43
66.61
64.42
62.96
56.11
49.07
14.12
9.16
Me
MeO
CO2Et
CO2Et
N
CO2Bn
f1 (ppm)

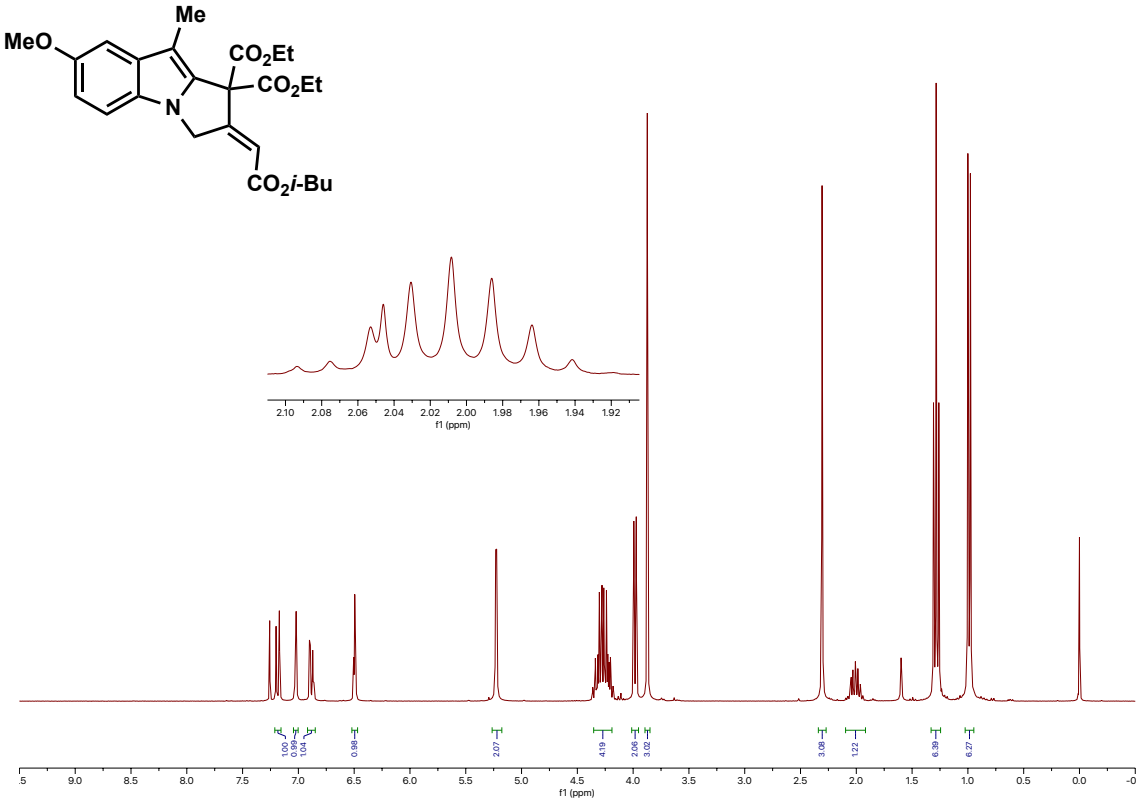
Me
MeO
CO2Et
CO2Et
N
CO2i-Bu
f1 (ppm)

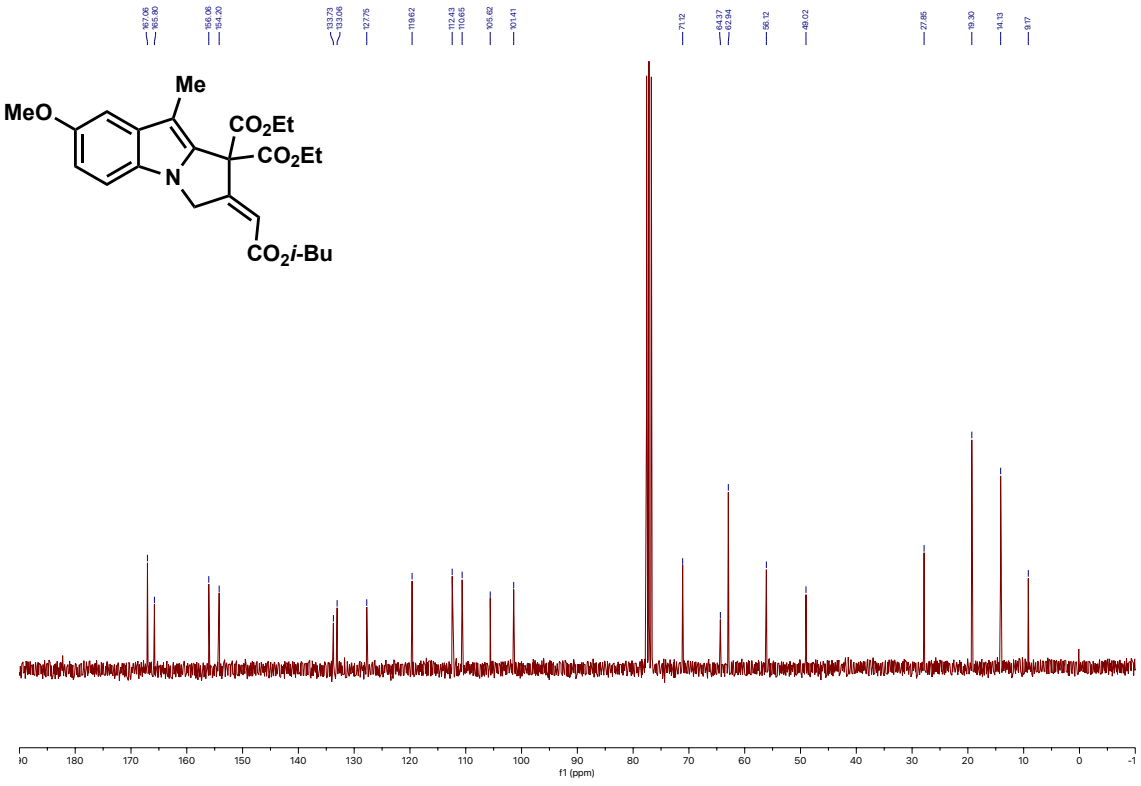
Me
MeO
CO2Et
CO2Et
N
CO2i-Bu
f1 (ppm)

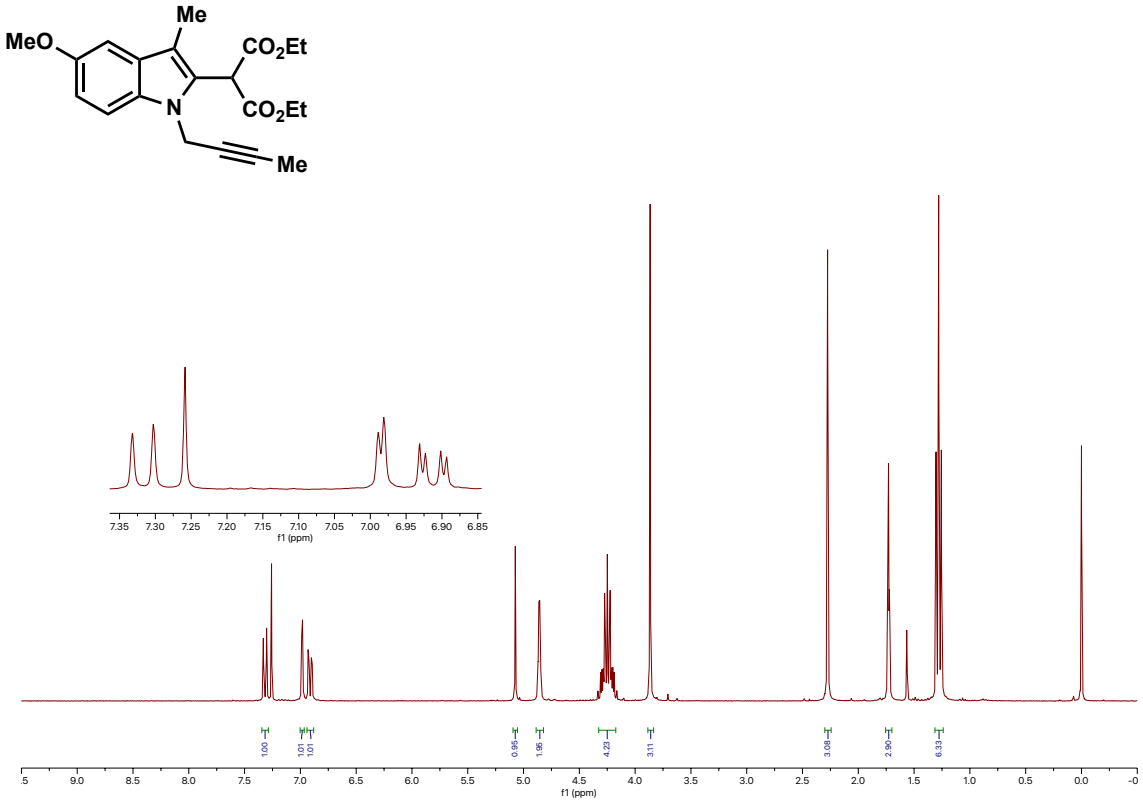
Me
MeO
CO2Et
CO2Et
N
Me
f1 (ppm)

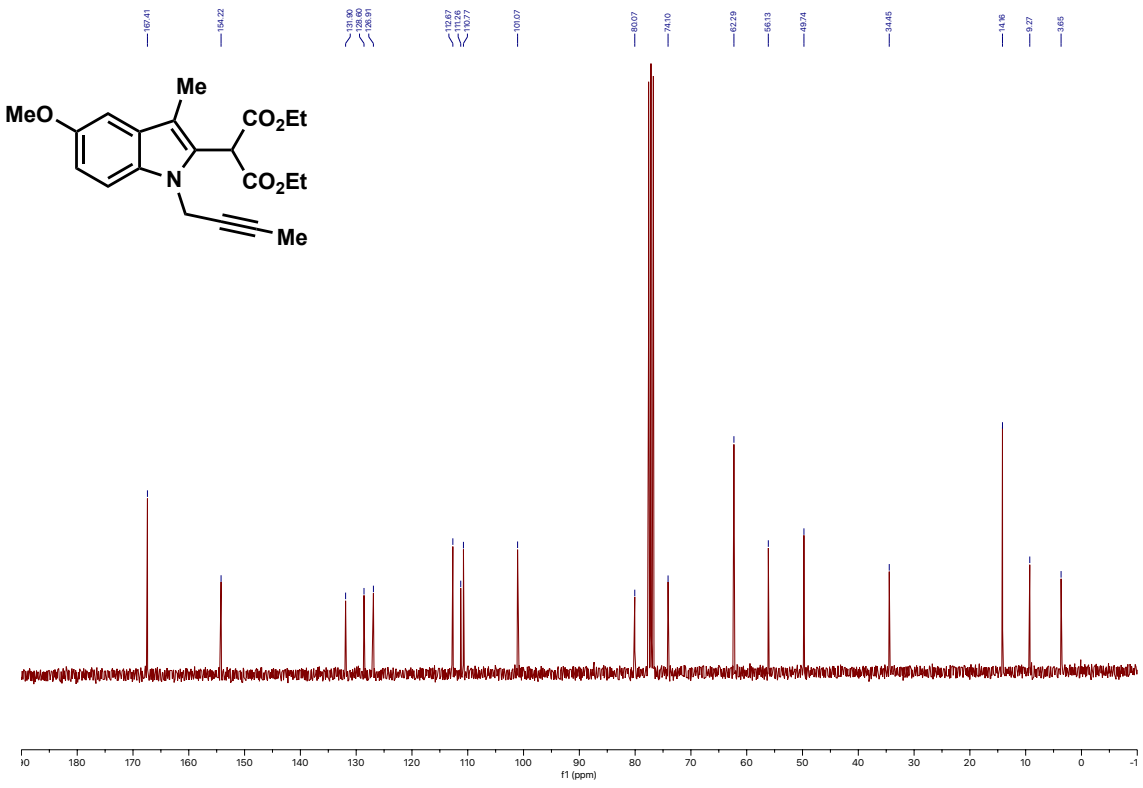
Me
MeO
CO2Et
CO2Et
N
Me
f1 (ppm)

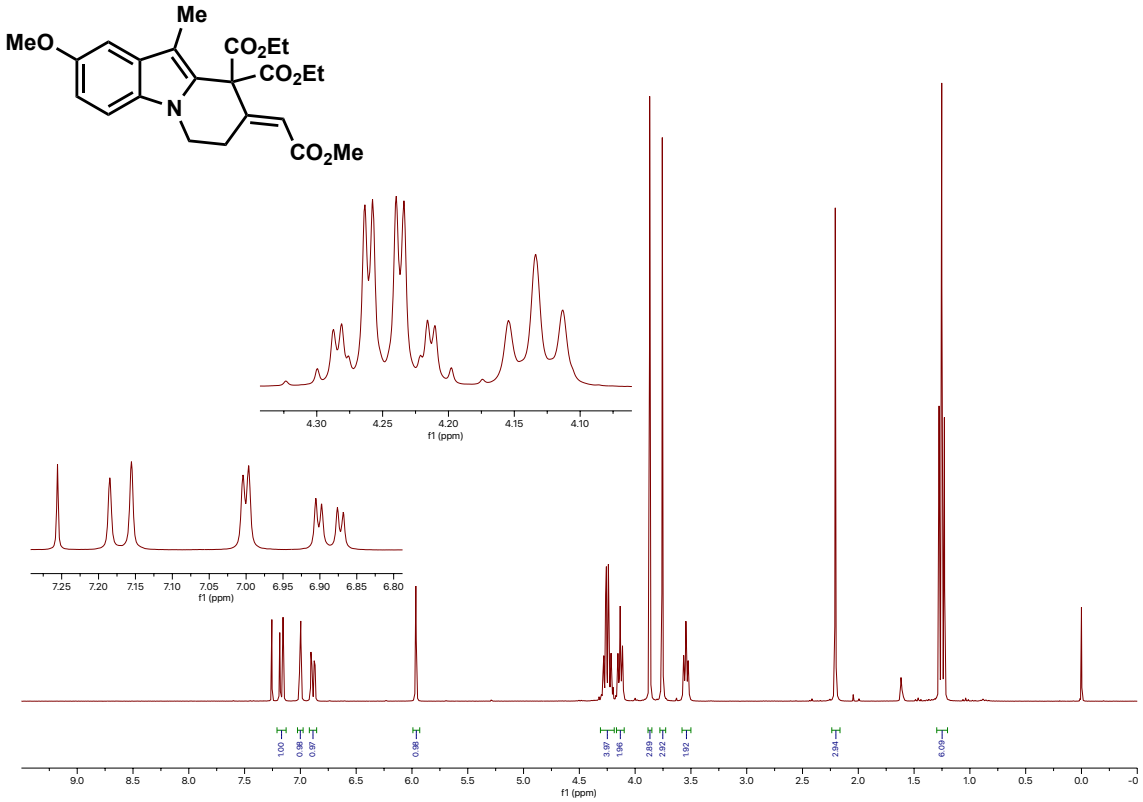
Me
MeO
CO2Et
CO2Et
N
CO2Me
f1 (ppm)

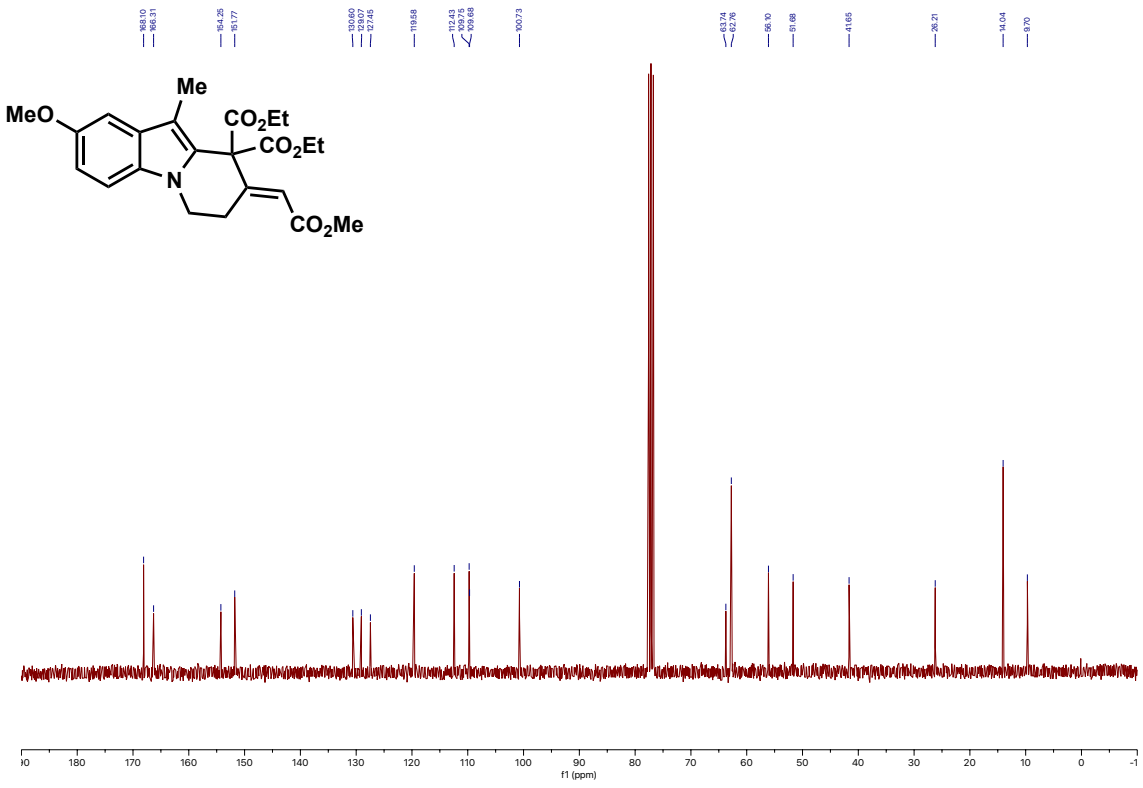
Me
MeO
CO2Et
CO2Et
N
CO2Me
f1 (ppm)

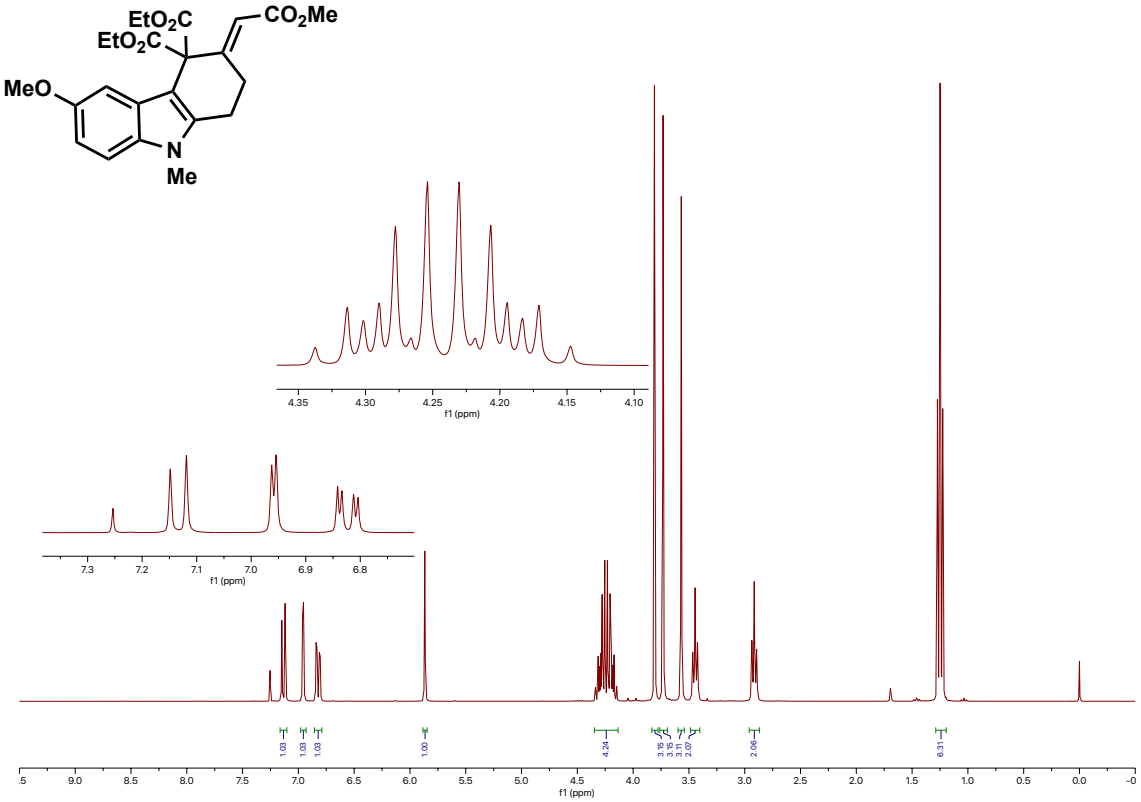
EtO2C
EtO2C
CO2Me
MeO
N
Me
f1 (ppm)

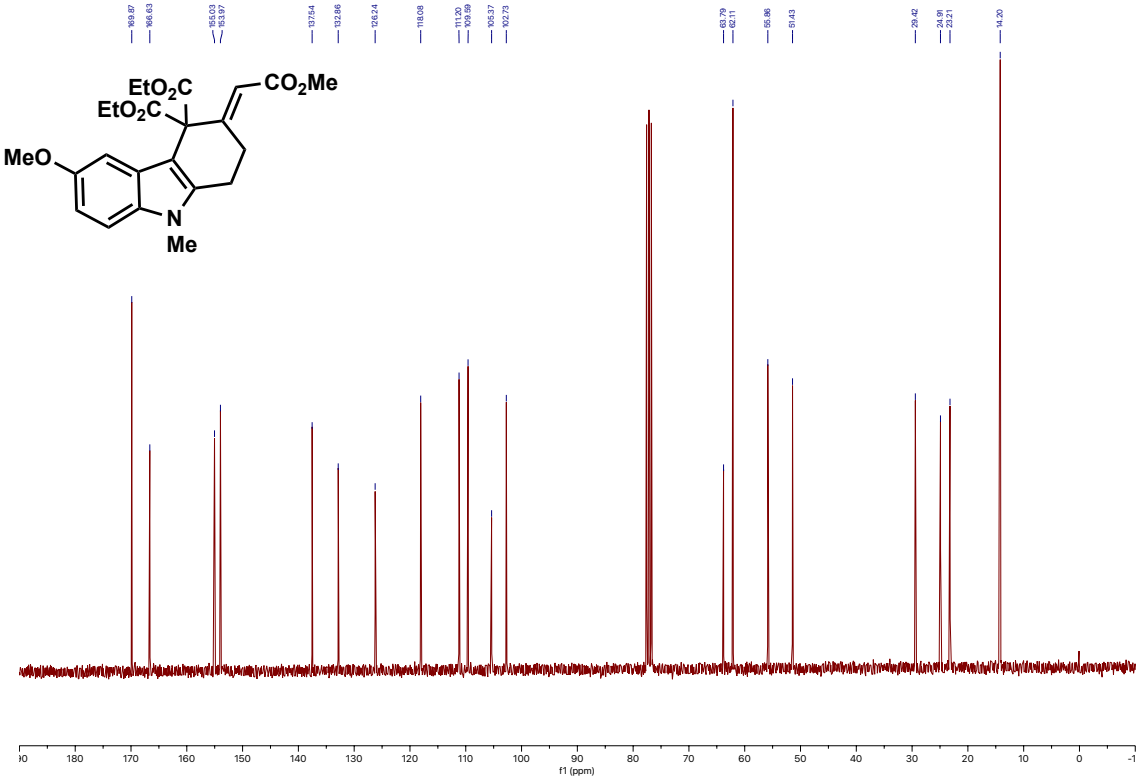
EtO2C
EtO2C
CO2Me
MeO
N
Me
f1 (ppm)

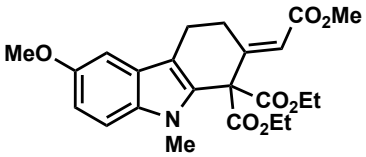
MeO
CO2Me
CO2Et
CO2Et
N
Me

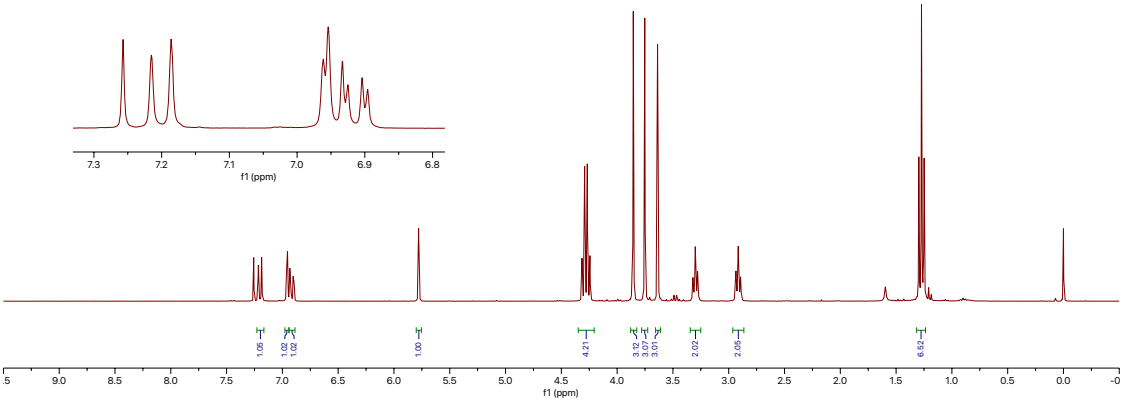
7.3
7.2
7.1
7.0
6.9
6.8
f1 (ppm)
1.05
1.02
1.02
1.00
4.21
3.12
3.07
3.01
2.02
2.08
6.52
f1 (ppm)

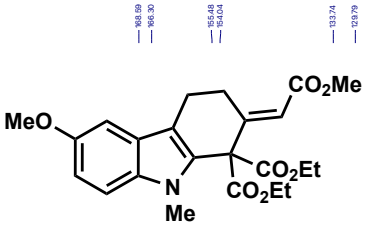
MeO
CO2Me
CO2Et
CO2Et
N
Me

168.89
166.30
155.48
154.04
133.74
129.79
125.58
118.03
112.70
112.54
110.50
100.69
64.63
62.69
55.96
51.39
31.30
25.87
21.70
13.94
f1 (ppm)

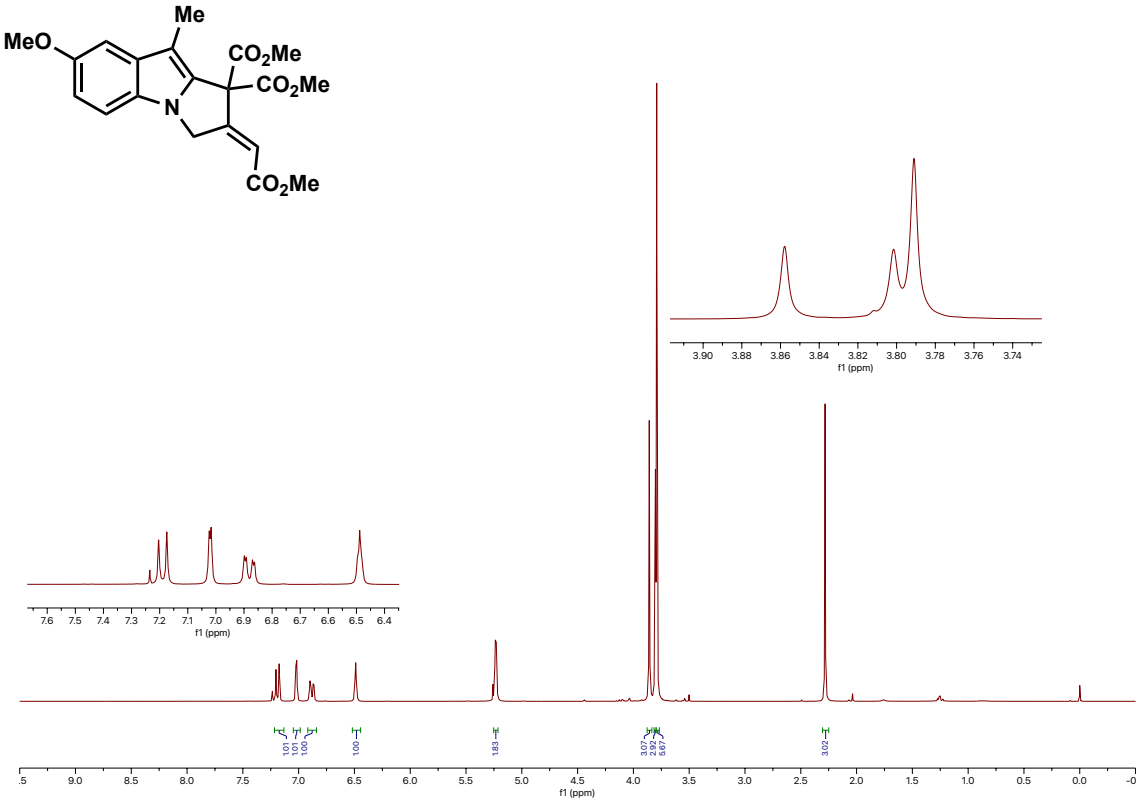
Me
MeO
CO2Me
CO2Me
N
CO2Me
f1 (ppm)

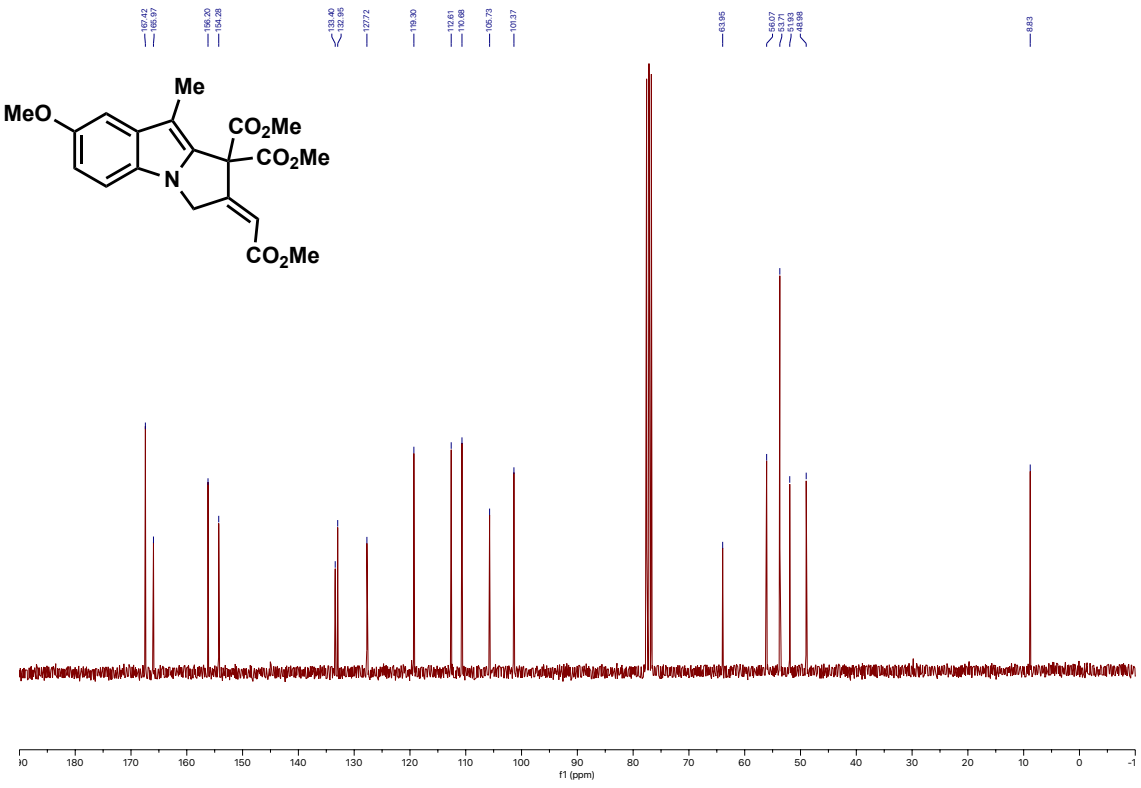
Me
MeO
CO2Me
CO2Me
N
CO2Me
f1 (ppm)

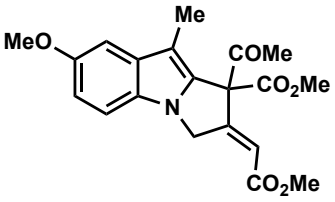
Me
MeO
COMe
CO2Me
N
CO2Me

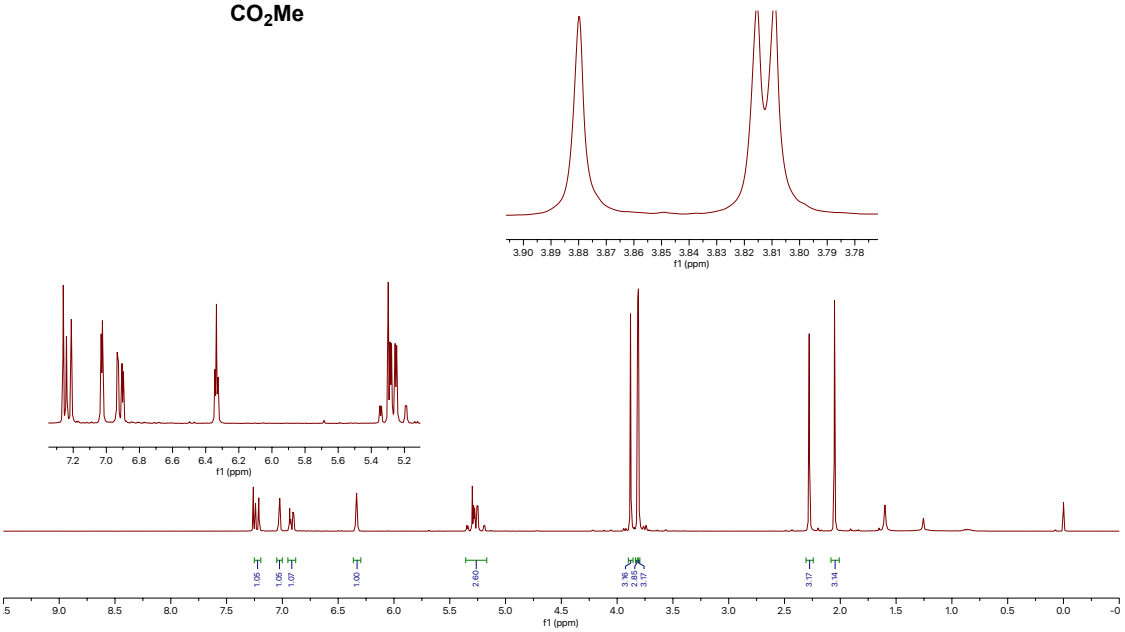
f1 (ppm)

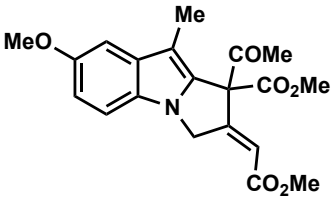
Me
MeO
COMe
CO2Me
N
CO2Me

f1 (ppm)

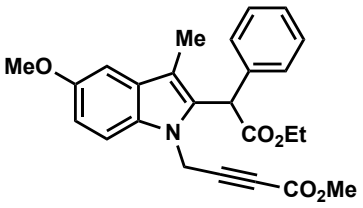
Me
MeO
N
CO2Et
CO2Me

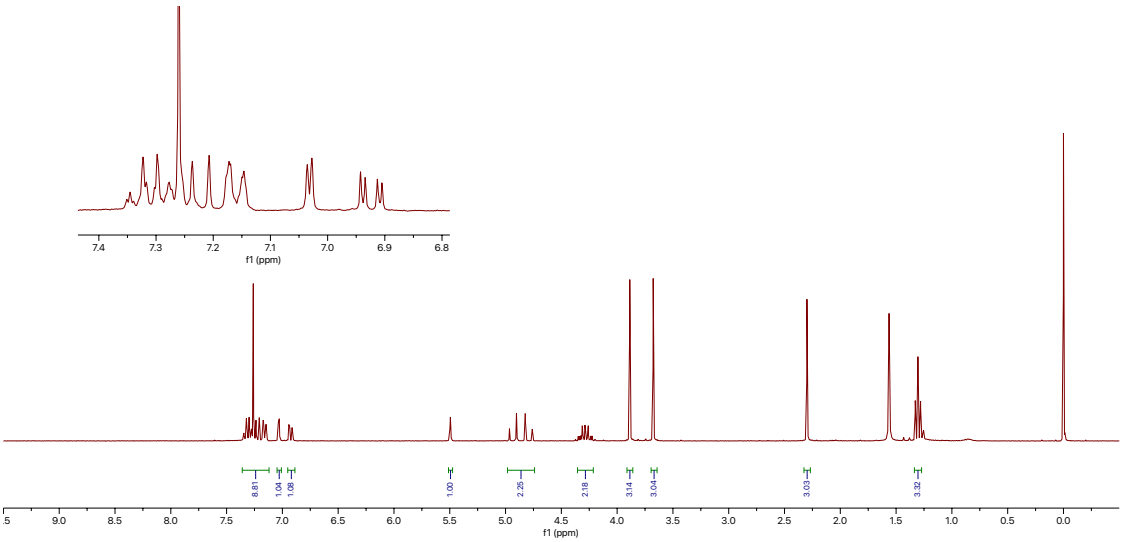
7.4
7.3
7.2
7.1
7.0
6.9
6.8
f1 (ppm)
8.81
1.04
1.08
1.00
2.25
2.18
3.14
3.04
3.03
3.32
f1 (ppm)

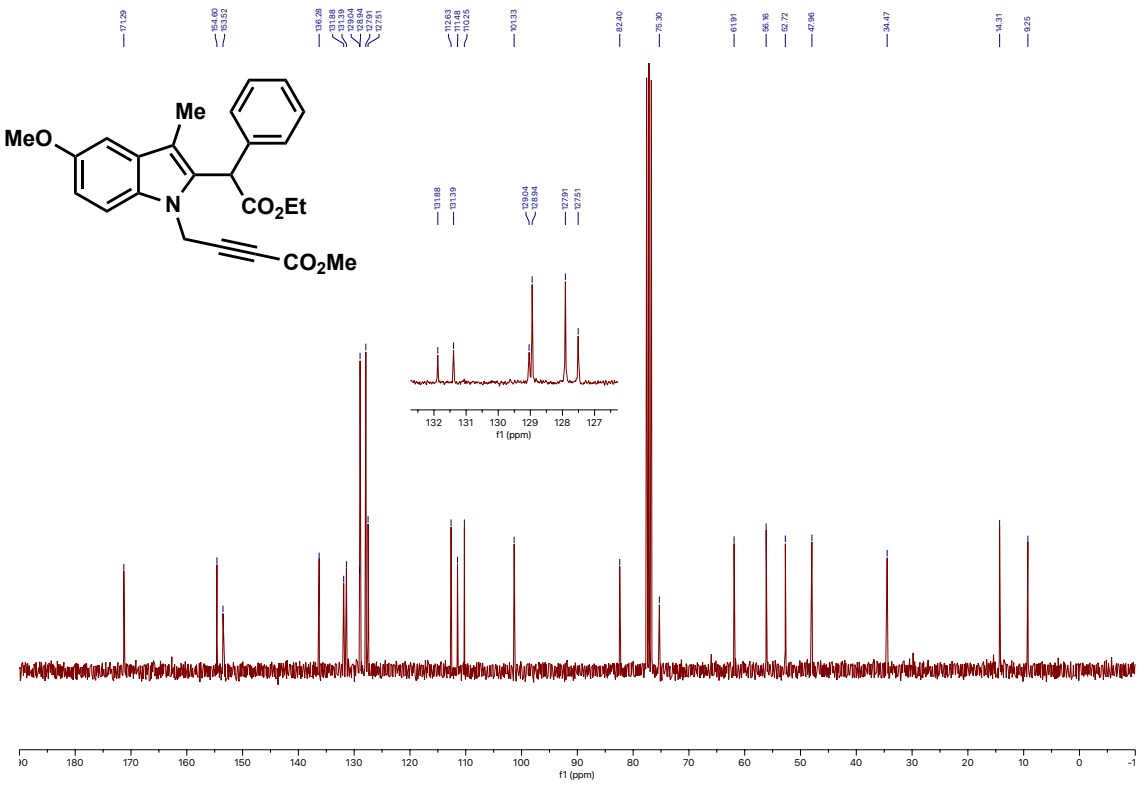
171.29
154.60
153.52
136.28
131.88
131.39
129.04
128.94
127.91
127.51
112.63
111.48
110.25
101.33
82.40
76.30
61.91
56.16
52.72
47.96
34.47
14.31
9.25
Me
MeO
N
CO2Et
CO2Me
131.88
131.39
129.04
128.94
127.91
127.51
132
131
130
129
128
127
f1 (ppm)
f1 (ppm)

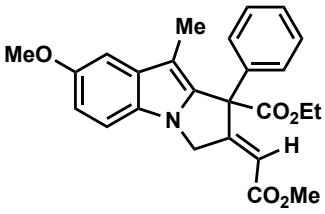
Me
MeO
N
CO2Et
H
CO2Me

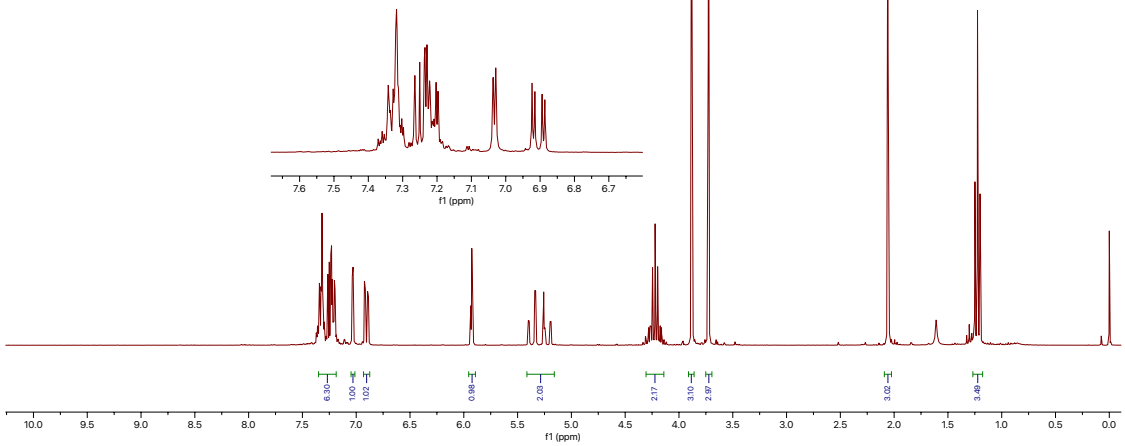
7.6 7.5 7.4 7.3 7.2 7.1 7.0 6.9 6.8 6.7
f1 (ppm)
6.30
1.00
1.02
0.98
2.03
2.17
3.10
2.97
3.02
3.49
10.0 9.5 9.0 8.5 8.0 7.5 7.0 6.5 6.0 5.5 5.0 4.5 4.0 3.5 3.0 2.5 2.0 1.5 1.0 0.5 0.0
f1 (ppm)

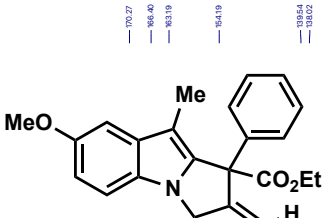
Me
MeO
N
CO2Et
H
CO2Me

170.27
166.40
163.19
154.19
139.54
138.02
133.20
128.84
127.89
127.74
127.52
119.03
112.02
110.61
104.77
101.31
69.53
69.47
66.12
61.69
48.68
14.11
9.01
128.84
127.89
127.74
127.52
129.4 129.2 129.0 128.8 128.6 128.4 128.2 128.0 127.8 127.6 127.4
f1 (ppm)
180 170 160 150 140 130 120 110 100 90 80 70 60 50 40 30 20 10 0
f1 (ppm)

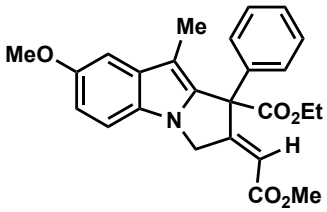
Me
MeO
CO2Et
N
H
CO2Me

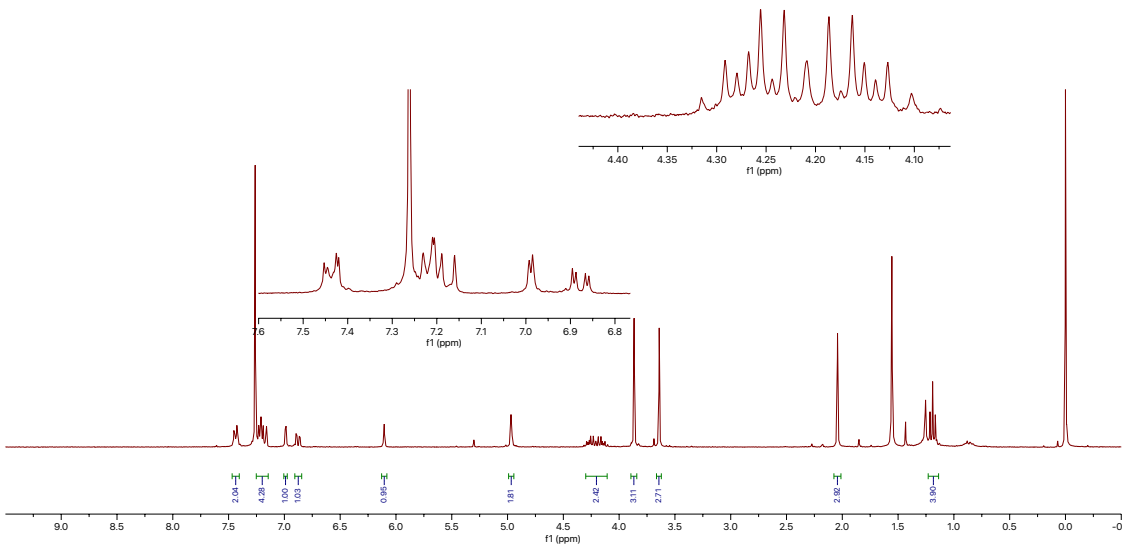
4.40 4.35 4.30 4.25 4.20 4.15 4.10
f1 (ppm)
7.6 7.5 7.4 7.3 7.2 7.1 7.0 6.9 6.8
f1 (ppm)
2.04 4.28 1.00 1.03 0.95 1.81 2.42 3.11 2.71 2.92 3.90
9.0 8.5 8.0 7.5 7.0 6.5 6.0 5.5 5.0 4.5 4.0 3.5 3.0 2.5 2.0 1.5 1.0 0.5 0.0 -0
f1 (ppm)

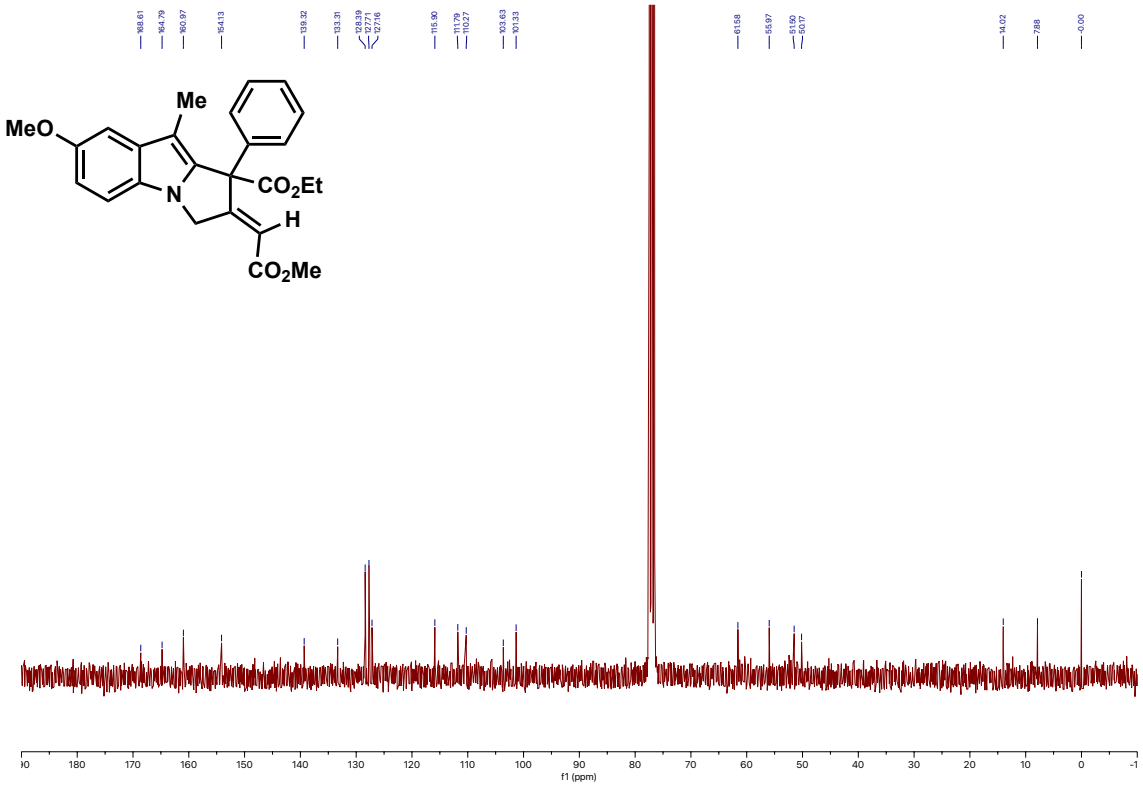
168.61
164.79
160.97
154.13
139.32
133.31
128.39
127.71
127.16
115.90
111.79
110.27
103.63
101.33
61.58
55.97
51.50
50.17
14.02
7.88
-0.00
Me
MeO
CO2Et
N
H
CO2Me
180 170 160 150 140 130 120 110 100 90 80 70 60 50 40 30 20 10 0 -1
f1 (ppm)

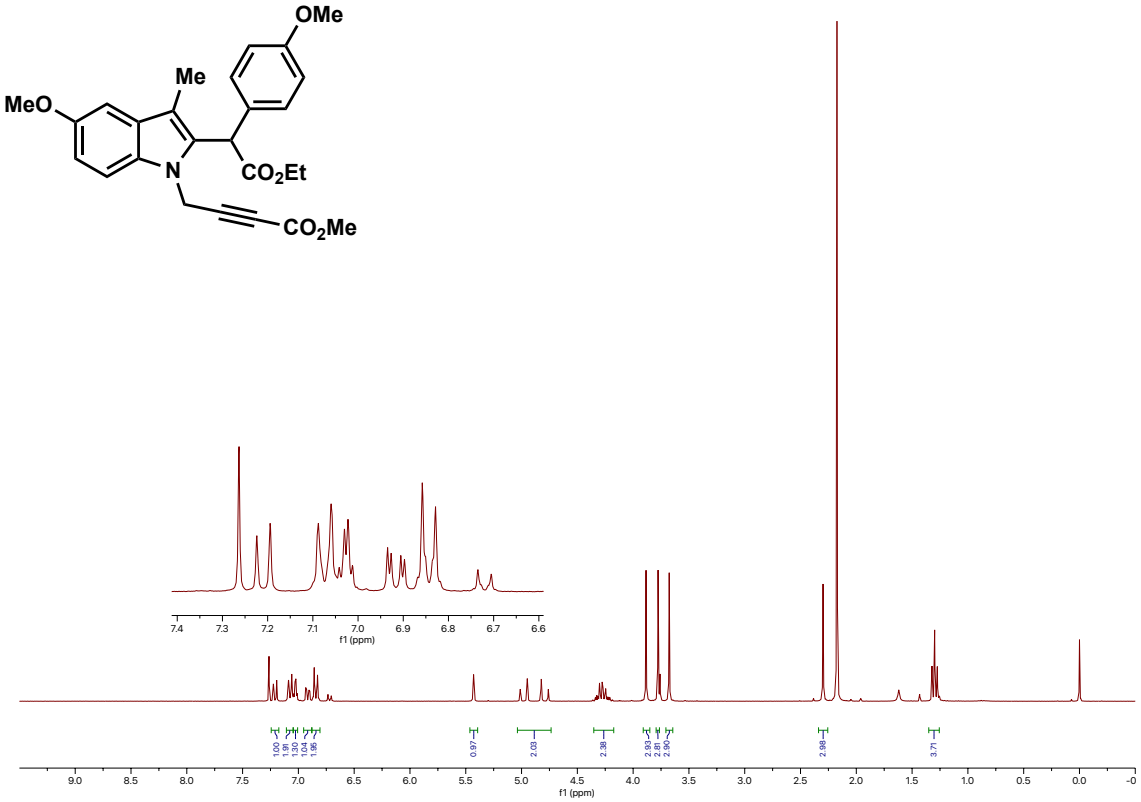
OMe
Me
MeO
N
CO2Et
CO2Me
f1 (ppm)

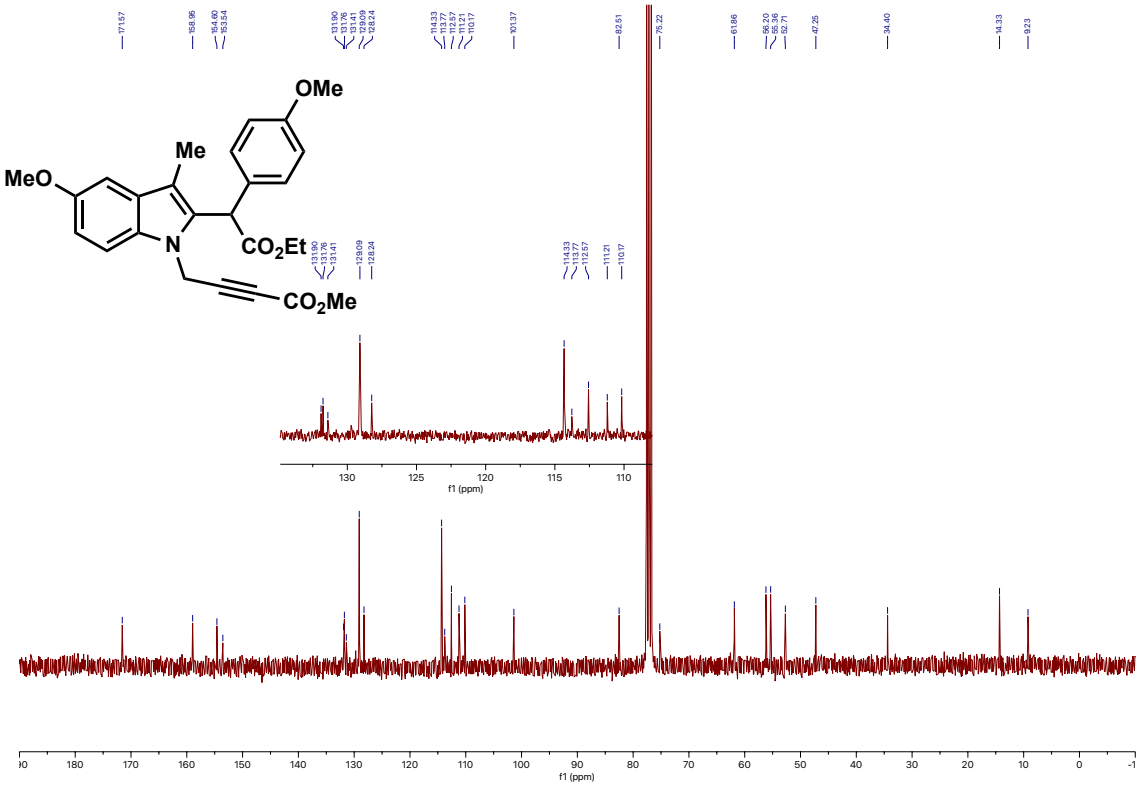
OMe
Me
MeO
N
CO2Et
CO2Me
f1 (ppm)

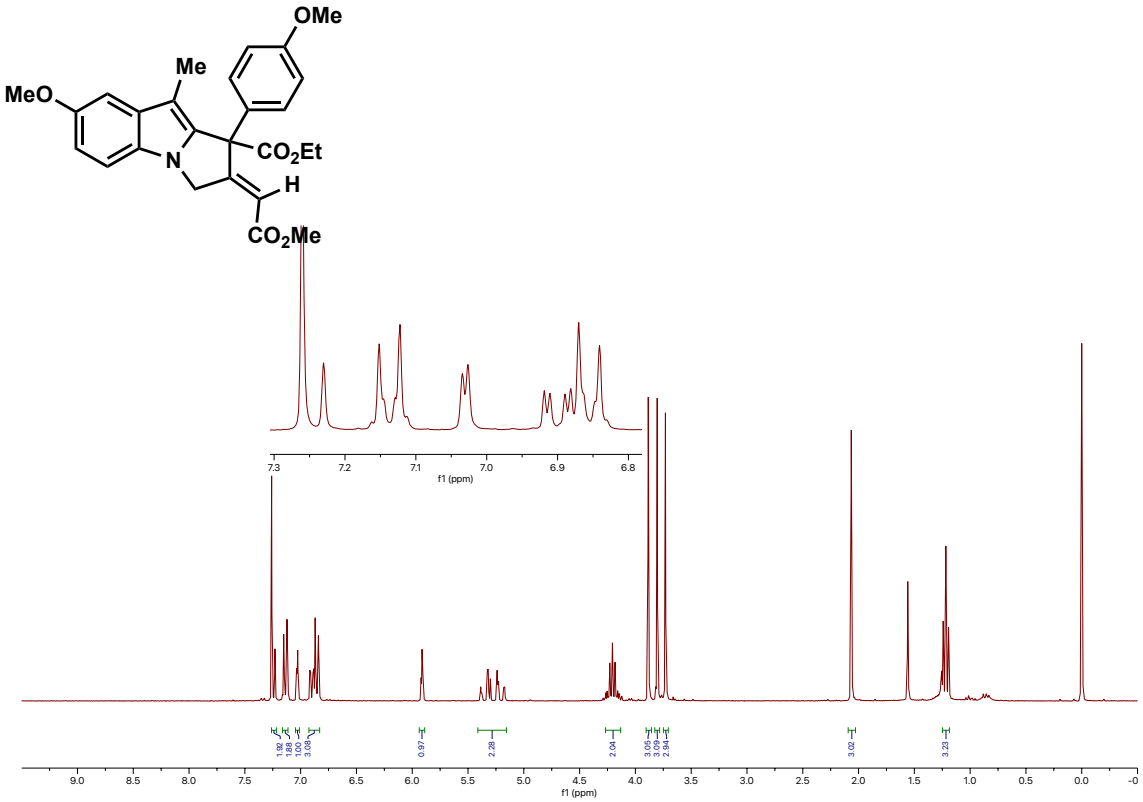
OMe
Me
MeO
N
CO2Et
H
CO2Me
f1 (ppm)

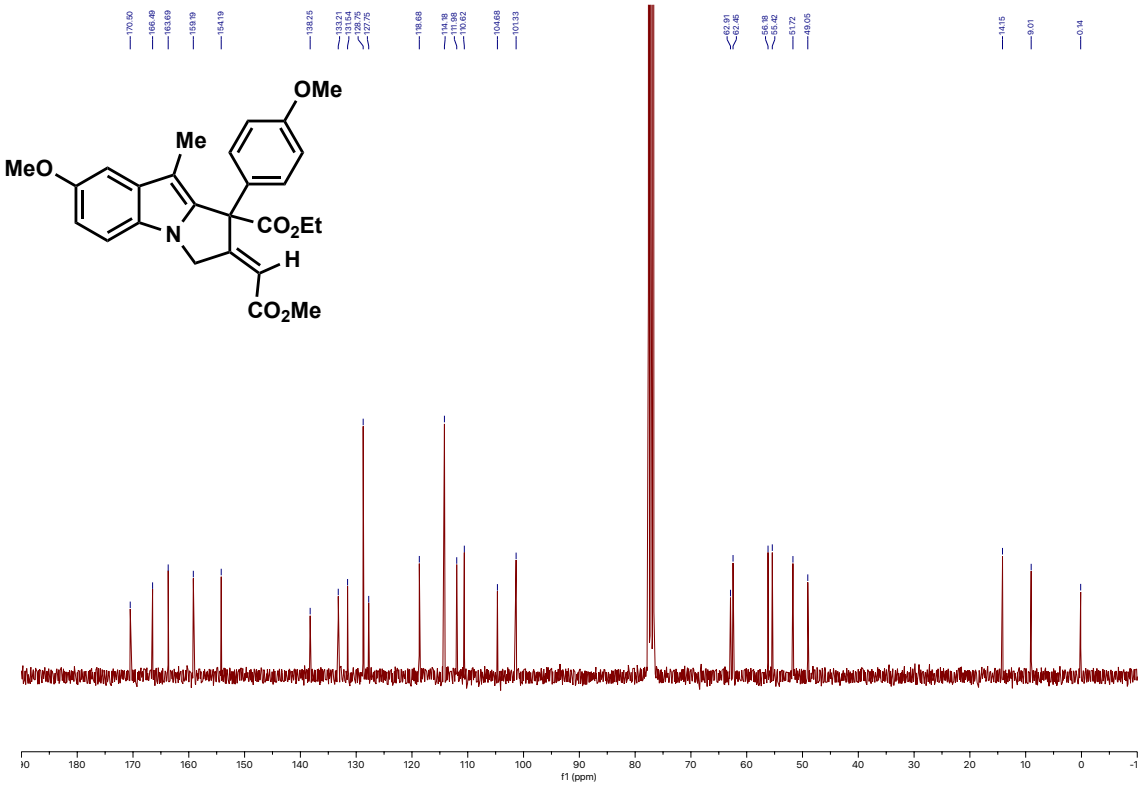
170.50
166.49
163.69
159.19
154.19
138.25
133.21
131.54
129.75
127.75
118.68
114.18
111.98
110.62
104.68
101.33
62.91
62.46
56.18
55.42
51.72
49.05
14.15
9.01
0.14
OMe
Me
MeO
N
CO2Et
H
CO2Me
f1 (ppm)

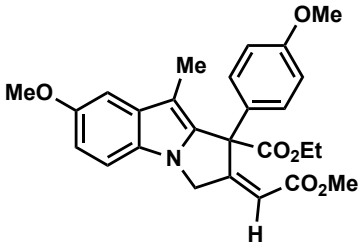
OMe
Me
MeO
N
CO2Et
CO2Me
H

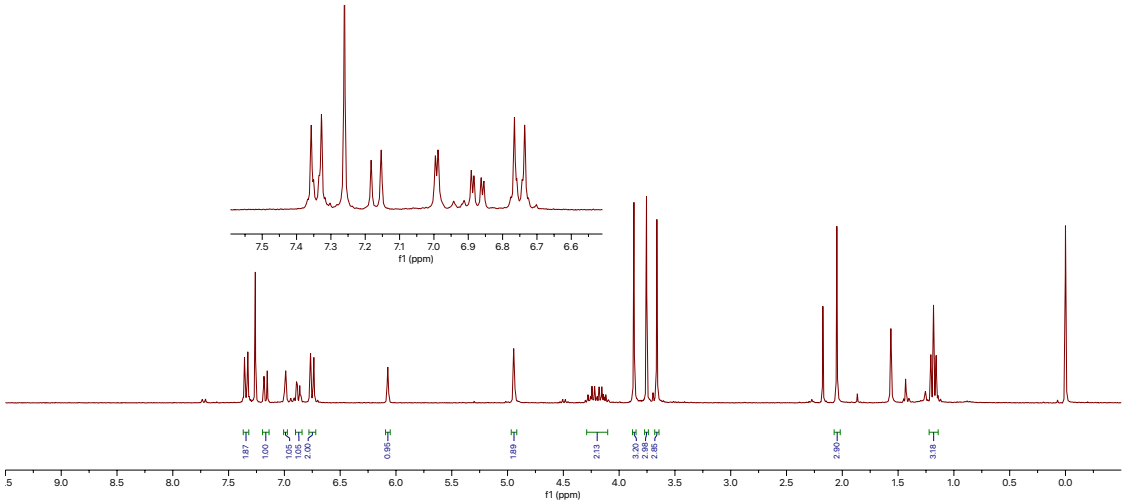
7.5 7.4 7.3 7.2 7.1 7.0 6.9 6.8 6.7 6.6
f1 (ppm)
1.87
1.00
1.05
1.05
2.00
0.95
1.89
2.13
3.20
2.98
2.85
2.90
3.18
f1 (ppm)

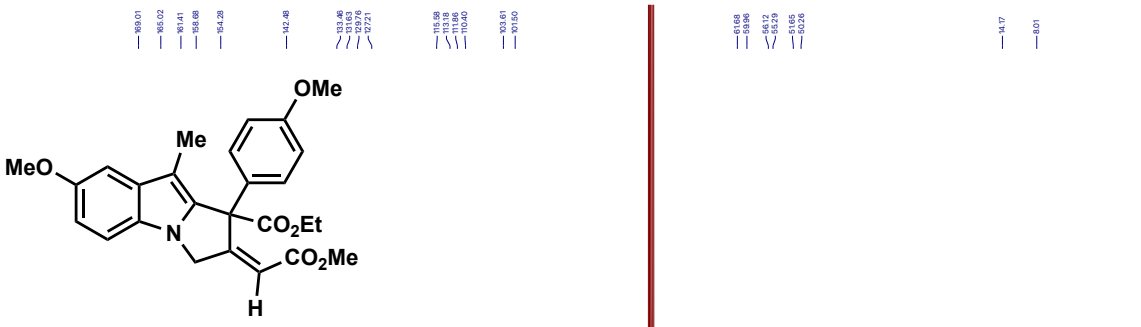
169.01
165.02
161.41
158.68
154.28
142.48
133.46
131.63
130.76
127.21
115.98
113.18
111.66
110.40
103.61
101.50
61.68
59.96
56.12
55.29
51.65
50.26
14.17
8.01

OMe
Me
MeO
N
CO2Et
CO2Me
H

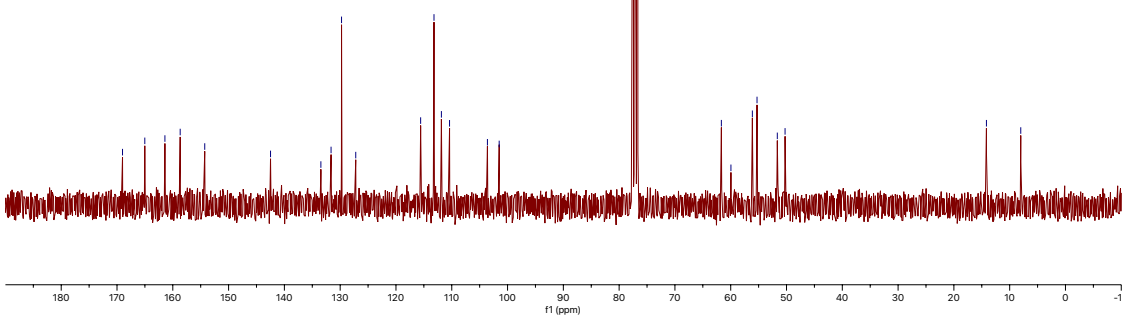
180 170 160 150 140 130 120 110 100 90 80 70 60 50 40 30 20 10 0 -1
f1 (ppm)

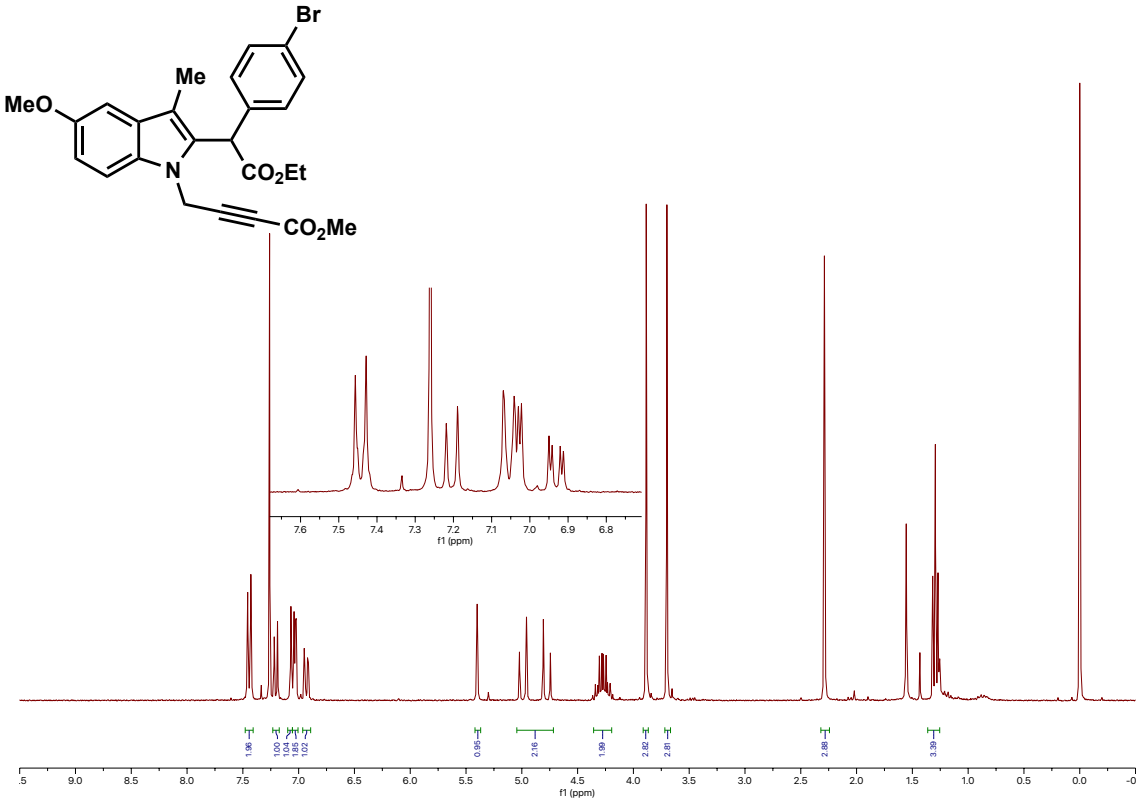
Br
Me
MeO
N
CO2Et
CO2Me
f1 (ppm)

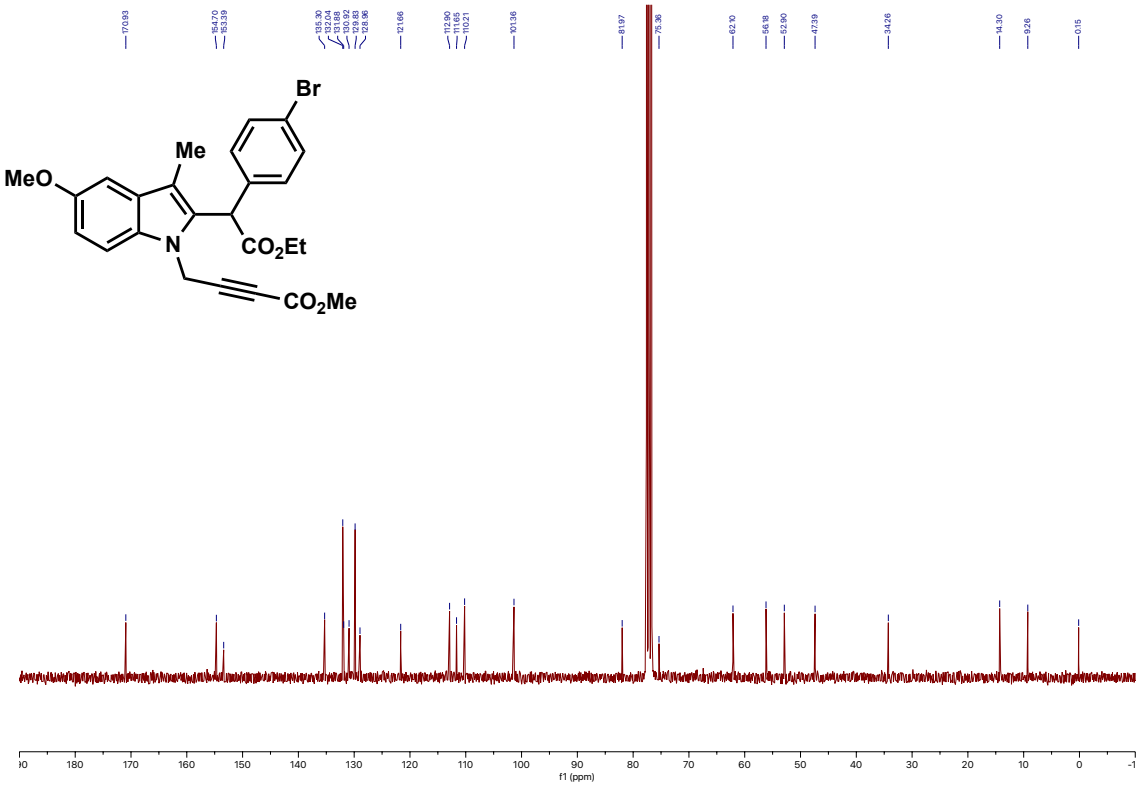
Br
Me
MeO
N
CO2Et
CO2Me
f1 (ppm)

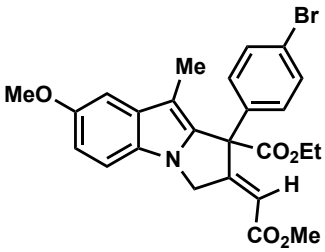
Br
Me
MeO
N
CO2Et
H
CO2Me

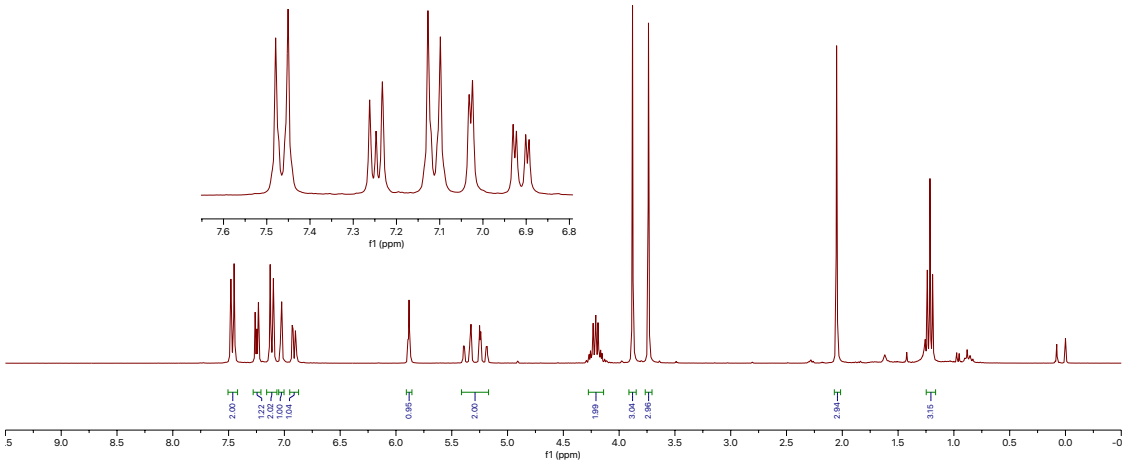
f1 (ppm)

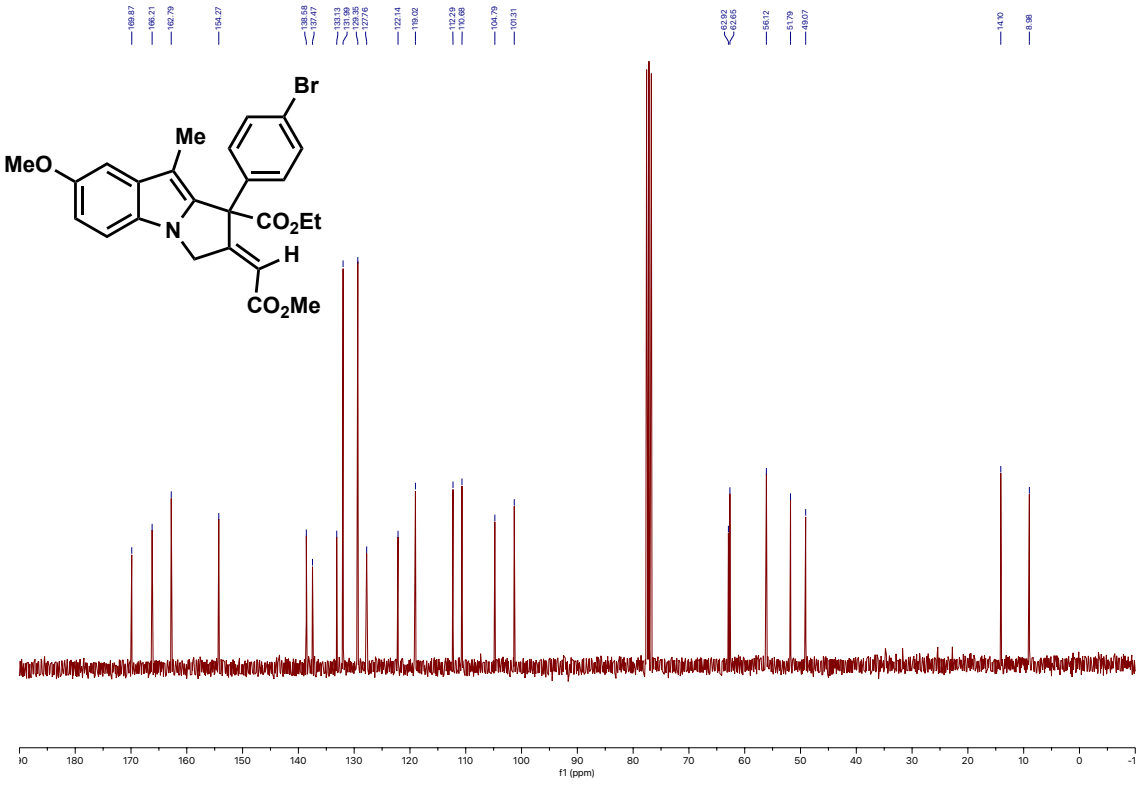
Br
Me
MeO
N
CO2Et
H
CO2Me
f1 (ppm)

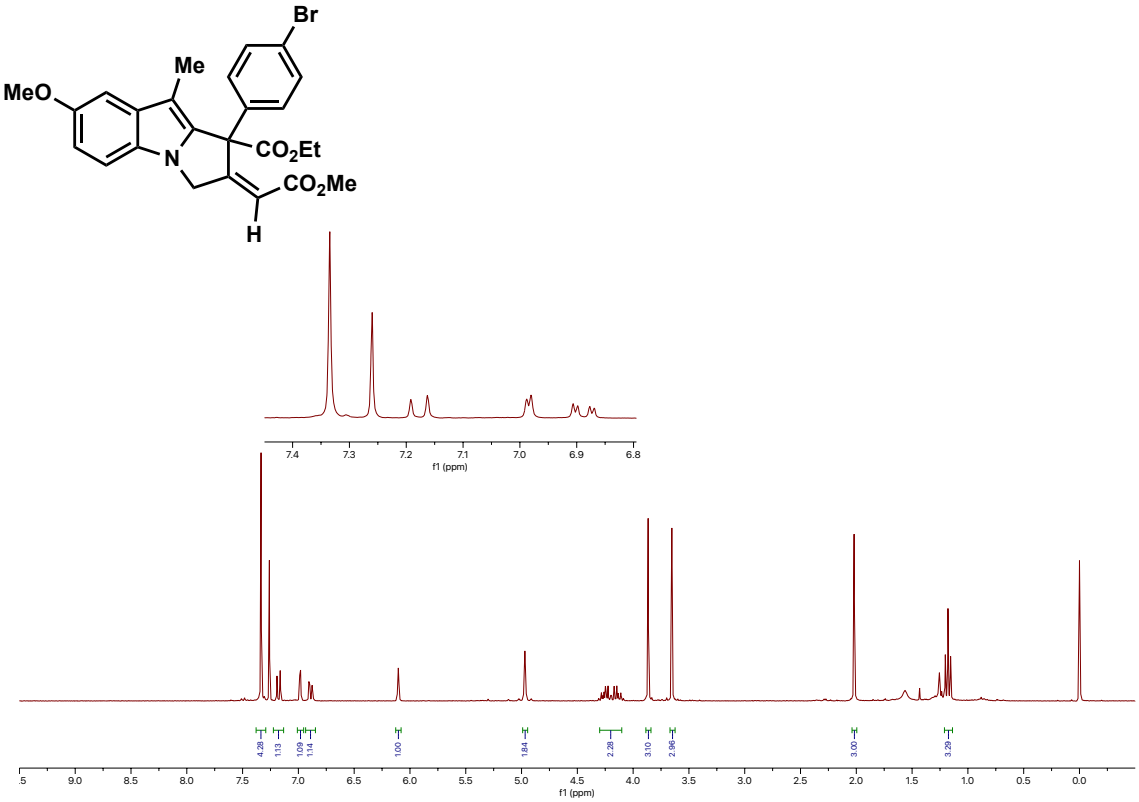
Br
Me
MeO
N
CO2Et
CO2Me
H
f1 (ppm)

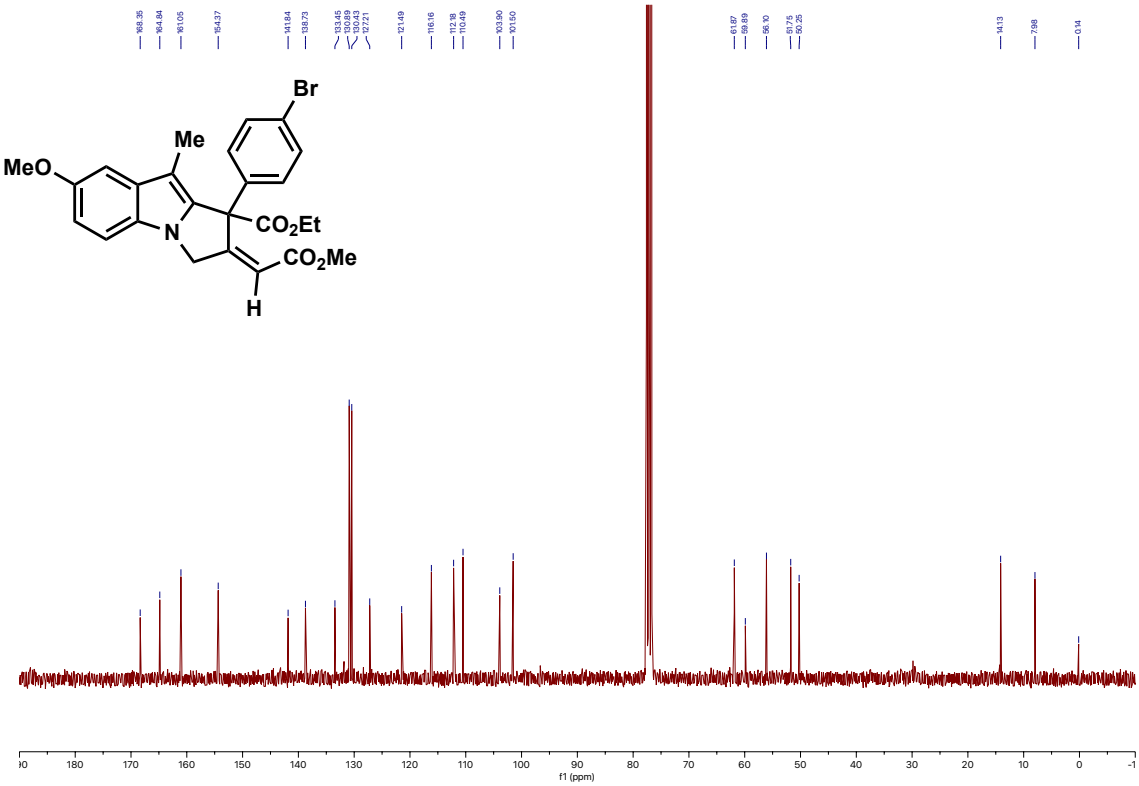
Br
Me
MeO
N
CO2Et
CO2Me
H
f1 (ppm)

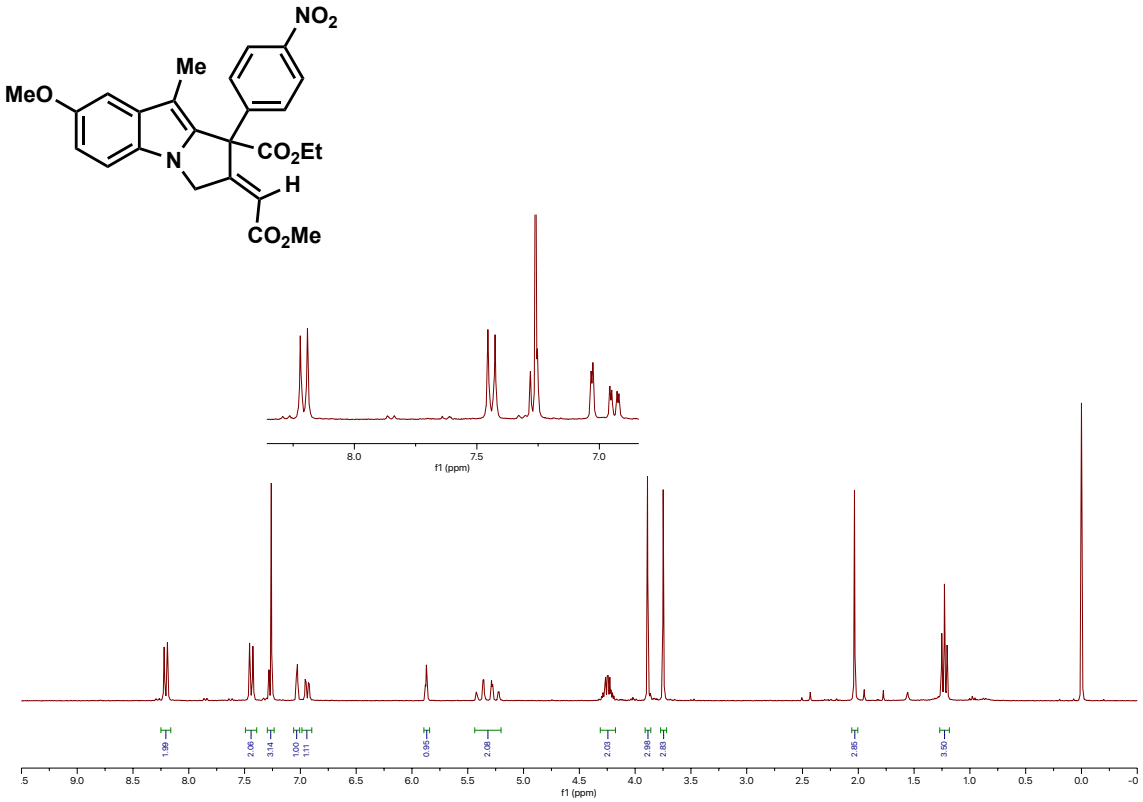
NO2
Me
MeO
CO2Et
N
H
CO2Me
f1 (ppm)

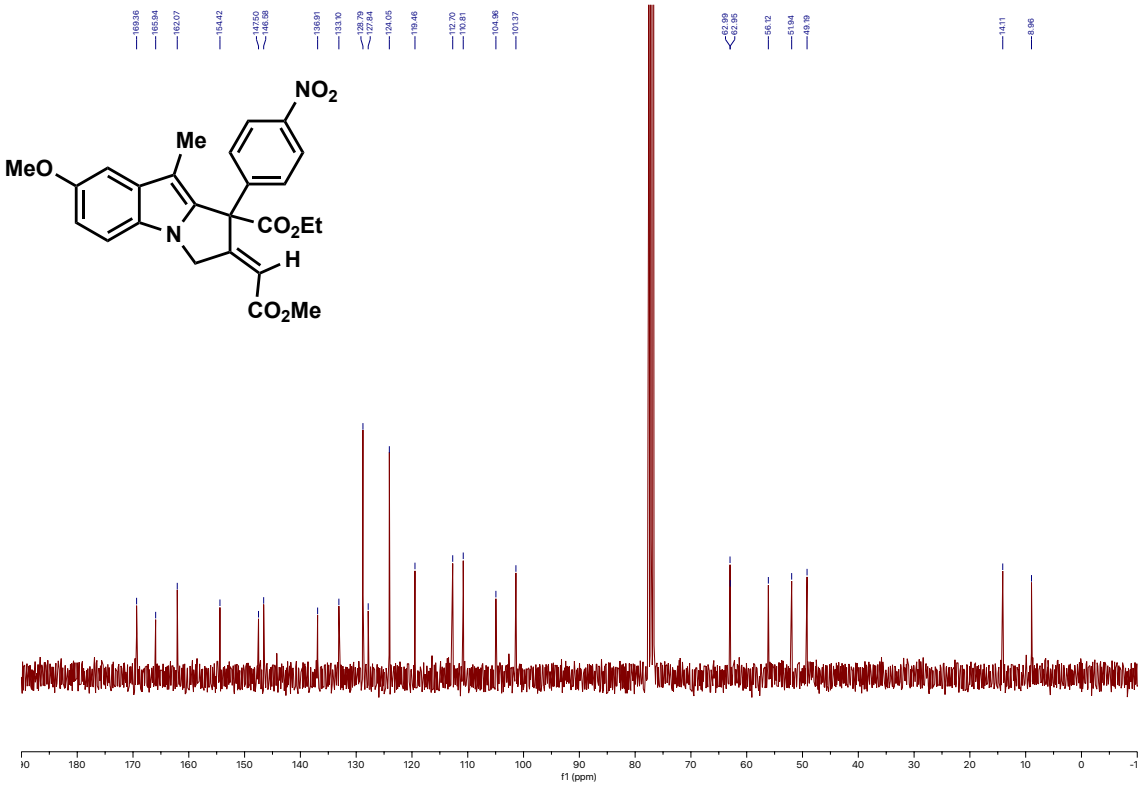
NO2
Me
MeO
CO2Et
N
H
CO2Me
f1 (ppm)

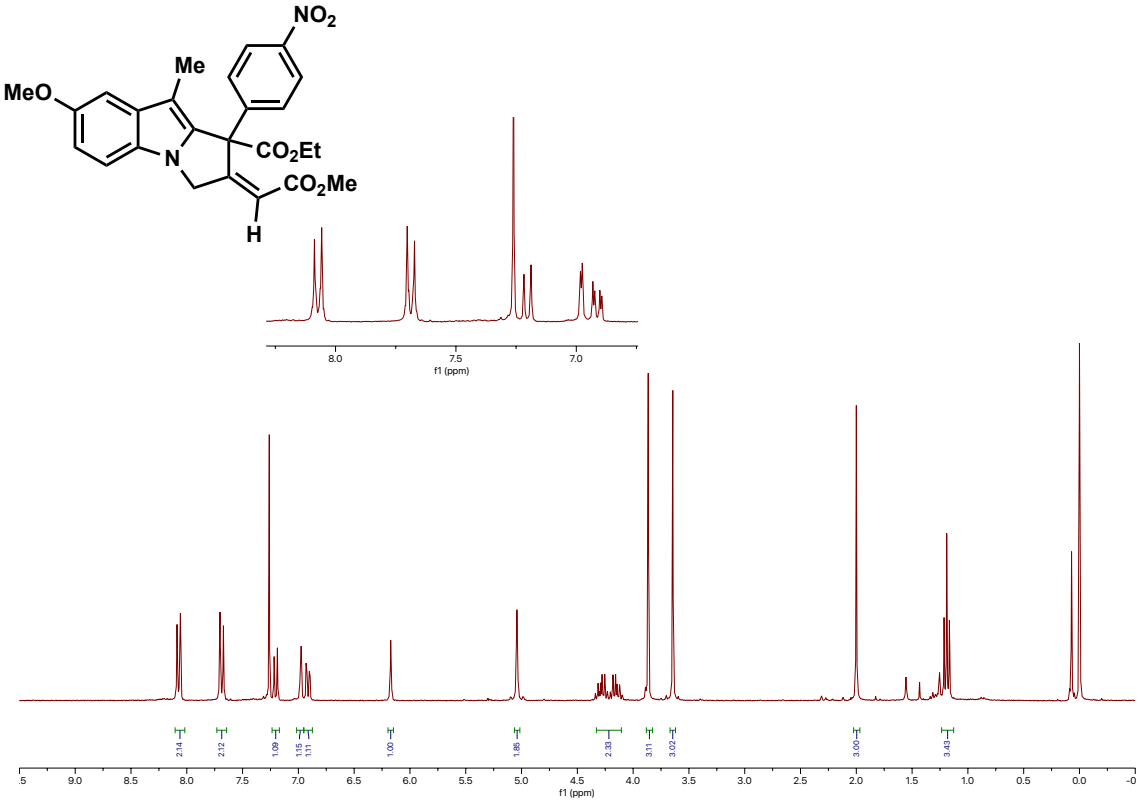
NO2
Me
MeO
CO2Et
CO2Me
H
N
f1 (ppm)

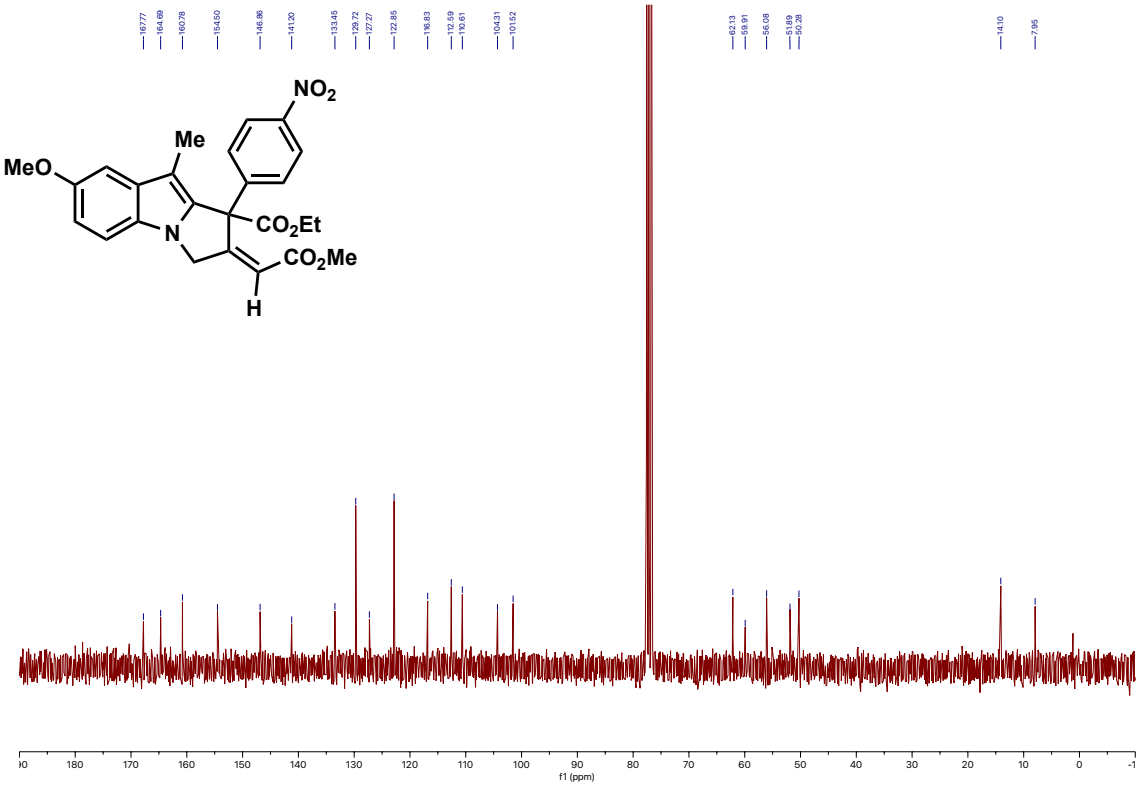
NO2
Me
MeO
CO2Et
CO2Me
H
N
f1 (ppm)

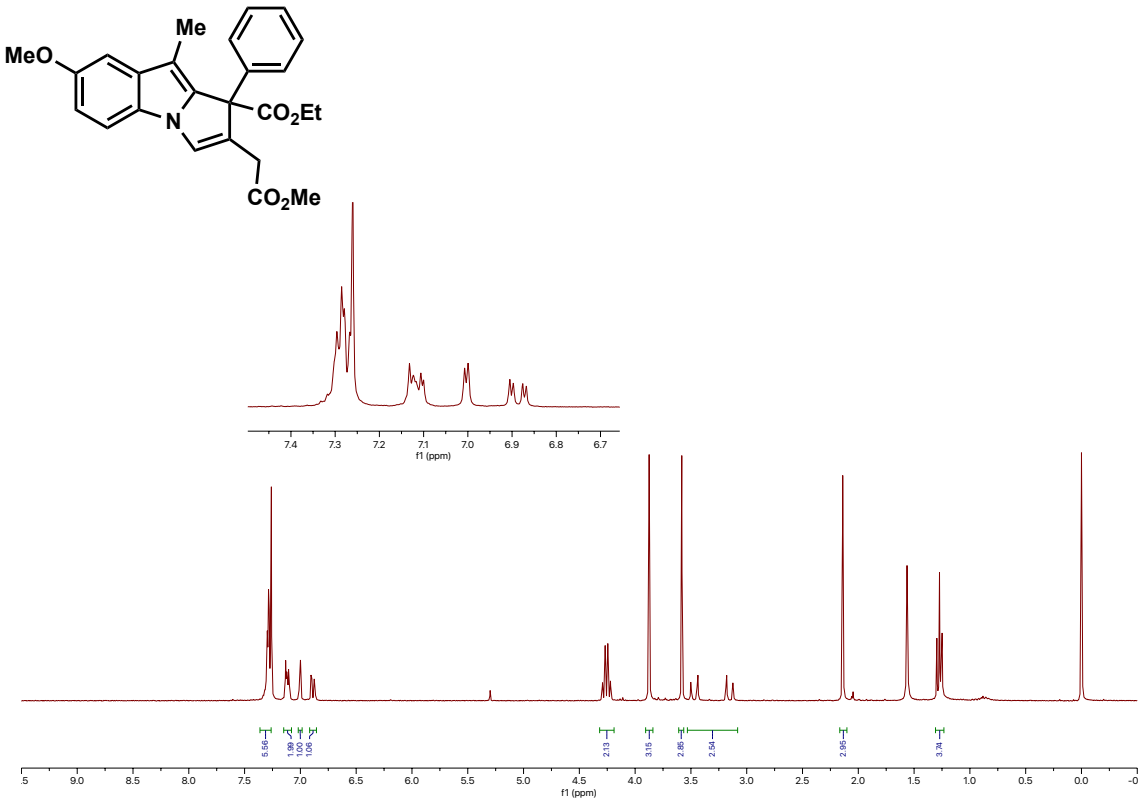
Me
MeO
N
CO2Et
CO2Me
f1 (ppm)

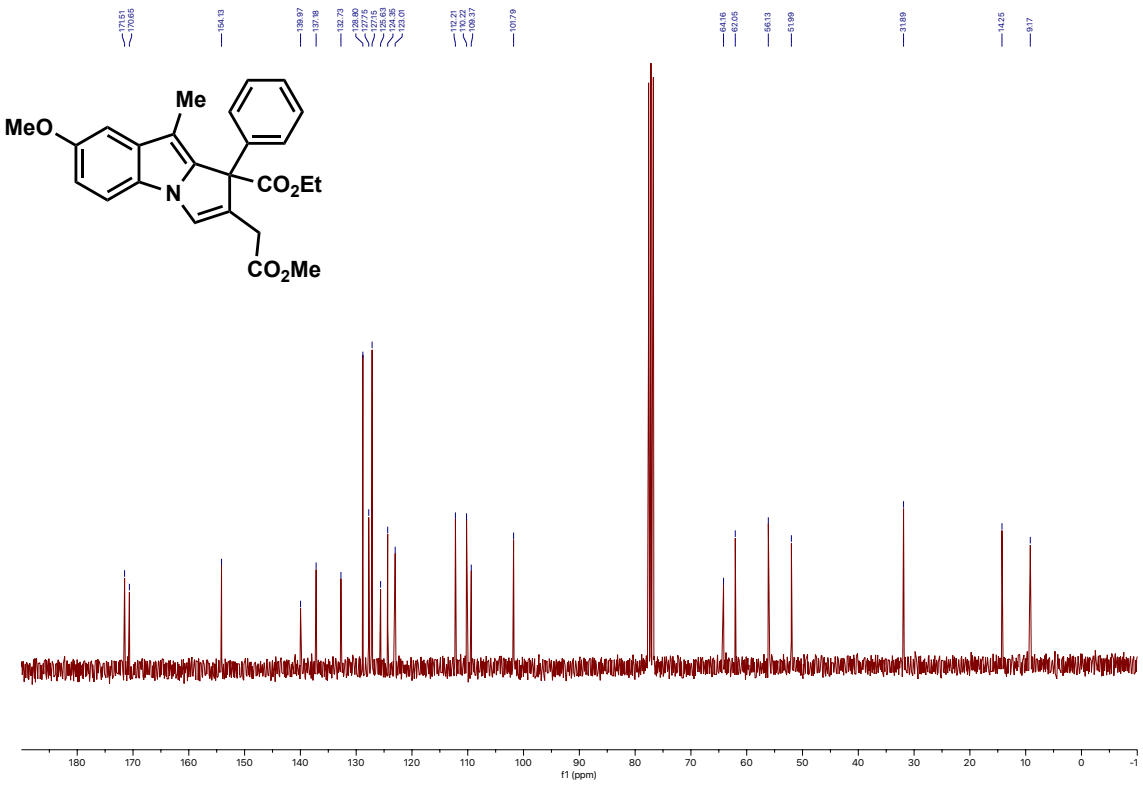
Me
MeO
N
CO2Et
CO2Me
f1 (ppm)

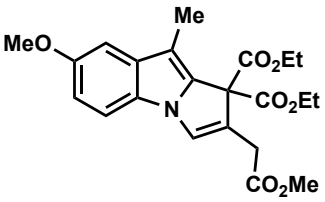
Me
MeO
CO2Et
CO2Et
N
CO2Me

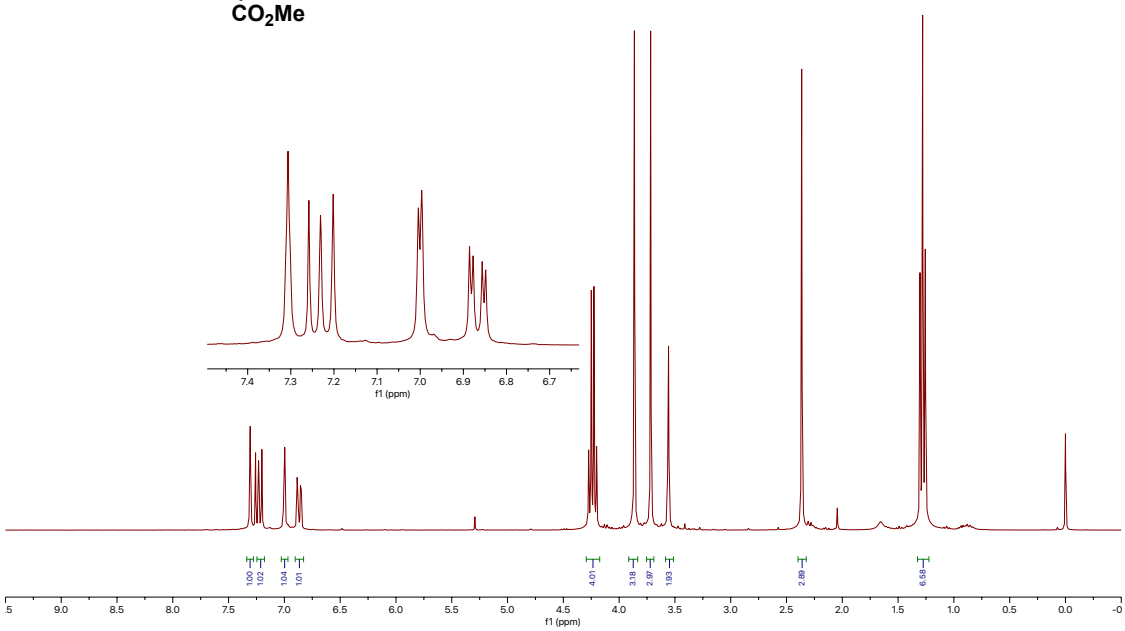
7.4
7.3
7.2
7.1
7.0
6.9
6.8
6.7
f1 (ppm)
1.00
1.02
1.04
1.01
4.01
3.18
2.97
1.93
2.89
6.58
f1 (ppm)

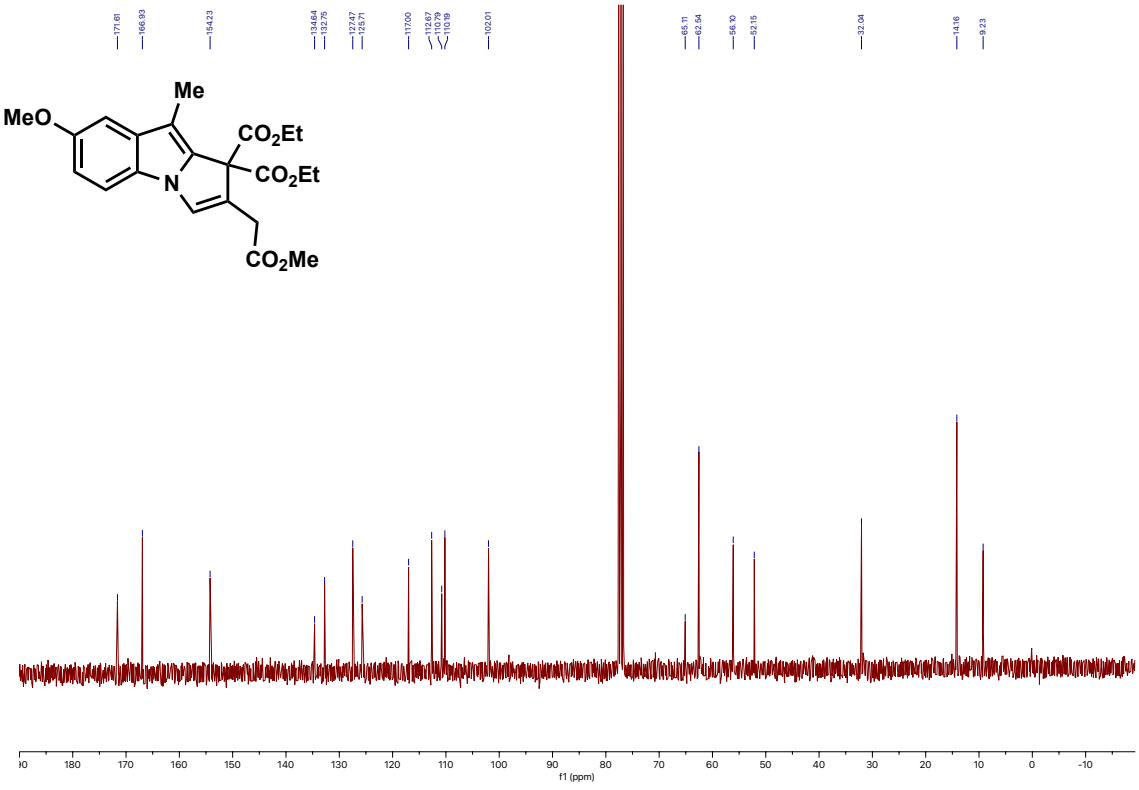
171.61
166.93
154.23
134.64
132.75
127.47
125.71
117.00
112.67
110.79
110.19
102.01
65.11
62.84
56.10
52.15
32.04
14.16
9.23
Me
MeO
CO2Et
CO2Et
N
CO2Me
f1 (ppm)

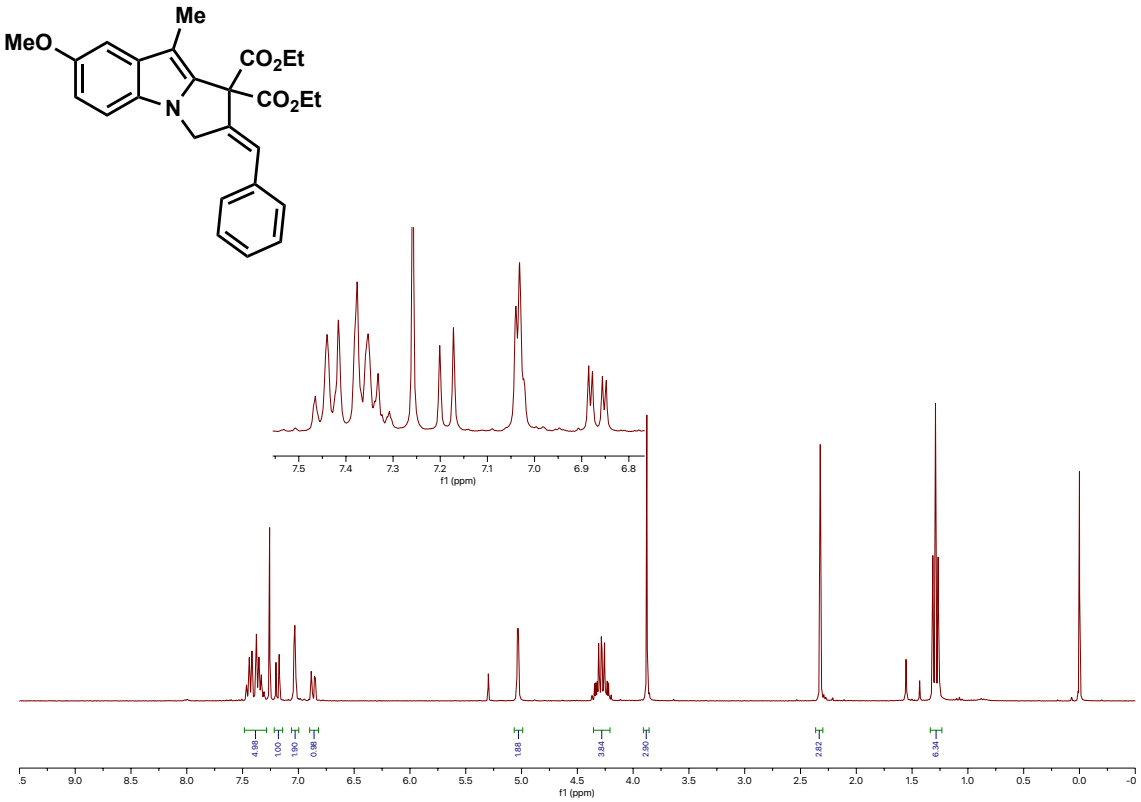
Me
MeO
CO2Et
CO2Et
N
f1 (ppm)

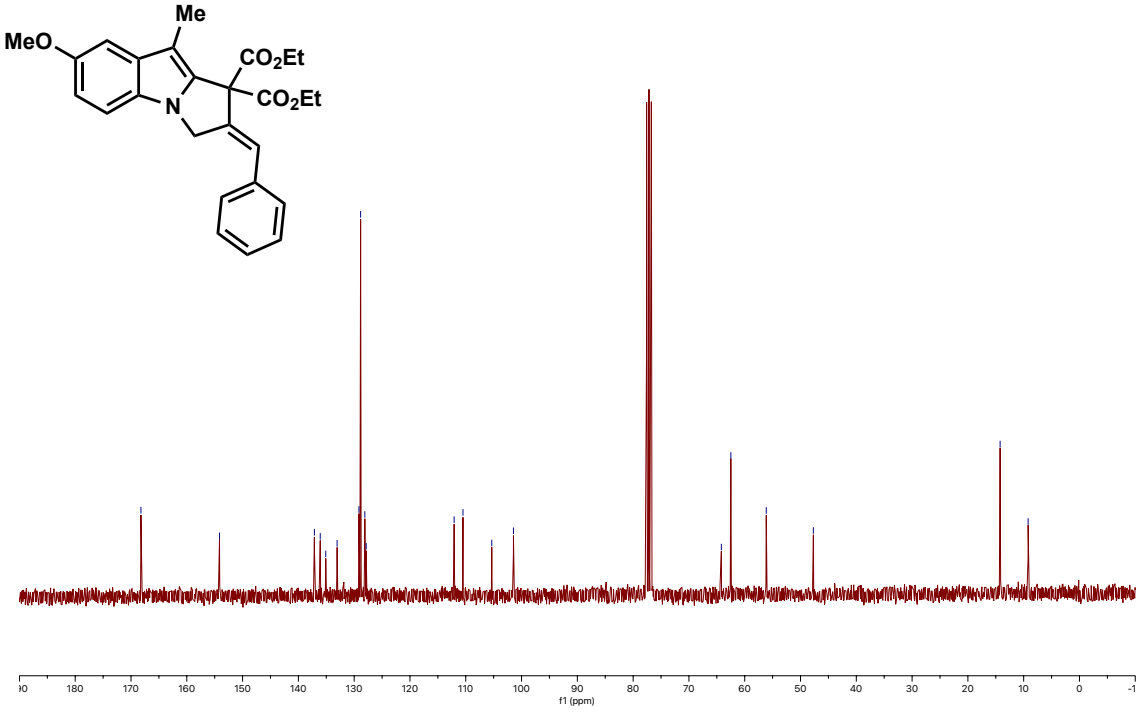
Me
MeO
CO2Et
CO2Et
N
f1 (ppm)

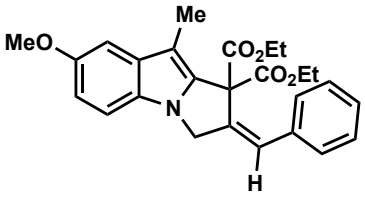
Me
MeO
CO2Et
CO2Et
N
H

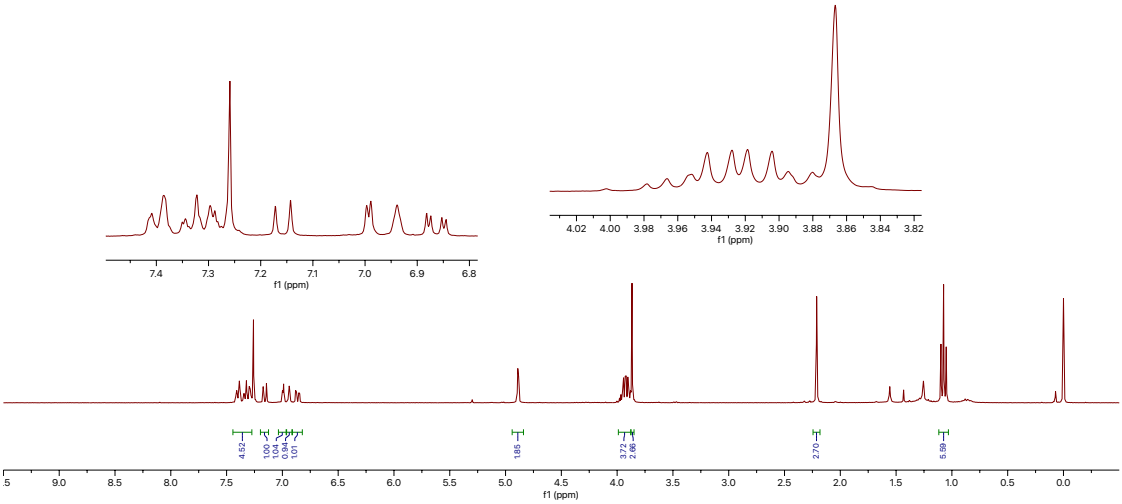
7.4 7.3 7.2 7.1 7.0 6.9 6.8
f1 (ppm)
4.02 4.00 3.98 3.96 3.94 3.92 3.90 3.88 3.86 3.84 3.82
f1 (ppm)
4.52 1.00 1.04 0.94 1.01 1.85 3.72 2.86 2.70 5.99
9.0 8.5 8.0 7.5 7.0 6.5 6.0 5.5 5.0 4.5 4.0 3.5 3.0 2.5 2.0 1.5 1.0 0.5 0.0
f1 (ppm)

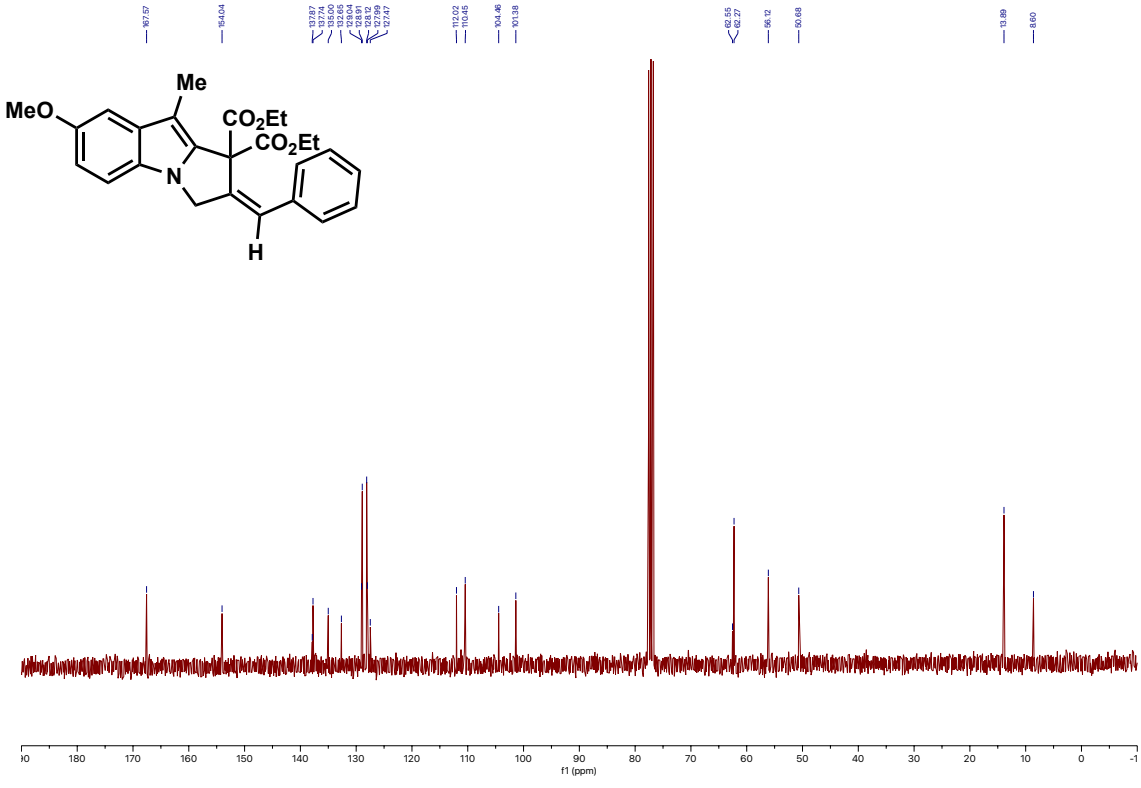
167.57
154.04
137.87
137.74
135.00
132.65
129.04
128.91
128.12
127.99
127.47
112.02
110.45
104.46
101.38
62.55
62.27
56.12
50.68
13.89
8.60
Me
MeO
CO2Et
CO2Et
N
H
180 170 160 150 140 130 120 110 100 90 80 70 60 50 40 30 20 10 0
f1 (ppm)

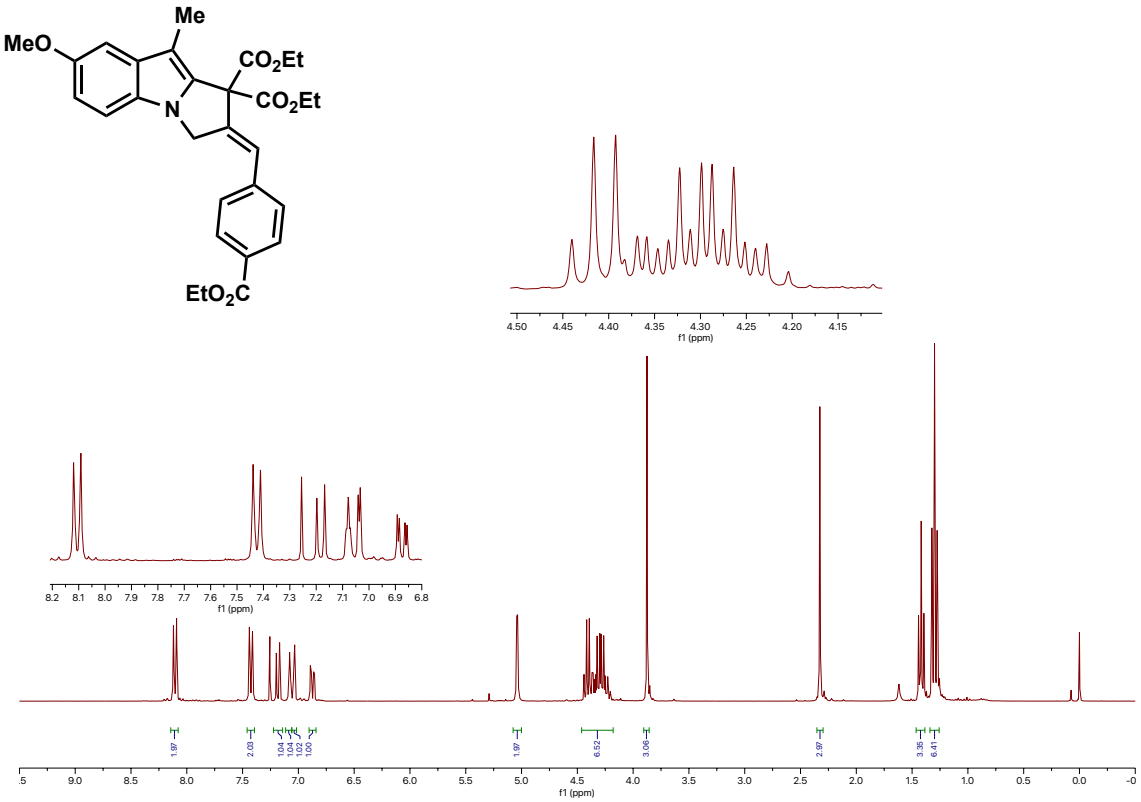
Me
MeO
CO2Et
CO2Et
N
EtO2C
f1 (ppm)

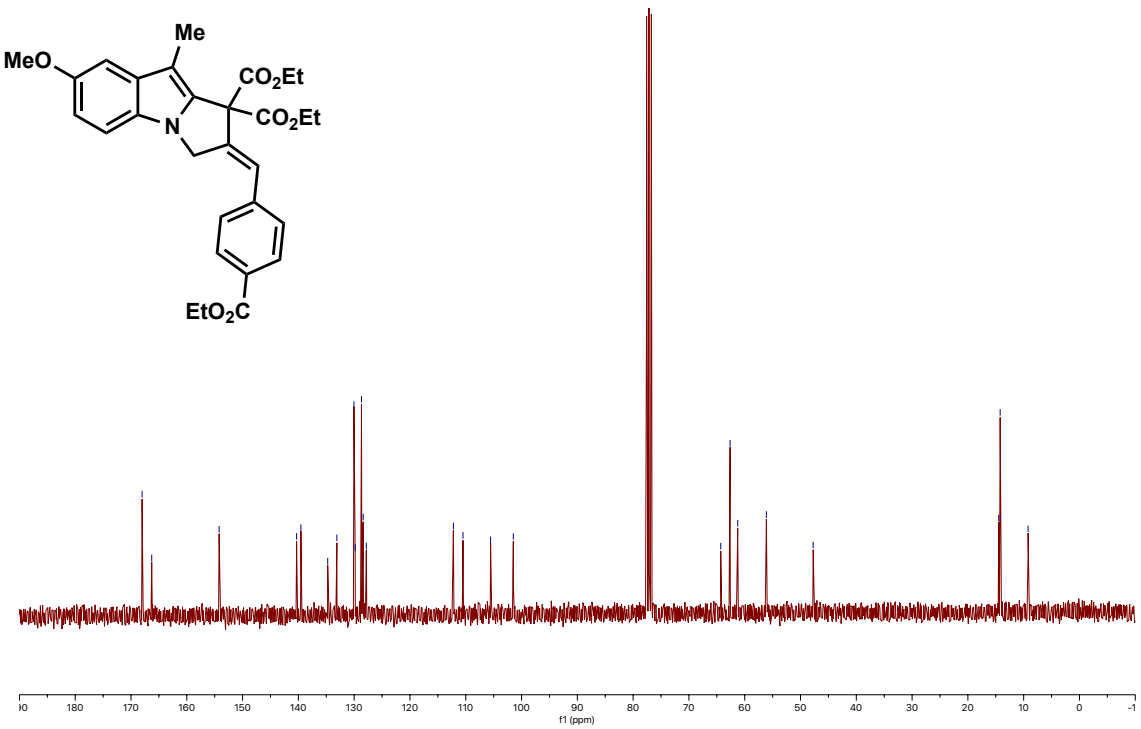
Me
MeO
CO2Et
CO2Et
N
EtO2C
f1 (ppm)

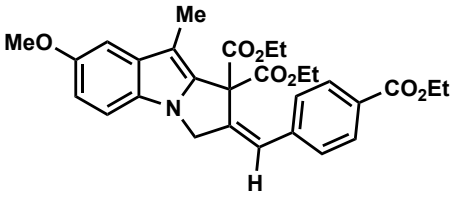
Me
MeO
CO2Et
CO2Et
CO2Et
N
H

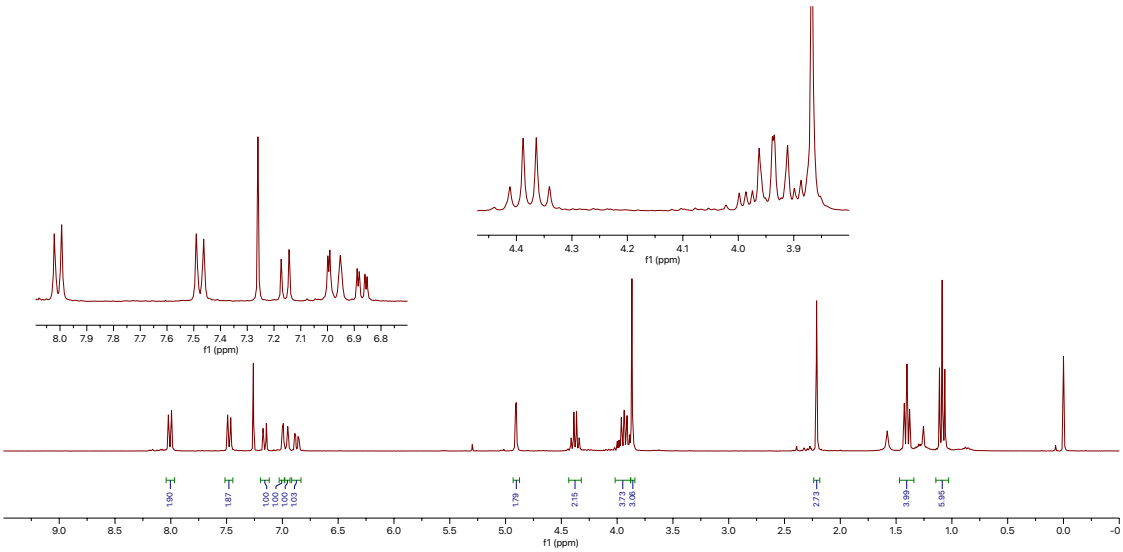
f1 (ppm)

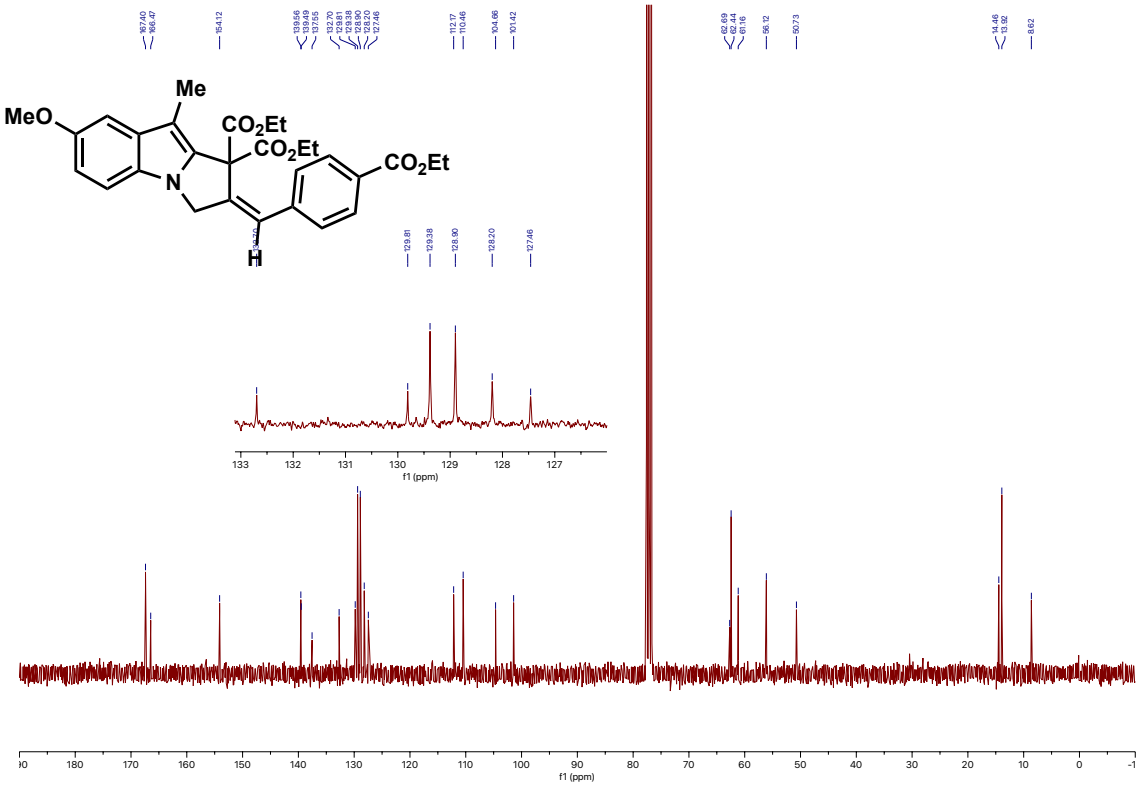
Me
MeO
CO2Et
CO2Et
CO2Et
N
H
f1 (ppm)

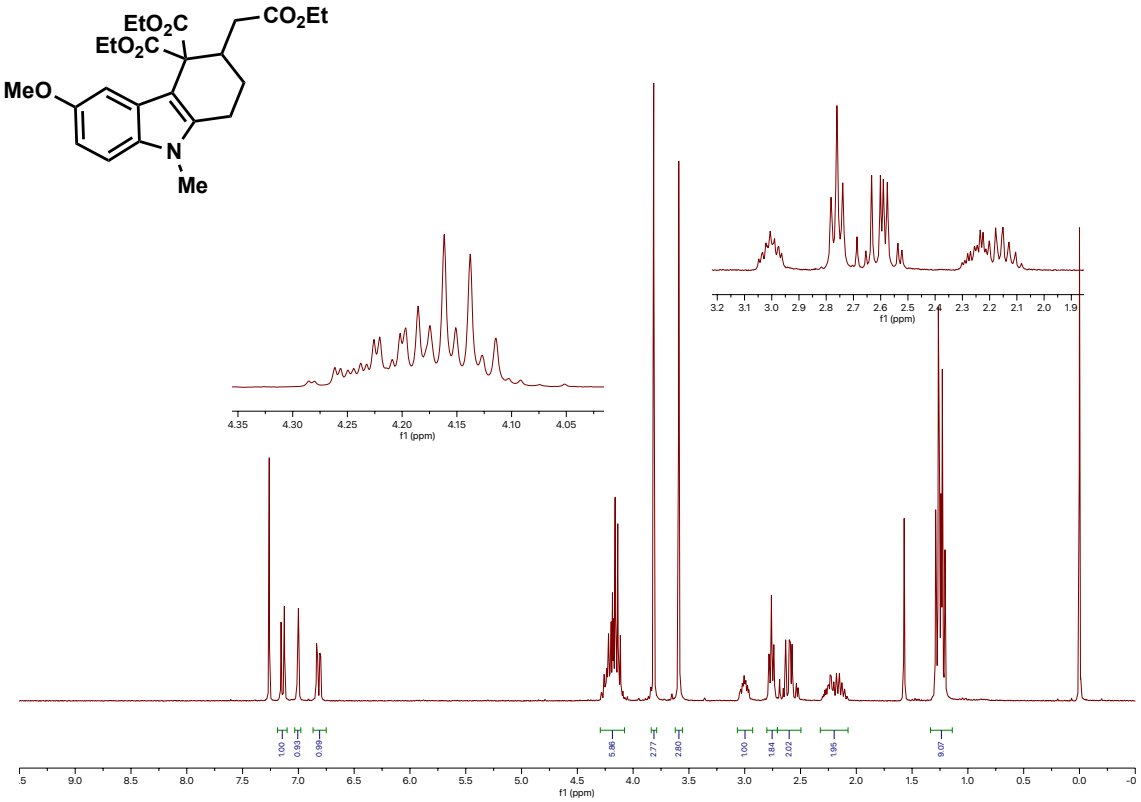
EtO2C
EtO2C
CO2Et
MeO
N
Me
f1 (ppm)

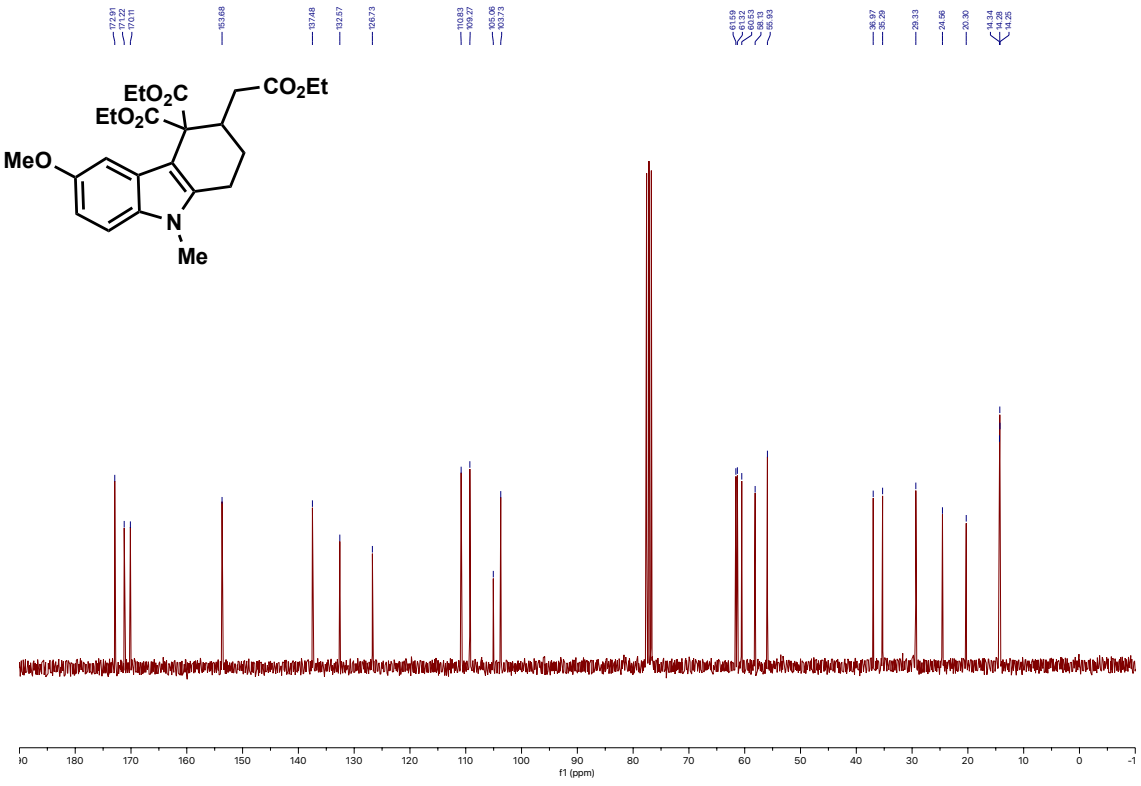
EtO2C
EtO2C
CO2Et
MeO
N
Me
f1 (ppm)

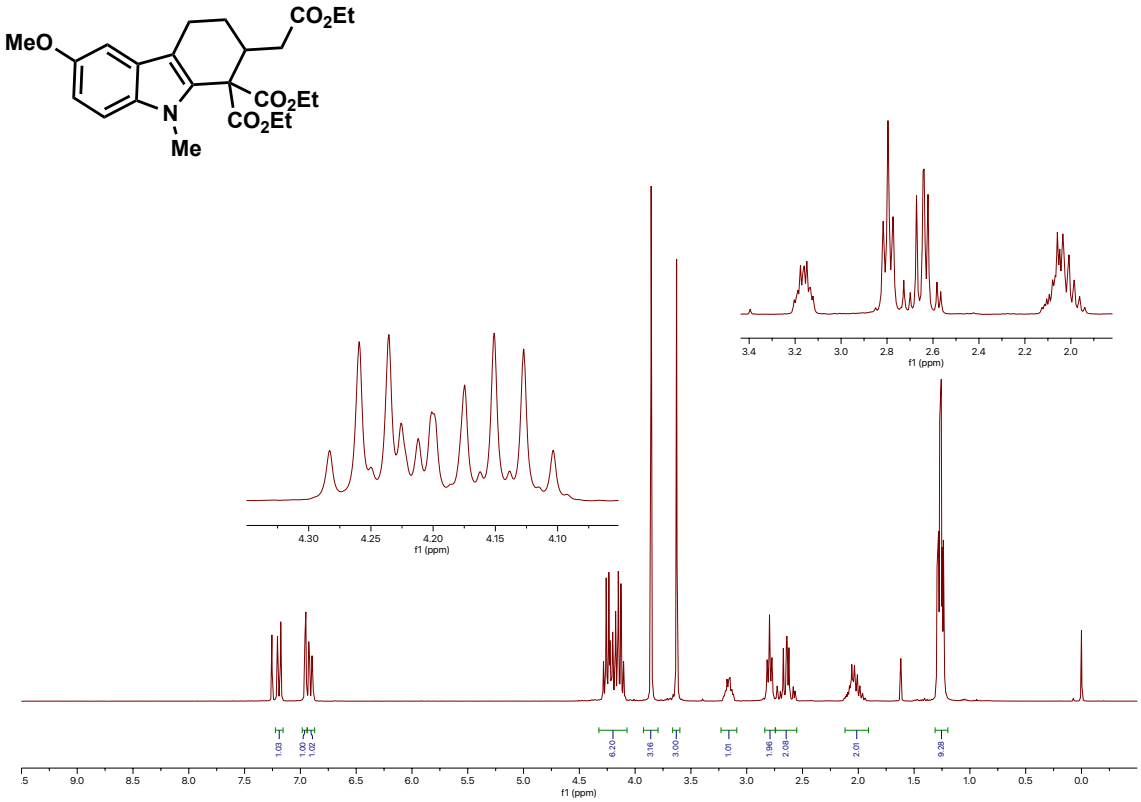
MeO
CO2Et
CO2Et
CO2Et
N
Me
f1 (ppm)

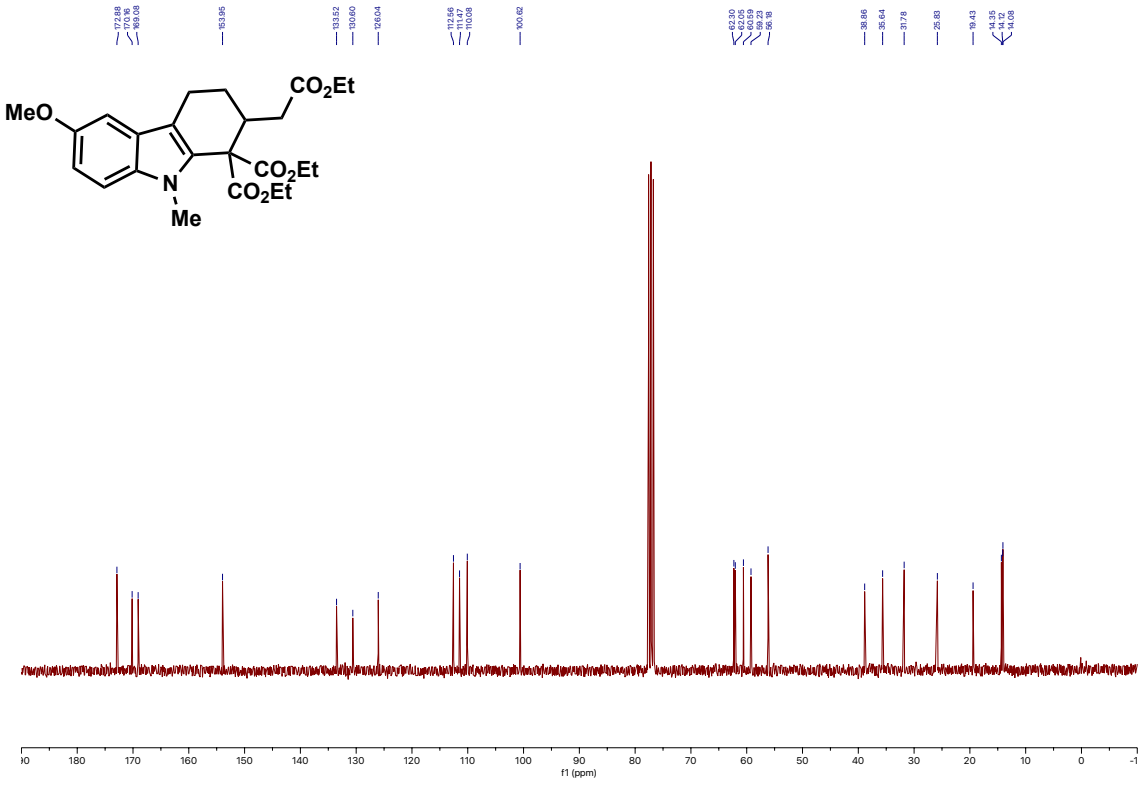
MeO
CO2Et
CO2Et
CO2Et
N
Me
f1 (ppm)

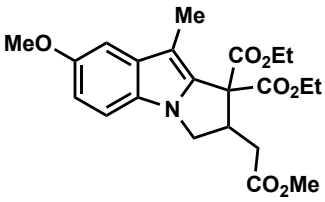
Me
MeO
CO2Et
CO2Et
N
CO2Me

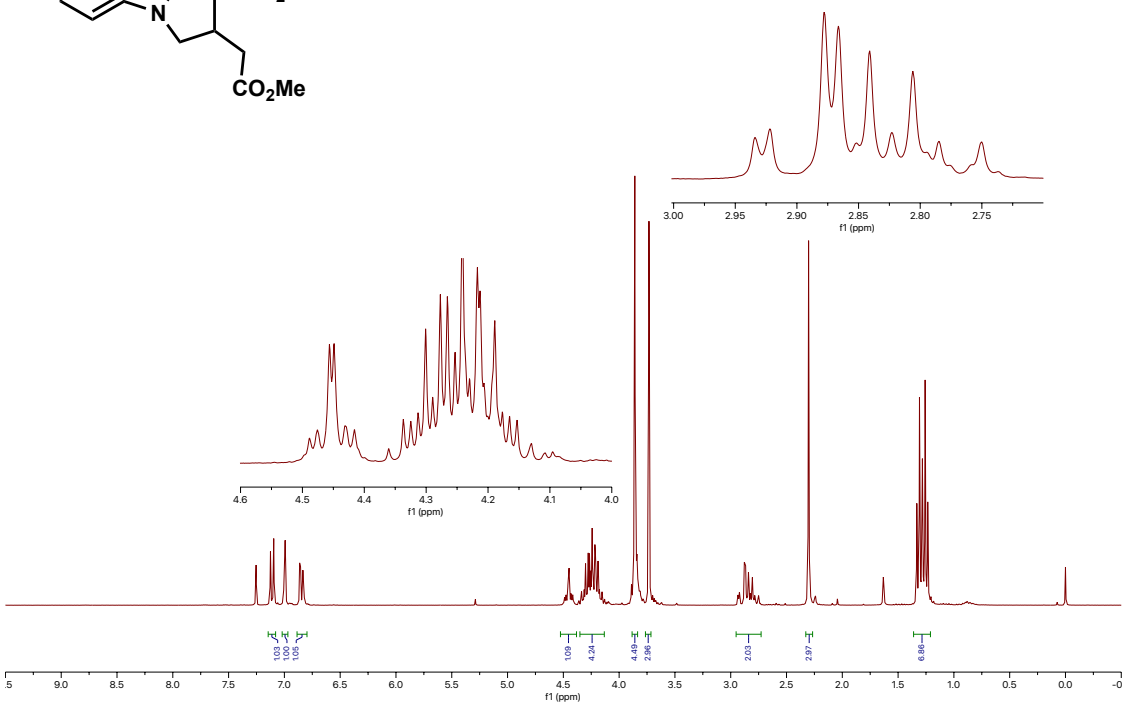
f1 (ppm)

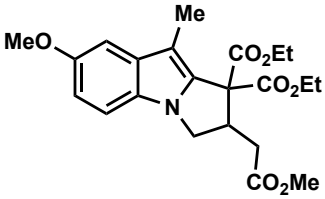
Me
MeO
CO2Et
CO2Et
N
CO2Me

f1 (ppm)

X-ray Crystallographic Analysis of **81**

Experimental details

Single-crystal X-ray diffraction data was collected at 100(2) K on a XtaLAB Synergy-S, Dualflex, HyPix-6000HE diffractometer using Cu *K*α radiation (λ = 1.5406 Å). Crystal was mounted on nylon CryoLoops with Paraton-N. The data collection and reduction were processed within *CrysAlisPro* (Rigaku OD, 2019). A multi-scan absorption correction was applied to the collected reflections. Using Olex^2 [1], the structure was solved with the ShelXT [2] structure solution program using Intrinsic Phasing and refined with the ShelXL [3] refinement package using Least Squares minimisation. All non-hydrogen atoms were refined anisotropically. The organic hydrogen atoms were generated geometrically.

1. Dolomanov, O.V., Bourhis, L.J., Gildea, R.J, Howard, J.A.K. & Puschmann, H. (2009), *J. Appl. Cryst*. 42, 339-341.
2. Sheldrick, G.M. (2015). *Acta Cryst*. A71, 3-8.
3. Sheldrick, G.M. (2015). *Acta Cryst*. C71, 3-8.

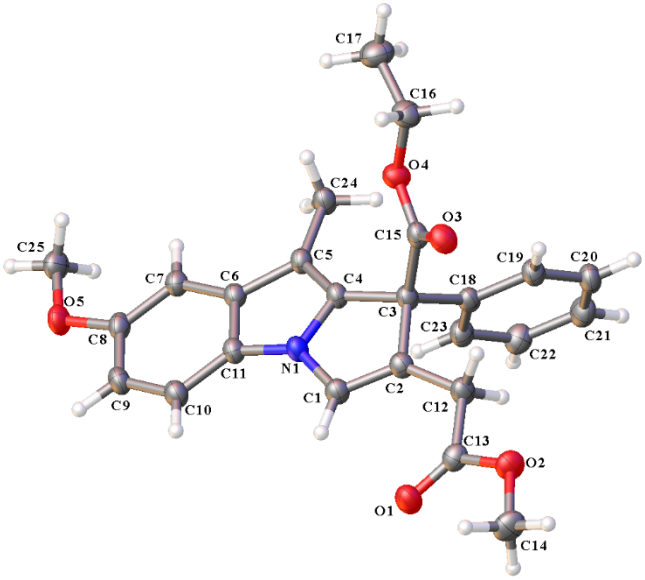

(Non-hydrogen atoms are represented by displacement ellipsoids at the 50% probability level).

Table S17 Crystal data and structure refinement

Empirical formula	$C_{25}H_{25}NO_5$
Formula weight	419.46
Temperature/K	100(2)
Crystal system	triclinic
Space group	*P*-1
a/Å	9.2549(5)
b/Å	10.9358(4)
c/Å	11.8353(5)
α/°	70.812(4)
β/°	83.459(4)
γ/°	69.525(4)
Volume/Å^3	1059.84(9)
Z	2
ρ_{calc}mg/mm^3	1.314
μ/mm^{-1}	0.747
F(000)	444.0
Crystal size/mm^3	0.264 × 0.147 × 0.1
2θ range for data collection	7.91 to 154.704°
Index ranges	$-11 \le h \le 11$, $-13 \le k \le 13$, $-14 \le l \le 14$
Reflections collected	17518
Independent reflections	4403[*R*(int) = 0.0522]
Data/restraints/parameters	4403/0/285
Goodness-of-fit on F^2	1.074
Final *R* indexes [$I>=2\sigma$ (I)]	R_1 = 0.0436, wR_2 = 0.1161
Final *R* indexes [all data]	R_1 = 0.0504, wR_2 = 0.1217
Largest diff. peak/hole / e Å^{-3}	0.25/-0.23

Table S18 Fractional Atomic Coordinates ($\times 10^4$) and Equivalent Isotropic Displacement Parameters ($Å^2 \times 10^3$). U_{eq} is defined as 1/3 of the trace of the orthogonalised U_{IJ} tensor.

Atom	*x*	*y*	*z*	U(eq)
O1	4980.7(13)	6614.1(12)	6436.3(9)	35.8(3)
O2	3274.1(13)	5834.9(11)	7700.2(9)	32.9(3)
O3	1922.2(12)	4757.6(11)	4554.6(9)	31.7(2)
O4	1409.0(12)	5600.5(10)	2588.2(9)	30.0(2)
O5	7097.9(12)	8942.5(12)	-1706.3(9)	33.6(3)
N1	4484.1(13)	7220.0(12)	2675.3(10)	24.6(3)
C1	4551.7(16)	6922.9(14)	3921.4(12)	25.6(3)
C2	3211.7(16)	6802.1(14)	4416.9(12)	25.2(3)
C3	2102.4(15)	7007.5(14)	3436.8(12)	24.1(3)
C4	3037.1(15)	7379.7(14)	2320.8(12)	23.6(3)
C5	2906.5(16)	7867.9(14)	1107.4(12)	23.9(3)
C6	4371.1(16)	8028.2(14)	672.1(12)	24.0(3)
C7	4923.0(16)	8484.2(14)	-492.2(12)	25.7(3)
C8	6413.0(17)	8518.5(15)	-617.3(13)	27.5(3)
C9	7354.9(17)	8117.5(16)	380.8(13)	29.7(3)
C10	6836.0(16)	7666.6(15)	1535.3(13)	28.6(3)
C11	5333.6(16)	7630.0(14)	1666.6(12)	24.3(3)
C12	2702.2(17)	6509.8(16)	5689.4(12)	29.5(3)
C13	3808.9(17)	6336.9(14)	6607.9(12)	27.2(3)
C14	4238(2)	5569.5(17)	8685.6(13)	37.1(4)
C15	1828.4(15)	5647.4(14)	3606.8(12)	25.2(3)

Atom	*x*	*y*	*z*	U(eq)
C16	1073(2)	4366.3(17)	2680.4(14)	35.0(3)
C17	703(2)	4461.9(19)	1448.7(16)	42.6(4)
C18	536.3(15)	8119.6(14)	3473.0(11)	24.6(3)
C19	-701.3(16)	7768.0(15)	4104.1(12)	27.2(3)
C20	-2084.5(17)	8786.2(17)	4191.7(13)	32.3(3)
C21	-2248.3(18)	10153.2(17)	3655.4(14)	34.8(3)
C22	-1019.1(19)	10511.1(16)	3016.2(13)	33.0(3)
C23	366.2(17)	9497.4(15)	2923.7(12)	28.7(3)
C24	1546.8(16)	8195.3(16)	357.0(12)	28.9(3)
C25	6205.0(19)	9345.9(18)	-2747.1(13)	34.8(3)

Table S19 Selected Bond Distances (Å)

Atom	Atom	Length/Å	Atom	Atom	Length/Å
O1	C13	1.2036(19)	C4	C5	1.3610(19)
O2	C13	1.3399(17)	C5	C6	1.4425(18)
O2	C14	1.4398(18)	C5	C24	1.4936(19)
O3	C15	1.2076(17)	C6	C7	1.4052(18)
O4	C15	1.3296(17)	C6	C11	1.4139(19)
O4	C16	1.4560(18)	C7	C8	1.382(2)
O5	C8	1.3801(16)	C8	C9	1.405(2)
O5	C25	1.419(2)	C9	C10	1.384(2)
N1	C1	1.4058(17)	C10	C11	1.394(2)
N1	C4	1.3843(18)	C12	C13	1.500(2)
N1	C11	1.3876(17)	C16	C17	1.497(2)
C1	C2	1.3406(19)	C18	C19	1.3936(19)
C2	C3	1.5456(19)	C18	C23	1.390(2)
C2	C12	1.4899(18)	C19	C20	1.392(2)
C3	C4	1.5137(18)	C20	C21	1.379(2)
C3	C15	1.540(2)	C21	C22	1.393(2)
C3	C18	1.5391(19)	C22	C23	1.392(2)

Table S20 Selected Bond Angles

Atom	Atom	Atom	Angle/°	Atom	Atom	Atom	Angle/°
C13	O2	C14	115.69(12)	C8	C7	C6	117.87(13)
C15	O4	C16	115.00(11)	O5	C8	C7	123.85(14)
C8	O5	C25	117.02(12)	O5	C8	C9	114.56(13)
C4	N1	C1	111.14(11)	C7	C8	C9	121.59(13)
C4	N1	C11	108.88(11)	C10	C9	C8	121.57(13)
C11	N1	C1	138.82(12)	C9	C10	C11	117.08(13)
C2	C1	N1	109.77(12)	N1	C11	C6	106.32(12)
C1	C2	C3	109.81(11)	N1	C11	C10	131.58(13)
C1	C2	C12	130.59(13)	C10	C11	C6	122.09(12)
C12	C2	C3	119.60(12)	C2	C12	C13	117.76(12)
C4	C3	C2	100.96(11)	O1	C13	O2	123.49(14)
C4	C3	C15	111.28(11)	O1	C13	C12	127.58(13)
C4	C3	C18	114.16(11)	O2	C13	C12	108.91(12)
C15	C3	C2	109.61(11)	O3	C15	O4	124.11(13)
C18	C3	C2	111.89(11)	O3	C15	C3	124.33(13)
C18	C3	C15	108.74(11)	O4	C15	C3	111.50(11)

Atom	Atom	Atom	Angle/°	Atom	Atom	Atom	Angle/°
N1	C4	C3	107.86(11)	O4	C16	C17	107.47(13)
C5	C4	N1	110.80(12)	C19	C18	C3	120.74(12)
C5	C4	C3	141.26(13)	C23	C18	C3	120.01(12)
C4	C5	C6	105.59(12)	C23	C18	C19	119.16(13)
C4	C5	C24	128.36(12)	C20	C19	C18	120.32(14)
C6	C5	C24	126.05(12)	C21	C20	C19	120.49(14)
C7	C6	C5	131.79(13)	C20	C21	C22	119.46(14)
C7	C6	C11	119.81(13)	C23	C22	C21	120.31(14)
C11	C6	C5	108.41(11)	C18	C23	C22	120.24(13)

Table S21 Selected Torsion Angles

A	B	C	D	Angle/°	A	B	C	D	Angle/°
O5	C8	C9	C10	179.99(13)	C6	C7	C8	O5	179.96(13)
N1	C1	C2	C3	1.06(16)	C6	C7	C8	C9	-0.2(2)
N1	C1	C2	C12	-179.38(14)	C7	C6	C11	N1	-179.24(12)
N1	C4	C5	C6	-0.15(15)	C7	C6	C11	C10	-0.3(2)
N1	C4	C5	C24	-179.50(13)	C7	C8	C9	C10	0.2(2)
C1	N1	C4	C3	-6.57(15)	C8	C9	C10	C11	-0.2(2)
C1	N1	C4	C5	170.82(12)	C9	C10	C11	N1	178.86(14)
C1	N1	C11	C6	-166.87(15)	C9	C10	C11	C6	0.2(2)
C1	N1	C11	C10	14.3(3)	C11	N1	C1	C2	169.22(16)
C1	C2	C3	C4	-4.65(15)	C11	N1	C4	C3	-176.67(11)
C1	C2	C3	C15	112.83(13)	C11	N1	C4	C5	0.71(16)
C1	C2	C3	C18	-126.46(13)	C11	C6	C7	C8	0.3(2)

A	B	C	D	Angle/°	A	B	C	D	Angle/°
C1	C2	C12	C13	1.3(2)	C12	C2	C3	C4	175.73(12)
C2	C3	C4	N1	6.56(14)	C12	C2	C3	C15	-66.79(16)
C2	C3	C4	C5	-169.53(18)	C12	C2	C3	C18	53.92(16)
C2	C3	C15	O3	26.90(18)	C14	O2	C13	O1	-3.2(2)
C2	C3	C15	O4	-155.85(11)	C14	O2	C13	C12	178.15(12)
C2	C3	C18	C19	-94.22(15)	C15	O4	C16	C17	-177.19(13)
C2	C3	C18	C23	82.49(15)	C15	C3	C4	N1	-109.70(13)
C2	C12	C13	O1	12.7(2)	C15	C3	C4	C5	74.2(2)
C2	C12	C13	O2	-168.63(12)	C15	C3	C18	C19	26.99(17)
C3	C2	C12	C13	-179.19(12)	C15	C3	C18	C23	-156.29(12)
C3	C4	C5	C6	175.87(17)	C16	O4	C15	O3	-0.6(2)
C3	C4	C5	C24	-3.5(3)	C16	O4	C15	C3	-177.89(11)
C3	C18	C19	C20	176.13(13)	C18	C3	C4	N1	126.76(12)
C3	C18	C23	C22	-176.04(13)	C18	C3	C4	C5	-49.3(2)
C4	N1	C1	C2	3.52(16)	C18	C3	C15	O3	-95.70(15)
C4	N1	C11	C6	-0.96(15)	C18	C3	C15	O4	81.55(13)
C4	N1	C11	C10	-179.76(15)	C18	C19	C20	C21	0.1(2)
C4	C3	C15	O3	137.72(14)	C19	C18	C23	C22	0.7(2)
C4	C3	C15	O4	-45.03(15)	C19	C20	C21	C22	0.4(2)
C4	C3	C18	C19	151.90(13)	C20	C21	C22	C23	-0.3(2)
C4	C3	C18	C23	-31.39(18)	C21	C22	C23	C18	-0.3(2)
C4	C5	C6	C7	179.68(14)	C23	C18	C19	C20	-0.6(2)
C4	C5	C6	C11	-0.46(15)	C24	C5	C6	C7	-1.0(2)
C5	C6	C7	C8	-179.85(14)	C24	C5	C6	C11	178.92(13)
C5	C6	C11	N1	0.87(15)	C25	O5	C8	C7	-0.8(2)
C5	C6	C11	C10	179.81(13)	C25	O5	C8	C9	179.35(13)

Chapter 2: Total Synthesis of Tanshinone IIA

2.1 Tanshinone Natural Products

2.1.1 Isolation and Applications

The use of natural plant material as medicines for the treatment of pain and disease is a practice that dates back to the dawn of mankind. Our understanding of the mechanism behind how these medications work in the body has come a long way since the days of Hippocrates. Isolation of specific metabolites from flora and fauna has given scientists incredible insight into how certain traditional medicines work in the human body.[1,2] Isolation of bioactive compounds, herein referred to as natural products, has also allowed for not only treatment of illness directly using these natural products, but inspiration for further medical advances through chemical derivatization of the isolated compounds.

One such class of natural products are the abietane diterpenoids known as tanshinones. Tanshinone natural products were originally isolated from the *Salvia miltiorrhiza*, the plant known as Danshen (or Tanshen in Chinese) which has been used in traditional Chinese medicine to treat many heart conditions, arthritis, and hepatits.[3] Parent compounds tanshinone I (**3**) and tanshinone IIA (**2**) were first isolated in 1934 by Nakao and Fukushima from the alcoholic extraction of the plant roots (Scheme 2.1).[4] Since this first isolation over 40 members of the family containing the same general structural cores composed of a tri-carbocyclic ring system (A,B,C) and an oxygen containing heterocyclic ring (D) have been identified.[5,6] The most abundant compounds contained in an extraction

are cryptotanshinone (**1**), tanshinone IIA (**2**), tanshinone I (**3**), dihydrotanshinone I (**4**), tanshinlactone (**5**), and neo-tanshinlactone (**6**) (Scheme 2.1).[3]

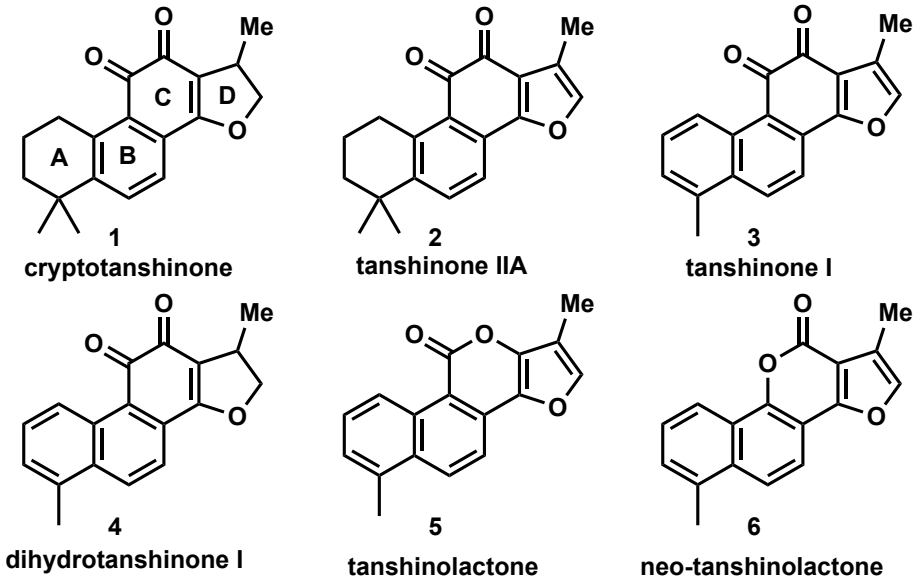

Scheme 2.1: Select examples of tanshinones.

Many of the tanshinone family members have been studied thoroughly for their cardiovascular benefits, with several commercial sources being prescribed as medical treatments.[7–9] More recently, however, some members of the tanshinone family have been investigated for their anti-cancer activity. Cryptotanshinone and tanshinone IIA have been the most extensively studied, followed by tanshinone I and dihydrotanshinone I.[10–12] As such, pharmaceutical companies desire large quantities of these compounds to manufacture profitable drugs. However, due to overharvesting in the wild, most of the feedstocks for these compounds are cultivated. The drawbacks of harvesting natural product molecules from cultivation are that crops take nearly 20 months to fully develop, and they suffer from the same degradation many crops suffer from such as destruction by herbivores, or

contamination from pesticide residues or heavy metals.[3] Thus, industry turns to the application of synthetic chemistry to circumvent the need for agricultural sources.

2.1.2 Previous Synthetic Efforts

Total syntheses of certain tanshinones have been reported as early as 1968, when Baillie and Thompson reported the first synthesis of tanshinone I using a Feist-Benary reaction as the key furan ring forming step.[13] Since then tanshinone I has been synthesized at least 5 other times.[13–15] Tanshinone IIA has received significant attention from synthetic chemists as well, due to the challenge associated with forming the fused cyclohexane ring containing a benzylic geminal dimethyl group. The first synthesis of tanshinone IIA was reported in 1968 by Kakisawa, who accomplished the synthesis in 16 steps from the advanced starting material, 1,2,4-trimethoxybenzene.[16] His strategy relied on a cyclodehydration of a tertiary alcohol formed from ester **7** to furnish the A ring in **8**, and a base catalyzed cyclization to form the D ring in **10** (Scheme 2.2).

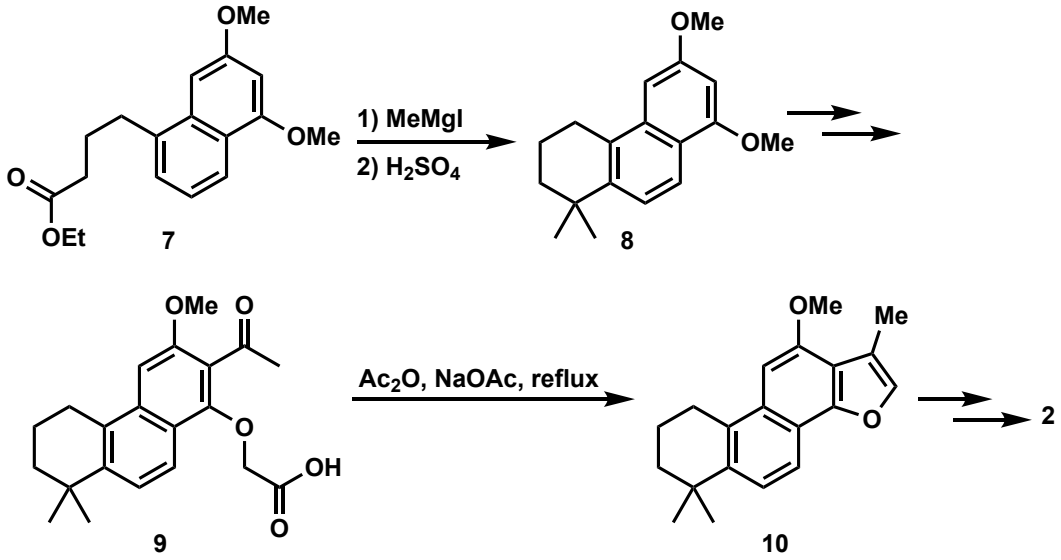

Scheme 2.2: Key ring forming steps in Kakisawa's synthesis of tanshinone IIA.

While the initial report by Kakisawa is historically important in that it is the first time this molecule was ever synthesized in a lab, and displayed several unique/interesting transformations, drawbacks of this initial approach included the high step count and the harsh conditions needed for many of the transformations. In contrast, Kakisawa, in collaboration with Inouye, published an alternate route to the molecule a year later in 1969. This route featured a key Diels-Alder reaction between 3-methylbenzofuran-4,7-quinone (**12**) and 6,6-dimethyl-1-vinylcyclohexene (**11**) to form the B ring and furnish tetracyclic compound **13** (Scheme 2.3). A structural rearrangement was then employed to install the D ring, which upon oxidation provided tanshinone IIA in 6 steps from the advanced intermediates **11** and **12**.[17] This route has served as a benchmark method for the formation of many different members of the tanshinone family varying the substitution on diene and dienophile.[18,19]

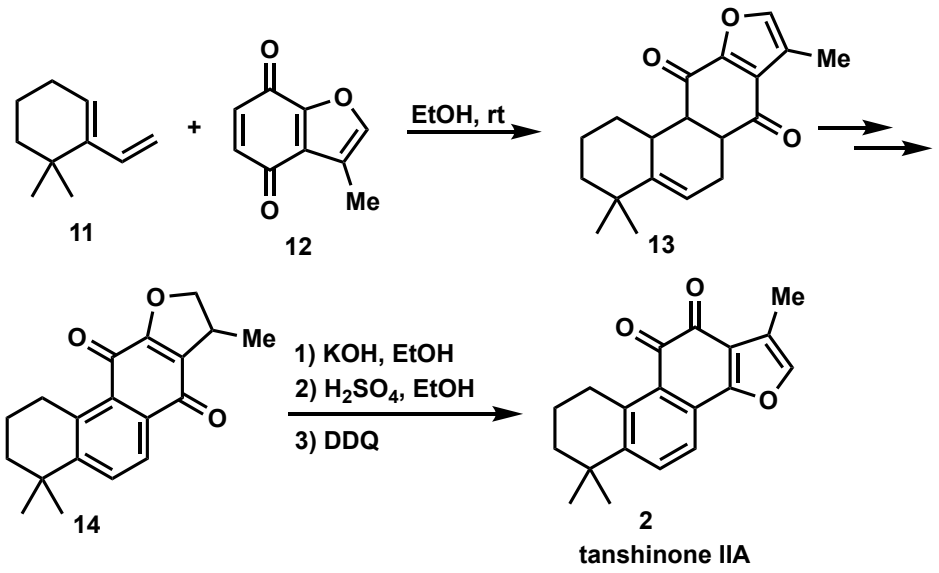

Scheme 2.3: Diels-Alder strategy for synthesis of tanshinone IIA by Kakisawa and Inouye.

Another landmark synthesis of tanshinone IIA was reported in 1995 by Danheiser. The synthetic strategy is initiated by the use of traditional reactions such as Negishi coupling[20] and Friedel-Crafts cyclization to furnish the A ring, providing bicyclic intermediate **17** (Scheme 2.4). Next, **17** was converted into the α-diazocarbonyl **18**, which was then utilized in an intriguing tandem photochemical Wolff rearrangement / [2+2]cycloaddition / 4π-electrocyclic cleavage / 6π-electrocyclization reaction (commonly referred to as the Danheiser benazannulation[21]) to furnish the C ring in **20**. After a series of functional group interconversions tanshinone IIA was isolated in an overall 11 steps.[22] This synthesis is noteworthy because it is one of the few reported syntheses that furnishes the C ring, as well as rings A and D. However, the cost of building these three rings may be lost in terms of chemical efficiency, as the multiple ring formations resulted in a high step count associated with this route. Also, while the yields of many steps are moderate to high, they require complex reagents that are not commercially available.

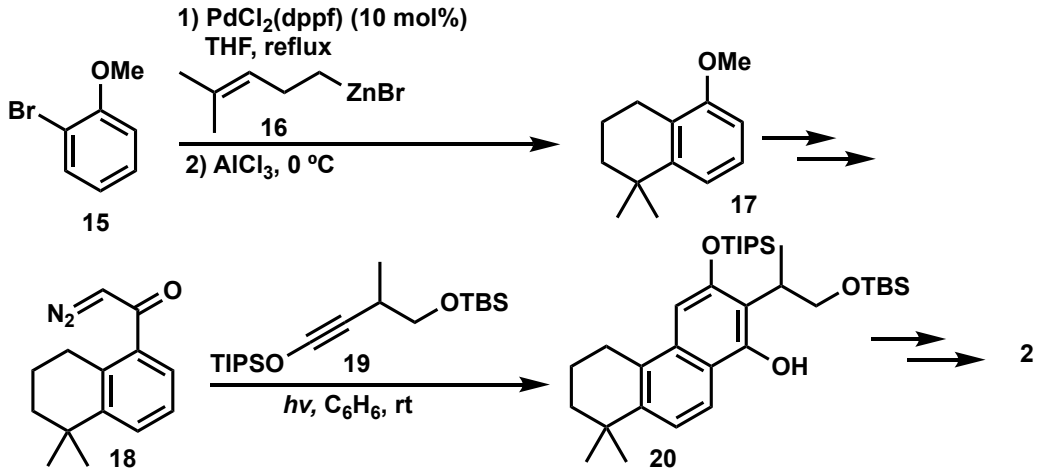

Scheme 2.4: Photochemical annulation strategy for the synthesis of tanshinone IIA by Danheiser.

In 2003, Jiang and coworkers reported a novel 12 step synthesis of tanshinone IIA. Their synthesis began from commercially available 1,5-naphthalenediol, which structurally provided the foundation of the B and C rings of natural product. The A ring was installed in 4 steps from the starting material, and another 3 steps gave aryl bromide **21**.[22] Next, a SmI_2 promoted cyclization between the aryl bromide moiety and the alkene in a 5-*exo*-*trig* processes provided the D ring in **22** (Scheme 2.5). With **22** in hand the next pivotal synthetic challenge was the installation of the diketone moiety on the C ring. It is important to note that this strategy differs from previous works, where the functional groups required to form the diketone were preinstalled in the starting materials. In contrast, the route undertaken by Jiang required installation of this functionality after the tetracyclic ring system was constructed. To complete this challenge, **22** was nitrated under mild conditions to provide nitro adduct **23**, which then underwent a subsequent reduction to the corresponding amine via catalytic hydrogenation. The synthesis was finished by treating the amine with Frémy's

salt to generate the diketone and DDQ to aromatize the furan ring and deliver tanshinone IIA.[22]

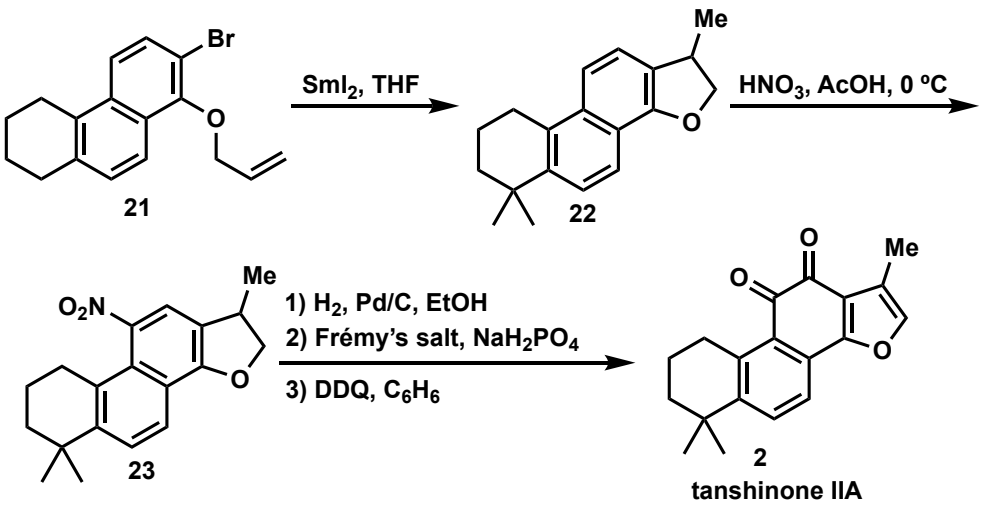

Scheme 2.5: Remote functionalization strategy in the synthesis of tanshinone IIA by Jiang.

The most recent total synthesis of tanshinone IIA was reported in 2020 by Huang *et al.*[23] Their synthesis starts from a similar intermediate (**24**) to Danheiser's synthesis, that is easily prepared in 2 steps from phenol (Scheme 2.6). Through a 5-step sequence, alcohol **24** was converted into β-keto ester **25** which was subjected to base catalyzed conditions to furnish the furan D ring in **26**. All that remained was to close the C ring, which they accomplished by first converting **26** to diester **27** followed by an acyloin condensation reaction with sodium metal which completed the synthesis of tanshinone IIA in 12 overall steps (Scheme 2.6).[23]

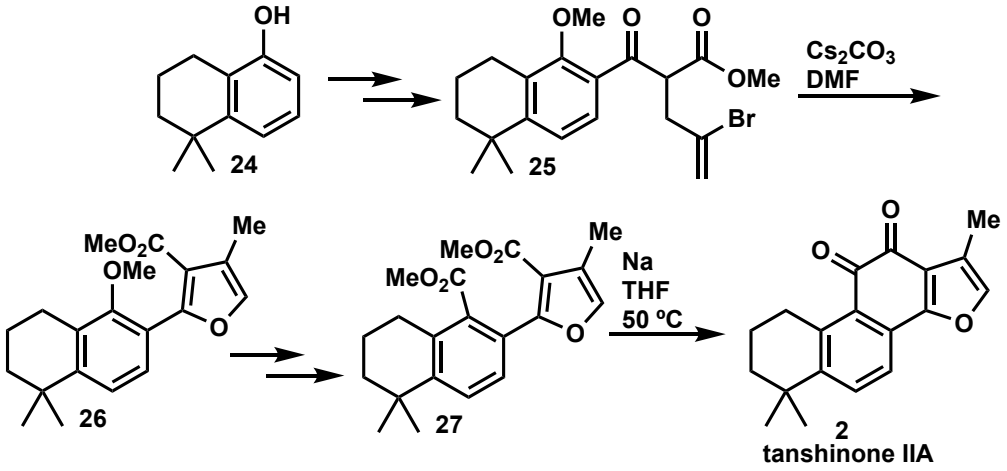

Scheme 2.6: Total synthesis of tanshinone IIA by Huang.

While these previous syntheses show the ingenuity of organic chemistry in fabricating complex molecules, it is evident after analysing these synthetic strategies that there are some drawbacks. For example, many routes that start from simple building blocks result in moderately high overall step counts. Conversely, if one starts from more complex products, the starting material is less available for general chemists and thus has a very niche use. Kakisawa and Inouye tried to circumvent these issues via their Diels-Alder strategy, however, that key reaction suffers from low yield and issues with stability and regioselectivity.[17] Therefore, developing alternative strategies to access tanshinones are of great importance in making these molecules readily available.

2.1.2 Project Objectives and Initial Retrosynthetic Analysis en Route to Tanshinone IIA

The goal for this project was to develop an efficient synthesis to tanshinone IIA, using strategic transformations to lower the step count below previous reports while also increasing chemical efficiency. Taking inspiration from Huang's synthesis, it was

envisioned that the final *ortho*-quinone ring could be furnished via a similar acyloin condensation of diester **27** (Scheme 2.7). Examining this molecule, a very simple bond disconnection arises by severing the biaryl bond to give two coupling partners. Thus the main strategy would be centered around developing conditions to achieve this bond formation through oxidative biaryl coupling methodology. The two simplest starting materials for this transformation were envisioned to be ethyl furoate **29**, and tetralin acid derivative **28** which contains a carboxylic acid group that could ideally control the regiochemical outcome of the coupling step by use as a directing group.

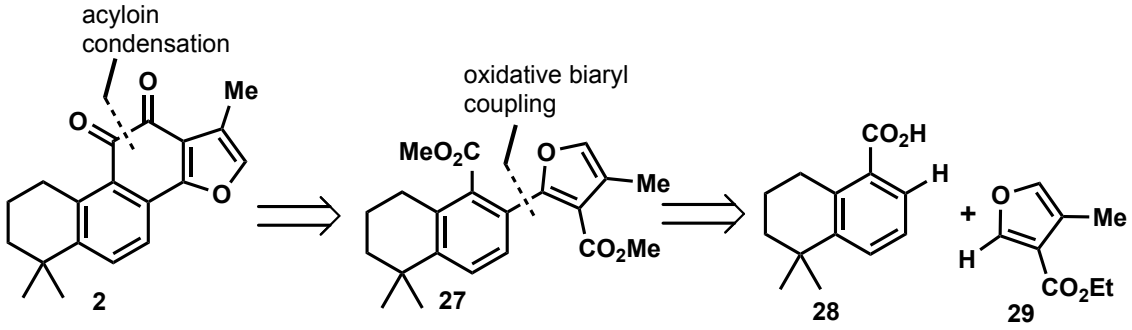

Scheme 2.7: Retrosynthetic analysis of the proposed route to tanshinone IIA.

2.2 Results and Discussion

2.2.1 Synthesis of Starting Materials

From the onset of this project, the interest in constructing the molecular complexity of tanshinone IIA from simple, cheap, readily available feedstock starting materials was one of the main goals. To this end, it was envisioned that required biaryl coupling partner **28**, a functionalized tetralin system containing both the A and B rings of the natural product, could be accessed from commercially available *o*-toluic acid via a selective C–H functionalization annulation strategy (Scheme 2.7). The importance of *o*-toluic acid in

achieving these synthetic goals was threefold; the starting material is cheap ($0.14/g from Sigma-Aldrich), the aryl ring represents the B ring of the natural product, and the carboxylic acid group can be utilized as an important directing group to control site selectivity of the required functionalization chemistry.

Inspired by previous methods on directing group enabled lateral metalation chemistry, an approach where metalation occurs at the benzylic (side chain) position of an alkyl substituted aromatic system, lateral to the directing group,[24] exploration began into metalation of *o*-toluic acid. Screening various alkyl lithium bases, it was found that treatment of **30** with 2.2 equivalents of *t*-BuLi at –78 °C, followed by the addition of prenyl bromide as an electrophile, delivered alkene **31** in an excellent 97% yield on multigram scale (Scheme 2.8). Subjecting alkene **31** to traditional Friedel-Crafts conditions furnished the desired carboxylic acid coupling partner **28** in excellent yield, again on multigram scale.

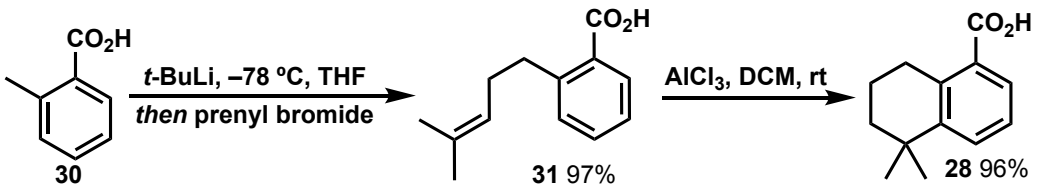

*Scheme 2.8: Two-step synthesis of key carboxylic acid **28**.*

Next the focus shifted to synthesizing the desired furan coupling partner. Previous members of our group had experimented with a method of synthesizing furans using a Diels-Alder reaction between oxazoles and alkynes, which was initially reported by Liotta.[25] To make use of this procedure we also needed access to the appropriate oxazole, which could be synthesized from isocyanide **33** (Scheme 2.9),[26] which is commercially

available, but for the purpose of this experiment was readily synthesized on a multigram scale from benzylamine **32**.

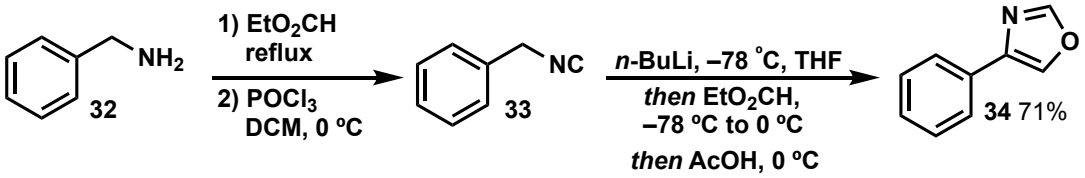

*Scheme 2.9: Synthesis of oxazole **34.***

With oxazole **34** in hand, what came next was to explore the [4+2]/retro [4+2] reaction of **34** with ethyl 2-butynoate to construct **29** (Table 1). It is important to note that based on previous experience with this type of transformation in the Grover group (unpublished results) all reactions were run without solvent, and a catalytic amount of hydroquinone was added to inhibit polymerization.[27] Initial attempts at the cycloaddition, using traditional heating in a sealed tube, following the preliminary procedure reported by Liotta,[25] suffered from long reaction times; however, **29** was obtained in moderate yield (Table 2.1 entry 1). Unfortunately, attempts to increase the yield of the reaction or decrease the reaction time by using higher temperatures under these traditional heating conditions proved unsatisfactory. It was found that through some sequential variation in conditions (Table 1 entries 2-5), the yield of the transformation could be increased, while simultaneously lowering the reaction time, temperature, and amount of oxazole used by performing the reaction in a microwavewave reactor. Thus the second coupling partner furoate **29** was able to be isolated in 74% yield on a gram scale.

Table 2.1: Optimization of the Diels-Alder reaction.

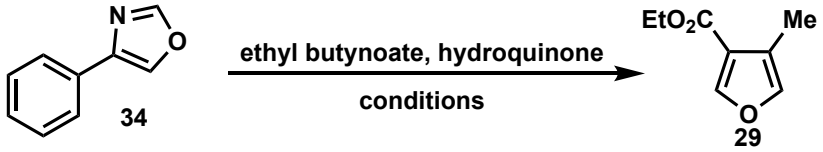

Entry	Equivalents of oxazole **34**	Temperature (source)	Time	Yield of **29**
1	2.5	240 ºC (heating mantle)	72 h	60%
2	2.5	240 ºC (microwave reactor)	1.5 h	59%
3	2.5	220 ºC (microwave reactor)	1.5 h	65%
4	2.0	220 ºC (microwave reactor)	2 h	74%
5	1.5	220 ºC (microwave reactor)	2 h	66%

2.2.2 Initial Coupling Attempts

Now that both coupling partners had been obtained, the oxidative biaryl coupling reaction was ready to be attempted. It was theorized that the carboxylic acid moiety of **28** could serve as a directing group to ensure a regioselective coupling, on the basis that benzoic acids and their derivatives have been shown to undergo various *ortho*-functionalization reactions via directed C–H activation pathways with transition metals.[28,29] Inspired by a previous report where benzoic acids are used to direct regioselective coupling with furan derivatives (Scheme 2.10A),[30] both carboxylic acid **28** and furan ester **29** were subjected to Rh(III) catalyzed coupling conditions (Scheme 2.10 B).

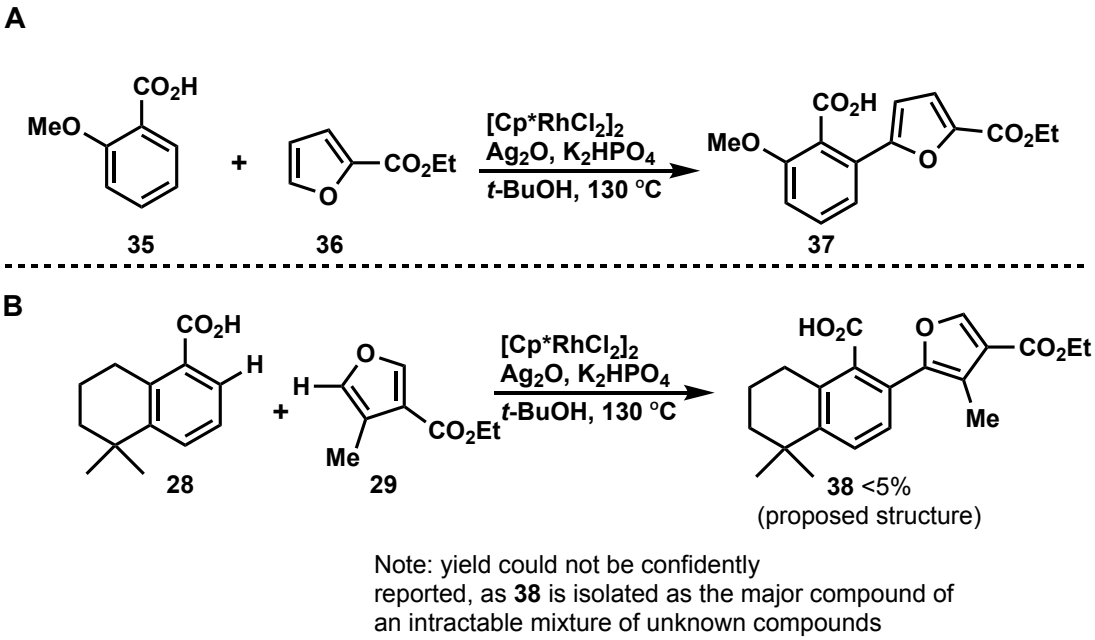

*Scheme 2.10: A: Rh(III) catalyzed coupling between benzoic acids and furans.[30] B: Rh(III) catalyzed coupling attempts between **28** and **29.***

Interestingly, while these reaction conditions led to a significant amount of recovered starting material, a trace amount of an impure compound containing both the furan and tetralin ring systems was also isolated. The tentative structure of this compound has been assigned as coupling product **38** where unfortunately the furan has coupled at the C5 position instead of the desired C2 position. Assignment of this structure was based on the presence of the aliphatic signals of the tetralin piece (Figure 2.1); 2.88 ppm (triplet), 1.84 ppm (multiplet), and 1.69 ppm (multiplet) as well as the aromatic signals H_d at 7.49 ppm and H_c 7.25 ppm (Figure 2.2). The furan C2 (H_a) position is observed as a singlet at 7.97 ppm, and the furan methyl group (H_b) is also observed as a singlet at 2.31 ppm. Of importance in determining the connectivity of furan to the tetralin ring system are the signals at 7.97 and 2.31 ppm. If the desired coupling were to occur, it is expected that there would be coupling between H_a and H_b as is observed in the NMR of the furan **29**

(see experimental for further details). As both H_a and H_b are represented as singlets, our current structural assignment is **38**. Note that due to time constraints, further characterization of this undesired coupling product was not completed.

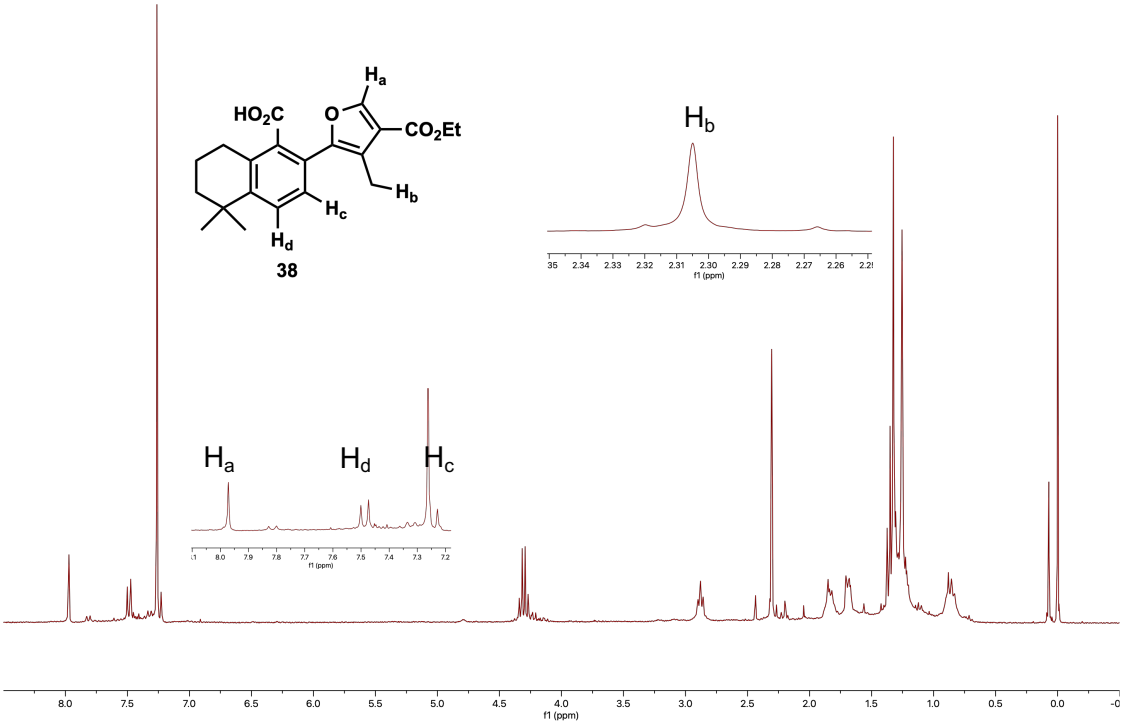

*Figure 2.1: ^{1}H NMR spectrum of undesired coupled product **38.***

Despite this undesirable result, valuable information was still obtained from this experiment; it was clear that the carboxylic acid could act as an effective directing group for the coupling under metal catalysis. Thus alternate reaction conditions were explored, taking inspiration from various literature sources which utilized carboxylic acids as directing groups in transition metal catalyzed C–H functionalization reactions.[31–33] While many of these reaction conditions resulted only in recovery of starting materials, one set of conditions in particular generated another interesting result. When the two coupling (**28**

and **29**) partners were reacted under palladium(II) catalysis (Scheme 2.11), the only other observed product apart from starting material was dimer **39**. Through a similar analysis to the previous Rh(III)-coupling product, the ^{1}H NMR spectrum of **39** did not show coupling between the methyl group of the furan and the C5 position indicating that the dimerization had occurred between the C5 carbons.

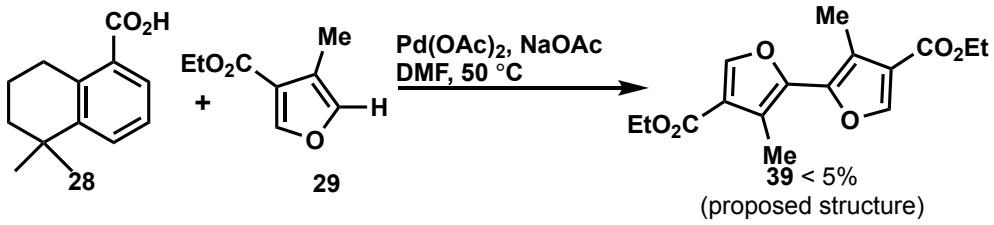

Scheme 2.11: Palladium-catalyzed biaryl coupling attempt

This result (Scheme 2.11), along with the initial rhodium-catalyzed coupling attempt (Scheme 2.10 B), potentially indicated that if an oxidative biaryl coupling between **28** and **29** were to be successful, the inherent electronics of the furan (C2 less electron rich then C5) in the C–H activation step with metal catalyst, may always favour the undesired coupling product. To avoid this electronic bias it was theorized that transforming ester **29** into a carboxylic acid could provide a second directing group to coordinate to the catalyst and thus lead to activation of the C2–H furan. Further literature searching revealed a previous report where benzoic acids were shown to undergo dimerization using Rh(III) catalysts (Scheme 2.12).[33]

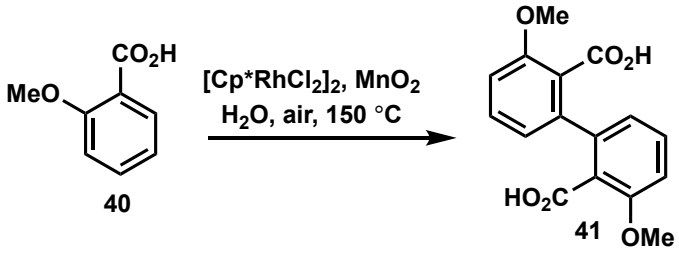

Scheme 2.12: Rh(III)-catalyzed dimerization of benzoic acids by Li.

To test the feasibility of this double directing group involved biaryl coupling strategy, furan ester **29** was hydrolyzed with aqueous potassium hydroxide in refluxing ethanol, to deliver furoic acid **42** in excellent yield (Scheme 2.13).With this new coupling partner in hand the same initial rhodium catalyzed biaryl coupling that delivered the undesired product coupling through the C5 position of the ethyl furoate was attempted (Scheme 2.10 B).[30] Attempting this reaction with the two different carboxylic acids (**28** and **42**), the only observable product other than recovered starting materials was another dimer **43** (Scheme 2.13). The connectivity of this dimer was proposed due to the fact that the C5 proton is now seen as a quartet, and the furan methyl protons are seen as a doublet (Scheme 2.13).

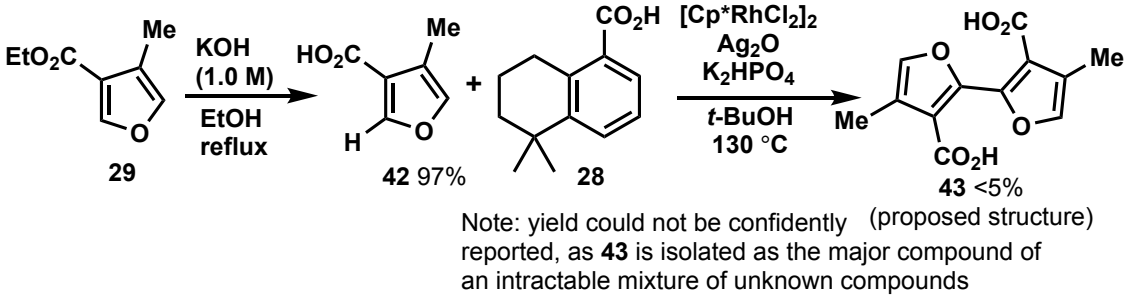

Scheme 2.13: Rhodium-catalyzed cross-coupling attempt using carboxylic acids.

While this result was again undesirable for the construction of tanshinone IIA, it indicated that the use of the carboxylic acid on the furan could potentially control the selectivity in the coupling. Further attempts at other coupling reactions using alternate palladium or rhodium catalyzed conditions were met with further challenges.[31,33] Attempted coupling with palladium acetate led to coupling of the two partners, however it proceeded through the C5 position of the furan resulting in dimer **44** (Scheme 2.14). Utilizing alternate rhodium catalysts with different solvents produced intractable mixtures of products (Scheme 2.14).

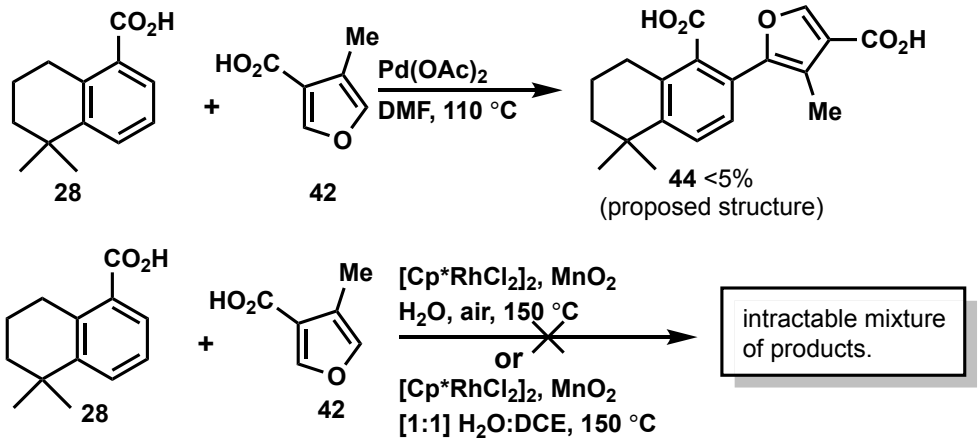

Scheme 2.14: Further attempts at carboxylic acid cross-coupling.

Frustrated by the lack of desired coupling between the two partners, it was theorized that perhaps converting one to an aryl halide would be beneficial in aiding in the reaction. This was supported by a literature procedure where 3-ethyl furoate **46** was selectively coupled with aryl bromides under palladium catalysis (Scheme 2.15 A).[34] To explore this new coupling route, it was decided to directly convert readily accessible tetralin carboxylic acid **28** into the corresponding aryl iodide **48** (Scheme 2.15 B). This selective

functionalization was achieved by employing carboxylic acid directed palladium(II) C–H activation conditions developed by Yu and coworkers[35] to construct *ortho*-iodoaryl carboxylic acid **48**. Notably, this transformation can be completed on a gram scale, in good overall yield, with no indication of other iodinated products.

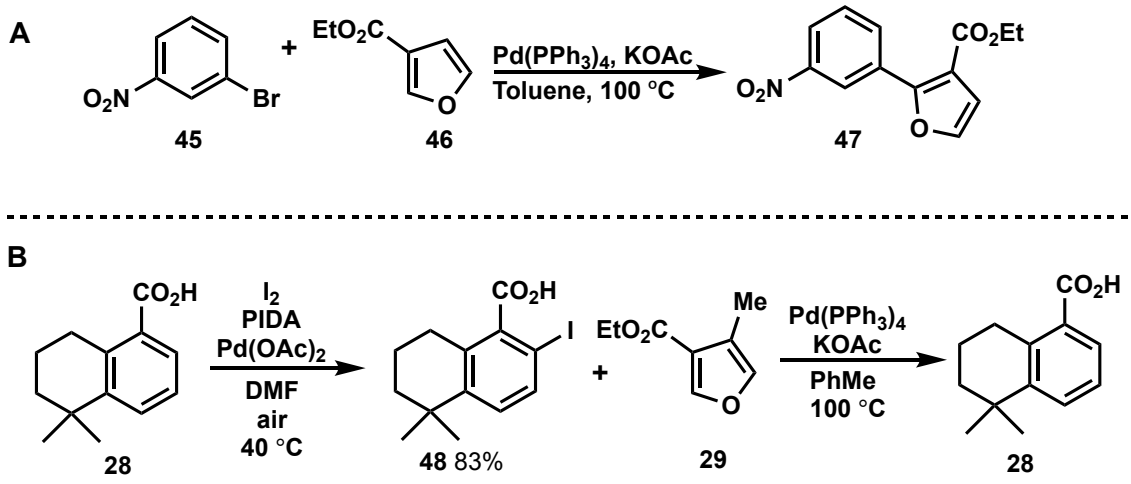

*Scheme 2.15: A: Literature reported coupling of aryl bromides with furan esters. B: Iodination and subsequent coupling attempt with furoate **29**.*

Iodide **48** was then subjected to the above mentioned coupling conditions with furan ester **29** (Scheme 2.15 B). Despite the fact that the paper reports decent yields as well as regiocontrol over the coupling site,[34] the only product that was isolated, other than recovered starting material **29**, was de-iodinated acid **28**. This result illustrated that palladium could undergo an oxidative addition into the C–I bond, however, protodepalladation,[36] potentially aided by the carboxylic acid, under these conditions limited a desired cross coupling pathway.

With facile access to aryl iodide **48** the next strategy to be explored was the possibility of forming the desired carbon–carbon bond by a palladium-catalyzed C–H

arylation of furoic acid **42** with **48** (Scheme 2.16).[37] Over the past 15 years, starting from one of the preliminary reports by Daugulis in 2007,[38] the palladium(II)-catalyzed, *ortho*-C–H arylation of benzoic acid derivatives with aryl iodides by a proposed Pd(II) → Pd(IV) cycle has become a very useful method for generating biaryl compounds. Unfortunately, subjecting **42** and **48** to similar palladium coupling conditions,[39,40] yielded mainly the de-iodinated tetralin product **28**, along with a very small amount of material that appeared to be a complex mixture of compounds by ^{1}H NMR analysis. One such compound in this mixture that was compiled from multiple coupling attempts was revealed to be dimer **49** which was confirmed by X-ray crystallography (Scheme 2.16).

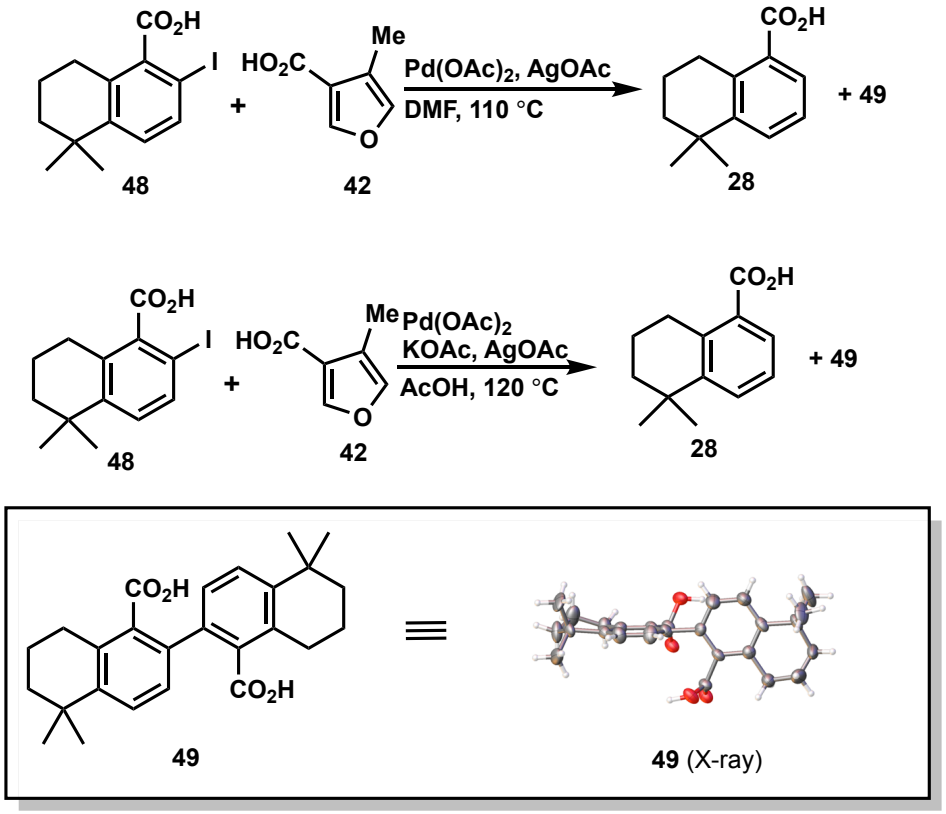

Scheme 2.16: Further attempts at directed couplings using aryl iodides.

Exploring alternate solutions, it was theorized that simply transforming the furoic acid into an aryl iodide and attempting the coupling with this different halide could furnish the desired carbon–carbon bond. Thus furoic acid **42** was treated with LDA and iodine to obtain iodofuran **50** in excellent yield on a gram scale (Scheme 2.17).[41] However, even with this different aryl halide coupling partner the result was still the same, the reaction conditions delivered more de-iodinated product **41** (Scheme 2.17).[42]

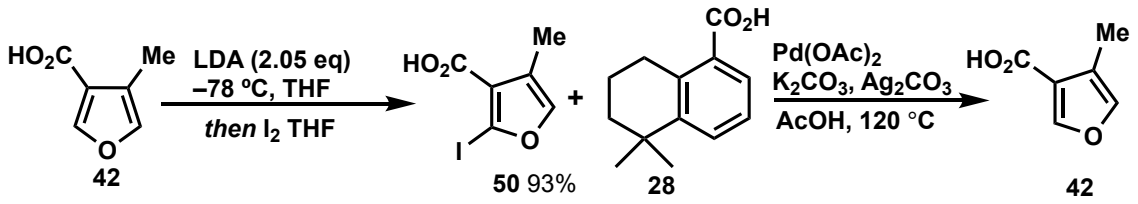

*Scheme 2.17: Synthesis and coupling attempt of iodofuran **50** with aryl carboxylic acid*

Observing that all coupling attempts with aryl iodides **48** or **50** containing an *ortho*-carboxylic acid moiety resulted mainly in dehalogenation, regardless of the efforts to keep the reactions dry, it was theorized that the carboxylic acid itself may be detrimental to the desired cross coupling. Thus the iodo-acid **48** was methylated to iodo-ester **51** with the hopes of combating this recurring issue (Scheme 2.18).[43] Although ester **51** is only isolated in a modest 70% yield, the base mediated conditions reported in Scheme 2.18 are important as attempts to esterify the carboxylic acid under acidic Fischer conditions (EtOH or MeOH, H_2SO_4, reflux) resulted in de-iodination and decomposition.

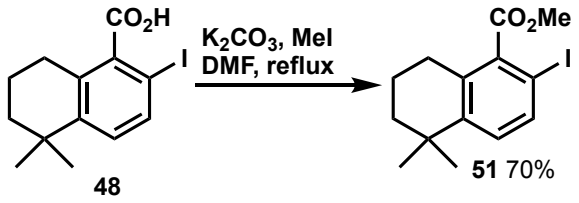

*Scheme 2.18: Esterification of aryl iodo-carboxylic acid **48.***

In the interest of accomplishing the desired coupling, it was decided that a traditional coupling reaction may be more fruitful than continuing to battle all the challenges associated with the C–H arylation coupling strategy. Thus, attempts to transform furoic acid **42** into a suitable coupling partner with preinstalled functionality were investigated. Unfortunately, initial attempts to metallate **42** at the C2 position and quench with $B(OMe)_3$ then aqueous HCl to provide the boronic acid were unsuccessful. Gratifyingly, metallation of **42** with 2.05 equivalents of BuLi, followed by addition of tributyltinchloride furnished organostannane **53** (Scheme 2.19).[41] This yield is approximate due to the presence of butyl impurities that could not be removed.

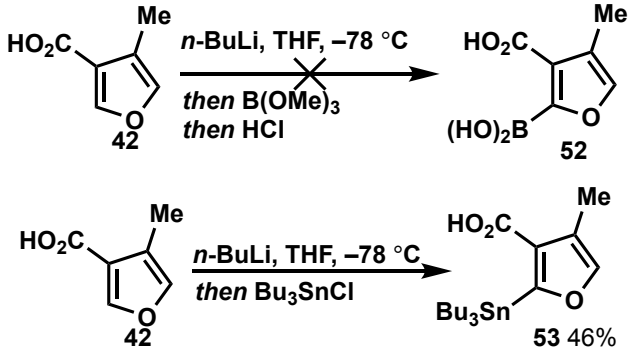

Scheme 2.19: Synthesis attempts of alternate coupling partners.

Now having access to aryl iodide **51** and crude organostannane **53**, a Stille coupling was then attempted. Treatment of **51** and **53** with $PdCl_2(PPh_3)_2$ in THF at 80 ºC provided the first indication of desired coupling product **54** (Scheme 2.20).[44] In addition to the desired product this reaction also yielded significant amounts of de-iodinated ester and furoic acid product arising from a loss of the iodine and tributyltin groups respectively.

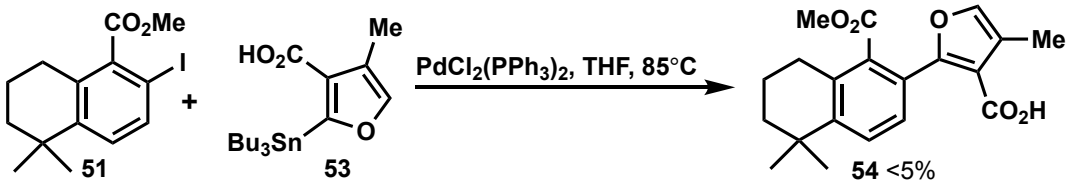

*Scheme 2.20: Synthesis of biaryl coupling product **54** via Stille coupling.*

The connectivity was determined by analyzing the ^1H NMR in the same way as previous coupled products (Figure 2.2). Noticeably, H_a is now observed as a quartet, and H_b is observed to be a doublet. This indicates that the coupling must be through the C2 position of the furan as was desired.

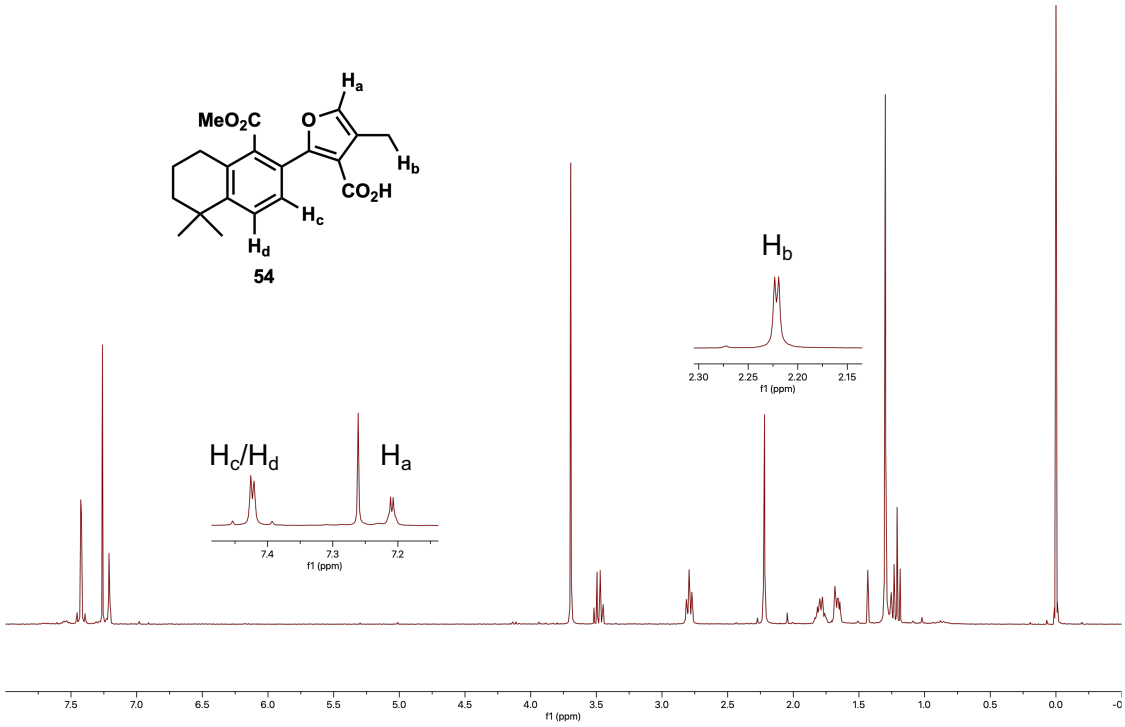

*Figure 2.2: ^{1}H NMR spectrum of desired coupled product **54.***

Again, it was hypothesized that the de-iodination could possibly be a result of the carboxylic acid acting as a proton source for protodemetallation/protodehalogenation. Thus, the strategy pivoted to coupling two suitably functionalized esters. An added advantage of this approach is that the ester groups would be required for the final ring closing step to access the C ring of natural product. The first attempt at altering the coupling partner was to convert iodo-ester **51** to a boronic ester **55**. Using traditional Miyaura borylation conditions accomplished this in moderate yield,[45] however, the yield decreased substantially on larger scale (Scheme 2.21).

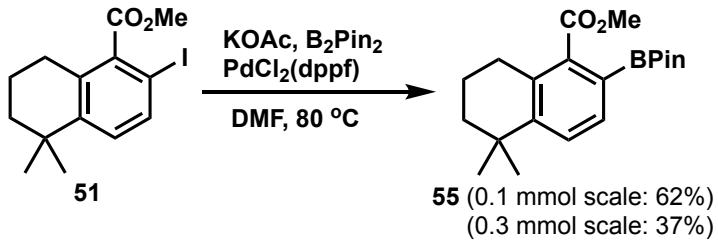

*Scheme 2.21: Synthesis of boronic ester **55** via Miyaura borylation.*

It was found that access to **55** could be improved, while also circumventing the need for an aryl iodide by applying an iridium-catalyzed C–H borylation strategy. Pleasingly, when ester **56**, which can be synthesized in near quantitative yield from carboxylic acid **28** by Fischer esterification, was subjected to iridium-catalyzed *ortho*-borylation,[46] boronic ester **55** was isolated in 97% yield (Scheme 2.22). Interestingly, this reaction was not only high yielding but also highly regioselective, as boronic ester **55** was the only observed product. Ultimately, this approach provided a very simple and high yielding route to the boronic ester coupling partner and thus a Suzuki reaction seemed like the most obvious next step to furnish the desired C–C bond.

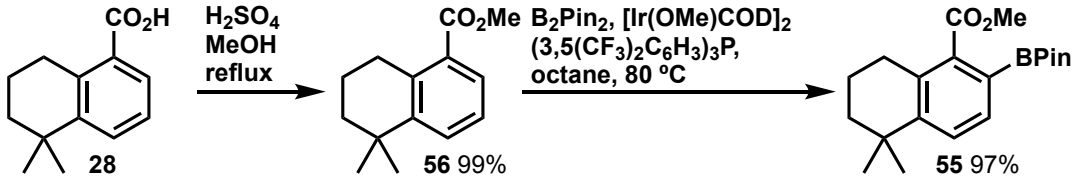

*Scheme 2.22: Two-step synthesis of boronic ester **54** using iridium catalysis.*

Returning to iodo-furoic acid **50,** attempts at making it an organoboron or organotin reagent were challenging and low yielding. Thus, it was esterified to give iodo-ester **57** which would act as the new aryl iodide for the desired coupling (Scheme 2.23).[43] Alternatively, direct metallation of furoate **29** was attempted using Hauser's base to

generate iodo-ester **58** (Scheme 2.23).[47] The initial attempt was low yielding; therefore the route was carried through using the methyl ester iodide **57,** as it could be accessed more reliably. However, this direct metallation strategy could reduce overall step count once optimized.

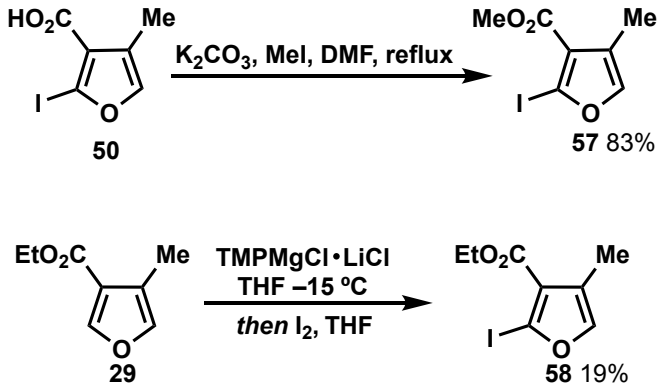

Scheme 2.23: Strategies for synthesis of iodo-furan coupling partners.

With **55** and **57** in hand the strategy to furnish the desired coupling product through a Suzuki reaction was attempted. Initial attempts at accomplishing this with similar conditions to the initial Miyaura borylation were fairly low yielding (Scheme 2.24), and thus alternative conditions were explored. XPhos Pd G2 is a bench stable catalyst that was developed for cross-coupling reactions,[48] and using this palladium catalyst in tandem with additional XPhos ligand was able to accomplish this transformation in excellent yield to give diester **59** (Scheme 2.24).

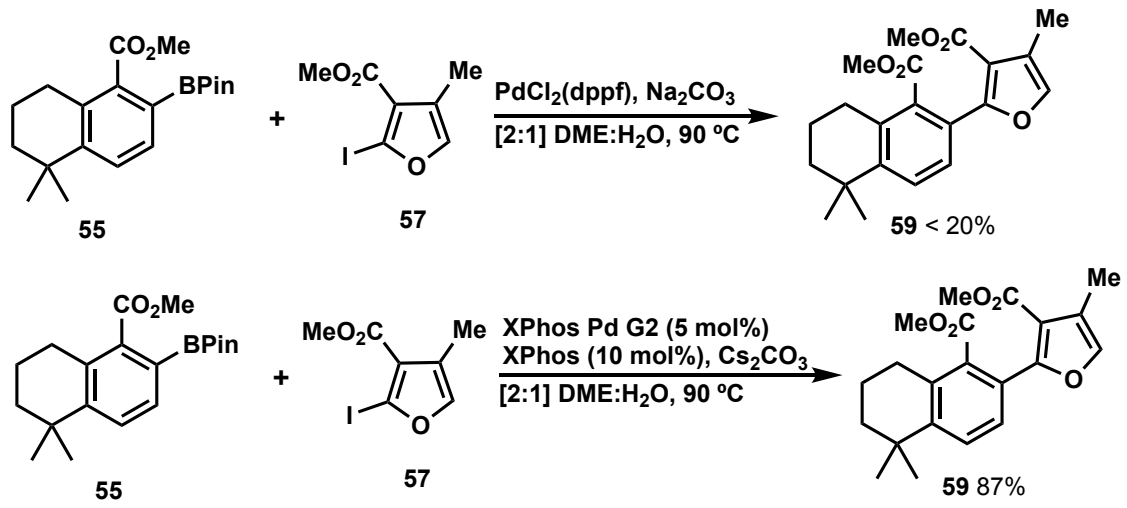

*Scheme 2.24: Attempts at forming diester **59** using Suzuki reaction.*

Now that a reliable route to diester **59** had been realized, what remained was to furnish the final C ring and complete the total synthesis of tanshinone IIA. Taking inspiration from Huang's synthesis,[23] it was envisioned that the final ring could be furnished via an acyloin condensation between the two esters to yield the *ortho*-quinone moiety. Unfortunately, recreating this result by heating diester **59** with sodium metal only delivered recovered starting material (Scheme 2.25). Amount of material on hand limited this to one attempt.

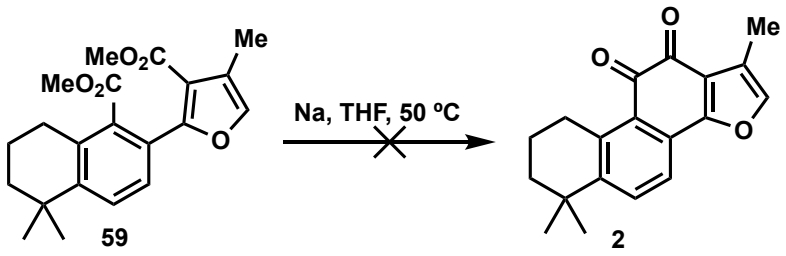

*Scheme 2.25: Failed acyloin condensation of diester **59.***

Searching for alternate strategies to furnish the *ortho*-quinone ring, a similar transformation in which a diester of biphenyl was subjected to a Brook rearrangement using trialkyltinlithium reagents to give phenanthrenequinone was identified (Scheme 2.26).[49] Mechanistically this occurs via a direct addition of Me_3SnLi to one of the esters in **60**, generating a stannyl adduct **61**, which can undergo a rearrangement to give an oxy carbanion **62** that can perform an intramolecular addition to the nearby ester and furnish phenanthrenequinone **63** upon protic workup.

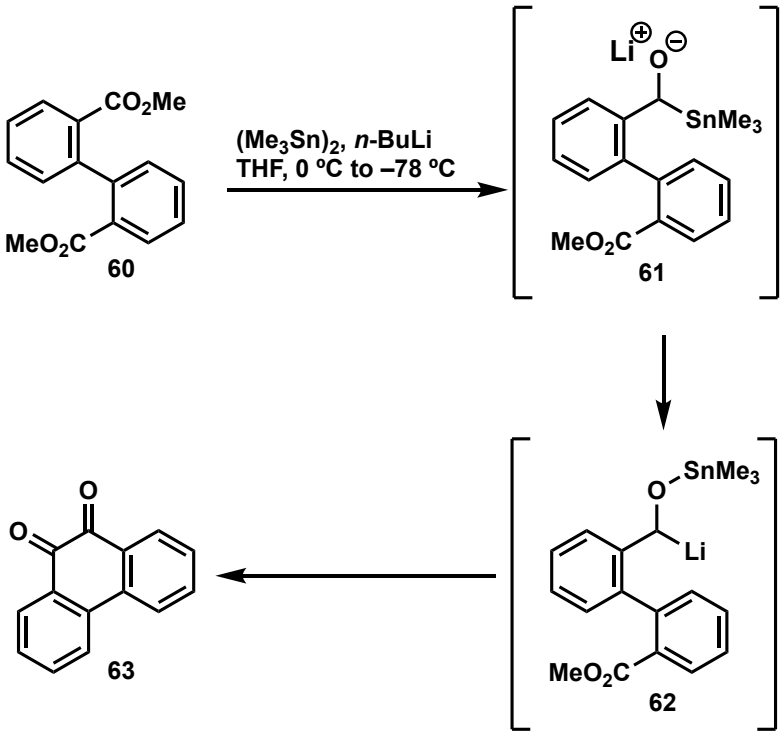

Scheme 2.26: Mechanism of Stanna-Brook rearrangement by Sardina.

Applying this methodology to diester **59** pleasingly delivered tanshinone IIA (**2**) as a 4:1 mixture with recovered starting material (Scheme 2.27). The product was isolated as an intensely red solid, with ^{1}H proton NMR signals matching literature data exactly. It

should be noted that the starting material is inseparable from the product, however diagnostic signals for the natural product could still be observed (see experimental for further explanation). Attempts to ensure complete conversion of starting material to the target molecule are ongoing.

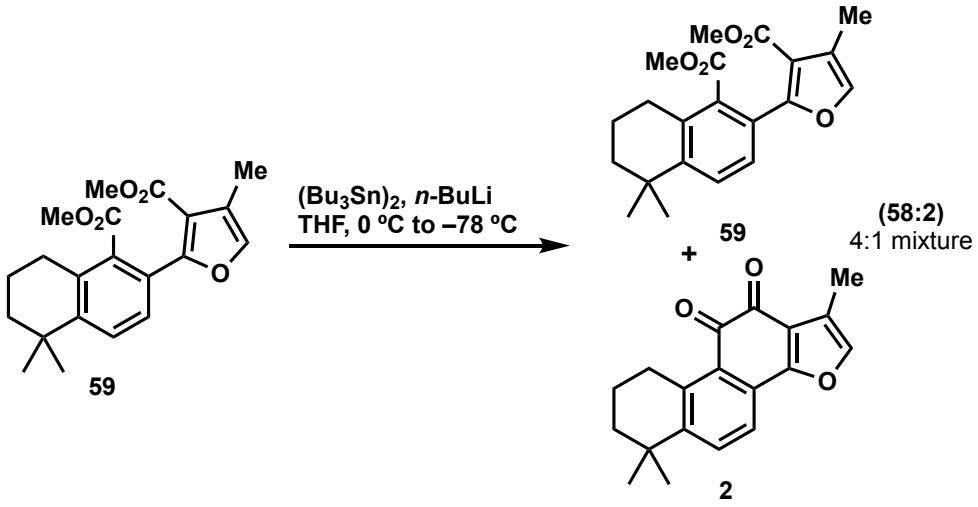

Scheme 2.27: Stanna-Brook rearrangement allows the synthesis of tanshinone IIA.

In conclusion, controlling the regioselectivity of biaryl couplings is a challenging endeavor. It was discovered that the use of directing groups can hinder reaction development as much as they can aid it. Combatting this hinderance required C–H functionalization on each coupling partner to use a more traditional cross coupling strategy. This allowed for the completed synthesis of tanshinone IIA in 7 longest linear steps from commercially available isocyanide **33**.

2.3 Experimental

2.3.1: General procedures

Unless otherwise stated, all reactions were performed in flame-dried glassware under a nitrogen atmosphere. Microwave heating was performed on an Anton Paar Monowave 50 +P system in a sealed tube. Dry solvents were obtained from Sigma Aldrich SureSeal™ bottles or by passing these solvents through activated alumina columns. Unless stated elsewhere, chemicals were purchased from commercial suppliers and used directly as received. Reactions were monitored by thin layer chromatography (TLC) on Silicycle Siliaplate™ glass backed TLC plates (250 μm thickness, 60 Å porosity, F-254 indicator) and visualized by UV irradiation or development with anisaldehyde stain. Volatile solvents were removed under reduced pressure using a rotary evaporator. All column chromatography was performed using Silicycle SiliaFlash® F60, 230-400 mesh silica gel (40-63 μm). ^{1}H and ^{13}C NMR spectra were measured on a Bruker Avance III 300 MHz multinuclear spectrometer or a Bruker AVANCE 500 MHz spectrometer, using $CDCl_3$ as solvent. Except when noted otherwise, chemical shifts are reported relative to the residual solvent signal (^{1}H NMR = 7.26 ($CHCl_3$); ^{13}C NMR = 77.16 ($CDCl_3$)). Coupling constants (*J*) are given in Hz. NMR data is reported as follows: chemical shift (multiplicity, coupling constant, number of hydrogens). Splitting is reported with the following symbols: s = singlet, bs = broad singlet, d = doublet, t = triplet, dd = doublet of doublets, q = quartet, m = multiplet. Infrared (IR) spectra were recorded using neat samples on a Bruker Alpha spectrometer. High resolution mass spectrometry (HRMS) data were obtained using an Agilent 6200 series instrument, employing a TOF mass analyzer. Melting points (**MP**)

were obtained on an OptiMelt instrument (a digital apparatus) produced by Stanford Research Systems by scanning temperature ranges from 40 - 150 °C at a rate of 3 °C/min.

2.3.2: Synthetic procedures

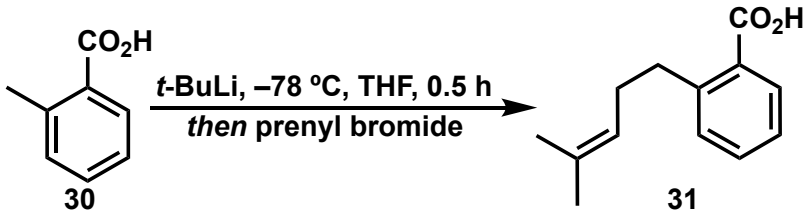

Procedure:
To a flame dried round bottom flask under N_2 was added *o*-toluic acid **30** (2.63 g, 19.3 mmol, 1.0 eq) and dissolved in dry THF (77.2 mL). The solution was cooled to –78 ºC and *t*-BuLi (25.0 mL, 42.5 mmol 2.2 eq) was added slowly via cannula over 15 min. When the addition of base was complete, the reaction mixture was stirred at –78 ºC for 15 min, then at room temperature for another 15 min. The reaction mixture was then cooled back to -78 ºC and prenyl bromide (5.57 mL, 48.2 mmol, 2.5 eq) was added dropwise, and the reaction mixture was allowed to stir for 12 h warming to room temperature. The crude reaction mixture was poured into EtOAc and washed with NaOH solution (x3). The combined aqueous layers were acidified to approx. pH 2.0 with 20% HCl and extracted with Et_2O (x3). The combined organic layers were washed with water (x2), brine (x2), dried over $MgSO_4$, and concentrated *in vacuo* to give carboxylic acid **31** (3.82 g, 18.7 mmol, 97%) as a white solid which was used without further purification.
R_f = 0.60, 25% EtOAc in hexanes.
Melting Point: 70.4 ºC – 73.8 ºC
^{1}H-NMR (300 MHz, $CDCl_3$) δ = 8.04 (dd, *J* = 8.1, 1.4 Hz, 1H), 7.48 (td, *J* = 7.7, 1.4 Hz, 1H), 7.31 – 7.27 (m, 2H), 5.22 (ddt, *J* = 7.3, 4.2, 1.3 Hz, 1H), 3.09 – 3.02 (m, 2H), 2.32 (q, *J* = 7.5 Hz, 2H), 1.72 – 1.69 (m, 3H), 1.54 (s, 3H);
^{13}C NMR (75 MHz, $CDCl_3$) δ = 173.6, 145.4, 133.0, 132.5, 131.7, 131.6, 128.4, 126.1, 123.9, 34.9, 30.5, 25.9, 17.6;
IR(neat): ν_{max} = 2951, 2856, 2639, 1695, 1402, 1266, 917, 745 cm^{-1};
HRMS (EI+) calc'd for $C_{13}H_{16}O_2$ $[M]^+$ 204.1150, found 204.1140. For $C_{13}H_{15}O_2$ $[M\text{-}H]^-$ 203.1078, found 203.1068.

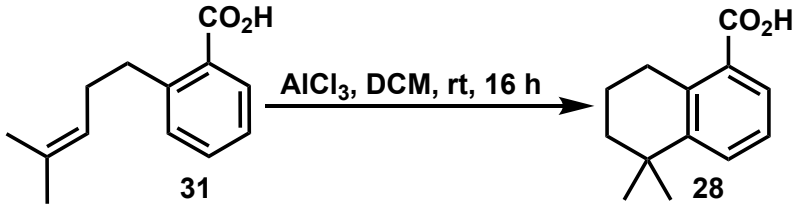

Procedure:

To a flame dried round bottom flask was added carboxylic acid **31** (3.82 g, 18.7 mmol, 1.0 eq), $AlCl_3$ (2.99 g, 22.4 mmol, 1.2 eq) and DCM (74.8 mL). The reaction mixture was let stir open to air for 16 h. The crude reaction mixture was then poured into water and extracted with DCM (x3). The combined organic layers were then washed with NaOH solution (x3). The combined aqueous was then acidified with 20% HCl and extracted with Et_2O (x3). The combined organic layers were washed with water, brine, dried over $MgSO_4$, and concentrated *in vacuo* to give cyclized carboxylic acid **28** (3.66 g, 17.9 mmol, 96%) as a white solid which was used without further purification.
R_f = 0.47, 25% EtOAc in hexanes.
Melting Point: 128.7 ºC-130.9 ºC
^{1}H-NMR (300 MHz, $CDCl_3$) δ = 7.81 (dd, *J* = 7.7, 1.3 Hz, 1H), 7.57 (dd, *J* = 7.9, 1.1 Hz, 1H), 7.22 (t, *J* = 7.4 Hz, 1H), 3.13 (t, *J* = 6.3 Hz, 2H), 1.84 – 1.76 (m, 2H), 1.67 (dd, *J* = 6.0, 2.3 Hz, 2H), 1.31 (s, 6H);
^{13}C NMR (75 MHz, $CDCl_3$) δ = 174.5, 147.4, 138.8, 131.9, 129.1, 128.8, 125.5, 38.6, 34.5, 32.3, 29.3, 19.5;
IR(neat): ν_{max} = 3064, 2932, 2859, 1680, 1579, 1251, 924, 783 cm^{-1};
HRMS (EI+) calc'd for $C_{13}H_{16}O_2$ $[M]^+$ 204.1150, found 204.1136. For $C_{13}H_{15}O_2$ $[M-H]^-$ 203.1078, found 203.1062.

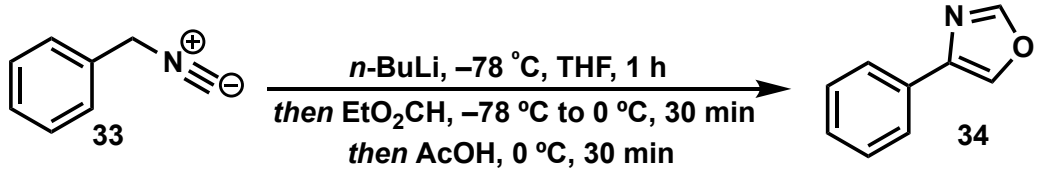

Procedure:
To a flame dried round bottom flask under N_2 was added isocyanide **33** (6.86 g, 58.6 mmol, 1.0 eq) and dissolved in THF (136 mL). This solution was cooled to –78 ºC and *n*-BuLi (24.6 mL, 61.5 mmol, 1.05 eq) was added dropwise. The reaction mixture was stirred at –78 ºC for 1 h, then ethyl formate (7.1 mL, 88 mmol, 1.5 eq) was added dropwise and the reaction mixture was stirred for a further 30 min at –78 ºC. The reaction mixture was then warmed up to 0 ºC and allowed to stir for 30 min before conc. AcOH (3.4 mL, 59 mmol, 1.0 eq) was added and the reaction was allowed to stir at room temperature for 1 h. The reaction was poured into water and extracted with EtOAc (x3). The combined organic layers were washed with water, brine, dried over $MgSO_4$, and concentrated *in vacuo*. The crude residue was purified by flash column chromatography (4-20% Et_2O in hexanes) to give oxazole **34** (6.05 g, 41.7 mmol, 71%) as an orange oil.
R_f = 0.65, 25% EtOAc in hexanes.
^{1}H-NMR (300 MHz, $CDCl_3$) δ = 7.95 – 7.94 (m, 2H), 7.77 – 7.73 (m, 2H), 7.45 – 7.39 (m, 2H), 7.36 – 7.30 (m, 1H);
^{13}C NMR (75 MHz, $CDCl_3$) δ = 151.0, 140.1, 133.4, 130.4, 128.5, 127.9, 125.3;
IR(neat): ν_{max} = 3128, 3035, 1514, 1448, 1104, 1062, 911, 744 cm^{-1};
HRMS (EI+) calc'd for C_9H_7NO $[M]^+$ 145.0528, found 146.0526. For C_9H_8NO $[M+H]^+$ 146.0600, found 146.0599.

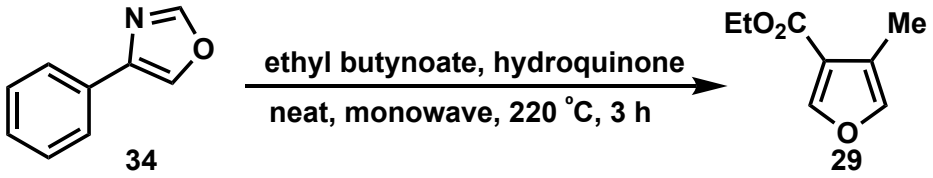

Procedure:
To a thick-walled reaction tube was added oxazole **34** (2.59 g, 17.8 mmol, 2.0 eq), ethyl butynoate (1.04 mL, 8.92 mmol, 1.0 eq), and hydroquinone (98.2 mg, 0.892 mmol, 10 mol%). The reaction mixture was reacted in a monowave reactor at 220 ºC for 3 h. The crude reaction mixture was purified by flash column chromatography (1-5% Et_2O in pentane) to give ethyl furoate **29** (1.03 g, 6.59 mmol, 74%) as a colorless oil.
R_f = 0.79, 25% EtOAc in hexanes.
^{1}H-NMR (300 MHz, $CDCl_3$) δ = 7.95 (d, *J* = 1.7 Hz, 1H), 7.21 (dq, *J* = 2.6, 1.2 Hz, 1H), 4.29 (q, *J* = 7.1 Hz, 2H), 2.19 (d, *J* = 1.2 Hz, 3H), 1.34 (t, *J* = 7.1 Hz, 3H);
^{13}C NMR (75 MHz, $CDCl_3$) δ = 163.9, 148.8, 141.1, 120.7, 119.1, 60.2, 14.5, 9.3;
IR(neat): ν_{max} = 2981, 2933, 1716, 1538, 1232, 1086, 1020, 772 cm^{-1};
HRMS (EI+) calc'd for $C_8H_{10}O_3$ $[M]^+$ 154.0630, found 154.0631. For $C_8H_{11}O_3$ $[M+H]^+$ 155.0703, found 155.0704.

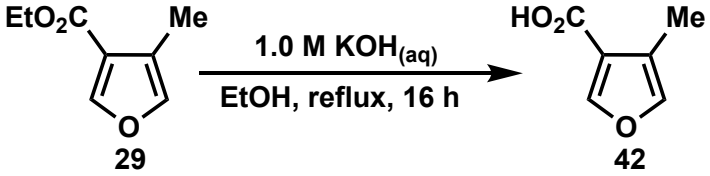

Procedure:
To a round bottom flask was added furoate **29** (1.00 g, 6.49 mmol, 1.0 eq) and dissolved in EtOH (13 mL). Subsequently 1.0 M KOH (7.1 mL, 7.1 mmol, 1.1 eq) was added, and the reaction mixture was refluxed with stirring for 16 h. The resulting reaction mixture was first poured into water and extracted with Et_2O (x2). The combined aqueous layers were then acidified to approx. pH 2.0 with 20% HCl and extracted with EtOAc (x3). The combined organic layers were washed with water (x2), brine (x2), dried over $MgSO_4$, and concentrated *in vacuo*. Carboxylic acid **42** (793 mg, 6.29 mmol, 97%) was isolated as a white solid and used without further purification.
R_f = 0.37, 25% EtOAc in hexanes.
Melting Point: 136.4 ºC – 140.8 ºC
^{1}H-NMR (300 MHz, $CDCl_3$) δ = 8.06 (d, *J* = 1.7 Hz, 1H), 7.24 (dq, *J* = 2.6, 1.3 Hz, 1H), 2.21 (d, *J* = 1.2 Hz, 3H);
^{13}C NMR (75 MHz, $CDCl_3$) δ = 169.6, 150.4, 141.5, 120.9, 118.4, 9.2;
IR(neat): ν_{max} = 2971, 2724, 2603, 1679, 1433, 1142, 1006, 767 cm^{-1};
HRMS (EI+) calc'd for $C_6H_6O_3$ $[M]^+$ 126.0317, found 126.0321. For $C_6H_5O_3$ $[M-H]^-$ 125.0244, found 125.0236.

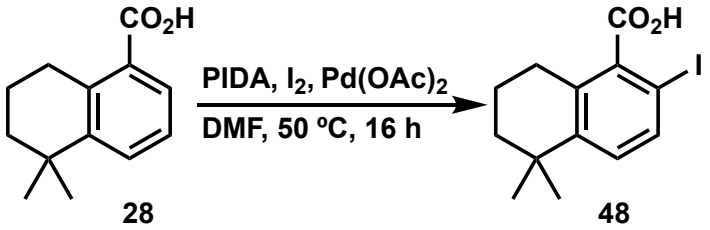

Procedure:
To a flame dried round bottom flask was added carboxylic acid **28** (500 mg, 2.45 mmol, 1.0 eq.), PIDA (789 mg, 2.45 mmol, 1.0 eq.), iodine (622 mg, 2.45 mmol, 1.0 eq), and $Pd(OAc)_2$ (27.5 mg, 0.122 mmol, 5 mol%) which were then dissolved in DMF (12.3 mL). The reaction flask was then capped with a septum and allowed to stir under an atmosphere of air at 50 ºC for 16 h. The crude reaction mixture was poured into H_2O and extracted with EtOAc (x3). The combined organic layers were washed with water (x2), brine (x2), dried over $MgSO_4$, and concentrated *in vacuo*. The residue was purified by flash column chromatography (5-20% EtOAc in hexanes) to afford *ortho*-iodo carboxylic acid **48** (679 mg, 2.06 mmol, 83%), as an off-white foam .
R_f = 0.38, 25% EtOAc in hexanes.
^{1}H-NMR (300 MHz, $CDCl_3$) δ = 7.61 (d, *J* = 8.4 Hz, 1H), 7.12 (d, *J* = 8.4 Hz, 1H), 2.85 (t, *J* = 6.3 Hz, 2H), 1.85 – 1.77 (m, 2H), 1.67 – 1.63 (m, 2H), 1.27 (s, 6H);
^{13}C NMR (75 MHz, $CDCl_3$) δ = 175.3, 146.6, 139.1, 136.3, 134.8, 129.9, 87.7, 38.3, 34.1, 31.8, 28.6, 19.2;
IR(neat): ν_{max} = 2955, 2631, 1695, 1433, 1254, 1112, 815, 691 cm^{-1};
HRMS (EI+) calc'd for $C_{13}H_{15}IO_2$ $[M]^+$ 330.0117, found 330.0084. For $C_{13}H_{14}IO_2$ $[M-H]^-$ 329.0044, found 329.0011.

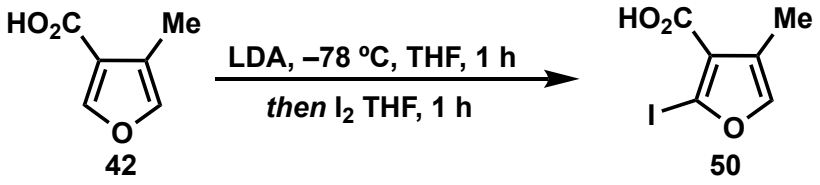

Procedure:
To a flame dried round bottom flask under N_2 was added furoic acid **42** (793 mg, 6.29 mmol, 1.0 eq.) and dissolved in dry THF (10.5 mL). To a freshly prepared solution of LDA made from *n*-BuLi (5.2 mL, 13 mmol, 2.0 eq) and distilled diisopropylamine (1.8 mL, 13 mmol, 2.0 eq) in dry THF (10.5 mL) was added the furoic acid solution dropwise at –78 ºC. The solution stirs for approx. 1 h, after which time a solution of iodine (1.63 g, 6.42 mmol, 1.02 eq) in dry THF (10.5 mL) was added dropwise to the reaction mixture. Once the addition of the iodide was complete, the reaction mixture was stirred for 1 h, warming up to room temperature. The reaction was quenched by addition of NH_4Cl and extracted with Et_2O (x3). The combined organic layers were washed with brine, dried over $MgSO_4$,

and concentrated *in vacuo*. The residue was purified via flash column chromatography (5-20% EtOAc in hexanes) to afford iodo acid **50** (1.47 g, 5.83 mmol, 93%) as a white solid.
R_f = 0.37, 25% EtOAc in hexanes.
Melting Point: 154.5 ºC – 156.8 ºC
^{1}H-NMR (500 MHz, $CDCl_3$) δ = 7.41 (q, *J* = 1.5 Hz, 1H), 2.22 (d, *J* = 1.4 Hz, 3H);
^{13}C NMR (75 MHz, $CDCl_3$) δ = 169.0, 146.1, 123.6, 123.3, 101.2, 10.4;
IR(neat): ν_{max} = 2971, 2628, 1677, 1506, 1291, 1105, 937, 764 cm^{-1};
HRMS (EI+) calc'd for $C_6H_5IO_3$ $[M]^+$ 251.9283, found 251.9276. For $C_6H_4IO_3$ $[M-H]^-$ 250.9211, found 250.9204.

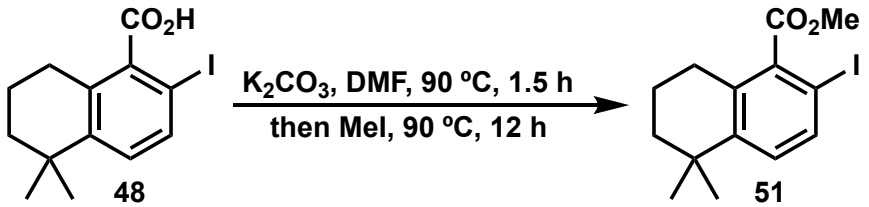

Procedure:
To a flame dried round bottom flask under N_2 was added *o*-iodo carboxylic acid **48** (1.33 g, 4.03 mmol, 1.0 eq), K_2CO_3 (1.67 g, 12.1 mmol, 3.0 eq), and DMF (17.5 mL). The reaction mixture was stirred at 90 ºC for 1.5 h, then MeI (0.50 mL, 8.1 mmol, 2.0 eq) was added and the reaction mixture was stirred at 90 ºC for 12 h. The reaction mixture was poured into water and extracted with Et_2O (x3). The combined organic layers were washed with water, brine, dried over $MgSO_4$ and concentrated *in vacuo*. The residue was purified via flash column chromatography (10% Et_2O in hexanes) to afford *o*-iodo methyl ester **51** (968 mg, 2.81 mmol, 70%) as a yellow oil.
R_f = 0.79, 25% EtOAc in hexanes.
^{1}H-NMR (300 MHz, $CDCl_3$) δ = 7.57 (d, *J* = 8.4 Hz, 1H), 7.09 (d, *J* = 8.4 Hz, 1H), 3.93 (s, 3H), 2.69 (t, *J* = 6.4 Hz, 2H), 1.81 – 1.73 (m, 2H), 1.64 – 1.60 (m, 2H), 1.25 (s, 6H);
^{13}C NMR (75 MHz, $CDCl_3$) δ = 170.0, 146.5, 139.9, 136.0, 134.9, 129.6, 88.1, 52.6, 38.2, 34.0, 31.6, 28.4, 19.1;
IR(neat): ν_{max} = 2952, 2884, 1729, 1435, 1245, 1122, 988, 773 cm^{-1};
HRMS (EI+) calc'd for $C_{14}H_{17}NO_2$ $[M]^+$ 344.0273, found 344.0265. For $C_{14}H_{18}NO_2$ $[M+H]^+$ 345.0346, found 345.0340.

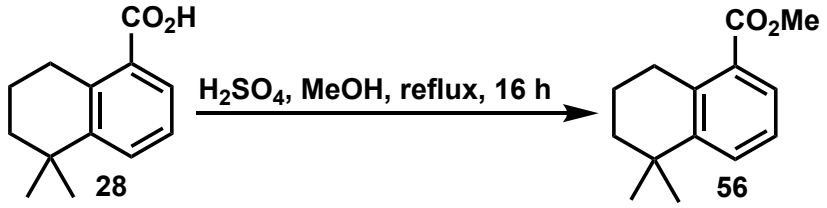

Procedure:
To a flame dried round bottom flask under N_2 was added carboxylic acid **28** (0.500 g, 2.45 mmol, 1.0 eq) and dissolved in MeOH (12.3 mL). Then conc. H_2SO_4 (0.16 mL, 2.9 mmol,

1.2 eq) was added dropwise and the reaction mixture was refluxed while stirring for 16 h. The reaction was quenched by the slow addition of $NaHCO_3$, poured into water, and extracted with Et_2O (x3). The combined organic layers were washed with water, brine, dried over $MgSO_4$ and concentrated *in vacuo*. The residue was purified via flash column chromatography (10% Et_2O in hexanes) to afford methyl ester **56** (532 mg, 2.44 mmol, 99%) as a white solid.

R_f = 0.79, 25% EtOAc in hexanes.

Melting Point: 31.1 ºC – 33.6 ºC

^{1}H-NMR (300 MHz, $CDCl_3$) δ = 7.58 (dd, *J* = 7.6, 1.4 Hz, 1H), 7.50 (dd, *J* = 7.9, 1.3 Hz, 1H), 7.18 (t, *J* = 7.8 Hz, 1H), 3.87 (s, 3H), 3.01 (t, *J* = 6.4 Hz, 2H), 1.82 – 1.73 (m, 2H), 1.70 – 1.64 (m, 2H), 1.29 (s, 6H);

^{13}C NMR (75 MHz, $CDCl_3$) δ = 169.1, 147.2, 137.4, 130.7, 130.6, 127.4, 125.4, 52.0, 38.7, 34.4, 32.2, 29.1, 19.5.

IR(neat): ν_{max} = 2950, 2867, 1713, 1449, 1258, 1108, 964, 766 cm^{-1};

HRMS (EI+) calc'd for $C_{14}H_{18}O_2$ $[M]^+$ 218.1307, found 218.1310. For $C_{14}H_{19}O_2$ $[M+H]^+$ 219.1380, found 219.1383.

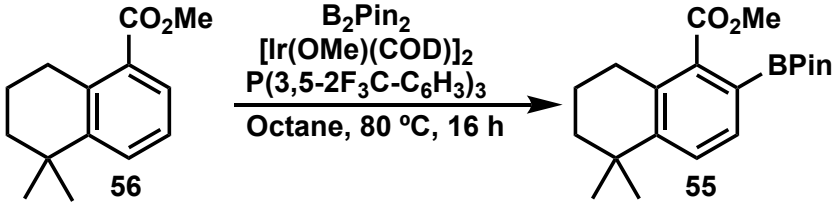

Procedure:

To a flame dried reaction tube was added ester **56** (129 mg, 0.590 mmol, 5.0 eq), B_2Pin_2 (30.0 mg, 0.118 mmol, 1.0 eq), iridium catalyst (1.17 mg, 0.00177 mmol, 1.5 mol%), and phosphine ligand (4.75 mg, 0.00708 mmol, 6 mol%), backfilled with N_2 and dissolved in distilled octane (0.740 mL). The reaction mixture was stirred at 80 ºC for 16 h. The reaction mixture was poured into water and extracted with Et_2O (x3). The combined organic layers were washed with water (x2), brine (x2), dried over $MgSO_4$ and concentrated *in vacuo*. The residue was purified via flash column chromatography (4-16% Et_2O in hexanes) to afford boronate ester **55** (39.2 mg, 0.114 mmol, 97%) as a white solid.

R_f = 0.73, 25% EtOAc in hexanes.

Melting Point: 118.3 ºC – 122.8 ºC

^{1}H-NMR (300 MHz, $CDCl_3$) δ = 7.57 (d, *J* = 7.9 Hz, 1H), 7.38 (d, *J* = 7.9 Hz, 1H), 3.87 (s, 3H), 2.74 (t, *J* = 6.3 Hz, 2H), 1.82 – 1.74 (m, 2H), 1.65 – 1.62 (m, 2H), 1.30 (s, 12H), 1.27 (s, 6H);

^{13}C NMR (75 MHz, $CDCl_3$) δ = 171.5, 149.6, 139.4, 132.4, 132.3, 127.6, 84.0, 52.1, 38.7, 34.5, 31.9, 27.7, 24.9, 19.3;

IR(neat): ν_{max} = 2975, 2868, 1725, 1594, 1251, 1129, 849, 679 cm^{-1}

HRMS (EI+) calc'd for $C_{20}H_{29}BO_4Na$ $[M+Na]^+$ 367.2051, found 367.2054.

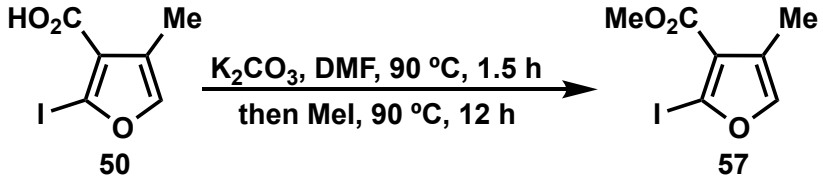

Procedure:
To a flame dried round bottom flask under N_2 was added *o*-iodofuroic acid **50** (1.47 g, 5.83 mmol, 1.0 eq), K_2CO_3 (2.42 g, 17.5 mmol, 3.0 eq), and DMF (25.3 mL). This mixture was stirred at 90 ºC for 1.5 h, then MeI (0.73 mL, 12 mmol, 2.0 eq) was added and the reaction mixture was stirred at 90 ºC for 12 h. The reaction mixture was poured into water and extracted with Et_2O (x3). The combined organic layers were washed with water, brine, dried over $MgSO_4$ and concentrated *in vacuo*. The residue was purified via flash column chromatography (Et_2O in hexanes) to afford iodo ester **57** (1.28 g, 4.81 mmol, 83%) as an off-white solid.
R_f = 0.69, 25% EtOAc in hexanes.
Melting Point: 55.2 ºC-57.6 ºC
^{1}H-NMR (300 MHz, $CDCl_3$) δ = 7.39 (q, *J* = 1.2 Hz, 1H), 3.86 (s, 3H), 2.19 (d, *J* = 1.3 Hz, 3H);
^{13}C NMR (75 MHz, $CDCl_3$) δ = 163.5,145.8, 124.0, 123.1, 99.2, 51.6, 10.3;
IR(neat): ν_{max} = 2952, 2841, 1711, 1494, 1286, 1099, 908, 755 cm^{-1};
HRMS (EI+) calc'd for $C_7H_7IO_3$ $[M]^+$ 265.9440, found 265.9436. For $C_7H_8IO_3$ $[M+H]^+$ 266.9513, found 266.9509.

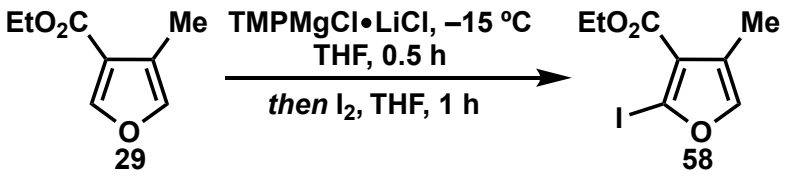

Procedure:
To a flame dried reaction tube under nitrogen was added furoate **29** (30.0 mg, 0.192 mmol, 1.0 eq) and dissolved in dry THF (0.200 mL). The furoate solution was cooled to –15 ºC and TMPMgClxLiCl (0.21 mL, 0.21 mmol, 1.1 eq) was added dropwise. The reaction mixture was stirred for 30 min at –15 ºC and then a solution of iodine (53.6 mg, 0.211 mmol, 1.1 eq) in dry THF (0.20 mL) was added dropwise. The reaction mixture was then stirred for approx. 1 h, warming to room temperature. The reaction was quenched by the addition of NH_4Cl and extracted with EtOAc (x3). The combined organic layers were washed with water, aqueous $Na_2S_2O_3$, and brine, dried over $MgSO_4$, and concentrated *in vacuo*. The residue was purified via flash column chromatography (10% Et_2O in hexanes) to afford iodo furoate **58** (10.3 mg, 0.0368 mmol, 19%) as a yellow oil.
R_f = 0.76, 25% EtOAc in hexanes.
^{1}H-NMR (300 MHz, $CDCl_3$) δ = 7.39 (q, *J* = 1.3 Hz, 1H), 4.33 (q, *J* = 7.1 Hz, 2H), 2.19 (d, *J* = 1.2 Hz, 3H), 1.39 (t, *J* = 7.1 Hz, 3H);
^{13}C NMR (75 MHz, $CDCl_3$) δ = 163.0, 145.8, 124.0, 123.2, 99.0, 60.7, 14.3, 10.3;

IR(neat): ν_{max} = 3115, 2932, 1698, 1501, 1294, 1165, 1089, 777 cm^{-1};
HRMS (EI+) calc'd for $C_8H_9IO_3$ $[M]^+$ 279.9596, found 279.9606. For $C_8H_{10}IO_3$ $[M+H]^+$ 280.9669, found 280.9678.

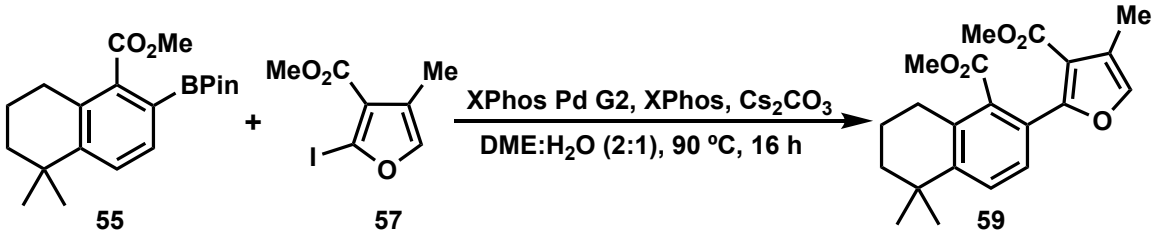

Procedure:
To a flame dried reaction tube was added boronate ester **55** (39.4 mg, 0.114 mmol, 1.0 eq.), iodo-ester **57** (30.3 mg, 0.114 mmol, 1.0 eq.), XPhos Pd G2 (4.5 mg, 0.0057 mmol, 5 mol%), Xphos ligand (5.4 mg, 0.011 mmol, 10 mol%), and Cs_2CO_3 (111 mg, 0.342 mmol, 3.0 eq.). Then the tube was evacuated under vacuum and backfilled with N_2. Degassed solvent (0.57 mL) was then added via syringe and the reaction mixture was left to stir at 90 ºC for 16 h. The crude reaction mixture was poured into H_2O and extracted with EtOAc (x3). The combined organic layers were washed with brine, dried over $MgSO_4$, and concentrated *in vacuo*. The residue was purified by flash column chromatography (2-10% Et_2O in hexanes) to afford diester **59** (35.4 mg, 0.0993 mmol, 87%), as a colorless oil.
$\mathbf{R_f}$ = 0.60, 25% EtOAc in hexanes.
^{1}H-NMR (500 MHz, $CDCl_3$) δ = 7.42 (q, *J* = 8.3 Hz, 2H), 7.20 (d, *J* = 1.2 Hz, 1H), 3.74 (s, 3H), 3.69 (s, 3H), 2.79 (t, *J* = 6.3 Hz, 2H), 2.20 (d, *J* = 1.2 Hz, 3H), 1.84 – 1.76 (m, 2H), 1.69 – 1.65 (m, 2H), 1.31 (s, 6H);
^{13}C NMR (75 MHz, $CDCl_3$) δ = 169.7, 164.6, 157.8, 148.1, 139.6, 134.0, 133.1, 128.2, 127.9, 126.1, 122.3, 114.7, 52.2, 51.4, 38.6, 34.5, 32.0, 28.3, 19.3, 10.2;
IR(neat): ν_{max} = 2950, 2866, 1716, 1436, 1218, 1078, 911, 729 cm^{-1};
HRMS (EI+) calc'd for $C_{21}H_{24}O_5$ $[M]^+$ 356.1624, found 356.1628. For $C_{21}H_{25}O_5$ $[M+H]^+$ 357.1697, found 357.1698.

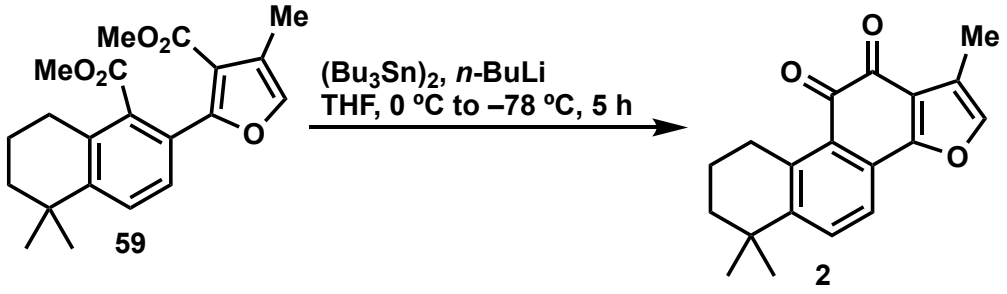

Procedure:

To a flame dried reaction tube under N_2 was added diester **59** (111 mg, 0.311 mmol, 1.0 eq.) and dissolved in THF (2.6 mL). In a separate flame dried reaction tube under N_2 was

added bis(tributyltin) (0.78 mL, 1.6 mmol, 5.0 eq.), dissolved in THF (4.2 mL) and cooled to 0 ºC. To the solution of bis(tributyltin) was then added *n*-BuLi (0.61 mL, 1.5 mmol, 4.9 eq.) dropwise and the reaction was allowed to stir at 0 ºC for 15 min before being cooled to –78 ºC. The diester solution was added to the reaction mixture dropwise at –78 ºC and allowed to stir for 5 h. The reaction was quenched by addition of NH_4Cl, the layers were separated and the aqueous layer was extracted with Et_2O (x3). The combined organic layers were washed with water, brine, dried over $MgSO_4$ and concentrated *in vacuo*. The residue was purified via flash column chromatography (4-20% Et_2O in hexanes) to give tanshinone IIA **2** as a red solid.

Note: the natural product was isolated as an approximately 4:1 mixture with unconsumed starting material **59**. See table below for comparison to literature values that allowed us to determine that we had indeed made the product.
R_f = 0.60, 25% EtOAc in hexanes.
^{1}H-NMR (500 MHz, $CDCl_3$) δ = 7.62 (d, *J* = 8.1 Hz, 1H), 7.54 (d, *J* = 8.1 Hz, 1H), 7.21 (d, *J* = 1.3 Hz, 1H), 3.18 (t, *J* = 6.4 Hz, 2H), 2.25 (d, *J* = 1.3 Hz, 3H).

Literature reported value:	This reported value:
7.62 (d, *J* = 8.2 Hz, 1H)	7.62 (d, *J* = 8.1 Hz, 1H)
7.54 (d, *J* = 8.1 Hz, 1H)	7.54 (d, *J* = 8.1 Hz, 1H)
7.22 (m, 1H)	7.21 (d, *J* = 1.3 Hz, 1H)
3.18 (t, *J* = 6.4 Hz, 2H)	3.18 (t, *J* = 6.4 Hz, 2H),
2.26 (d, *J* = 1.3 Hz, 3H)	2.25 (d, *J* = 1.3 Hz, 3H).
1.82–1.76 (m, 2H)	Overlap w/Starting material
1.67–1.64 (m, 2H)	Overlap w/Starting material
1.31 (s, 6H)	Overlap w/Starting material

References

(1) Cragg, G. M.; Newman, D. J. *Pure Appl. Chem.* **2005**, *77*, 7–24.

(2) Dias, D. A.; Urban, S.; Roessner, U. *Metabolites* **2012**, *2* , 303–336.

(3) Zhang, Y.; Jiang, P.; Ye, M.; Kim, S. H.; Jiang, C.; Lü, J. *Int. J. Mol. Sci.* **2012**, *13*, 13621–13666.

(4) Nakao, M.; Fukushima, T. *Yakugaku Zasshi* **1934**, *54*, 844–858.

(5) Wang, X.; Morris-Natschke, S. L.; Lee, K. H. *Med. Res. Rev.* **2007**, *27*, 133–148.

(6) Dong, Y.; Morris-Natschke, S. L.; Lee, K. H. *Nat. Prod. Rep.* **2011**, *28*, 529–542.

(7) Zeng, Y.; Song, J. X.; Shen, X. C. *Phyther. Res.* **2012**, *26*, 159–167.

(8) Gao, S.; Liu, Z.; Li, H.; Little, P. J.; Liu, P.; Xu, S. *Atherosclerosis* **2012**, *220*, 3–10.

(9) Jia, Y.; Huang, F.; Zhang, S.; Leung, S. W. *Int. J. Cardiol.* **2012**, *157*, 330–340.

(10) Chen, W.; Lu, Y.; Chen, G.; Huang, S. *Anticancer Agents Med. Chem.* **2012**, *13*, 979–987.

(11) Qiu, Y.; Li, C.; Wang, Q.; Zeng, X.; Ji, P. *Cancer Med.* **2018**, *7*, 397–407.

(12) Jiang, Z.; Gao, W.; Huang, L. *Front. Pharmacol.* **2019**, *10*, 1–14.

(13) Wu, N.; Ma, W. C.; Mao, S. J.; Wu, Y.; Jin, H. *J. Nat. Prod.* **2017**, *80*, 1697–1700.

(14) Wang, F.; Yang, H.; Yu, S.; Xue, Y.; Fan, Z.; Liang, G.; Geng, M.; Zhang, A.; Ding, C. *Org. Biomol. Chem.* **2018**, *16*, 3376–3381.

(15) Jiao, M.; Ding, C.; Zhang, A. *Tetrahedron* **2014**, *70*, 2976–2981.

(16) Kakisawa, H.; Tateishi, M.; Kusumi, T. *Tetrahedron Lett.* **1968**, *34*, 3783–3786.

(17) Kakisawa, H.; Inouye, Y. *Bull. Chem. Soc. Jpn.* **1969**, *42*, 3318–3323.

(18) Lee, J.; Snyder, J. K. *J. Org. Chem.* **1990**, *55*, 4995–5008.

(19) Lee, J.; Snyder, J. K. *J. Am. Chem. Soc.* **1989**, *111*, 1522–1524.

(20) King, A. O.; Okukado, N.; Negishi, E. I. *J. Chem. Soc. Chem. Commun.* **1977**, *19*, 683–684.

(21) Danheiser, R. L.; Brisbois, R. G.; Kowalczyk, J. J.; Miller, R. F. *J. Am. Chem. Soc.* **1990**, *112*, 3093–3100.

(22) Danheiser, R. L.; Casebier, D. S.; Firooznia, F. *J. Org. Chem.* **1995**, *60*, 8341–8350.

(23) Huang, H.; Song, C.; Wang, Z.; Li, M.; Chang, J. *Tetrahedron Lett.* **2020**, *61*, 152102.

(24) Chuc, L. T. N.; Chen, C. S.; Lo, W. S.; Shen, P. C.; Hsuan, Y. C.; Tsai, H. H. G.; Shieh, F. K.; Hou, D. R. *ACS Omega* **2017**, *2*, 698–711.

(25) Liotta, D.; Saindane, M.; Ott, W. *Tetrahedron Lett.* **1983**, *24*, 2473–2476.

(26) Solomin, V. V.; Radchenko, D. S.; Slobodyanyuk, E. Y.; Geraschenko, O. V.; Vashchenko, B. V.; Grygorenko, O. O. *Eur. J. Org. Chem.* **2019**, *18*, 2884–2898.

(27) Sample, T.; Hatch, L. *Org. Synth* **1988**, *6*, 454.

(28) Engle, K. M.; Mei, T.; Wasa, M.; Yu, J. *Acc. Chem. Res.* **2012**, *45*, 288–802.

(29) Font, M.; Quibell, J. M.; Perry, G. J. P.; Larrosa, I. *Chem. Commun.* **2017**, *53*, 5584–5597.

(30) Qin, X.; Li, X.; Huang, Q.; Liu, H.; Wu, D.; Guo, Q.; Lan, J.; Wang, R.; You, J.. *Angew. Chem. Int. Ed.* **2015**, *54*, 7167–7170.

(31) Dong, J. J.; Roy, D.; Roy, R. J.; Ionita, M.; Doucet, H. *Synthesis.* **2011**, *21*, 3530–3546.

(32) Wu, Z.; Luo, F.; Chen, S.; Li, Z.; Xiang, H.; Zhou, X. *Chem. Commun.* **2013**, *49*, 7653–7655.

(33) Gong, H.; Zeng, H.; Zhou, F.; Li, C. J. *Angew. Chem. Int. Ed.* **2015**, *54*, 5718–5721.

(34) Glover, B.; Harvey, K. A.; Liu, B.; Sharp, M. J.; Tymoschenko, M. F. *Org. Lett.* **2003**, *5*, 301–304.

(35) Mei, T. S.; Giri, R.; Maugel, N.; Yu, J. Q. *Angew. Chem. Int. Ed.* **2008**, *47*, 5215–5219.

(36) O'Duill, M. L.; *Synthesis.* **2018**, *50*, 4699–4714.

(37) Das, J.; Mal, D. K.; Maji, S.; Maiti, D. *ACS Catal.* **2021**, *11*, 4205–4229.

(38) Chiong, H. A.; Pham, Q. N.; Daugulis, O. *J. Am. Chem. Soc.* **2007**, *129*, 9879–

9884.

(39) Xu, Z.; Yang, T.; Lin, X.; Elliott, J. D.; Ren, F. *Tetrahedron Lett.* **2015**, *56*, 475–477.

(40) Arroniz, C.; Denis, J. G.; Ironmonger, A.; Rassias, G.; Larrosa, I. *Chem. Sci.* **2014**, *5*, 3509–3514.

(41) Kolodziejczyk, K.; Roiban, G. D.; Schnürch, M.; Mihovilovic, M. D.; Stanetty, P. *Monatsh.* **2009**, *140*, 1349–1359.

(42) Arroniz, C.; Ironmonger, A.; Rassias, G.; Larrosa, I. *Org. Lett.* **2013**, *15*, 910–913.

(43) Varni, A. J.; Fortney, A.; Baker, M. A.; Worch, J. C.; Qiu, Y.; Yaron, D.; Bernhard, S.; Noonan, K. J. T.; Kowalewski, T. *J. Am. Chem. Soc.* **2019**, *141*, 8858–8867.

(44) Vachal, P.; Toth, L. M. *Tetrahedron Lett.* **2004**, *45*, 7157–7161.

(45) Ishiyama, T.; Murata, M.; Miyaura, N. *J. Org. Chem.* **1995**, *60*, 7508–7510.

(46) Ishiyama, T.; Isou, H.; Kikuchi, T.; Miyaura, N. *Chem. Commun.* **2010**, *46*, 159–161.

(47) Krasovskiy, A.; Krasovskaya, V.; Knochel, P. *Angew. Chem. Int. Ed.* **2006**, *45*, 2958–2961.

(48) Martin, R.; Buchwald, S. L. *Acc. Chem. Res.* **2008**, *41*, 1461–1473.

(49) Paleo, M. R.; Calaza, M. I.; Graña, P.; Sardina, F. J. *Org. Lett.* **2004**, *6*, 1061–1063.

Appendix

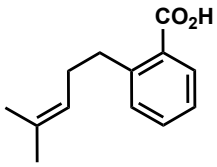
CO2H

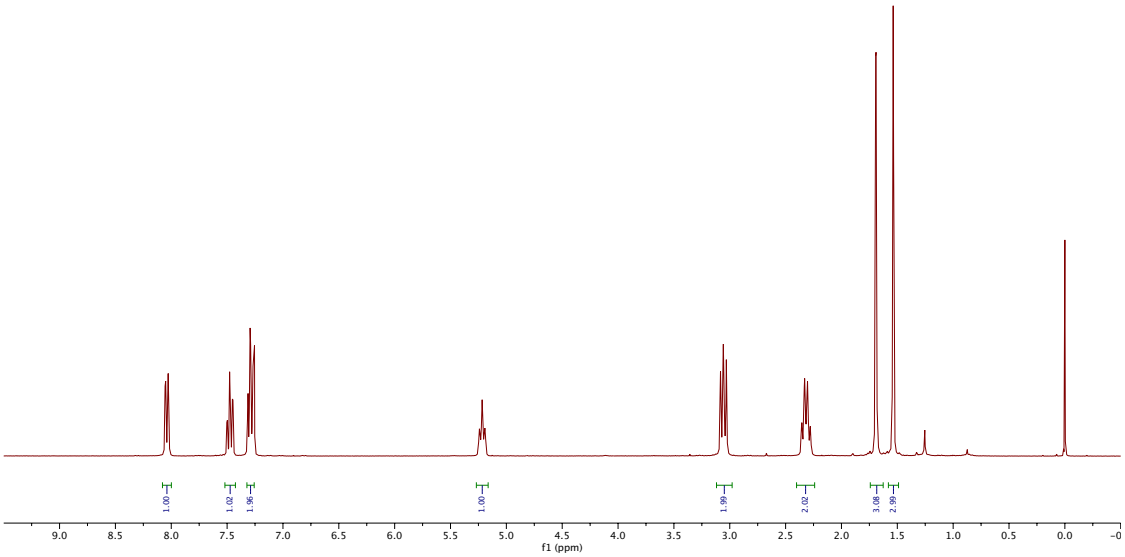
1.00
1.02
1.96
1.00
1.99
2.02
3.08
2.99
f1 (ppm)

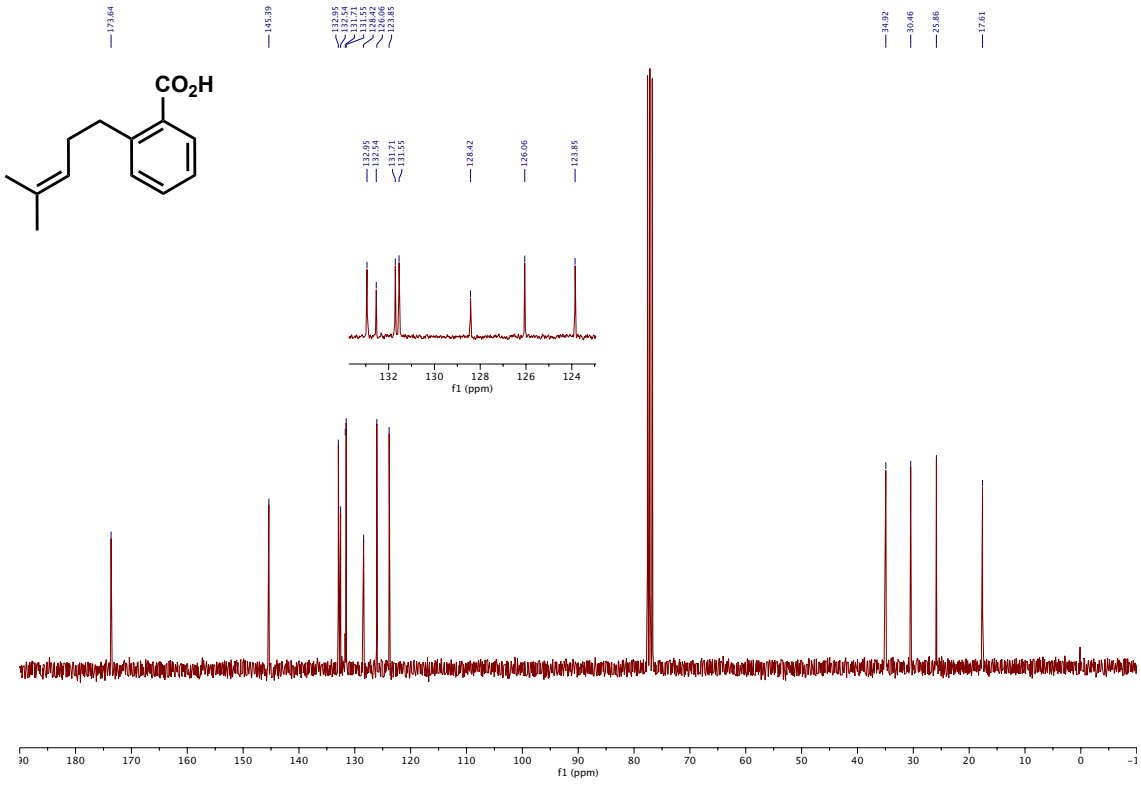
173.64
145.39
132.95
132.54
131.71
131.55
128.42
126.06
123.85
34.92
30.46
25.86
17.61
CO2H
f1 (ppm)

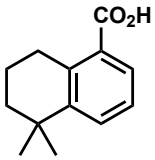
CO2H

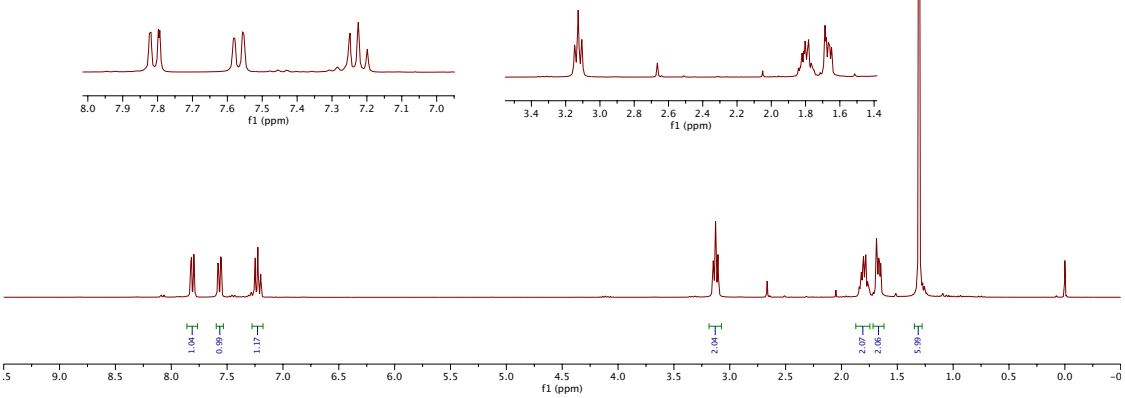
8.0 7.9 7.8 7.7 7.6 7.5 7.4 7.3 7.2 7.1 7.0
f1 (ppm)
3.4 3.2 3.0 2.8 2.6 2.4 2.2 2.0 1.8 1.6 1.4
f1 (ppm)
1.04
0.99
1.17
2.04
2.07
2.06
5.99
f1 (ppm)


174.48
147.37
138.83
131.89
130.33
128.83
125.51
38.59
34.45
32.98
29.34
19.53

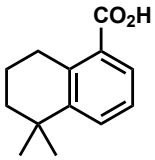
CO2H

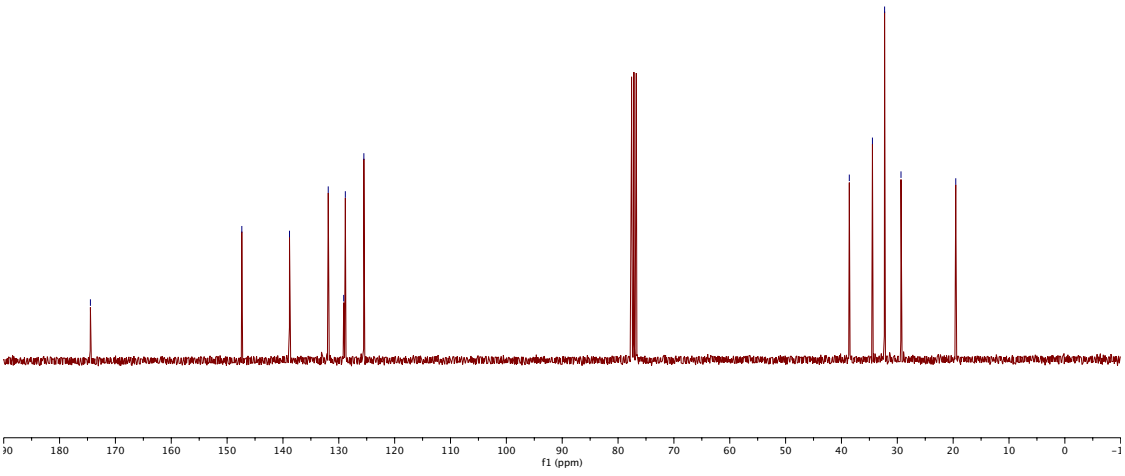
f1 (ppm)

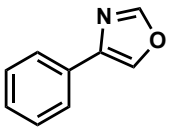

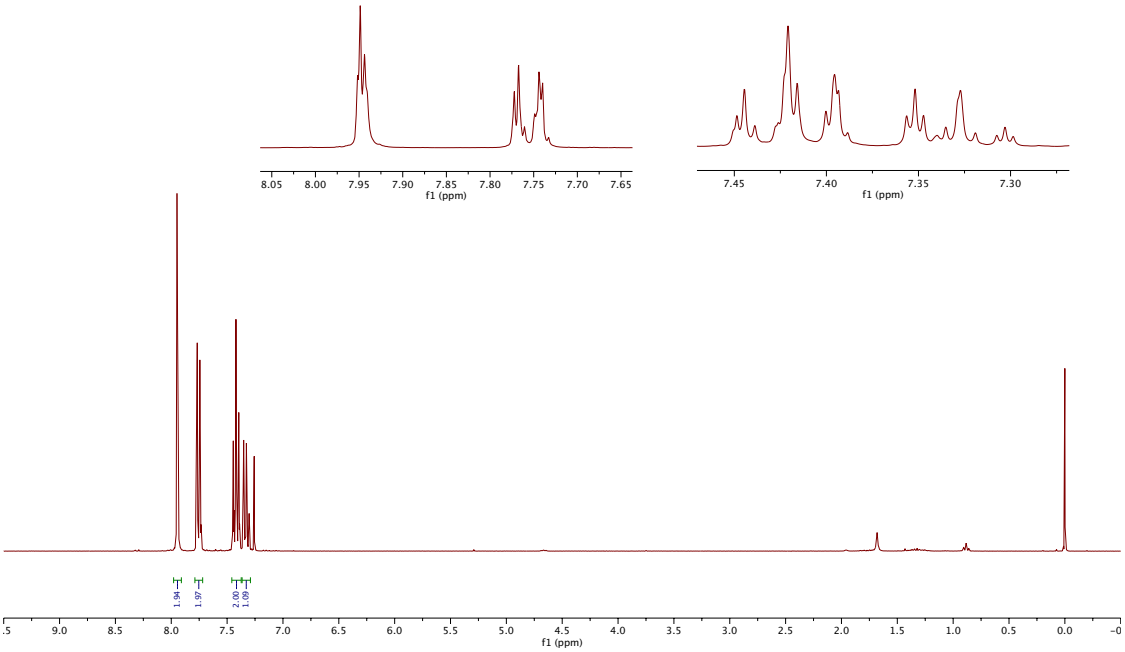
8.05 8.00 7.95 7.90 7.85 7.80 7.75 7.70 7.65
f1 (ppm)
7.45 7.40 7.35 7.30
f1 (ppm)
1.94
1.97
2.00
1.09
f1 (ppm)

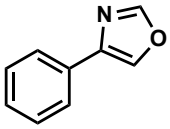

151.34
140.44
133.73
130.72
128.82
128.24
125.61
f1 (ppm)

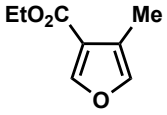
EtO2C
Me
O

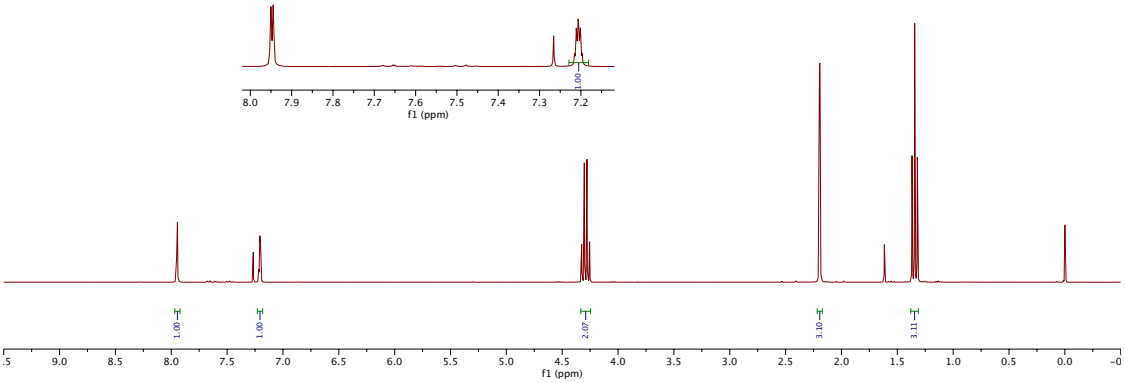
8.0 7.9 7.8 7.7 7.6 7.5 7.4 7.3 7.2
f1 (ppm)
1.00
1.00
2.07
3.10
3.11
9.0 8.5 8.0 7.5 7.0 6.5 6.0 5.5 5.0 4.5 4.0 3.5 3.0 2.5 2.0 1.5 1.0 0.5 0.0
f1 (ppm)

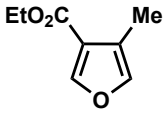
EtO2C
Me
O

163.94
148.79
141.07
120.73
119.09
60.19
14.46
9.26
180 170 160 150 140 130 120 110 100 90 80 70 60 50 40 30 20 10 0
f1 (ppm)

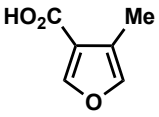
HO2C
Me
O

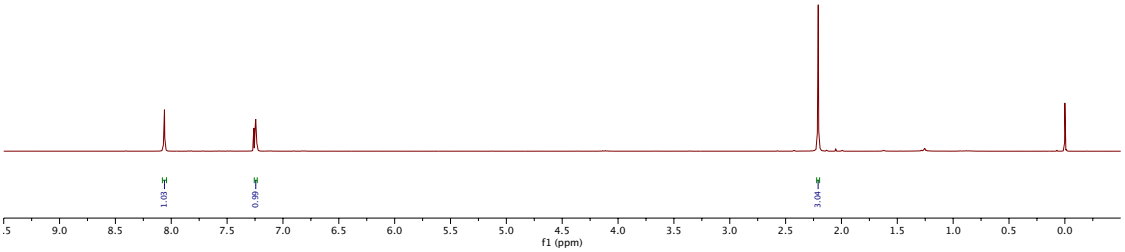
1.03
0.99
3.04
f1 (ppm)

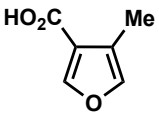
HO2C
Me
O

169.61
150.41
141.46
120.92
118.36
9.19
f1 (ppm)

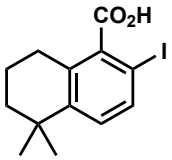
CO2H
I

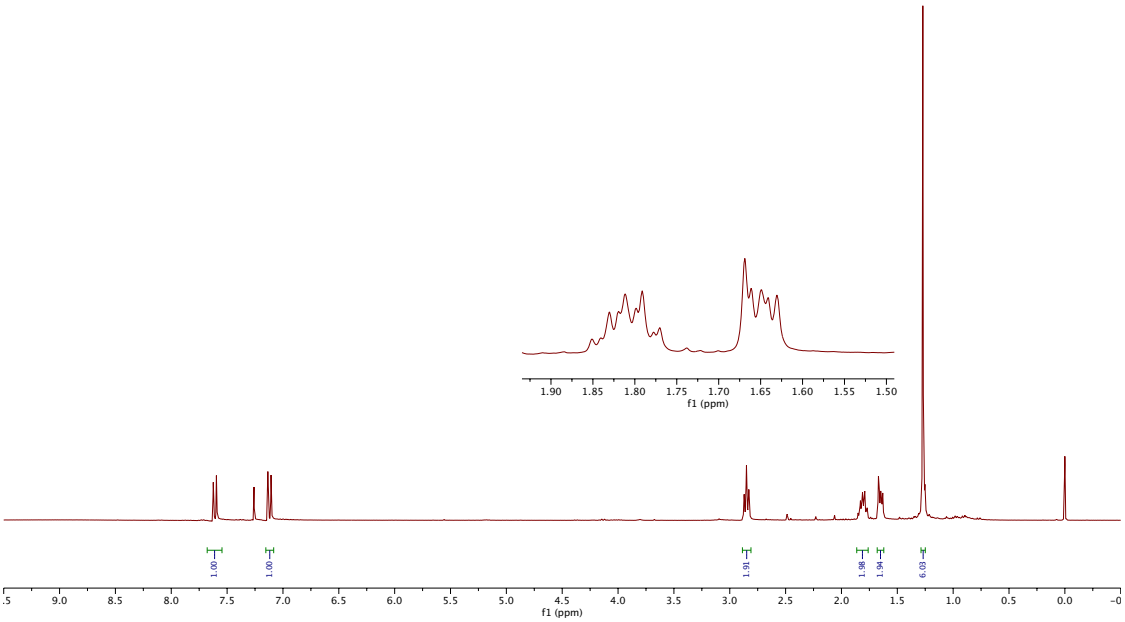
1.00
1.00
1.91
1.98
1.94
6.03
f1 (ppm)

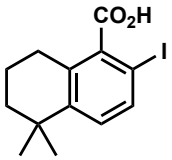
CO2H
I

175.31
146.64
139.10
136.72
134.80
129.93
87.69
38.26
34.15
31.75
26.87
19.22
f1 (ppm)

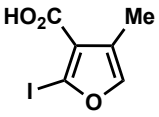
HO2C
Me
I
O

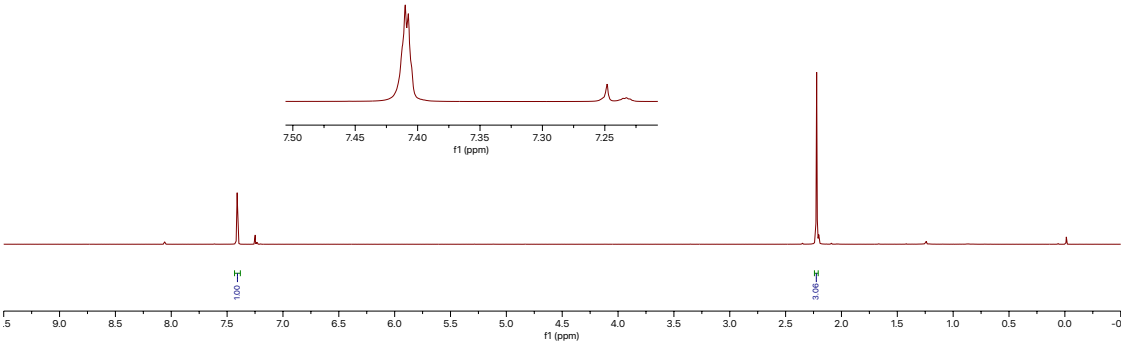
7.50
7.45
7.40
7.35
7.30
7.25
f1 (ppm)
1.00
3.06
f1 (ppm)

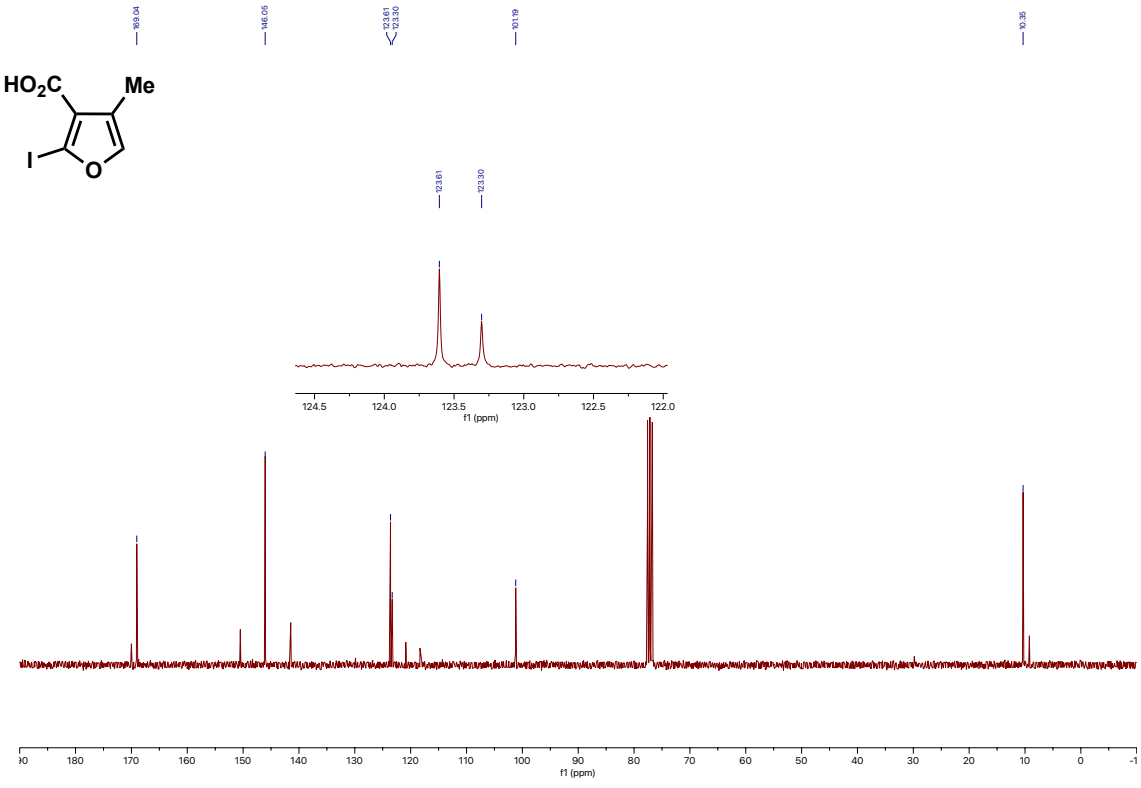
169.04
146.05
123.61
123.30
101.19
10.35
HO2C
Me
I
O
123.61
123.30
124.5
124.0
123.5
123.0
122.5
122.0
f1 (ppm)
f1 (ppm)

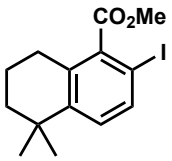
CO2Me
I

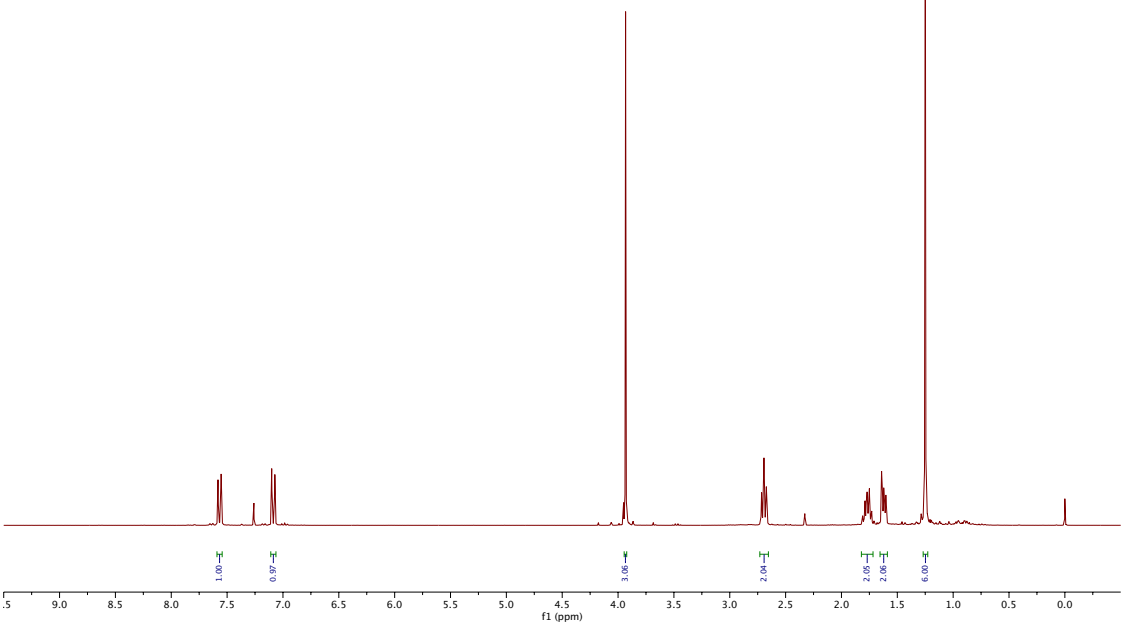
1.00
0.97
3.06
2.04
2.05
2.06
6.00
f1 (ppm)


169.97
146.47
139.94
136.02
134.93
129.55
88.11
52.56
38.20
34.01
31.64
24.40
19.11

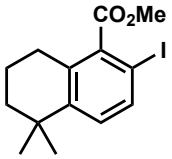
CO2Me
I

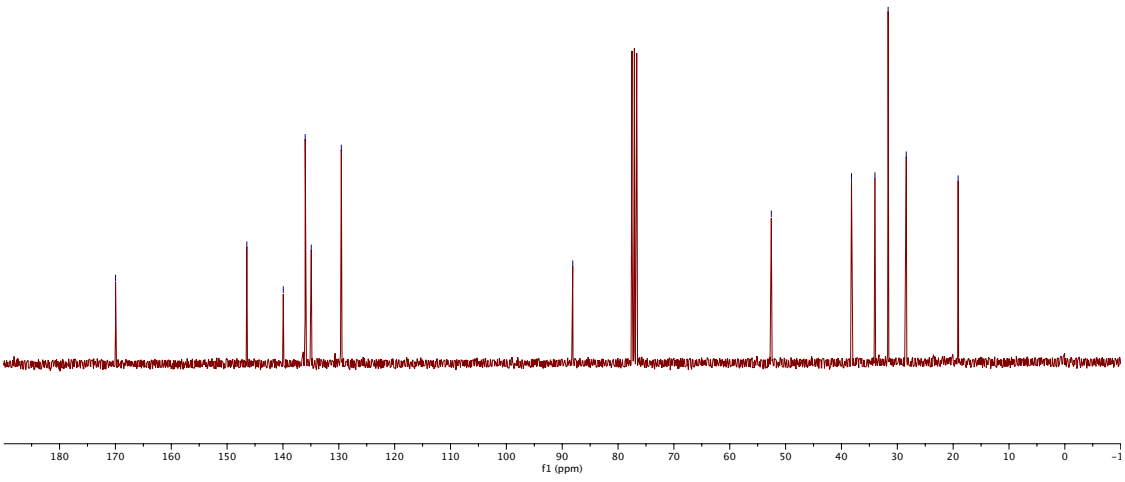
f1 (ppm)

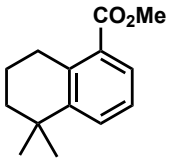
CO2Me

7.60 7.55 7.50 7.45 7.40 7.35 7.30 7.25 7.20 7.15
f1 (ppm)
1.80 1.75 1.70 1.65
f1 (ppm)
1.00
1.01
1.04
3.03
2.09
2.09
2.09
6.04
f1 (ppm)

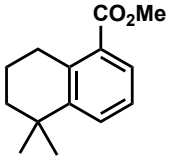
CO2Me

169.12
147.15
137.35
130.70
130.65
127.48
125.43
51.98
38.68
34.40
29.24
29.06
19.53
f1 (ppm)

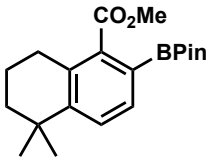
CO2Me
BPin

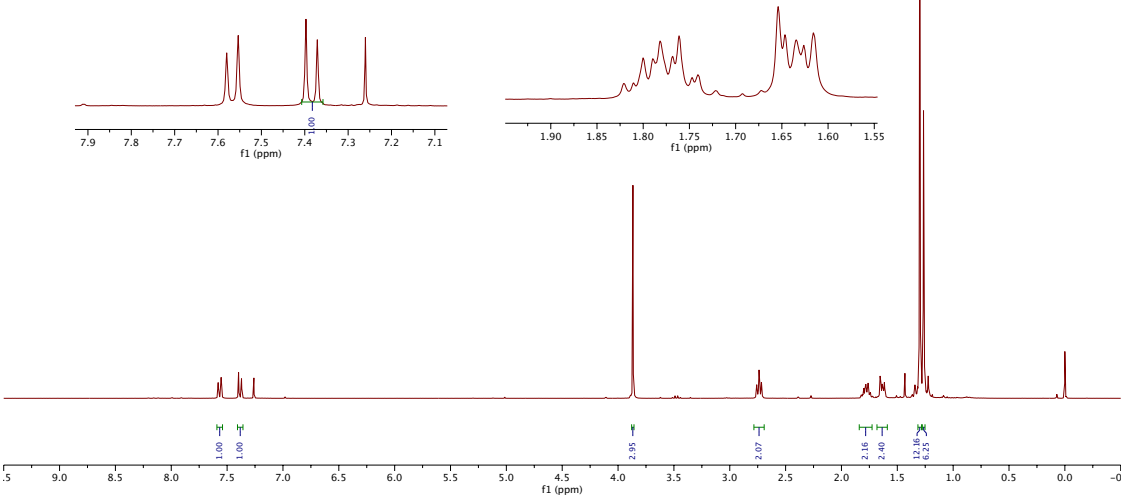
f1 (ppm)
1.00
1.00
2.95
2.07
2.16
2.40
12.16
6.25

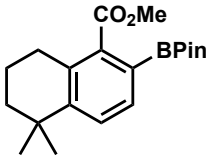
CO2Me
BPin

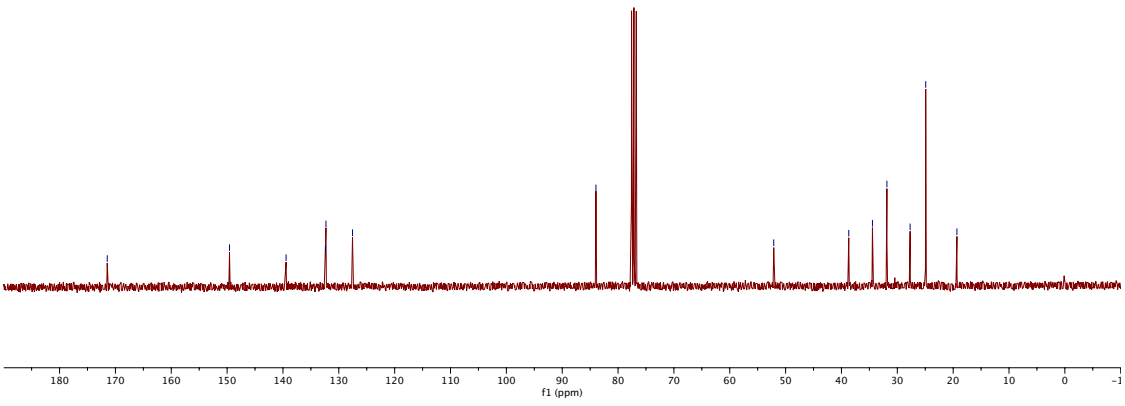
171.46
149.57
139.44
132.39
132.30
127.55
83.96
52.13
38.69
34.45
31.86
27.70
24.91
19.33
f1 (ppm)

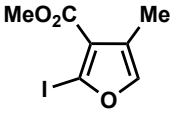
MeO2C
Me
I
O

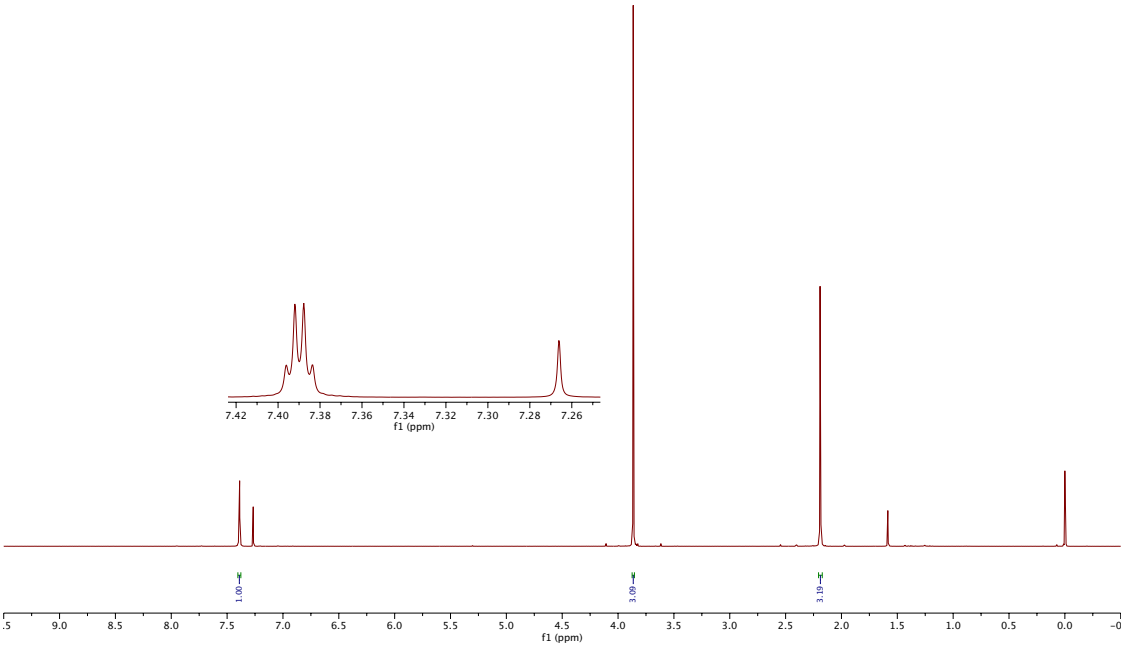
7.42 7.40 7.38 7.36 7.34 7.32 7.30 7.28 7.26
f1 (ppm)
1.00
3.09
3.19
9.5 9.0 8.5 8.0 7.5 7.0 6.5 6.0 5.5 5.0 4.5 4.0 3.5 3.0 2.5 2.0 1.5 1.0 0.5 0.0
f1 (ppm)

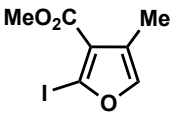
MeO2C
Me
I
O

163.46
145.80
132.96
123.14
99.20
51.55
10.30
190 180 170 160 150 140 130 120 110 100 90 80 70 60 50 40 30 20 10 0
f1 (ppm)

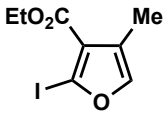
EtO2C
Me
I
O

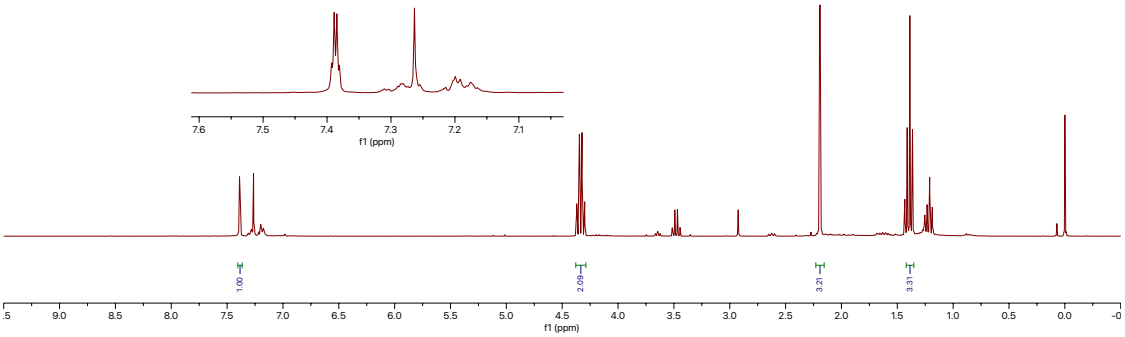
7.6
7.5
7.4
7.3
7.2
7.1
f1 (ppm)
1.00
2.09
3.21
3.31
f1 (ppm)

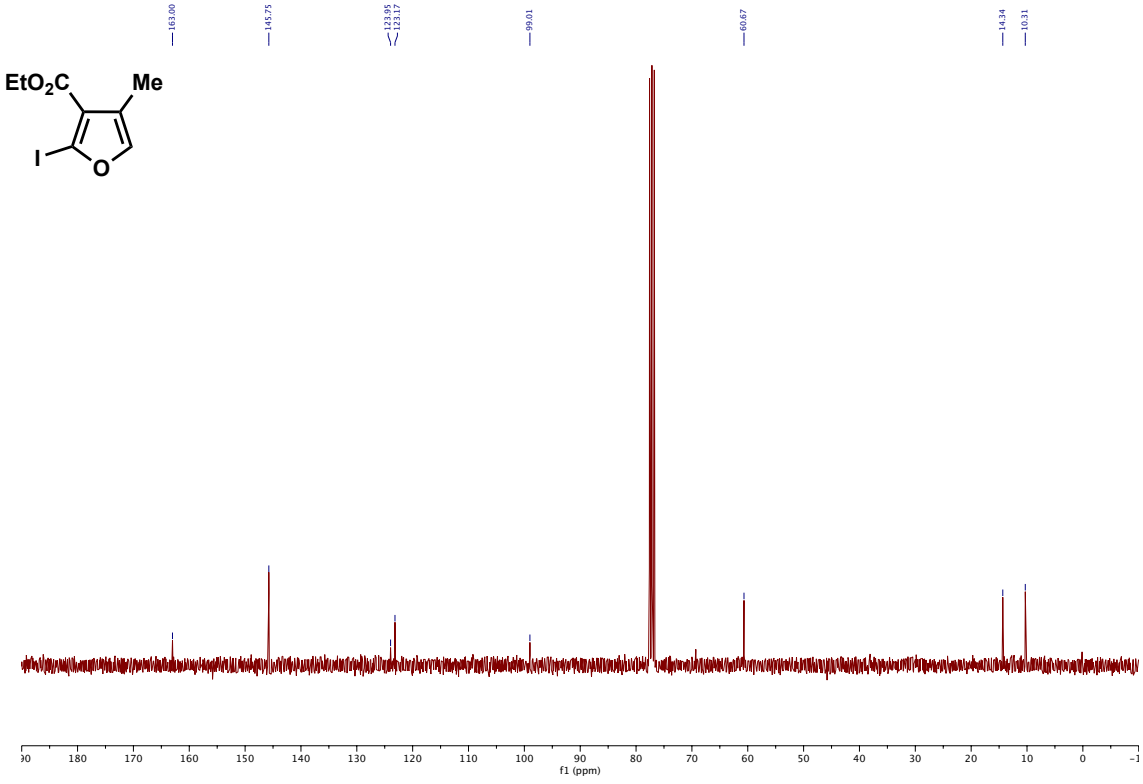
163.00
145.75
123.95
123.17
99.01
60.67
14.34
10.31
EtO2C
Me
I
O
f1 (ppm)

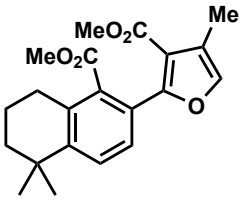
MeO2C
MeO2C
Me
O

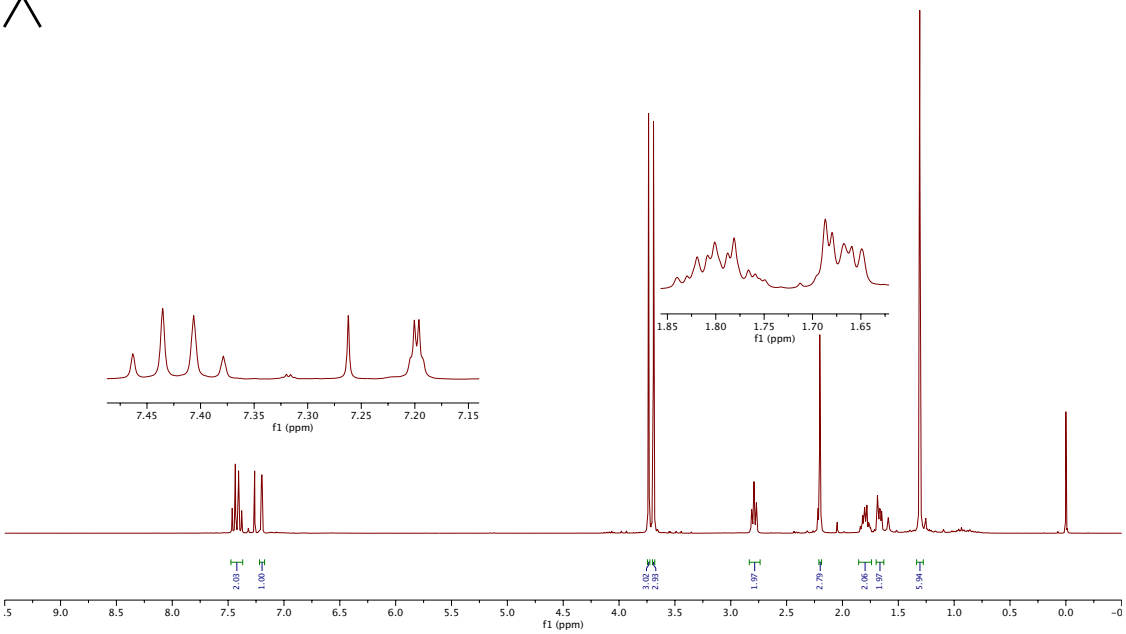
7.45 7.40 7.35 7.30 7.25 7.20 7.15
f1 (ppm)
1.85 1.80 1.75 1.70 1.65
f1 (ppm)
2.03
1.00
3.02
2.93
1.97
2.79
2.06
1.97
5.94
f1 (ppm)


169.72
164.56
157.80
148.06
139.57
134.00
133.09
128.24
127.80
126.14
122.33
114.73
52.19
51.38
38.56
34.47
31.95
28.34
19.34
10.20

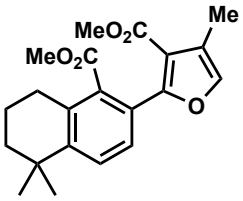
MeO2C
MeO2C
Me
O

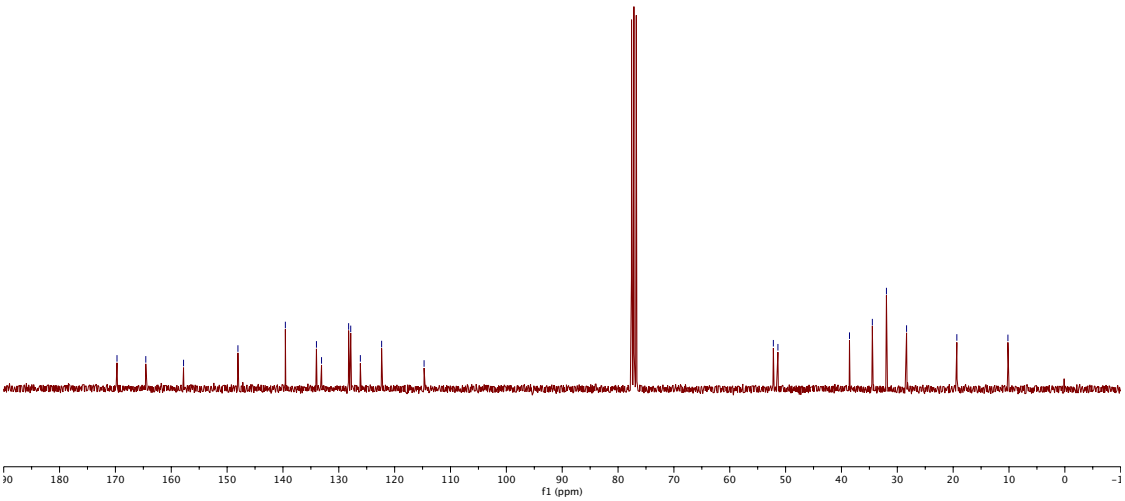
f1 (ppm)

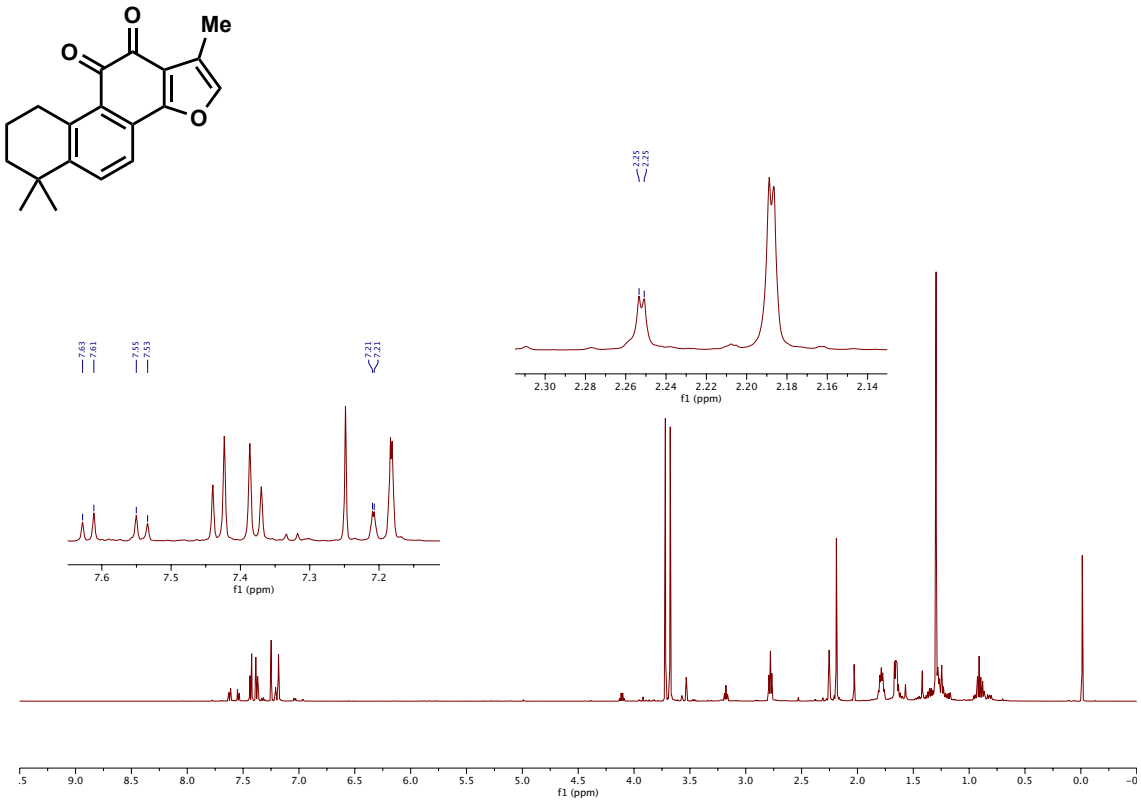
O
O
Me
O
7.63
7.61
7.55
7.53
7.21
7.21
2.25
2.25
f1 (ppm)
f1 (ppm)
f1 (ppm)

X-ray Crystallographic Analysis of **49**

Experimental details

Single-crystal X-ray diffraction data was collected at 293(2) K on a XtaLAB Synergy-S, Dualflex, HyPix-6000HE diffractometer using Cu *K*α radiation (λ = 1.5406 Å). Crystal was mounted on nylon CryoLoops with Paraton-N. The data collection and reduction were processed within *CrysAlisPro* (Rigaku OD, 2021). A multi-scan absorption correction was applied to the collected reflections. Using Olex2 [1], the structure was solved with the ShelXT [2] structure solution program using Intrinsic Phasing and refined with the ShelXL [3] refinement package using Least Squares minimisation. All non-hydrogen atoms were refined anisotropically. The carboxylic hydrogen atoms were located in difference Fourier maps and refined on a riding model. All other organic hydrogen atoms were generated geometrically. Because the compound is a weak anomalous scatterer and the s.u. of the Flack parameter is large, the absolute structure parameter is meaningless and removed from the CIF.

1. Dolomanov, O.V., Bourhis, L.J., Gildea, R.J, Howard, J.A.K. & Puschmann, H. (2009), *J. Appl. Cryst*. 42, 339-341.
2. Sheldrick, G.M. (2015). *Acta Cryst*. A71, 3-8.
3. Sheldrick, G.M. (2015). *Acta Cryst*. C71, 3-8.

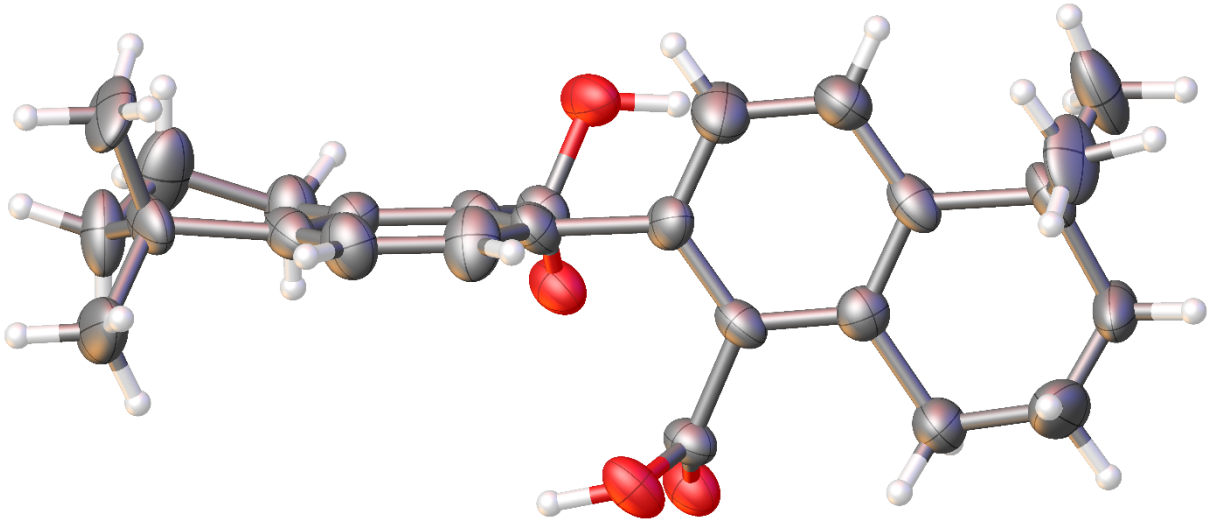

(Non-hydrogen atoms are represented by displacement ellipsoids at the 50% probability level).

List of Tables

Table 1. Crystal data and structure refinement

Table 2. Fractional Atomic Coordinates and Equivalent Isotropic Displacement Parameters

Table 3. Selected Bond Distances

Table 4. Selected Bond Angles

Table 5. Selected Torsion Angles

Table 1. Crystal data and structure refinement

Identification code	NT-D-145-F
Empirical formula	$C_{26}H_{30}O_4$
Formula weight	406.50
Temperature/K	293(2)
Crystal system	tetragonal
Space group	$P4_22_12$
a/Å	17.6425(2)
b/Å	17.6425(2)
c/Å	7.09565(14)
Volume/Å^3	2208.58(7)
Z	4
ρ_{calc}mg/mm^3	1.223
μ/mm^{-1}	0.647
F(000)	872.0
Crystal size/mm^3	0.334 × 0.121 × 0.078
2θ range for data collection	7.086 to 158.636°
Index ranges	$-22 \leq h \leq 17$, $-22 \leq k \leq 22$, $-8 \leq l \leq 8$
Reflections collected	28137
Independent reflections	2376[R(int) = 0.0530]
Data/restraints/parameters	2376/8/247
Goodness-of-fit on F^2	1.103
Final R indexes [I>=2σ (I)]	R_1 = 0.0775, wR_2 = 0.2278
Final R indexes [all data]	R_1 = 0.0835, wR_2 = 0.2373
Largest diff. peak/hole / e Å^{-3}	0.17/-0.20

Table 2. Fractional Atomic Coordinates ($\times 10^4$) and Equivalent Isotropic Displacement Parameters ($Å^2 \times 10^3$). U_{eq} is defined as 1/3 of the trace of the orthogonalised U_{IJ} tensor.

Atom	*x*	*y*	*z*	U(eq)
O1	5535(3)	5527(3)	3600(6)	74.8(13)
O2	6265(4)	4879(5)	1637(10)	80.2(19)
C1	6040(7)	5151(6)	3376(18)	61(2)
C2	6566(2)	4818(2)	4823(5)	58.4(13)
C3	6475(2)	4077.2(19)	5452(6)	62.6(14)
C4	6913(3)	3808(2)	6937(7)	94(2)
C5	7442(3)	4280(3)	7793(7)	84(3)
C6	7532(3)	5021(3)	7164(7)	68(2)
C7	7094(2)	5289.7(19)	5679(6)	65.2(14)
C8	7148(5)	6118(4)	5022(12)	83.2(18)
C9	7905(6)	6459(6)	5563(16)	116(4)
C10	8083(6)	6376(6)	7363(16)	98(4)
C11	8179(5)	5539(6)	7991(12)	79(3)
C12	8113(5)	5491(7)	10191(11)	125(4)
C13	8938(5)	5220(10)	7510(30)	116(4)
O3	6213(6)	4941(5)	13371(15)	67(2)
O4	5489(3)	5589(3)	11379(6)	69.4(13)
C14	6030(5)	5145(5)	11693(15)	59(2)
C15	6510(2)	4861(2)	10152(5)	58.1(14)
C16	6439(2)	4123(2)	9489(6)	67.1(16)
C17	6901(3)	3869(2)	8034(7)	72(2)
C18	7435(3)	4354(3)	7241(7)	69(2)
C19	7506(3)	5092(3)	7904(7)	69(2)
C20	7044(2)	5345.5(19)	9359(6)	57.3(13)
C21	7092(4)	6151(4)	10126(11)	74.5(18)
C22	7789(7)	6560(6)	9595(19)	125(4)
C23	8049(12)	6382(12)	7480(30)	169(11)
C24	8135(5)	5570(6)	7000(16)	78(2)
C25	8889(10)	5247(14)	7520(30)	122(3)
C26	8071(7)	5567(8)	4822(16)	122(3)

Table 3. Selected Bond Distances (Å)

Atom	Atom	Length/Å	Atom	Atom	Length/Å
O1	C1	1.122(11)	O3	C14	1.285(16)
O2	C1	1.382(16)	O4	C14	1.254(10)
C1	C2	1.504(10)	C14	C15	1.471(10)
C7	C2	1.3900	C19	C20	1.3900
C7	C6	1.3900	C19	C18	1.3900
C7	C8	1.537(8)	C19	C24	1.534(10)
C2	C3	1.3900	C20	C15	1.3900
C3	C3[1]	1.519(6)	C20	C21	1.525(8)
C3	C4	1.3900	C15	C16	1.3900
C4	C5	1.3900	C16	C16[2]	1.579(6)
C5	C6	1.3900	C16	C17	1.3900
C6	C11	1.575(9)	C17	C18	1.3900
C8	C9	1.514(12)	C21	C22	1.473(11)
C9	C10	1.323(15)	C22	C23	1.60(2)
C10	C11	1.552(16)	C23	C24	1.48(2)
C11	C12	1.568(12)	C24	C25	1.49(2)
C11	C13	1.493(15)	C24	C26	1.549(15)

[1]1-Y,1-X,1-Z; [2]1-Y,1-X,2-Z

Table 4. Selected Bond Angles

Atom	Atom	Atom	Angle/°	Atom	Atom	Atom	Angle/°
O1	C1	O2	124.1(10)	O3	C14	C15	116.7(7)
O1	C1	C2	128.6(11)	O4	C14	O3	122.1(10)
O2	C1	C2	107.2(7)	O4	C14	C15	121.2(8)
C2	C7	C6	120.0	C20	C19	C18	120.0
C2	C7	C8	118.6(4)	C20	C19	C24	123.9(5)
C6	C7	C8	121.3(4)	C18	C19	C24	116.0(5)
C7	C2	C1	118.5(6)	C19	C20	C21	122.2(4)
C3	C2	C1	121.1(6)	C15	C20	C19	120.0
C3	C2	C7	120.0	C15	C20	C21	117.8(4)
C2	C3	C3[1]	122.7(4)	C20	C15	C14	118.8(4)
C2	C3	C4	120.0	C16	C15	C14	121.2(4)
C4	C3	C3[1]	117.2(4)	C16	C15	C20	120.0
C5	C4	C3	120.0	C15	C16	C16[2]	119.3(4)
C4	C5	C6	120.0	C15	C16	C17	120.0
C7	C6	C11	119.1(5)	C17	C16	C16[2]	120.5(4)
C5	C6	C7	120.0	C16	C17	C18	120.0
C5	C6	C11	120.6(5)	C17	C18	C19	120.0
C9	C8	C7	110.8(6)	C22	C21	C20	114.3(7)
C10	C9	C8	114.2(9)	C21	C22	C23	112.5(11)
C9	C10	C11	114.1(9)	C24	C23	C22	115.7(15)
C10	C11	C6	111.5(6)	C19	C24	C26	111.3(8)
C10	C11	C12	109.3(9)	C23	C24	C19	111.2(8)
C12	C11	C6	106.6(8)	C23	C24	C25	113.8(16)
C13	C11	C6	110.2(8)	C23	C24	C26	103.0(12)
C13	C11	C10	113.0(11)	C25	C24	C19	109.4(10)
C13	C11	C12	106.0(9)	C25	C24	C26	108.0(11)

[1]1-Y,1-X,1-Z; [2]1-Y,1-X,2-Z

Table 5. Selected Torsion Angles

A	B	C	D	Angle/°	A	B	C	D	Angle/°
O1	C1	C2	C7	-74.7(16)	O3	C14	C15	C20	-101.8(8)
O1	C1	C2	C3	98.2(13)	O3	C14	C15	C16	78.1(9)
O2	C1	C2	C7	108.3(8)	O4	C14	C15	C20	75.2(9)
O2	C1	C2	C3	-78.7(10)	O4	C14	C15	C16	-104.9(7)
C1	C2	C3	C3[1]	8.8(7)	C14	C15	C16	C16[2]	-4.7(6)
C1	C2	C3	C4	-172.9(7)	C14	C15	C16	C17	-179.9(6)
C7	C2	C3	C3[1]	-178.4(5)	C19	C20	C15	C14	179.9(6)
C7	C2	C3	C4	0.0	C19	C20	C15	C16	0.0
C7	C6	C11	C10	15.9(10)	C19	C20	C21	C22	-16.1(11)
C7	C6	C11	C12	135.1(7)	C20	C19	C18	C17	0.0
C7	C6	C11	C13	-110.3(10)	C20	C19	C24	C23	-15.8(16)
C7	C8	C9	C10	-51.7(13)	C20	C19	C24	C25	110.8(12)
C2	C7	C6	C5	0.0	C20	C19	C24	C26	-130.0(8)
C2	C7	C6	C11	174.5(6)	C20	C15	C16	C16[2]	175.2(5)
C2	C7	C8	C9	-159.8(7)	C20	C15	C16	C17	0.0
C2	C3	C4	C5	0.0	C20	C21	C22	C23	38.5(17)
C3[1]	C3	C4	C5	178.4(4)	C15	C20	C21	C22	164.5(8)
C3	C4	C5	C6	0.0	C15	C16	C17	C18	0.0
C4	C5	C6	C7	0.0	C16[2]	C16	C17	C18	-175.1(5)
C4	C5	C6	C11	-174.4(6)	C16	C17	C18	C19	0.0
C5	C6	C11	C10	-169.6(7)	C18	C19	C20	C15	0.0
C5	C6	C11	C12	-50.5(8)	C18	C19	C20	C21	-179.4(5)
C5	C6	C11	C13	64.1(11)	C18	C19	C24	C23	167.0(13)
C6	C7	C2	C1	173.0(7)	C18	C19	C24	C25	-66.4(13)
C6	C7	C2	C3	0.0	C18	C19	C24	C26	52.8(9)
C6	C7	C8	C9	23.6(10)	C21	C20	C15	C14	-0.8(7)
C8	C7	C2	C1	-3.6(8)	C21	C20	C15	C16	179.4(5)
C8	C7	C2	C3	-176.6(5)	C21	C22	C23	C24	-53(2)
C8	C7	C6	C5	176.5(5)	C22	C23	C24	C19	39(2)
C8	C7	C6	C11	-9.0(7)	C22	C23	C24	C25	-84.7(17)
C8	C9	C10	C11	63.1(14)	C22	C23	C24	C26	158.7(15)
C9	C10	C11	C6	-43.4(13)	C24	C19	C20	C15	-177.1(7)
C9	C10	C11	C12	-161.0(9)	C24	C19	C20	C21	3.5(8)
C9	C10	C11	C13	81.3(12)	C24	C19	C18	C17	177.3(7)

[1]1-Y,1-X,1-Z; [2]1-Y,1-X,2-Z

Chapter 3: Summary and Future Work

3.1: Chapter 1 Summary

Chapter 1 of this thesis represents a new methodology for utilizing α-diazocarbonyl compounds in a tandem C–H insertion/annulation reaction for the construction of heterocycles. Using this tandem C–H functionalization/Michael-type annulation, a number of different fused indole substrates were synthesized. These transformations were accomplished using a single inexpensive copper catalyst system, which is a financial improvement over expensive rhodium or gold catalysts employed in similar known transformations. This tandem reaction proceeds in moderate to high yields, with many examples proceeding in a stereoselective fashion. Finally, the development of a one-pot C–H insertion/base promoted annulation sequence was established, allowing for an extension of this reaction manifold to include donor/acceptor diazo compounds and electron deficient alkene electrophiles. In total, 28 distinct ring fused products were produced in the project(Scheme 3.1).

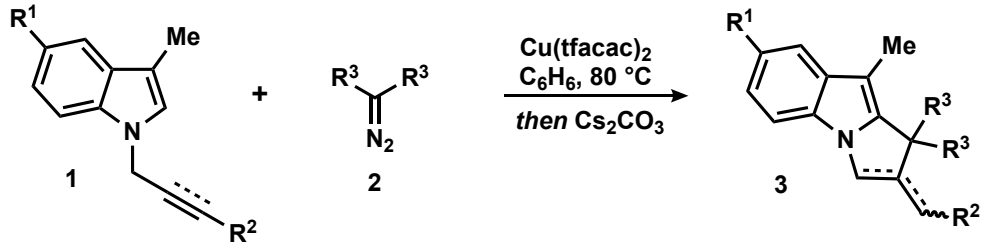

Scheme 3.1: Representative example of pyrroloindole synthesis.

Potential future expansions of the current reaction manifold (C–H insertion/annulation) would be to explore other compatible nucleophilic arenes (other than indole), along with exploration into other electrophiles. As mentioned in Chapter 1, this

area of research is well established with heteroatom nucleophiles (X–H insertion/annulation) and many different electrophiles have been explored, including carbonyls, imines, nitriles, and alkyl halides. In contrast, there has been very little research developed for the comparative C–H insertion processes. A thorough investigation into various electrophiles by consultation with X–H insertion/annulation literature would be a good place to start.

A tangentially related future project could also come from an interesting by-product that was formed in one example when exploring the reaction scope of the copper catalyzed reaction described in Chapter 1. Note, this substrate was not described in Chapter 1 as no desired annulation product was observed. In an attempt to extend the electrophile substrate an electron poor pyridine ring was installed on the alkyne (Scheme 3.2A). When this indole substrate (**4**) was subjected to reaction with diazo **5** under the optimized reaction conditions, product **6**, containing an unusual indolizine ring system, was isolated in ca. 20% yield. Interestingly, this product has lost one of the ester groups from the initial diazo reagent. It is envisioned that this reaction could be applied to general substituted 2-alkynylpyridine to develop a new method for the synthesis of substituted indolizine compounds (Scheme 3.2B). Optimizing the yield of the transformation is the most immediate goal. Once that is accomplished a broad substrate scope similar to that explored in Chapter 1 will be undertaken. This preliminary result should warrant further investigation.

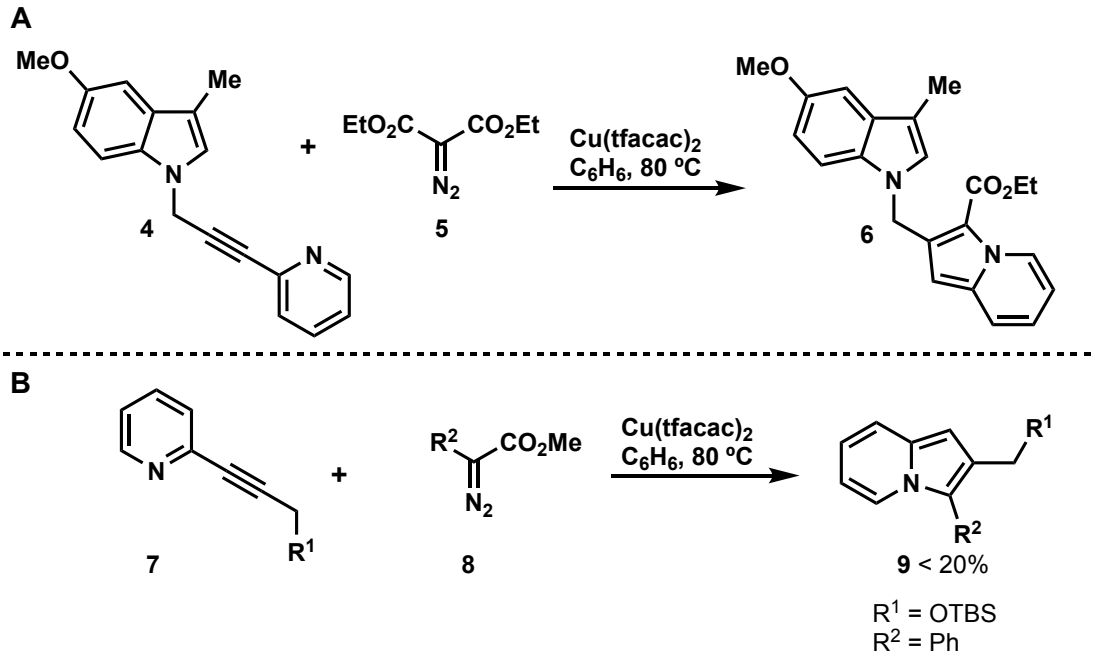

Scheme 3.2: A: Interesting result from attempted insertion/annulation. B: Initial attempts at the synthesis of indolizines via tandem insertion/annulation.

3.2: Chapter 2 Summary

Chapter 2 presents a total synthesis project of an abietane diterpenoid called tanshinone IIA. In summary, tanshinone IIA has been synthesized in a total 11 convergent steps, with the longest linear sequence being 7 steps from commercially available isocyanide **10**. This synthesis features access to coupling partners **14** and **19** from commercially available starting materials through multiple high yielding multigram scale transformations, as well as an interesting Stanna-Brook rearrangement to furnish the C ring of tanshinone IIA (Scheme 3.3). The most immediate work is to improve the final step in the synthesis to ensure complete conversion to the natural product.

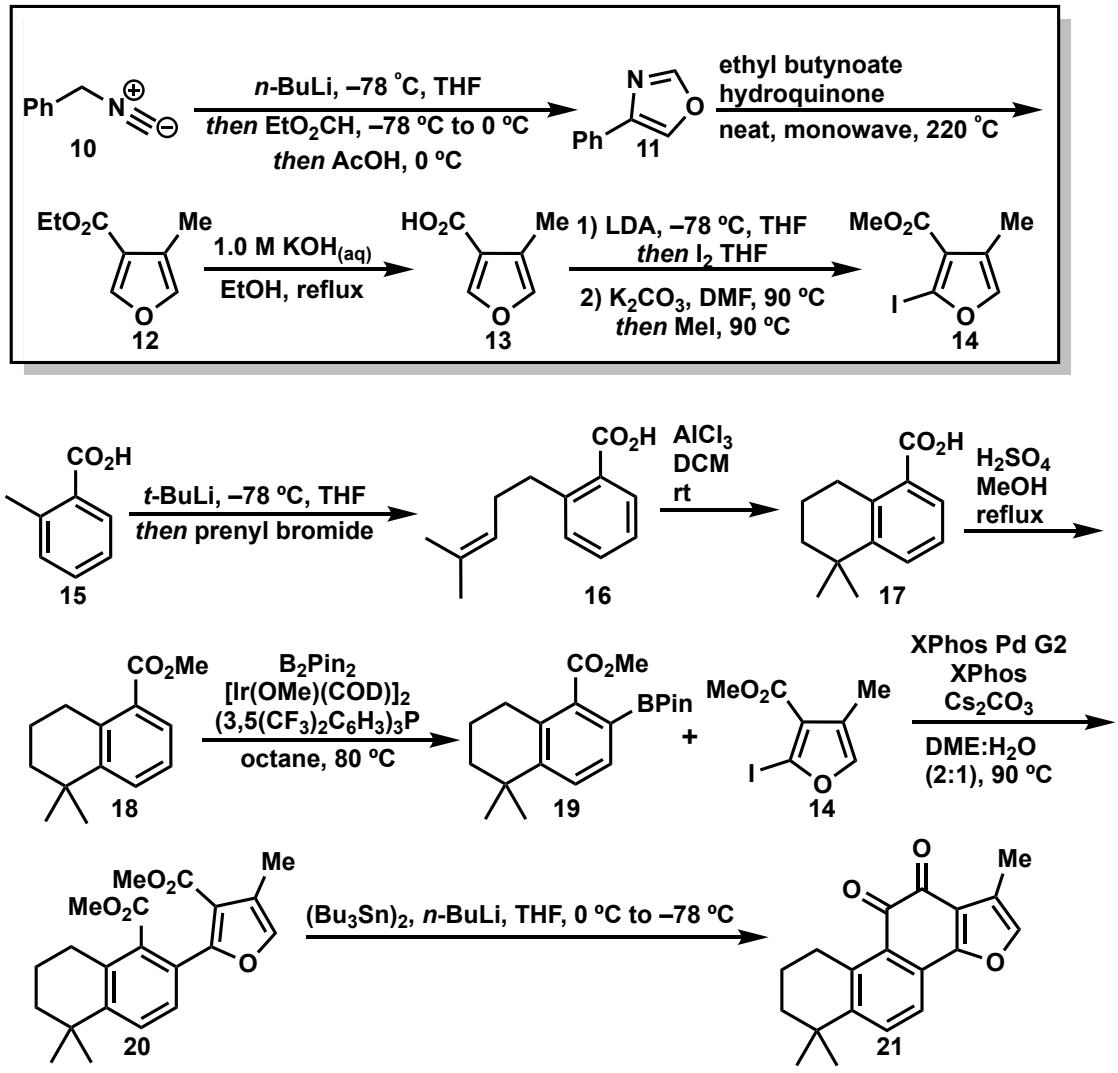

Scheme 3.3: Total synthesis of tanshinone IIA.

3.2.1: Potential Future Work

Further optimization of the current synthetic route for larger scale production of tanshinone IIA is being investigated. In particular the iridium borylation, Suzuki coupling, and final ring closure have only been completed on small scale. In addition to determining if the current route can be done on larger scale, alternative approaches to the biaryl cross coupling should be explored with intentions of improving the overall step count of the total

synthesis. A possible improvement can be realized through a one-pot Negishi coupling process. This involves selective metallation of furan **12**, followed by *in situ* transmetalation with Zinc and subsequent Negishi coupling with **22** to furnish a coupled product in one-pot.[1] Initial attempts at this transformation have been low yielding, but have shown that small amounts of coupled product can be formed through this method (Scheme 3.4). In essence, if optimized, this alternative coupling approach would cut down on the overall step count of the synthesis and make use of two intermediates (**12** and **22**) that have already be obtained in gram quantities.

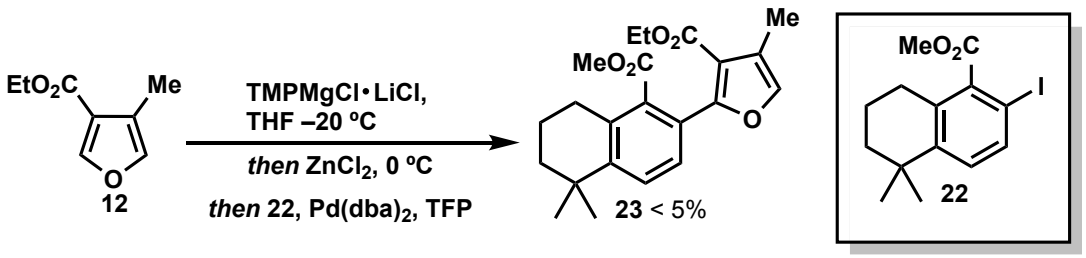

Scheme 3.4: One-pot Negishi coupling attempt.

Finally, it is also anticipated that other target members of this natural product family may be accessed using similar methodology. Both normiltirone **27** and miltirone **28** have been envisioned arising from the same carboxylic acid **26** (Scheme 3.5). This carboxylic acid has actually been isolated in 2 steps from *o*-iodo-ester **22**, via formylation and subsequent Horner-Wadsworth-Emmons reactions. Final steps to access these two natural products are currently underway.

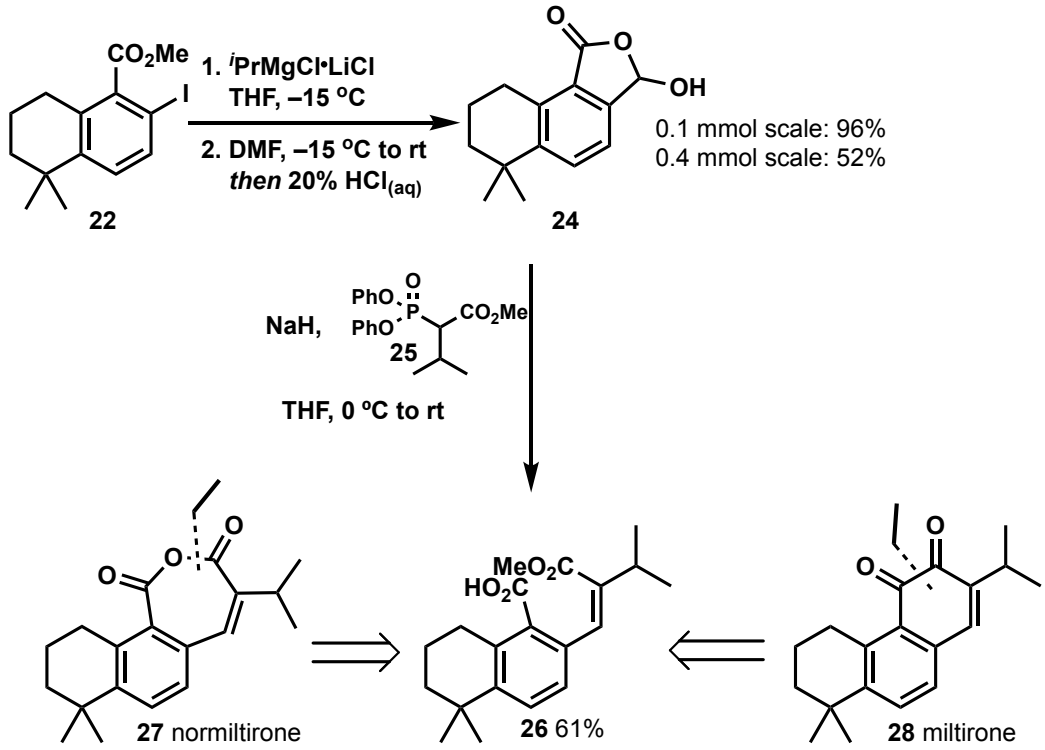

Scheme 3.5: Progress towards the synthesis of normiltirone and miltirone.

References

(1) Ren, H.; Krasovskiy, A.; Knochel, P. *Chem. Commun.* **2005**, 4, 543–545.